Multicomponent Porphyrins as Platforms for Applications with Nanomaterials and in DSSCs

Submitted by

Alina Meindl BSc

A thesis submitted to the University of Dublin, Trinity College for the degree of

Doctor of Philosophy

Under the supervision of Prof. Dr. Mathias O. Senge

Trinity College Dublin, the University of Dublin

2019

Declaration

I declare that this thesis has not been submitted as an exercise for a degree at this or any other university and it is entirely my own work.

I agree to deposit this thesis in the University's open access institutional repository or allow the Library to do so on my behalf, subject to Irish Copyright Legislation and Trinity College Library conditions of use and acknowledgement.

Furthermore, unpublished and/or published work of others, is duly acknowledged in the text wherever included.

Signed: _____

February 2019 Trinity College Dublin

Summary

The aim of this research was to investigate different multicomponent porphyrin systems. Special interest was put on donor-acceptor units, the specific molecular arrangement of units within the multicomponent systems as well as distinctive electronic properties such as those in conjugated and isolating systems.

Contemporary applications in optics, medicine, solar cells or material science are increasingly reliant on unsymmetrically substituted porphyrins. Due to their widespread uses and rise in demand, a comparative analysis of synthetic strategies for meso-substituted porphyrins was undertaken and the synthesis of different series of so-called A_2BC *push-pull* porphyrins was explored. The synthetic pathways used were applied to both 5,15-substituted and 5,10-substituted porphyrins, showcasing their flexibility and adaptability for different needs. This approach combines well-known reactions with a strategic and logical stepwise functionalisation allowing researchers to change and modify the electronic properties of these systems at various points of the syntheses. This facilitates the easy optimisation of the synthesis of systems of current interest, e.g., porphyrins for dye-sensitised solar cells (DSSC) or for use in nonlinear optics, as well as the fast generation of compound libraries

Furthermore, the linkage of an electronically isolating unit to a porphyrin was explored. Therefore, the cubane unit was chosen as an example of a non-conjugated hydrocarbon linker. One of the major objectives of this study was to gain deeper insights into the cubane C-C coupling chemistry, with a special focus on the synthesis of directly linked cubane-porphyrin systems and multi-porphyrin arrays with cubane as scaffold linker. First attempts were undertaken using the formation of a porphyrinyllithium species to couple a halogen-substituted cubane derivative to a porphyrin. While this proved unsuccessful, the utilisation of SET cross-coupling reactions showed promising results. The preparation of a suitable porphyrin–zinc species was achieved by adapting the iodine–metal exchange developed by the Osuka group.[1] Following optimisation of various reaction conditions, three different directly-linked cubane-substituted porphyrins were synthesised and isolated. Generally, the yields are low for these important classes of compounds, but nevertheless the first directly linked cubane–porphyrin system, a system which has not been reported before, was synthesised.

Besides electronically isolated systems also conjugated systems were investigated. Here, especially the distinct interaction of various porphyrin materials with different nanomaterials was of interest.

- One part involved the generation of synthetic methodologies for porphyrin-based supramolecular tectons for surface studies. The study aimed to generate porphyrins with directional anchoring groups with a special focus on organometallic coupling reactions for the introduction of benzoic acid moieties as anchor groups. Porphyrin monomers and dimers with one to four benzoic acid moieties were synthesised.
- Furthermore, interfacial charge transfer studies with the *push-pull* porphyrins developed above were undertaken. Here the interactions of the porphyrins and different nanomaterials, namely fullerene and graphene carboxylate, were investigated.
- Another interaction was explored through the synthesis of pyridine-substituted Pd porphyrins for their use in Metal-organic Frameworks. As purification of the Pd complexes proved to be difficult, the firt synthetic pathway was revised and the free-base 5,15-diphenyl-10,20-bis[(4-pyridyl)ethynyl]porphyrin was synthesised according to literature procedure.[2] However, the final metal insertion resulted in the formation of networks due to the interaction of the pyridine-substituted porphyrin with Pd. Therefore, the reaction pathway was altered again which resulted in the formation of the 5,15-diphenyl-10,20-bis[(4-pyridyl)ethynyl]porphyrin.
- Besides, to probe non-covalent interactions of various porphyrin systems with nanomaterials, also covalently linked porphyrins were investigated. Therefore, metal complexes of the 5-(4-ethynylphenyl)-10,20-diphenylporphyrin were synthesised to covalently link to the surface of an electrode. The ethynylphenyl linker was attached to the porphyrin through standard organolithium reaction. While the subsequent Ni insertion proceeded without difficulties, the Co insertion resulted in severe interactions between the porphyrin and silica or AlOX and consecutive degradation. Upon reconsideration of the synthetic pathway, the Co atom was inserted prior to the coupling reaction with the ethynylphenyl moiety. Furthermore, the protected 4-[(trimethylsilyl)ethynyl]phenylboronic acid pinacol ester was used to allow purification at this late stage of the

synthesis. This reduced the interaction with silica or ALOX significantly and gave the desired ethynylphenyl-appended porphyrin after deprotection.

Finally, the synthesis of bisanthracene-substituted porphyrins was attempted. These porphyrins are of interest for optoelectronic devices as they represent a class of highly conjugated systems which are electronically coupled and possess a large bathochromic shift in their absorption spectra. To obtain these systems the synthesis of bisanthracene building blocks as well as the following mono bromination was optimised. These valuable precursors were then subjected to Suzuki cross-coupling reactions in order to append the anthracene unit to the porphyrin. Dimers as well as trimers were synthesised with one and two bisanthracene units. Besides this, oxidative fusing reactions were explored for both the bisanthracene starting material and the anthracene-substituted porphyrins.

Publications

- **A. Meindl**, S. Plunkett, A. A. Ryan, K. J. Flanagan, S. Callaghan, M. O. Senge, Comparative Synthetic Strategies for the Generation of 5,10- and 5,15-Substituted *Push-Pull* Porphyrins, *Eur. J. Org. Chem*. **2017**, 3565-3583.

- **Cover Picture** "Comparative Synthetic Strategies for the Generation of 5,10- and 5,15-Substituted *Push-Pull* Porphyrins" *Eur. J. Org. Chem*. **2017**, 3565-3583.

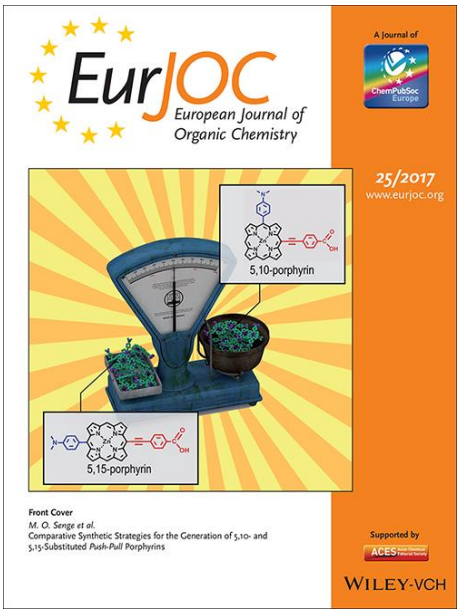

- **A. Meindl**, A. A. Ryan, K. J. Flanagan and M. O. Senge, Synthesis of Long-Wavelength Absorbing Porphyrin m-Benzoic Acids as Molecular Tectons for Surface Studies, *Heterocycles*, **2017,***8*, 1518-1541

- S. S. R. Bernhard, G. M. Locke, S. Plunkett, **A. Meindl**, K. J. Flanagan, and M. O. Senge, Cubane Cross-Coupling and Cubane–Porphyrin Arrays, *Chem. Eur. J.*, **2017**, *23*, 1-6.

- **Cover Picture** "Cubane Cross-Coupling and Cubane–Porphyrin Arrays" *Chem. Eur. J.*, **2017**, *23*, 1-6.

- M. O. Senge and **A. Meindl**, The Organic Synthesis and Reactivity of Porphyrins, in *Porphyrins for the 21st Century: Fundamentals*, Vol. 1, (P. J. Brother and M. O. Senge, eds.), Wiley, Weinheim, in press.

Conference Abstracts

Poster:

- A. A. Ryan, **A. Meindl**, M. Dizon, A. A. Carfolla and M. O. Senge " Different strategies for π-extended porphyrins in solution and on metal surfaces" in thirteenth Annual Symposium of the Centre for Synthesis and Chemical Biology (12.12.14), University College Dublin, Dublin, Ireland.
- L. Rogers, E. Burke-Murphy, C. Moylan, A. M. K. Sweed, M. Kielmann, **A. Meindl**, Y. M. Shaker, E. M. Scanlan and M. O. Senge "Biconjugated porphyrins for use in photodynamic therapy" in GDCH Wissenschaftsforum 2015 (30.8.-02.09.15), Dresden, Germany.
- L. Rogers, E. Burke-Murphy, C. Moylan, A. M. K. Sweed, M. Kielmann, **A. Meindl**, Y. M. Shaker, E. M. Scanlan and M. O. Senge "Synthetic pathways towards two classes of optimized photosensitizers (PSs) for use in photodynamic therapy (PDT)" in fourteenth Annual Symposium of the Centre for Synthesis and Chemical Biology (11.12.15), Royal College of Surgeons, Dublin, Ireland.
- S. Plunkett, S. Callaghan, **A. Meindl** and M. O. Senge " Synthesis of 5,10-disubstituted porphyrins and their stepwise functionalization" in fourteenth Annual Symposium of the Centre for Synthesis and Chemical Biology (11.12.15), Royal College of Surgeons, Dublin, Ireland.
- **A. Meindl**, S. Plunkett and M. O. Senge, "New Disubstituted Porphyrin Systems with Potential Application as Sensitizers in PDT and Photochemistry" in 4th ESp Photobiology school (20.6-25.6.16), Brixen, Italy.
- **A. Meindl** and M. O.Senge, "Methodologies Towards the Synthesis and Functionalisation of 5,10-Disubstituted Porphyrins" in Tetrapyrrole Discussion Group Meeting (21.03.16-22.03.16), John Moores University, Liverpool, UK.
- **A. Meindl**, S. Plunkett and M. O. Senge, "New Disubstituted Porphyrin Systems with Potential Application as Sensitizers in PDT and

Photochemistry" in fifteenth Annual Symposium of the Centre for Synthesis and Chemical Biology (09.12.16), Trinity College Dublin, Dublin, Ireland.

- **A. Meindl** and M. O. Senge, "Methodologies Towards the Synthesis and Functionalisation of 5,10-Disubstituted Porphyrins" in Tetrapyrrole Discussion Group Meeting (21.03.16-22.03.16), John Moores University, Liverpool, UK, page 18.

- **A. Meindl**, S. Plunkett and M. O. Senge, "New Disubstituted Porphyrin Systems with Potential Application as Sensitizers in PDT and Photochemistry" in 4th ESP Photobiology school (20.6-25.6.16), Brixen, Italy, page 19.

- **A. Meindl**, S. Plunkett and M. O. Senge, "New Disubstituted Porphyrin Systems with Potential Application as Sensitizers in PDT and Photochemistry" in fifteenth Annual Symposium of the Centre for Synthesis and Chemical Biology (09.12.16), Trinity College Dublin, Dublin, Ireland, Abstract P33.

- **A. Meindl**, S. Plunkett and M. O. Senge, „Synthesis and Functionalization of New Disubstituted Porphyrin Systems with Potential Application as Sensitizers in PDT and Photochemistry" in 17th Congress of the European Society for Photobiology (04.09.-08.09.2017), Pisa, Italy, abstract book: P036, page 120.

- **A. Meindl**, C. Moylan, L. Rogers, E. M. Scanlan and M. O. Senge, "Porphyrin-based Bioconjugates for Use in Photodynamic Therapy (PDT)" in 17th Congress of the European Society for Photobiology (04.09.-08.09.2017), Pisa, Italy, abstract book: P032, page 119

- **A. Meindl**, A. A. Ryan, A. A. Carfolla and M. O. Senge, "Towards Functional π-Extended Porphyrins – Solution and Surface Chemistry of Porphyrin Nanostructures" in GDCh-Wissenschaftsforum Chemie 2017 (10.09.-14.09.2017), Berlin, Germany, abstract book: ORG 064, page 77.

- **A. Meindl**, S. Plunkett, S. Callaghan and M. O. Senge, "Methodologies Towards the Synthesis and Functionalisation of Unsymmetrical Push-Pull Porphyrins" in GDCh-Wissenschaftsforum Chemie 2017 (10.09.-14.09.2017), Berlin, Germany, abstract book: ORG 063, page 77.

- **A. Meindl**, A. A. Ryan, A. A. Carfolla and M. O. Senge, “Towards Functional π-Extended Porphyrins – Solution and Surface Chemistry of Porphyrin Nanostructures” in CSCB 2017 (08.12.2017), Dublin, Ireland abstract book: P59.

- **A. Meindl**, S. S. R. Bernhard, S. L. Plunkett, G. M. Locke and M. O. Senge,” Development of New Tools for the Functionalization of Cubane” poster at Humboldt Colloquium “Moving Forward-The UK-German Research Network in a Changing World”, (15.03.-17.03.2018) Oxford, UK. Abstract book: page 231

- **A. Meindl** and M. O. Senge, “Methodologies Towards the Synthesis and Functionalization of Unsymmetrical Push-Pull Porphyrins” in International Conference on Porphyrins and Phthalocyanines (ICPP-10) (01.07.-06.07.2018), Munich, Germany, abstract book: page 523.

- **A. Meindl**, A. A. Ryan, A. A. Carfolla and M. O. Senge, “Towards Functional π-Extended Porphyrins – Solution and Surface Chemistry of Porphyrin Nanostructures” in International Conference on Porphyrins and Phthalocyanines (ICPP-10) (01.07.-06.07.2018), Munich, Germany, abstract book: page 524.

<u>Oral presentations:</u>

- **A. Meindl** and M. O. Senge, “Following Nature’s Footprints: A Comparative Synthetic Study of *Push-Pull* Porphyrins for Solar Cells” talk at Trinity College Dublin (06.03.2018) Dublin, Ireland.

- **A. Meindl**, and M. O. Senge, “Following Nature’s Footprints: A Comparative Synthetic Study of *Push-Pull* Porphyrins for Solar Cells” talk at Humboldt Colloquium “Moving Forward-The UK-German Research Network in a Changing World”, (15.03.-17.03.2018) Oxford, UK. Talk in Section 4: Chemistry, Geosciences, Applied Engineering, March 16th.

Acknowledgements

First of all, I would like to thank Prof. Dr. Mathias Senge for the opportunity to work in his research group and for his guidance, encouragement and support over the years. I would also like to thank Science Foundation Ireland for the financial support during my studies.

Furthermore, I would like to thank all members of the Senge group for making the lab a welcoming and enjoyable place to work. The atmosphere and support in the group truly made a big difference in the day to day life in the lab. I am very thankful for the close friendships that have formed over the years which have by far extended working hours and resulted in many great memories of fun evenings, weekends away, festivals, sport events, swimming and surfing in the freezing sea together and many more… Special thanks also to Jess and Gemma for proof-reading large parts of this thesis.

Many thanks to all the technical staff of the chemistry department, in particular, Dr. John O'Brien and Dr. Manuel Rüther for NMR analysis and to Dr. Martin Feeney and Dr. Gary Hessman for HRMS measurements.

Last but not least I would like to thank my family. Thank you to my parents for always being there for me, for your love and for encouraging me to take a step further, even if I had some doubts in the beginning. Without your constant support I wouldn't be the person I am today! Thanks also to my sisters Esther and Flora, for the many conversations, your support, the many jokes and your unfiltered truth, which helps me to stay on the ground! Finally, I would like to thank Eric for his permanent support and help and for listening to me and cheering me up after a bad day.

"*I have not failed. I've just found 10,000 ways that won't work*".

Thomas A. Edison

"Science, my lad, is made up of mistakes, but they are mistakes which it is useful to make, because they lead little by little to the truth."

Jules Verne

Die Normalität ist eine gepflasterte Straße: man kann gut darauf gehen - doch es wachsen keine Blumen auf ihr.

Vincent van Gogh

Abbreviations

Acac	Acetylacetonate
Ar	Aryl
BINAP	2,2'-Bis(diphenylphosphino)-1,1'-binaphthalene
B	Broad
C_{60}	Fullerene
CB	Conduction band
Calcd	Calculated
$CHCl_3$	Chloroform
Dba	Dibenzylideneacetone
DCM	Dichloromethane
DDQ	2,3-Dichloro-5,6-dicyano-1,4-benzoquinone
DEA	Diethylamine
DMF	*N*,*N*-Dimethylformamide
DPM	Dipyrromethane
DPEphos	Bis[(2-diphenylphosphino)phenyl]ether
DSSC	Dye-sensitised solar cells
ESI	Electrospray ionisation
Eq.	Equivalents
GCO	Graphene carboxylate
HRMS	High resolution mass spectrometry
MALDI	Matrix assisted laser desorption ionization
MeOH	Methanol
min	Minute
M.p.	Melting point
MW	Microwave
NBS	*N*-Bromosuccinimide
n-BuLi	*n*-Butyllithium
N.D.	Not determined
NLA	Non-linear absorption
NMR	Nuclear magnetic resonance

NLO	Non-linear optics
η-value	Power conversion efficiency
OEP	Octaethylporphyrin
PCE	Power conversion efficiency
Prep TLC	Preparative thin layer chromatography
OTf	Triflate
Ph	Phenyl
Ppm	Parts per million
R_f	Retention factor
rt	Room temperature
sat.	Saturated
TBAF	Tetra-*n*-butylammonium fluoride
TFA	Trifluoroacetic acid
THF	Tetrahydrofuran
TLC	Thin layer chromatography
TMS	Trimethylsilane
UV	Ultraviolet
Vis	Visible
v/v	Volume to volume
Xantphos	4,5-Bis(diphenylphosphino)-9,9-dimethylxanthene

Table of Contents

1 Introduction

1.1 An introduction to porphyrins

Porphyrins belong to the family of tetrapyrrolic macrocycles. These molecules have been widely studied due to their prevalence in nature as well as the fundamental role they play in plant, bacteria and animal life. Porphyrins are integral to photosynthesis, oxygen transport in the blood and they play a significant role in the functioning of the brain and nervous system (vitamin B12). The name porphyrin originates from the Greek word porphura which stands for red/purple. Some prominent members of the tetrapyrrolic family are shown in Figure 1.1.[3] The porphyrin skeleton, which was first proposed by Küster in 1912,[4] consists of four pyrrole units which are linked *via* methine bridges. Fischer provided the synthetic proof of this proposed structure in 1929 when he succeeded in synthesising heme for the first time.[5] This seminal work led to a strong interest and a significant body of follow-up research on these versatile molecules.

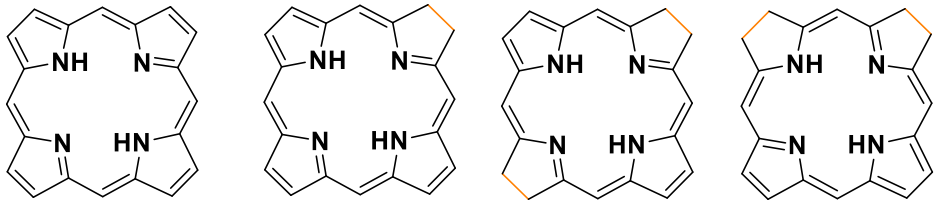

Figure 1.1. Some members of the tetrapyrrole family**.**

1.1.1 Structure of porphyrins

Porphyrins are derivatives of the unsubstituted parent molecule porphine (Fig. 1.1). The molecule consists of four pyrrole rings resulting in two pyrrolenine and two pyrrole units connected through methine bridges (Fig. 1.2). The macrocycle consists of 22 electons with only 18 being part of the aromatic system, therefore obeying Hückel's rule for aromaticity (4n+2).[6] This is due to the 4π electrons not involved in the aromatic system of the porphyrin possessing more of a double bond character. As mentioned before, this structure was first postulated by W. Küster in 1912.[4] Later on, it was shown that the trans-NH-tautomer was the most stable form, as shown in Figure 1.2. Three different types of carbon atoms can be

found in a porphyrin macrocycle. There are α and β carbons present on the pyrrole ring as well as the meso-carbons next to the methine bridges (Fig. 1.2). α-carbon atoms can be found at position 1,4,6,9,11,14,16 and 19 whereas β-carbons are present at position 2, 3, 7, 8, 12, 13, 17, and 18. Only four meso-carbons exist on a porphyrin macrocycle, namely the carbon atoms at position 5, 10, 15 and 20 (Fig. 1.2).

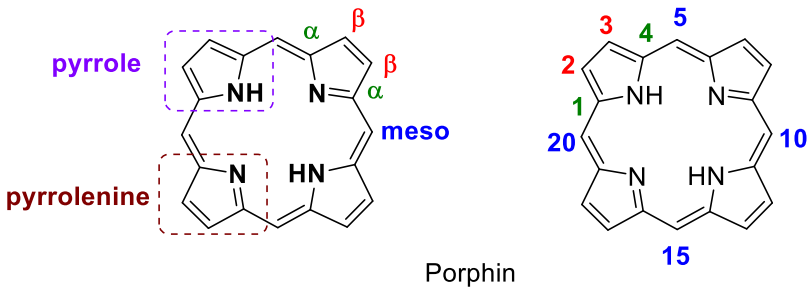

Figure 1.2. Different parts and Nomenclature of the porphyrin core.

Meso and β- carbons in particular can undergo a plethora of reactions, such as substitution, addition, nitration, acylation, etc.[7] Furthermore, the properties of this molecule can be changed and fine-tuned through modifications of the porphyrin core; for example, through variation of the protons on the inner nitrogen atoms. The dianionic or dicationic porphyrin species can be formed through the loss and gain of protons. Additionally, the inner porphyrin core can be modified through metallation.[8] A large variety of metal ions can be inserted into the porphyrin more or less readily, depending on the size of the metal. The type of metal, which is inserted into the porphyrin, also plays a role when it comes to further functionalisation reactions. A divalent ion, such as Zn^{2+} or Ni^{2+}, helps to activate the meso-position of the porphyrins towards nucleophilic attacks, while electrophilic metals can deactivate the meso-position and activate the β-positions thereafter. This versatility, together with their optical properties and their chemical stability makes them ideal candidates for a wide range of applications such as optoelectronics, medical applications such as PDT or surface chemistry,[9]

1.2 Synthesis of meso-substituted porphyrins

Meso-substituted porphyrins represent the synthetically most accessible class of tetrapyrroles. Even though they cannot be used as direct counterparts to naturally occurring porphyrins, they still play an integral role in a wide range of applications such as material science, synthetic methods development, and fundamental studies. Various syntheses now exist and enable chemists to attach different substituents to the porphyrin core in a defined manner.[7] This allows to design porphyrins specifically targeted for certain applications. In practical terms, their synthesis often necessitates only the use of aldehydes for the C_m part in pyrrole condensation reactions, which gives a broad scope to quickly generate systems with alkyl, aryl, heterocyclic, functional and organometallic groups, or even other porphyrins. This has made meso-substituted porphyrins the standard workhorses of many contemporary studies.

Fundamentally, the synthesis of porphyrins comes down to symmetry considerations (Fig. 1.3). If the target structure **1.1** is symmetrical then a simple *tetra*merization of the pyrrole precursor(s) will suffice, if not, more elaborate syntheses and starting materials must be employed. The former typically involves the condensation of either four α-substituted pyrroles or (β-substituted) pyrroles with an aldehyde carrying the meso-substituent (**1.2**). In the latter case, one can employ various approaches, be it the 'total' synthesis of a linear tetrapyrrole **1.3** followed by cyclisation, the reaction of smaller building blocks, *e.g.*, a tripyrrane and a pyrrole [3+1] or of two dipyrrins [2+2] (**1.4**). Furthermore, partial synthesis using preformed porphyrins **1.5**, or even 'mixed' condensations of different pyrroles/aldehydes can be considered. The reaction preferentially gives the desired regioisomer, or the stamina of the chemist is sufficient for the required chromatographic purification.

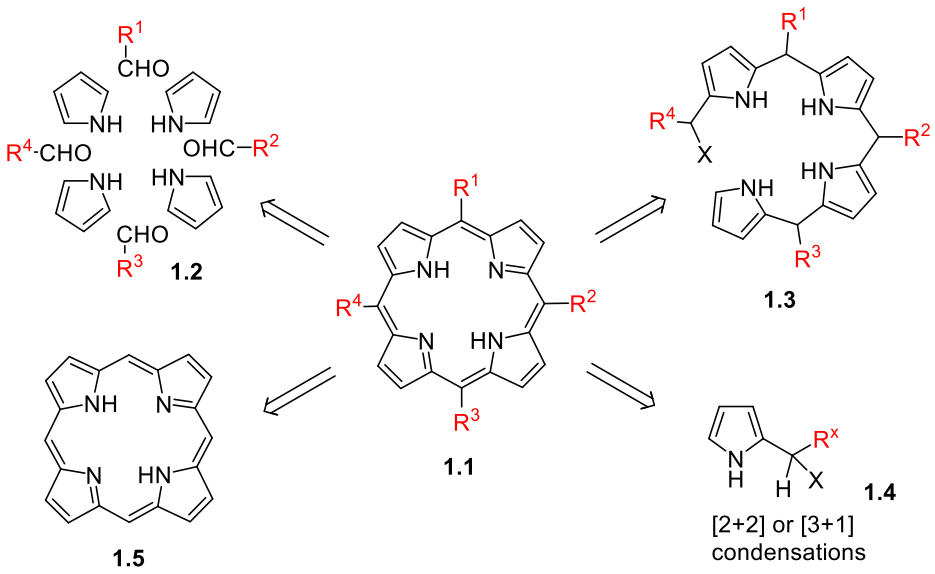

Figure 1.3. Retrosynthetic analysis of porphyrin syntheses. Similar symmetry considerations apply for meso- and β-substituted porphyrins.

1.2.1 Synthesis of A_4-porphyrins

The most easily prepared porphyrins are the symmetric A_4-type systems. Here, 5,10,15,20-tetraphenylporphyrin (H_2TPP) stands out as the prime example which we will encounter frequently. Its synthesis was first investigated by Rothemund in 1935. He reacted a range of aliphatic and aromatic aldehydes with pyrrole in MeOH and obtained the respective porphyrins in low yields, typically not exceeding 5%.[10] The reactions were performed in sealed tubes, using high concentrations in the absence of an oxidant and required high reaction temperatures. In addition, significant amounts of the corresponding chlorin were isolated as side product, requiring follow-up oxidation. Subsequent modifications included the use of other solvents or metal salts, which benefits reactions with some, but not all, aldehydes and results in the formation of metal complexes.

Adler-Longo method: A more general method, which is still frequently used, was developed by Adler, Longo and co-workers in 1964.[11] Initially developed for H_2TPP, they used benzaldehyde, pyrrole and an acidic solvent with heating to reflux under atmospheric conditions. Optimised conditions employing propionic acid and higher concentrations gave improved yields. However, the porphyrin is still contaminated with the corresponding chlorin, similar to the Rothemund method. Contemporary practices of this *Adler-Longo method* involve heating of equimolar amounts of aldehyde and pyrrole in propionic acid for 30 minutes in air and filtering off the porphyrin after cooling. The chlorin component is often oxidised in the crude reaction mixture with DDQ or chloranil prior to purification and

porphyrins such as H_2TPP can routinely be prepared in >20% yield.[12] Use of other acids, *e.g.*, acetic acid can increase the yields to 35-40%, but propionic acid is preferred as it typically allows crystallisation of the products directly from the reaction mixture.[13] The reaction mechanism was investigated in detail by Dolphin and he proposed the porphyrinogen, *i.e.* the cyclic nonaromatic tetrapyrrole, as the key intermediate in aldehyde-pyrrole condensation reactions. Using UV/vis spectroscopy he suggested sequential oxidations from the porphyrinogen *via* porphodimethene to the fully aromatised porphyrin. This was confirmed by isolation of the porphyrinogen and subsequent (photo)chemical oxidation to the porphyrin.[14]

The detailed reaction mechanism for the synthesis of H_2TPP is shown in Figure 1.4. In the first step, the oxygen of the benzaldehyde is protonated by the acid and the pyrrole attacks the carbonyl group. After deprotonation of the substituted α-position, the aromaticity in the pyrrole is restored. Protonation of the hydroxyl group is then followed by loss of water and formation of a carbocation. This carbocation is then attacked by another pyrrole molecule and the previous steps are repeated to form the porphyrinogen **1.7** after the fourth attack of a pyrrole molecule. The preference of cyclotetramerisation over simple polymerisation can be explained on the basis of steric considerations. In particular for β-substituted pyrroles (see below), the steric hindrance (see inset in Fig. 1.4) between the residues is minimised in a cyclic arrangement as in **1.6**, which also presents the reactive partners for cyclotetramerisation in the close vicinity.[15] The porphyrinogen is then subsequently oxidised to the porphomethene **1.8** and then *via* the porphodimethene **1.9** stepwise to the porphyrin **1.10**.

This method opened the pathway to the widespread use of meso-substituted porphyrins with various substituents, ranging from simple alkyl residues over *p*-, *m*- or *o*-substituted aryl units to more complex systems such as the ‘picket fence’ porphyrins or capped, strapped, cofacial and other superstructured systems.[13]

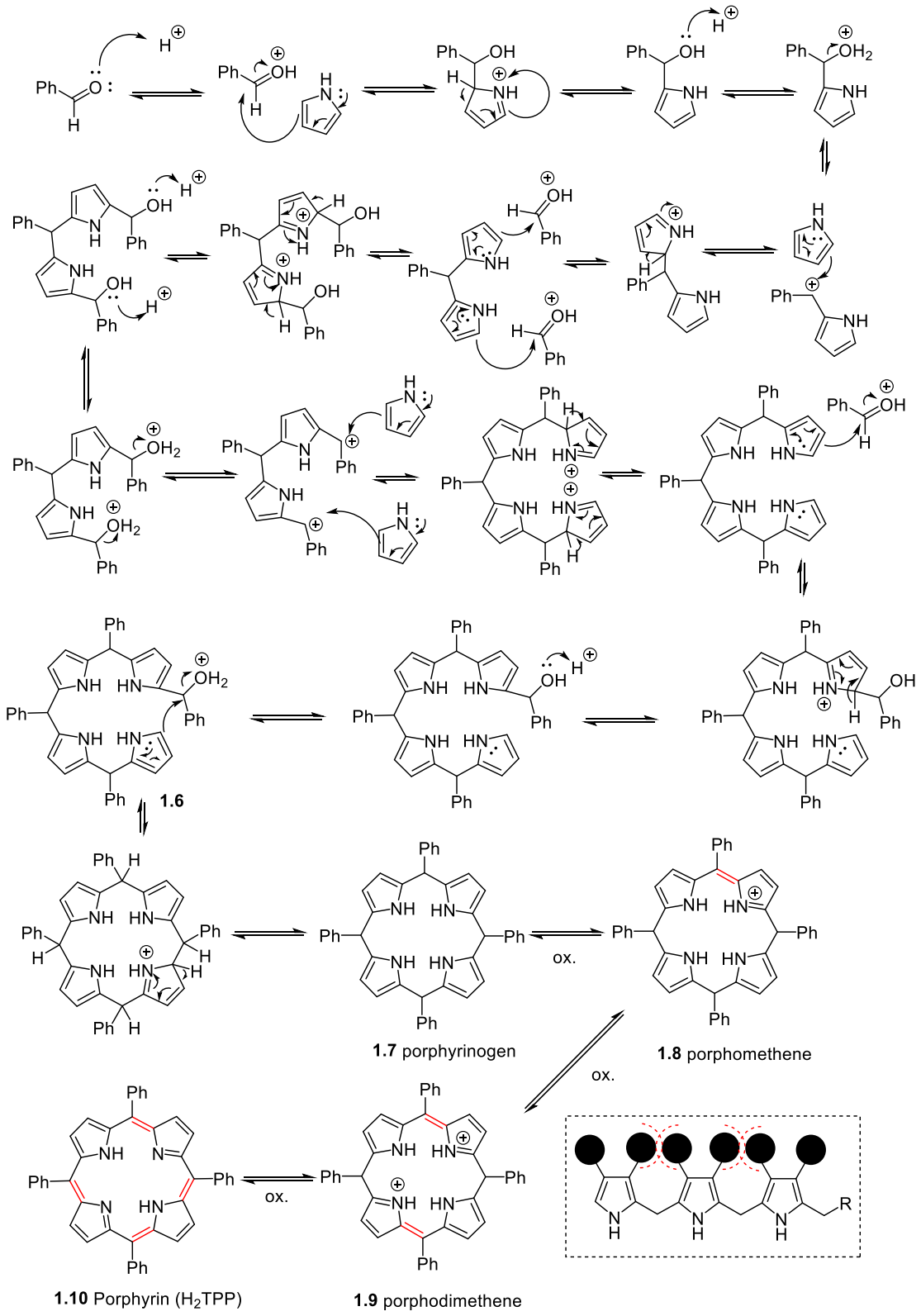

Figure 1.4. Reaction mechanism for the formation of 5,10,15,20-tetraphenylporphyrin (H_2TPP).

The experimental procedure has seen many modifications over the years, primarily with regard to solvent and acid-catalysis. For example, H_2TPP **1.10** can be prepared using DMF and $AlCl_3$ as a catalyst in 30% yield in two hours without

formation of the chlorin side product. Similar to the synthesis for β-substituted porphyrins, where the C_m-carbon is often brought into the reaction as a pyrrole α-residue, pyrrole-carbinols can be used under Adler-Longo conditions for both alkyl- and arylporphyrin synthesis in low to moderate yields.[16]

Lindsey method: The most general and versatile development in this area stems from Lindsey's persistent efforts to develop mild and general conditions for the synthesis of porphyrins.[13, 17] He considered that both pyrrole and benzaldehyde are reactive molecules, which should be able to react under milder conditions. Aryl aldehydes tend to react with nucleophiles and an acid catalyst at room temperature. Therefore, this should also work in pyrrole-aldehyde condensations, as pyrrole is very reactive towards S_EAr. Additionally, the biosynthesis of natural porphyrins proceeds *via* porphyrinogen intermediates with subsequent oxidation to the porphyrin.

Ultimately, these considerations resulted in the development of the 'Lindsey method', a two-step, one-flask condensation method for meso-substituted porphyrins which, is now a cornerstone of the canon of porphyrin chemistry.[18] It consists of the reaction of pyrrole and an aldehyde in DCM with trifluoroacetic acid (TFA) or BF_3-etherate at room temperature. The final porphyrin is formed through oxidation of the initially formed porphyrinogen in a second step. For example, H_2TPP can be synthesised in 35-40% yield with this method. The reaction is very sensitive to the concentration of the reactants and the acid catalyst. Typically, a higher concentration of TFA is necessary compared to BF_3-etherate. DDQ is widely used to oxidise porphyrins and formally three DDQ molecules are necessary to oxidise one porphyrinogen, *i.e.* remove six hydrogen atoms, to a porphyrin. Due to the cost of DDQ, large-scale syntheses often employ the (less effective) *p*-chloranil as an oxidant. This methodology works very well for a broad range of aldehydes due to the mild conditions at room temperature for both condensation and oxidation, and its versatility has made this strategy the standard method for C_m-substituted porphyrins.[13] It is compatible with various benzaldehydes, including sterically hindered ones, organometallic units, protected carbohydrates, and many more; and yields of up to 50% can be achieved.

The reaction is critically depended on all ingredients and may require adaptation for a specific target material. For example, 2,6-disubstituted aryl aldehydes with electron-donating groups react better with BF_3-etherate and ethanol as co-catalyst. In fact, mesitylaldehyde will not react without the presence of the latter. The

concentration of the acid catalyst is crucial as well and needs to balance the maximisation of yield of porphyrinogen with minimisation of any side products. The latter comprises dipyrromethanes and pyrrole-red, among others, and are formed at high acid concentrations.

Comparison: At this stage, the Rothemund method has no real benefit over other methods. The Adler-Longo method is suitable for condensations with relatively stable aldehydes that can survive boiling propionic acid and for the synthesis of porphyrins on a preparative scale if the product crystallises easily. However, it is not the method of choice for 2,6-disubstituted aryl and aliphatic aldehydes. The Lindsey method uses the mildest reaction conditions of all three methods and can be used with a broad range of aldehydes. It usually gives superior yields compared to the other two methods. Furthermore, it works very well for sterically hindered, aliphatic, and sensitive aldehydes. A drawback is the more involved work-up, which normally includes column chromatography.

1.2.2 Unsymmetric porphyrins with different meso-substituents

The synthesis of porphyrins with a defined number of either identical meso-substituents (A_x-porphyrins) or different ones (*e.g.*, ABCD-porphyrins **1.14**) requires the skills to introduce the meso-substituents in a controlled manner. Simple pyrrole condensation reactions will yield mixtures and thus, this area mainly relies on reactions using building blocks with more than one pyrrole unit (Fig. 1.5). A typical example is the use of dipyrromethanes **1.11**, *i.e.* dipyrrins with two pyrroles. Many of the methods described in the following sections were initially developed for β-substituted porphyrins and trace their lineage to Fischer's efforts.[19] Advancements in this area for meso-substituted porphyrins came late, primarily after 1990 when interest in β-substituted porphyrins waned.[13]

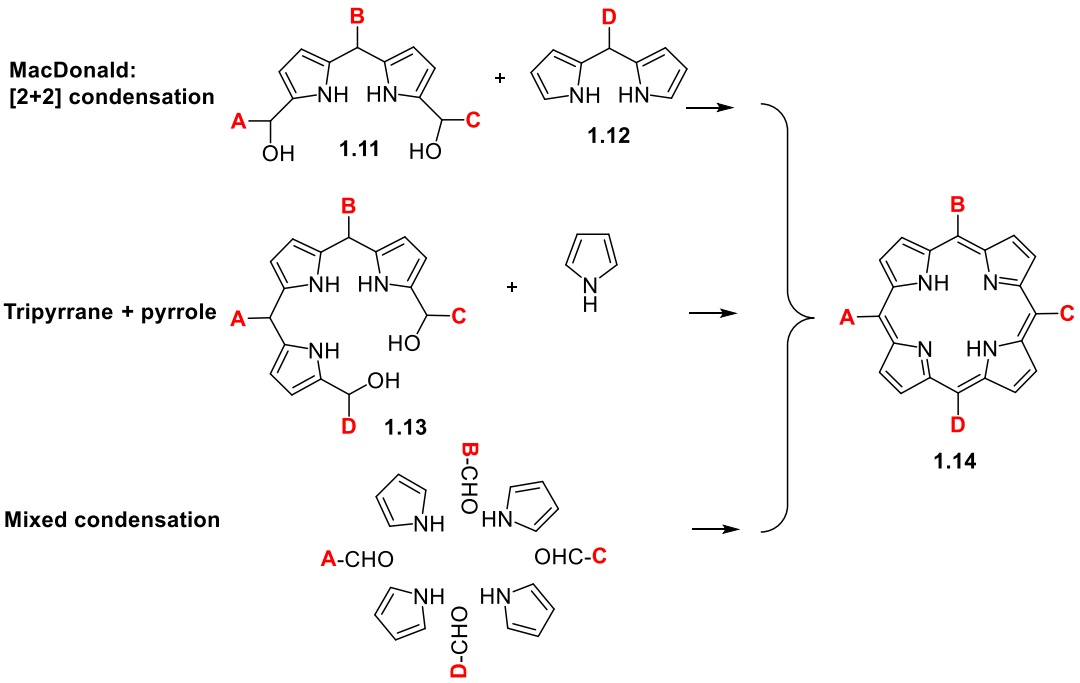

Figure 1.5. Different condensation methodologies towards the synthesis of ABCD porphyrins.

1.2.2.1 ABCD-porphyrins via condensation reactions

MacDonald–type [3+1] and [2+2] routes towards ABCD-porphyrins: A typical synthesis of ABCD-type systems can be achieved through the use of 1,9-diacyldipyrromethanes and goes back to concepts developed in the groundbreaking work of MacDonald and co-workers for β-substituted porphyrins.[20] This compound is reduced with $NaBH_4$ to the dipyrromethane-dicarbinol **1.11**, which is followed by the condensation with a dipyrromethane **1.12** and subsequent oxidation (Fig. 1.5). Scrambling, *i.e.* the cleavage of preformed pyrrole systems followed by recondensation in a different arrangement, is a troublesome side reaction of many porphyrin condensations, but this could be remedied in many cases giving access to various ABCD-porphyrins.[17]

Condensation with dipyrromethane-carbinols can be catalysed by Lewis acids, which are ineffective in the condensation of aldehydes and pyrrole/dipyrromethanes. But caution must be taken with the order of substituents when applying this to the condensation of dipyrromethane-dicarbinol and dipyrromethane. Substituents on the meso-position of the dipyrromethane-dicarbinol should be stable during the acylation and ketone reduction steps, while the substituent on the dipyrromethane only has to be stable during the milder condensation and oxidation steps. Furthermore, scrambling can be addressed in

part by the choice of substituents. Thus, alkyl groups or an absence of substituents on the carbinol give the lowest amount of scrambling, while basic heterocycles result in low yields or scrambled products.[17] Even though optimisations were investigated for this method, many aspects of the optimal conditions are still the original ones introduced by MacDonald. Yields of up to 60% can be achieved and only very little by-products are formed.[21] Many variants of this strategy have been employed, for example, the acid-catalysed condensation of functionalised tripyrranes **1.13** with pyrrole (Fig. 1.5).

Mixed pyrrole condensation: As seen above, pyrrole condensation reactions are a technically simple approach to porphyrins. Hence, pyrrole is often employed in mixed condensation reactions with different aldehydes. While this method looks deceptively simple, it has major drawbacks in practical terms for unsymmetrical porphyrins. Mixed condensations tend to yield a mix of various porphyrins with different degrees of substitution, which are often very hard or even impossible to separate. For example, reaction with just two different aldehydes already yields a mixture of six different porphyrins and may serve to illustrate the pitfalls of this approach (Fig. 1.6). The product mixture includes the two A_4- and B_4-porphyrins (**1.15** and **1.20**, respectively), as well as the A_3B- (**1.16**), 5,10-A_2B_2- (**1.17** 'cis'), 5,15-A_2B_2- (**1.18** 'trans') andAB_3-type (**1.19**) porphyrins. Naturally, separation of this mixture may require elaborate chromatography depending on factors such as the polarity of the two meso-substituents.[22]

Statistically, the porphyrin formation follows a binomial distribution as shown in Fig. 1.6 for a 1:1 ratio. The ratio of the expected porphyrins can be tuned by varying the ratio of aldehydes used. For example, the A_3B porphyrin **1.16** is often the desired compound in mixed condensations and can be maximized with a ratio of 3:1 of aldehyde A and B to give 31.64% A_4-, 42.19% A_3B-, 14.06% 5,10-A_2B_2-, 7.03% 5,15-A_2B_2-, 4.69% AB_3-, and 0.39% B_4-porphyrin.

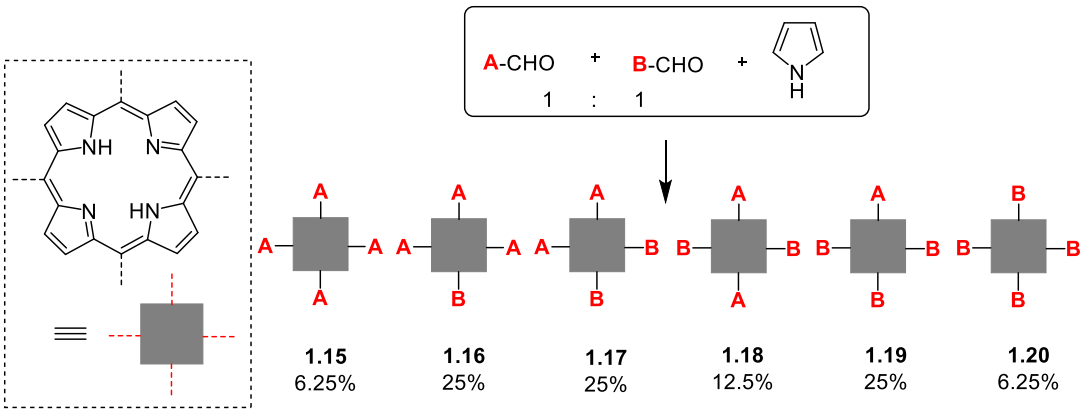

Figure 1.6. Mixed condensation of two aldehydes with pyrrole.

However, these yields are only theoretical and the actual isolated yield depends on the reactivity of the aldehydes as well as on the ease of separation of the different porphyrins. In reality, isolated yields for A_3B-porphyrin *via* this route tend to be around 5% compared to an overall porphyrin yield of 20%. In special circumstances, the desired porphyrin can be obtained in high yield due to kinetic control, but this is not a general case. Acid-labile groups tend to cause problems as does the use of hindered groups, which can result in the quantitative formation of porphodimethenes.[13, 17]

1.2.2.2 'trans'-5,15-A_2B_2-porphyrins

Dipyrromethane and aldehyde condensation route: 5,15-Disubstituted A_2-porphyrins are very useful for various applications and represent standard starting materials for many contemporary uses of porphyrins. Mixed aldehyde condensation gives access to both the 5,15- and 5,10-systems but separation is often very difficult due to the frequently similar polarities of the products. A more strategic and rational synthesis is again a [2+2] condensation (Fig. 1.7). This reaction involves the condensation of dipyrromethane **1.21** and an aldehyde under acid-catalysed conditions and presents one of the easiest and most often used strategies towards A_2B_2- **1.18** (M = 2H) or A_2-porphyrins.

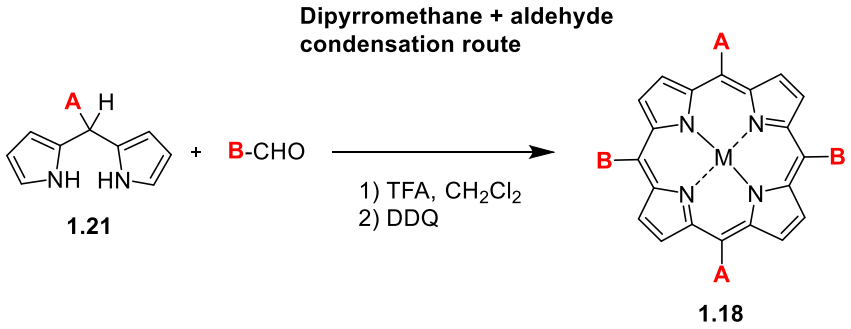

Figure 1.7. Synthesis of '*trans*'-A_2B_2-porphyrins.

Dipyrromethanes are very similar to simple pyrrole in terms of their stability and electrophilicity, although they are prone to oxidation at the C_m bridge to dipyrromethenes or dipyrroketones.[22] The tendency for scrambling during these reactions depends largely on the meso-substituents used. While *ortho*-aryl-substituents result in hardly any scrambling, non-bulky aryl or alkyl groups result in a mixture of porphyrins.[17] A_2- or A_2B_2-porphyrins can be synthesised when an α-free dipyrromethane is used with aldehydes. Many of the initial experiments utilised β-substituted dipyrromethanes, as most known procedures for the synthesis of dipyrromethanes were established in the context of studies on naturally occurring porphyrins.[19] Today, β-unsubstituted dipyrromethanes are readily available and give strategic access to '*trans*' $A_2(B_2)$-porphyrins. The reaction is suitable for a wide range of aldehydes and can normally be performed under standard conditions. Sometimes exchange reactions occur, resulting in '*cis*'-substituted porphyrins **1.17**. In general, this happens far less with sterically hindered dipyrromethanes (*e.g.*, 5-mesityldipyrromethane) and is more pronounced for less hindered systems such as 5-phenyldipyrromethane.[22]

1.2.2.3 'trans'-5,15-A_2-porphyrins

The synthesis of A_2-5,15-disubstituted porphyrins, formally a sub-group of the A_2B_2-porphyrins **1.18**, is well established and they are some of the most widely used starting materials in contemporary porphyrin chemistry. They allow a facile entry to strapped porphyrins, polymers and, *via* functionalisation of the unsubstituted meso-positions, give rise to more unsymmetrical A_2BC-type systems. Their synthesis is easy and requires only the reaction of unsubstituted dipyrromethane with various aldehydes under acid-catalysed conditions. There is

also significant scope to utilise other synthetic approaches. The various approaches are exemplified in Figure 1.8 for 5,15-diphenylporphyrin **1.22**.[22]

A straightforward method uses one equivalent of unsubstituted dipyrromethane **1.26** with one equivalent of benzaldehyde in DCM and an acid catalyst at room temperature. 5,15-A_2-porphyrins are obtained in good yields and can easily be isolated *via* column chromatography. The [2+2] methodology is widely used with yields typically in the 20-30% range and allows better control of the C_m-substituents compared to mixed condensations. It is equally amenable to the synthesis of 5,15-dialkylporphyrins. For example, 5,15-dihexylporphyrin has been reported in a yield of 27% with a work-up consisting of just filtration of the compound through silica gel with DCM and recrystallization.[23]

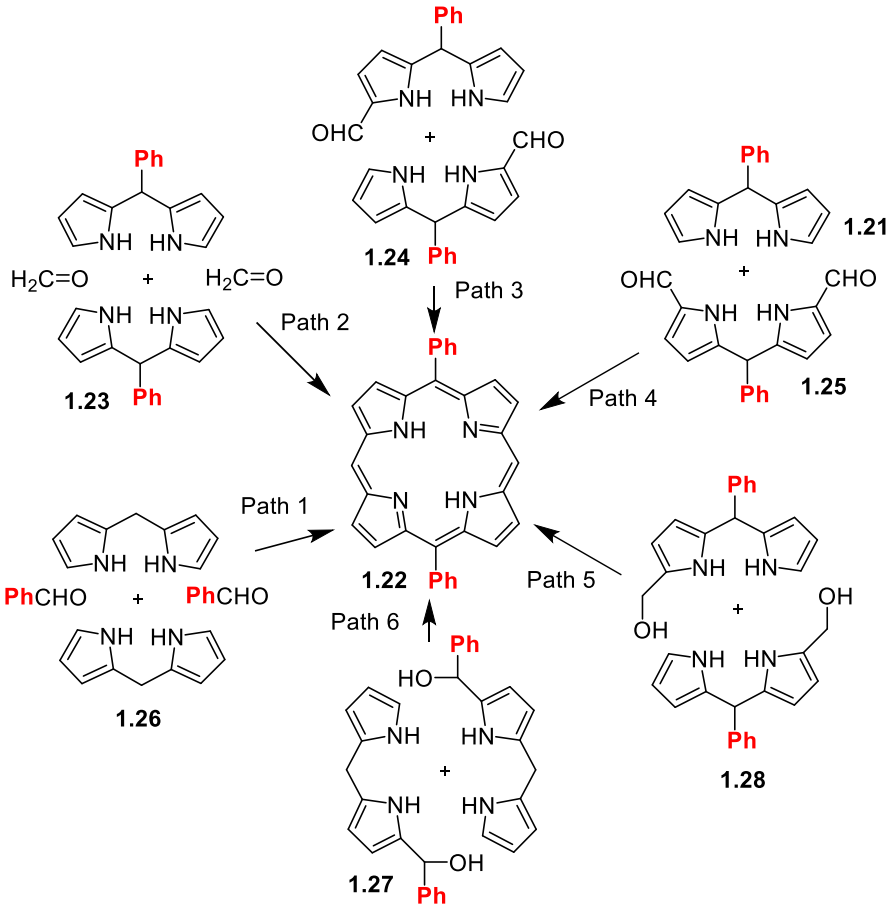

Figure 1.8. Synthesis of 5,15-A_2-porphyrins illustrated for 5,15-diphenylporphyrin **1.22**.

5,15-Diphenylporphyrin was first described by Treibs and Häberle in 1968[24] and the requirement for two different C_m-positions allows the use of several different [2+2] approaches. One pathway is the aforementioned condensation of

unsubstituted dipyrromethane **1.26** with benzaldehyde using TFA as catalyst (Fig. 1.8 Path 1). Oxidation of the condensation products with chloranil gave yields of about 25-40%. Another option is the condensation of 5-phenyldipyrromethane **1.23** with formaldehyde (Fig. 1.8, Path 2). Initially developed by Baldwin *et al.* for β-alkyl-substituted diphenylporphyrins, this method used trichloroacetic acid as catalyst and oxidation with air.[25] The application of this procedure to diphenylporphyrins by Brückner *et al.* gave yields of about 30%.[26] Tetraphenylporphyrin was obtained as a side product from acid-catalysed scrambling, but only in yields of <1%.

In other pathways, the dipyrrolic compound with the linking carbon in the condensation carries either a hydroxymethyl substituent (**1.27**, **1.28**, Path 5, 6) or a formyl group (**1.24**, **1.25**, Path 3, 4). However, these methods require more synthetic steps to form the dipyrromethene species (Path 4-6), as well as reduction of the carbonyl group to form the sensitive hydroxymethyl substituents (Path 5, 6). Path 4 represents a classic MacDonald-type approach, whereas Path 3 and 5 are other options to prepare 5,15-diphenylporphyrin *via* acid-catalysed self-condensation.[22]

1.2.2.4 A- and 5,10-A_2-porphyrins

Even though many different methods exist today to synthesise nearly any meso-substituted porphyrin, some remain harder to obtain than others. One example is the meso-monosubstituted A-porphyrin **1.29**. Even though this type is often mentioned in publications, it is mostly formed as a side product. On the other hand, less is often more, as such systems represent a superior starting material for the strategic synthesis of unsymmetric porphyrins *via* stepwise functionalisation. One possible synthesis would be the condensation of bilane with an aldehyde. Yet, due to their instability, bilanes are hard to synthesise and handle.[27]

A simpler approach was designed by Wiehe *et al.* which utilised formylpyrrole **1.30**, an “A”-aldehyde and dipyrromethane **1.26** (Fig. 1.9).[28] Herein, a pyrrole aldehyde is condensed with dipyrromethane and an aldehyde under acid-catalysed conditions. The so-called [2+1+1] approach is straightforward, tolerates a broad range of different functional (A) groups and gives yields between 2-15%. Additional products are formed, as in other ‘mixed-condensations’, notably the disubstituted porphyrins from scrambling. However, in terms of yields, the

electronic properties of the aldehydes are often less significant than the solubility of the products. In this case, the disubstituted porphyrin is by far less soluble than the monosubstituted compound, which makes separation significantly easier. Sometimes the A-porphyrin can be isolated as the sole product (*e.g.*, A = 4-nitrophenyl, 4-methoxyphenyl, *tert*-butyl) allowing for large-scale synthesis.[13]

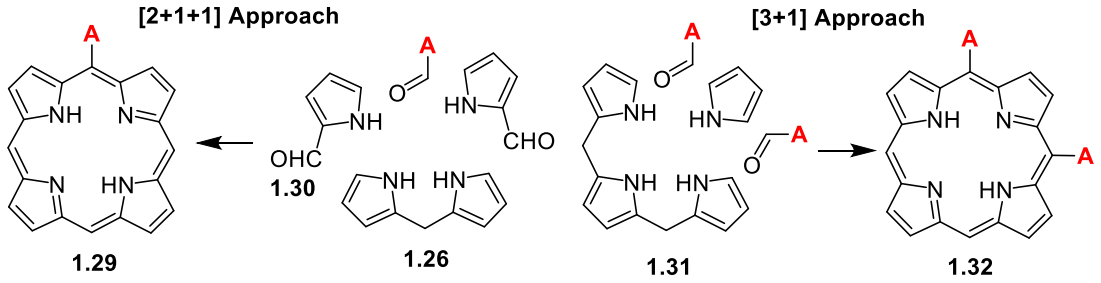

Figure 1.9. Synthesis of A- and '*cis*'-5,10-A_2-porphyrins.

A similar situation existed for 5,10-disubstituted porphyrins **1.32**, where two neighbouring meso-residues carry substituents. For 5,10-diphenylporphyrin, i.e. the regioisomer of **1.22**, Briñas and Brückner reported a logical 'total synthesis' involving the condensation of dicarbinol-dipyrromethane with dipyrromethane.[29] More general are [3+1] condensation reactions using tripyrrane **1.31** together with an aldehyde and acid as catalyst. Tripyrrane can be obtained *via* condensation of 2,5-bis(hydroxymethyl)pyrrole and pyrrole, with yields of up to 12%. Similar to the synthesis of monosubstituted porphyrins, here the A-porphyrin **1.29** is formed as a side product but can be easily separated from the target compound. This synthesis is amenable to aromatic and aliphatic aldehydes.[30]

1.3 Step-wise functionalisation of meso-substituted porphyrins

Nowadays, a lot of applications in optics, material science and photomedicine require unsymmetrically substituted compounds such as **1.33** (Fig. 1.10).[31] Thus, interest has shifted towards the use of mixed meso-substituted porphyrins resulting in less symmetric systems. This trend leads to extensive research in the development of new synthetic routes and functionalisation methods to make this desired class of porphyrins more easily available.

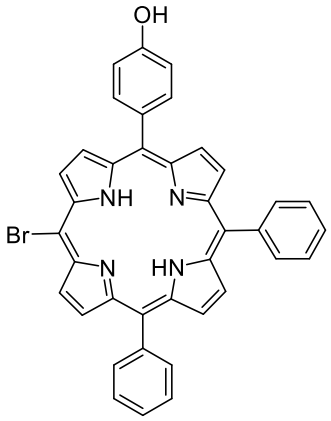

1.33

Figure 1.10. Example of an unsymmetrically substituted porphyrin.

While total synthesis or mixed condensation are methods which have been known for a long time, they often suffer from practical pitfalls. Therefore, the investigation into more versatile and controlled methods was inevitable. This can be achieved through a plethora of functional group conversions which range from nucleophilic substitution reactions to palladium cross-coupling reactions and some of the more important ones will be discussed here.

1.3.1 Reactivity of porphyrins

The reactivity of porphyrins is governed by many factors, ranging from electronic and steric effects to more special features such as macrocycle conformation, coordination state in complexes, aggregation and more.[32] Much of the fundamental chemistry can be explained by consideration of the electron density distribution in the macrocycle and the effect exerted thereon by core and peripheral substituents and other contributors (Fig.1.11). The C_m are generally more reactive in reactions with nucleophiles, radicals or electrophiles, as compared to the C_b (**1.34**). This is counteracted to some extent by sterically hindered residues at neighbouring β-positions (**1.35**), which may shield the meso-position against attack (and *vice versa* for β). The electronic character of the macrocycle is most easily manipulated by metallation (M, **1.34**). Metal complexes with Mg(II), Zn(II), Cd(II) (d^0, d^{10}) have increased electron density and lower oxidation potential. On the other hand, Sn(IV) or Fe(III) (d^1–d^5) complexes have lower electron densities and show high reactivity at the β-positions with nucleophiles. The former complexes are relatively labile towards acid and other metals are often difficult to remove from the porphyrin core. Thus, Ni(II) and Cu(II)

(d^6–d^9) are often the compromise of choice in synthetic reactions, while Zn(II) is preferred over Mg(II) in chlorophyll-related studies. Naturally, the π-system can be modulated *via* protonation or deprotonation of free base systems. However, many irreversible, secondary reactions with acids and bases may occur under these conditions.

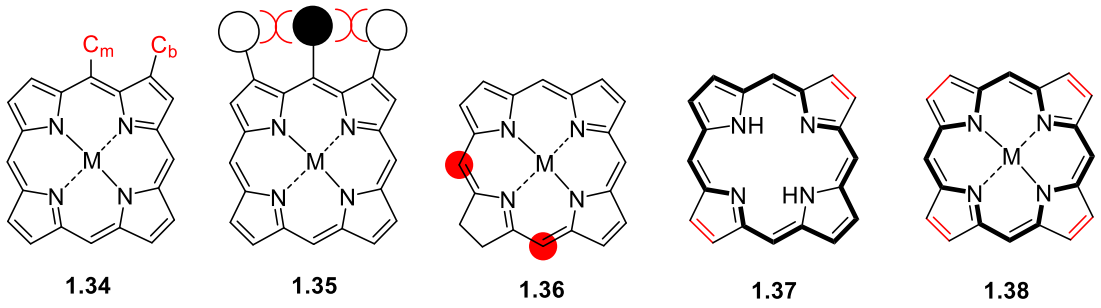

1.34 1.35 1.36 1.37 1.38

Figure 1.11. Reactivity considerations and aromatic delocalization pathways in porphyrins.

Various aspects of porphyrin reactivity can also be illustrated by analysis of the π-delocalisation pathways (Fig. 1.11). Only 18 of the 22 π-electrons are involved in the aromatic system [Hückel 4n+2 rule, n=4] and hence, in free base porphyrins, the β-β'-bonds are not equivalent. The two not involved in the delocalisation pathway (**1.37**) have double bond character and will undergo standard addition reactions. This also explains the easy formation of chlorins (2,3-dihydroporphyrins) and bacteriochlorins (2,3,12,13-tetrahydroporphyrins), which show higher reactivity next to the reduced pyrrole ring (**1.36**). This gives rise to different N–H tautomers in substituted (hydro)porphyrins with the N21, N23-tautomer (shown in **1.37**) being considered thermodynamically more stable. In metalloporphyrins and dications or tetraanions the various possible tautomeric forms are equivalent (**1.38**) and thus there is no difference in β-β' reactivity of the pyrrole units in symmetric porphyrins. Consideration of the delocalisation pathway in tautomers also provides a rationale for directive effects in substituted porphyrins; although this is sometimes complicated by steric and macrocycle conformation effects. Reactions at the α-position are rare; they are only found during oxygenation or rearrangement reactions.

1.3.2 Electrophilic reactions

Historically, electrophilic substitution and addition reactions provided the main entry into functionalised porphyrins. Taking into account the aforementioned

influence of central metals and steric effects, substitution reactions can specifically target either the meso- or β-positions. Porphyrins readily undergo deuteration at the meso-positions, can be halogenated, nitrated, and participate in Friedel-Crafts and Vilsmeier reactions. Other examples include cyanation, mercuration, methylation, and more.[32b]

1.3.2.1 Vilsmeier formylation

Vilsmeier formylation is a classic reaction for the introduction of C-substituents into porphyrins.[33] Developed by Inhoffen,[34] the reaction is typically performed with Ni(II) or Cu(II) complexes (stable under acidic conditions) and uses DMF/$POCl_3$ for generation of the Vilsmeier complex, followed by base hydrolysis. Porphyrin or β-substituted systems (**1.39**) will undergo meso-monoformylation to **1.40**, while prolonged reaction with excess reagent will result in diformylation to **1.41** (Fig. 1.12). The reaction of meso-substituted porphyrins such as Ni(II)TPP will result in 2-formylporphyrins **1.42**. Formylporphyrins have been used widely for transformations, although most derivatives are today more easily prepared *via* organometallic reactions.

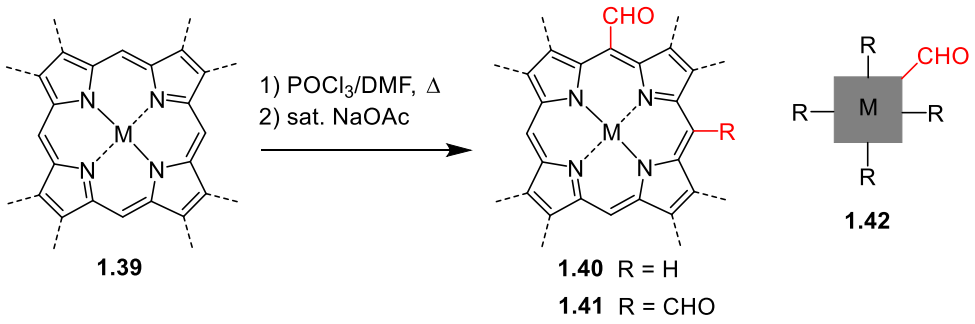

Figure 1.12. Vilsmeier formylation of porphyrins.

1.3.2.2 Halogenation

The standard halogens F, Cl, Br, and I can all be introduced at the meso- and/or β-positions. Selectivity and regiochemistry are primarily controlled by steric considerations, *e.g.*, iodination is more likely at unhindered β-positions, as is bromination; while fluorination and chlorination preferentially occur at the meso-positions. Over the years the whole cornucopia of possible halogenation reagents has been used with varying success,[15, 35] even in reactions with unsubstituted porphyrin **1.5**.[36] β-Substituted porphyrins can be meso-halogenated (X = F, Cl,

Br), although the degree of halogenation is difficult to control and radical conditions might promote reactions in alkyl side chains.[37]

β-Perhalogenated porphyrins **1.44** are easily prepared for X = Cl and Br *via* reaction of 5,10,5,20-tetraarylporphyrins **1.43** with NCS and NBS (Fig.1.13).[38] Bromine can also be used, but will always give perbromination and can degrade free base porphyrins. These highly electron deficient and often nonplanar systems have found wide use as oxidation catalysts.[39] Contemporary methods[38, 40] allow selective β-halogenations giving access to 5,10,15,20-tetraarylporphyrins with 1, 2, 4, 6 and 8 β-halogen atoms, which in turn serve as precursors for porphyrins with mixed substituent types.[41] The key regiochemical consideration is that halogenation is directed to the pyrrole ring opposite one carrying electron-withdrawing substituents (*e.g.*, other halogen atoms or NO_2), thus, in **1.45** X^1 is followed by X^2. β-Fluoroporphyrins are better prepared *via* condensation reactions with fluoropyrroles.[42]

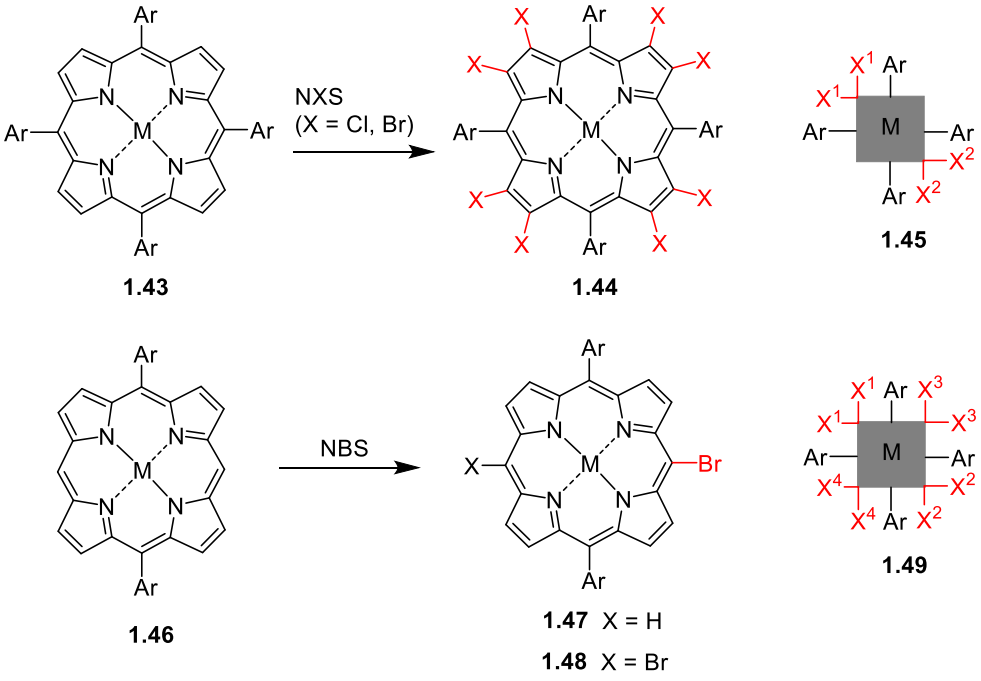

Figure 1.13. Halogenated porphyrins**.**

Halogenated porphyrins are the most important construction materials in contemporary porphyrin chemistry.[7] This relates to their utility in transition metal-catalysed reactions and many current syntheses use 5,15-disubstituted porphyrin **1.46** building blocks. For example, regioselective meso-mono- (**1.47)** or dibromination (**1.48)** is possible, as is meso-monoiodination to **1.49**.[43]

1.3.2.3 Nitration

Similar to other reactions nitration proceeds preferentially at the meso-position. For example, the reaction of octaethylporphyrin (H_2OEP) **1.50** with nitric acid in acetic acid gives the mononitrated product **1.51**, while HNO_3 in sulfuric acid gives the mono- to trinitrated products with disubstitution following the 5,15-pattern (Fig. 1.14).[44] Complete meso-nitration is achieved with $Zn(NO_3)_2$ to yield the metalloporphyrin **1.52**.[45] The nitro group in **1.51** and other porphyrins can be reduced with $SnCl_2$/HCl or $NaBH_4$/Pd/C to the aminoporphyrin.[46] The latter is highly reactive and behaves similar to meso-oxoporphyrins, *i.e.*, in acid it forms phlorins such as **1.53**. β-Nitration of meso-arylporphyrins is possible as well; notably, compounds with one to eight β-nitro groups **1.54** have been prepared using HNO_3/CF_3SO_3H/$(CF_3SO_2)_2O$ mixtures.[47]

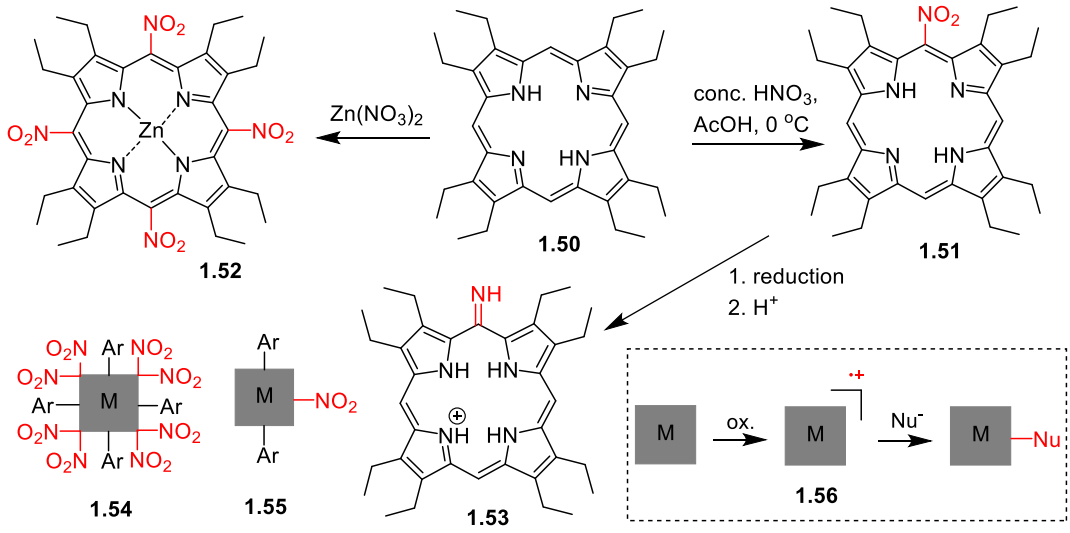

Figure 1.14. Nitration of porphyrins (inset: the reaction of porphyrin π-cation radicals).

Nitroporphyrins can also be prepared using an oxidising agent and nitrite, and this illustrates another fundamental reaction of porphyrins. (Metallo)porphyrins are easily oxidised to π-cation radicals **1.56** and these electrophiles can be trapped with various nucleophiles.[48]

1.3.3 Nucleophilic reactions

Porphyrins are known to undergo a range of nucleophilic substitution reactions, again predominantly at the meso-position. Many possibilities for nucleophilic reactions exist,[15, 49] but they often require activation of the porphyrin system *via* oxidation, appropriate central metals, steric effects, or the presence of electron-withdrawing substituents.[50] In the following, the exemplary and classic case of electron deficient porphyrins and the use of strong nucleophiles such as RLi reagents for nucleophilic aromatic substitution reactions is discussed.

1.3.3.1 C–H activation with organolithium reagents

A more generally applicable method is the reaction of porphyrins with organolithium reagents. This reaction from our laboratory was developed in 1998 by Kalisch and Senge[51] and gave rise to significant follow-up studies.[50, 52] At that time functionalisation on the β-position had been explored more widely, and fewer synthetic methods existed for substitution of the meso-position. S_NAr reactions are often limited to special cases or depend upon activation of the porphyrin core, such as with electron-withdrawing substituents, metals or steric effects, and therefore require synthetic modifications prior to substitution. Thus, while it was perhaps counterintuitive to attack an electron-rich, heteroaromatic system with nucleophiles, surprisingly, 'standard' porphyrins submitted readily to reactions with RLi.

As shown in Fig. 1.15, Ni(II)OEP **1.57** underwent direct meso-substitution with alkyl or aryl residues, without activation of the porphyrin, giving excellent and often quantitative yields. This methodology utilises organolithium reagents to perform a nucleophilic aromatic substitution on the porphyrin core. The reaction gives facile access to a broad spectrum of highly substituted porphyrins with various functional groups (as long as they are tolerated under the conditions used for the preparation of the RLi reagent) without cumbersome multi-step syntheses or mixed-condensation reactions. The reaction is compatible with both free base porphyrins and metal complexes, such as Zn(II), Cu(II), Co(II) and Ni(II). Usually, the trend is that alkyllithium compounds tend to give higher yields with metalloporphyrins, while substitutions with aryllithium reagents work better with free base porphyrins.[53]

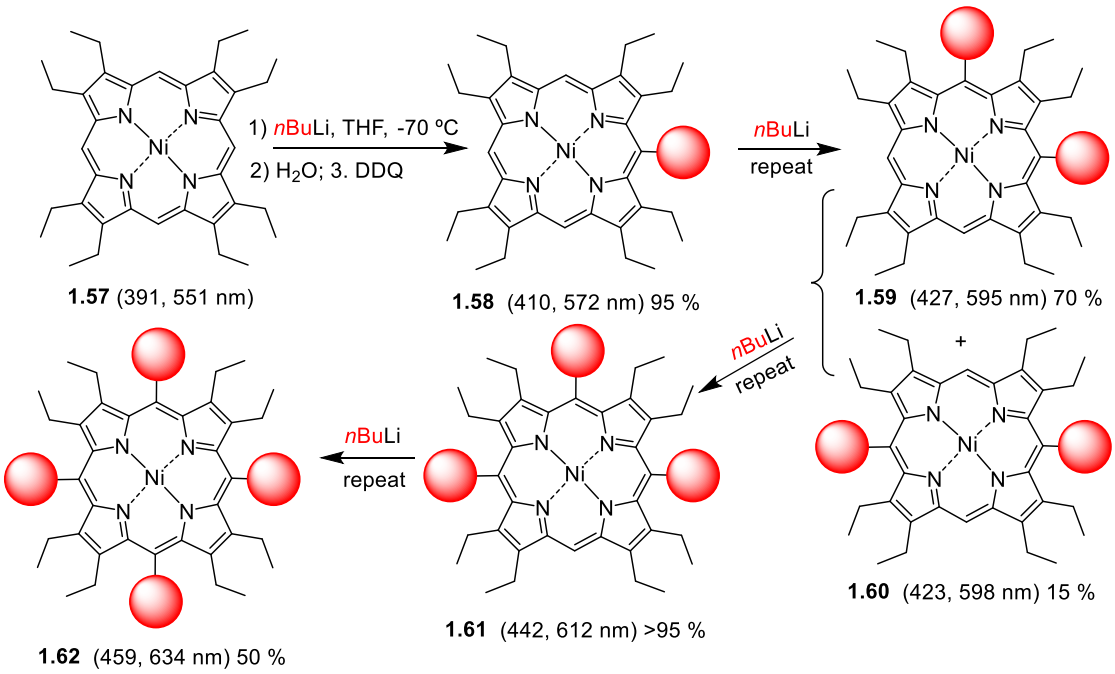

Figure 1.15. Reaction of Ni(II)OEP with *n*BuLi. Numbers in brackets refer to the main absorption maxima in DCM.

The general reaction mechanism follows an addition-oxidation sequence. The nucleophile attacks the meso-position of a porphyrin leading to a Meisenheimer-type complex as an intermediate. In the following steps, this complex is hydrolysed and oxidised to yield the substituted porphyrin. The reaction mechanism can depend on the steric aspects and conformation of the porphyrin, as well as on the steric bulk of the organolithium reagents. Further investigation, using spectroscopic and deuterium labelling studies, showed that the reaction mechanism follows two different pathways, depending on whether either metalloporphyrins or free base porphyrins are being used (Fig. 1.16). The metalloporphyrin forms a porphodimethene anion **1.66** while the free base porphyrin results in a phlorin anion **1.64**.[54] One limitation is that organolithium reagents are not compatible with very reactive substituents. Usually, these reactions are performed at low temperatures between –100 and –40 °C, depending on the starting material and the organolithium reagent used. However, the reaction can be repeated, giving easy and selective access to porphyrins with one (**1.58**), two (**1.59**, **1.60**), three (**1.61**), and four (**1.62**) meso-substituents. Such systems are examples of highly substituted nonplanar porphyrins. The impact of increasing the numbers of meso-substituents and the concomitant increase in the macrocycle nonplanarity is clearly shown in the bathochromic shift of the absorption maxima for the porphyrins shown in Fig. 1.15.

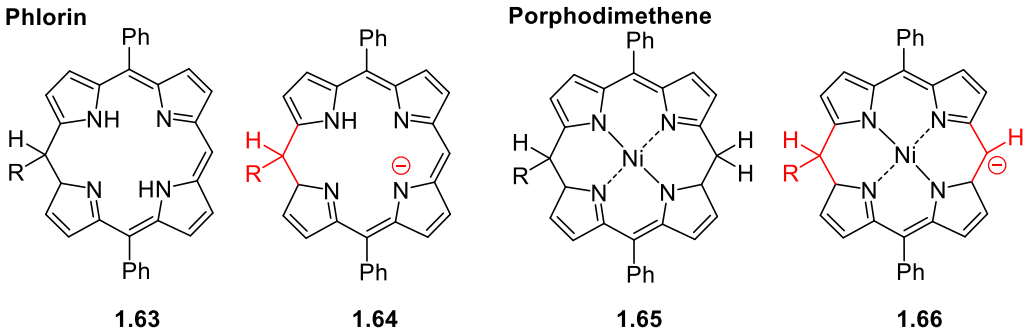

Figure 1.16. Intermediates in the reaction of porphyrins with RLi.

The possibility to introduce four meso-substituents in a step-wise manner also allowed the synthesis of porphyrins with four different C_m-residues, *i.e.*, OEP-type ABCD-porphyrins **1.75** (Fig. 1.17) utilising a sequence as that shown for **1.57→→→→1.62** (Fig. 1.15).[55] Here, the predominant localisation of the negative charge on the meso-carbon opposite to the one attacked results in a regioselective preference of the second substitution in the 10-position (as in **1.59**). This was more distinctive for meso-aryl substituents than -alkyl derivatives.[50]

This versatile method can be used not only to synthesise mono-, di-, tri- and tetra-meso-substituted porphyrins with different residues **1.75**, but also directly meso-meso-linked bisporphyrins **1.75**, phlorins, porphodimethenes (**1.70** or **1.71**), and chlorins (**1.69**) (Fig. 1.17).[56] The key aspect here is the generation of the anionic intermediate **1.68** from **1.67** and how this is used in subsequent transformations. Quenching with water followed by oxidation will yield the porphyrin, while trapping with an organic electrophile at low temperature will yield A,B-disubstituted porphyrins **1.72** in a one-pot reaction.[43b]

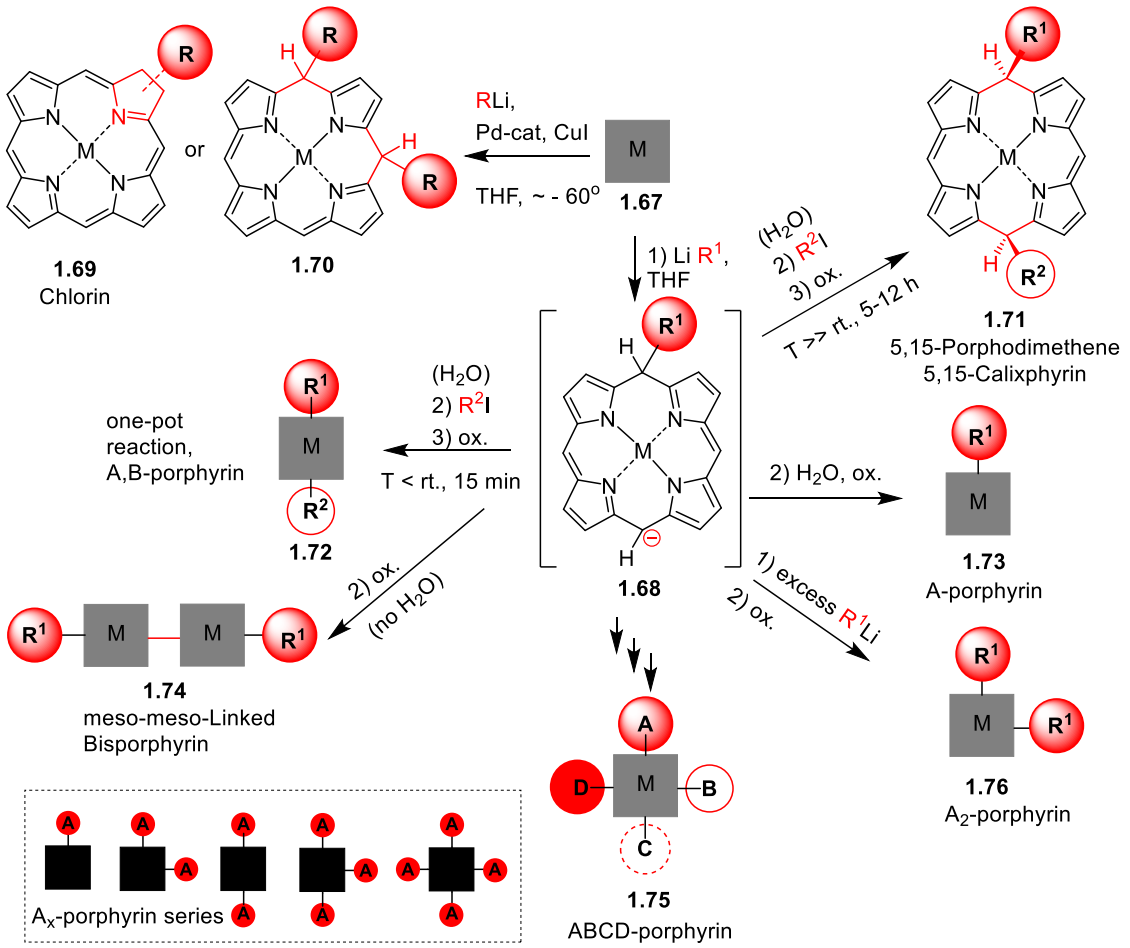

Figure 1.17. Synthetic scope of using organolithium reagents for porphyrin modifications.

If the electrophile is added at higher temperatures, then the intermediate becomes locked in a roof-type conformation which cannot be oxidised to the porphyrin level and 5,15-porphodimethenes **1.71** are obtained.[57] Skipping the hydrolysis step and instead having direct oxidation of the intermediate **1.68** yields an anion radical which can dimerise to **1.74**.[58]

The use of an organolithium reagent also offered the first rational entry into "less-substituted" porphyrins and the completion of the A_x-type porphyrin series (inset, Fig. 1.17) through functionalisation of unsubstituted porphyrin **1.5** (naturally, in practice the symmetric compounds are more easily prepared by simple condensation reactions). The synthesis and use of porphyrin was cumbersome and plagued by low yields as well as its extremely low solubility (due to π-stacking), and this hampered synthetic advances therewith.[59] This was overcome by preparation of the free base **1.5** *via* acid-catalysed thermal dealkylation of the highly nonplanar porphyrin 5,10,15,20-tetra(*tert*-butyl)porphyrin or its β-substituted analogues.[60] The reaction of **1.5** *in situ* with RLi as outlined above then gave a

high yielding synthesis of 5-substituted **1.68**[28] or, with excess RLi, 5,10-disubstituted porphyrin **1.76**. [30] Formally, these reactions are the initial steps in the synthesis of 5,10,15,20-tetrasubstituted ABCD-type porphyrins **1.75** from **1.5**.[7, 61]

This method can also be used for substitution of the β-position. This depends on the steric bulk of the RLi reagent, where larger ones such as *t*BuLi undergo nucleophilic β-addition reactions to yield chlorins **1.69**.[57b, 62]

1.3.3.2 Nitroporphyrins and porphyrin thioethers

Nitro groups have a highly electron-withdrawing effect and can act as good leaving groups. Thus, compounds as those described in 3.5.2.3 can undergo reactions with nucleophiles. In general, β-nitroporphyrins are more reactive than meso-nitroporphyrins. Depending on whether ‘’hard’’ or ‘’soft’’ nucleophiles are used, different substitution mechanisms apply.

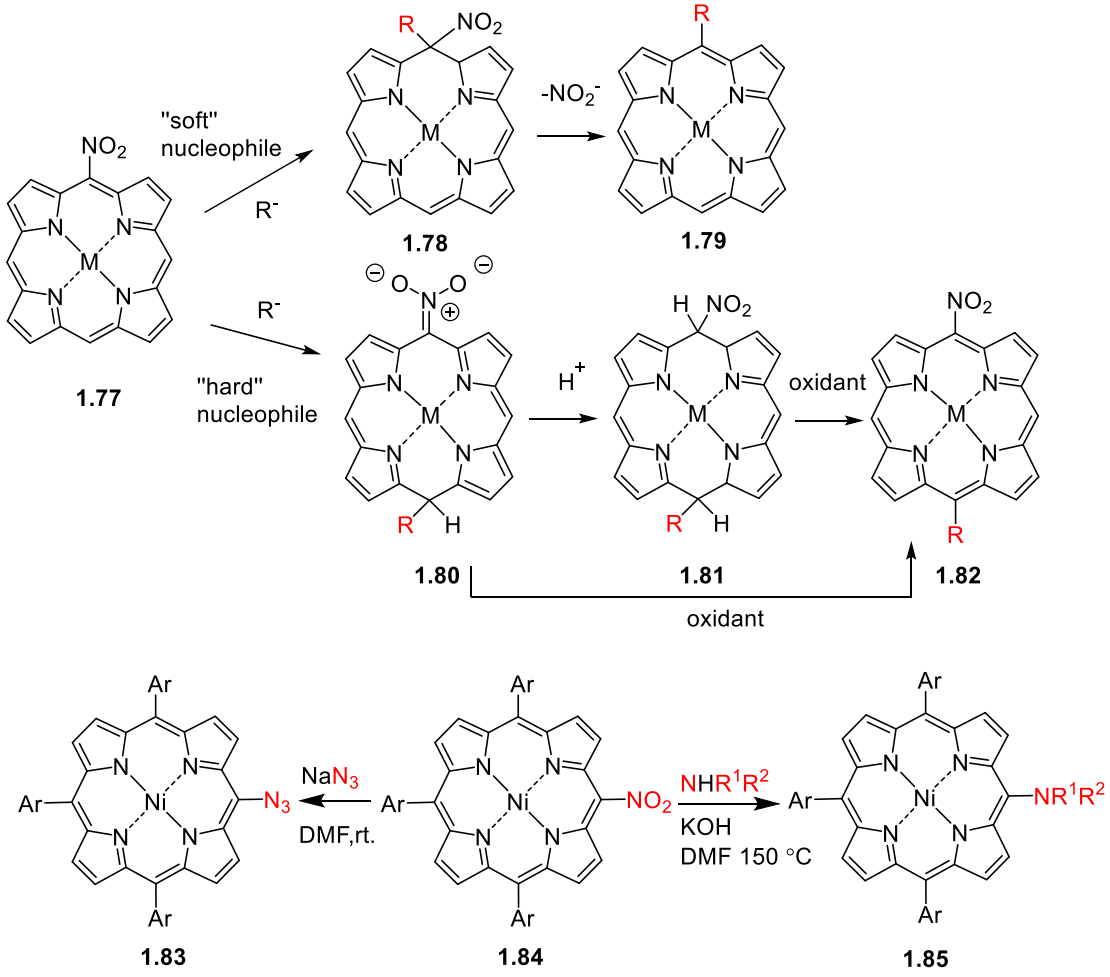

Figure 1.18 Nucleophilic substitution of 5-nitroporphyrins.

When 5-nitroporphyrin **1.77** is treated with ‘’hard’’ nucleophiles such as methylmagnesium iodide or benzyl oxide, a 5,15-meso-addition (‘*trans*’) to **1.82** occurs while ‘’soft’’ nucleophiles, such as thiolates or benzaldoxime anions, result in an *ipso*-substitution (**1.78**) followed by denitration to **1.79** (Fig. 1.18).[63]

Similar results were obtained for 2-nitroporphyrins, where the attack of ‘’soft’’ nucleophiles results in an *ipso*-attack and the reaction with ‘’hard’’ nucleophiles results in an attack on the adjacent β-pyrrolic position. This was exemplified in Crossley’s reaction of 2-nitro-TPP with Grignard reagents. These first involve a nucleophilic addition, *i.e.*, give a 2-substituted-3-nitrochlorin which rapidly eliminates nitrous acid to reform the porphyrin system.[64]

The reaction of nickel(II) nitroporphyrins **1.84** with nitrogen-based nucleophiles such as sodium azide to **1.83** or primary or secondary aryl- and alkylamines to **1.85** are of practical utility. As shown by Devillers *et al*. the use of amines with electron-donating or -withdrawing groups requires a basic catalyst, while the azide anion is nucleophilic enough to react without any catalyst (Fig. 1.18).[65] Various compounds could easily be synthesized *via* this method, including NH-bridged porphyrin dimers. Such reactions were first observed by Gong and Dolphin, who studied reactions of the free base 2,3,7,8,12,13,17,18-octaethyl-5,10,15,20-tetranitroporphyrin **1.90** with halides (Fig. 1.19).[66]

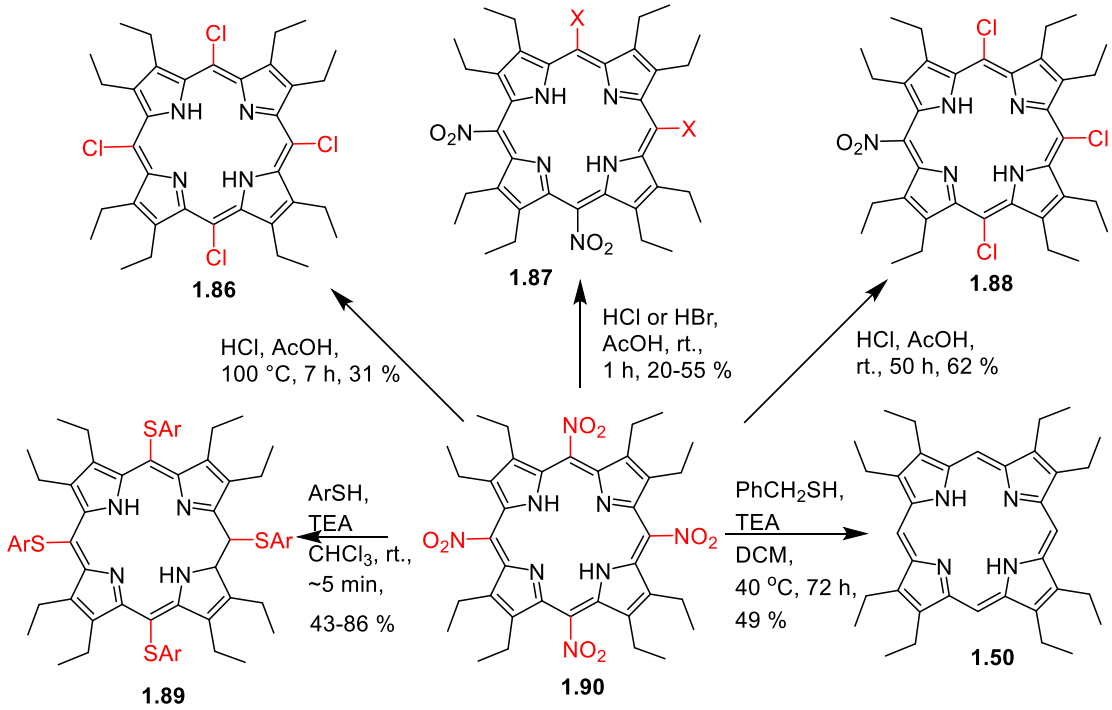

Figure 1.19 Nucleophilic substitution and denitration reactions of 2,3,7,8,12,13,17,18-octaethyl-5,10,15,20-tetranitroporphyrin.

The reaction proceeds *via* an addition-elimination pathway to form a Jackson-Meisenheimer complex, followed by elimination of the nitro group to yield the *ipso*-substituted products. The degree of substitution could be controlled through variation of the reaction conditions, ranging from replacement of all four nitro groups by halides (**1.86**) to partial substitution, as in **1.87** or **1.88**.

More recently *S*-nucleophiles were shown to yield the respective tetrasubstituted thioethers **1.89** in high yield.[67] Next to substitution, step-wise denitration to **1.90** was also observed as a competing process under basic conditions.

Another intriguing reaction was the formation of bisporphyrin thioethers *via* a similar mechanism. Studies on the 'unmasking' of porphyrin-thioethers with an isooctyl-3-mercaptopropionate group **1.91**, *i.e.*, attempting to generate the free thiol, resulted in the formation of the bisporphyrin thioethers **1.95** in good yield (Fig. 1.20).[68] Nucleophiles containing sulfur groups often require activation of the system (good leaving groups, strong bases, high temperatures, metal catalysts). Therefore, it was very surprising that the formation of sulfur-linked dimers could be achieved through simple treatment with base at room temperature.

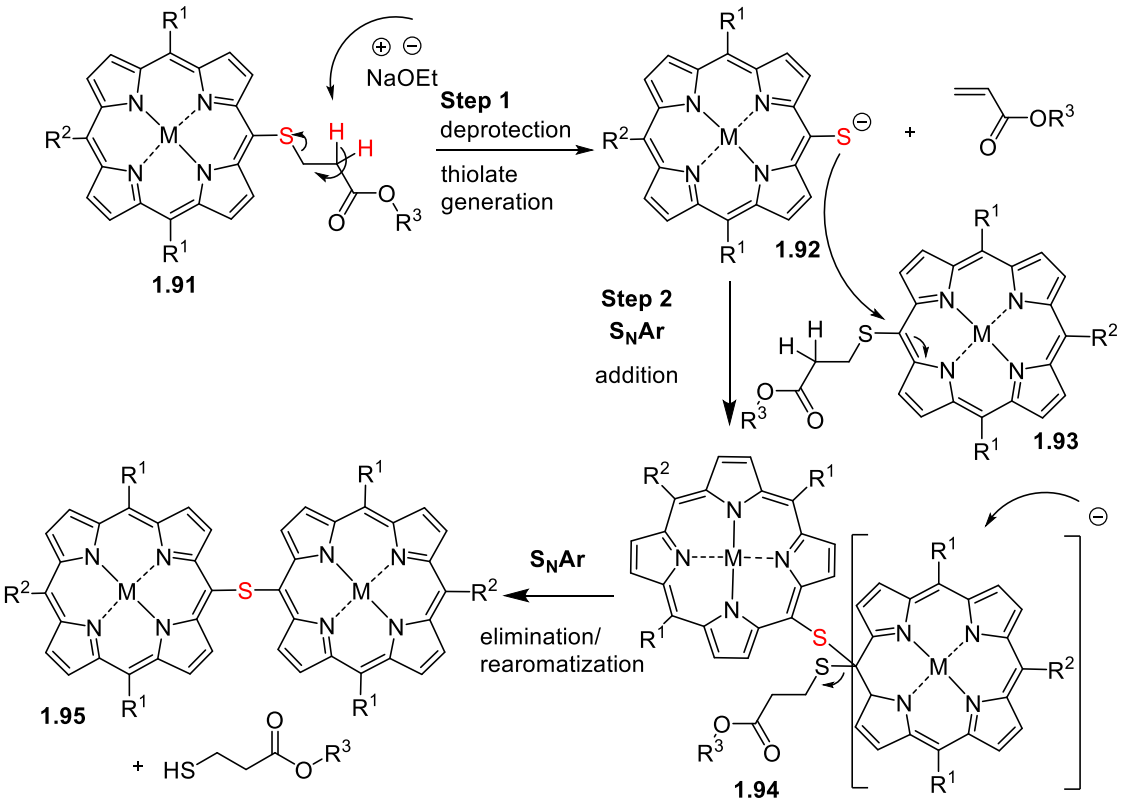

Figure 1.20 Synthesis of bisporphyrin thioethers *via* thiolate displacement.

These systems were considered rather inactive, but substitution occurred nevertheless. The reaction mechanism includes a base-mediated deprotection of a

porphyrin thiol, followed by a S_NAr reaction. The deprotected porphyrin thiolate **1.92** acts as a very strong nucleophile and attacks the, as of yet, unreacted starting material to form the bisporphyrin, most likely *via* a phlorin intermediate **1.94**.

1.3.4 Transition metal-catalysed reactions

Organometallic reactions are currently the most widely used means to modify a porphyrin. Initially developed for small molecules, their application in C–C- and C–heteroatom-bond formation on the porphyrin macrocycle has been the main driving force behind the explosion in porphyrin research and applications in recent decades. The use of organolithium reagents for C–H activation has already been highlighted. Therefore, the next focus lies on the use of transition metal (catalysts) for transformations directly at the porphyrin ring system. An excellent survey of synthetically useful organometallic reactions was recently published by Shinokubu and co-workers.[69] It nicely sets the various reactions in the context of their synthetic utility.

Most of these reactions require however prior activation of the porphyrin macrocycle through halogenation. This makes halogenation reactions an incredibly important tool for the synthesis of starting materials for organometallic coupling reactions.[70] One difficulty concerning these reactions is that for asymmetric porphyrins often only one halogen atom at a time is required on the porphyrin core. Due to the electron density on the meso-positions of the porphyrin, these positions are very reactive towards electrophilic substitution and it might be difficult to obtain regioselectivity. Some degree of control can be gained by adopting the reaction temperature and the eq. of the bromination agent used. To achieve for example monobromination the reaction can be performed at 0 °C as well as with only 0.9-1 eq. brominating agent. However, most of the time still some side products will form to a minor extent.

1.3.4.1 C–C bond formation

Since the advent of transition metal-catalysed reactions in the second half of the last century, C–C bond forming reactions have become a mainstay of synthetic organic chemistry. Most of them have also been subsequently applied to porphyrins. Typically, this involved the transfer and then optimisation of reactions initially developed for simple aromatic compounds to porphyrinoids. The most

important examples which result in C-C bond formation directly at the macrocycle are grouped according to the metal involved in the catalytic reaction in the following sections.

1.3.4.1.1 Palladium-catalysed reactions

The central method to achieve step-wise functionalisation of porphyrins is palladium-catalysed cross-coupling in its many variants, similar to some of those used for C–H activation.[69, 71] A functionalisation of the aromatic macrocycle,*e.g.*, halogenation (**1.96**), is needed first in most cases. Typically, the reaction mechanism involves an oxidative addition of the Pd(0) complex (**1.97**), followed by substitution of the halogen by a nucleophile (**1.98**). The cycle is completed by reductive elimination of the palladium complex, which simultaneously forms the desired coupling product **1.99** and regenerates the catalyst (Fig. 1.21).

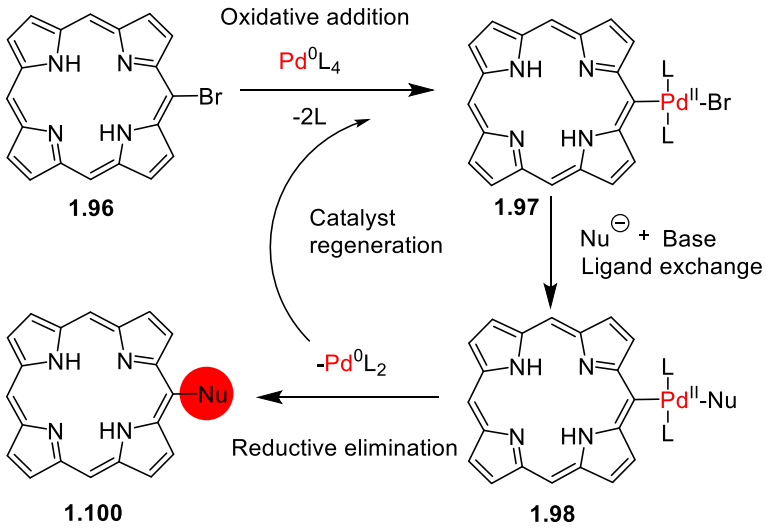

Figure 1.21. General mechanism of Pd-catalysis.

Porphyrin chemists began to apply such reactions in the 1990s. A host of reaction types are now available, the primary distinction being in what form the second reaction partner (the Nu in Fig. 1.21) is fed into the reaction sequence. Therien and co-workers reported the first palladium-catalysed reaction with porphyrins utilising organozinc (Negishi coupling) and organotin (Stille reaction) nucleophiles in 1993 and these reactions can be applied to both the meso- and β-positions.[72]

Suzuki-Miyaura – Boron: One of the best-known palladium-catalysed coupling reactions is the Suzuki reaction which has been used in porphyrin

chemistry now for two decades.[73] Here, the porphyrin can either be used as the organohalide (*i.e.*, bromoporphyrins) or as the attacking nucleophile. The latter can be achieved by reversing the polarity of the porphyrin *via* the synthesis of boronyl porphyrins (typically prepared from bromoporphyrins). The mechanism follows the general palladium-catalysed reaction mechanism (Fig. 1.21). In the first step, the organopalladium species is formed *via* oxidative addition to **1.101** (Fig. 1.22). Next, complex **1.102** reacts with a base to yield intermediate **1.103**. Meanwhile, the boronic acid **1.104** is activated with a base to give the boronate complex **1.105**. This activation is necessary to facilitate transmetallation to compound **1.106**. The catalytic cycle is completed with reductive elimination, delivering the desired product **1.107**.

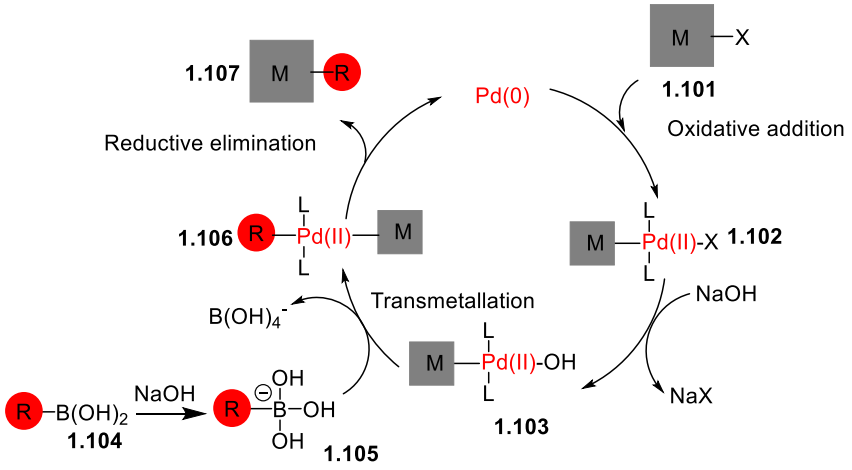

Figure 1.22. Illustration of the Suzuki-Miyaura reaction mechanism with porphyrins. Note, R can also be a porphyrin to be coupled with either another organic residue or a (different) porphyrin.

This strategy can be used to synthesise a broad range of alkyl and aryl meso- and β-substituted porphyrins. The reaction conditions are normally relatively mild, require only hours and give, depending on the substituents used, excellent yields.

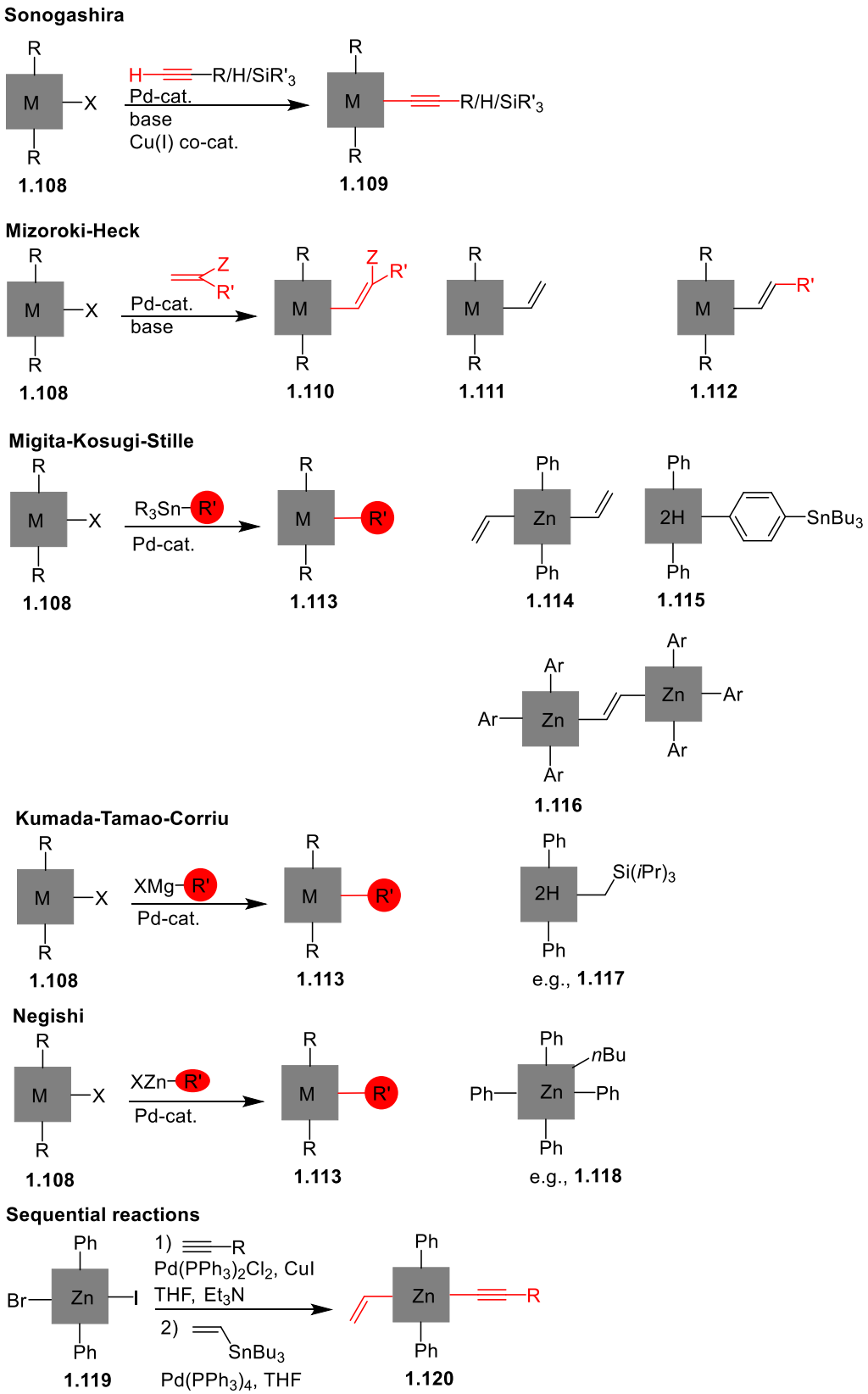

Figure 1.23. Examples of other Pd-catalysed coupling reactions with porphyrins. Note, various combinations and use of porphyrin reactants other than those shown are possible.

Sonogashira – CΞC-R: Another coupling reaction using palladium is the Sonogashira cross-coupling reaction. It is the method of choice to generate alkynyl-substituted porphyrins through the introduction of ethynyl compounds. The groups of van Lier and Therien were the first to apply this method to porphyrins in 1994.[74] Reactions of haloporphyrins using a range of acetylene derivatives worked well with β-alkyl- and meso-arylporphyrins and is now routinely used with all types of halo-, tosyl- and boronylated porphyrins (**1.108→1.109**) (Fig. 1.23). Porphyrin chemistry is hard to imagine without this versatile method, and numerous compounds have been generated with it, mostly using CuI as a co-catalyst and $Pd(PPh_3)_4$, $PdCl_2(PPh_3)_2$, or $Pd_2(dba)_3$ as a catalyst. To avoid metal insertion during the reaction, metallated porphyrins must be used. Even though a few copper-free methods exist, applications for them are still limited. Alkynyl-linked bis- and oligoporphyrins are frequently employed due to the rigid conjugating linker(s) in biomimetic chemistry, photonics, and the synthesis of superstructured molecules.[74b, 75]

Heck – alkenyl: The Mizoroki-Heck reaction was first used with porphyrins by Gauler and Risch in 1998.[76] Since then this reaction type has been used to introduce alkenyl substituents into the meso- or β-positions.[77] Some examples for alkenes which have been applied to Heck reactions are acrylates, styrenes and acrylonitrile (**1.108→1.110**). Usually, bromoporphyrins are used as the coupling partner, but vinylporphyrins such as **1.111** or protoporphyrin IX also react,[78] and this method can be used to modify the peripheral positions of a porphyrin. The mechanism of the Heck-reaction is slightly different from that of other Pd-catalysed reactions. The first step is an oxidative addition, followed by coordination and migratory insertion of the olefin to palladium. A subsequent bond rotation moves the two aryl groups *trans* to each other and results in β-hydride elimination to form the desired coupling product. The catalyst is then regained by base-mediated reductive elimination.

Stille, Negishi, and Kumada – tin, zinc, magnesium: Further variations of the catalytic Pd-cycle are exemplified in the use of organometallic Sn, Zn, and Mg compounds. The Migita-Kosugi-Stille reaction is a coupling between bromoporphyrins and tin reagents with a Pd-catalyst (**1.108→1.113**).[72] Even though organotin reagents are very cheap to synthesise, the number of applications with porphyrins are limited.[43b] The reaction mechanism is very similar to Suzuki coupling (Fig. 1.23), aside from the fact that the boronic acids have to be

activated with a base, whereas the tin reagents used in the transmetallation step react on their own. First used for the synthesis of vinylporphyrins (**1.113**)[72], a number of substitution patterns, including those of porphyrin organotin compounds (**1.115**)[79], are known. Organotin compounds are also a complementary method for introducing alkenyl (**1.116**)[80] and alkynyl residues[81], the latter up to eight times[82].

Related catalytic reactions include the use of Grignard reagents (Kumada-Tamao-Corriu coupling) (**1.108→1.113**). Thus far, this has been used for the synthesis of silylmethyl porphyrins **1.114** using catalytic $Pd_2dba_3/Ph_2P(O)H$].[83] In contrast, organozinc reactions (Negishi coupling, **1.108→1.113**) have been used for longer [72], and for both aryl and alkyl residues[84]. Such reactions may also be executed in sequence, *e.g.*, by using bishalogenated porphyrins **1.119** in consecutive Songashira and Stille reactions to give **1.120**.[85] Many other reactions involving Pd-catalysts for C–C-coupling reactions with porphyrinoids are known; for an almost complete list see reference.[69] Some of these include homocouplings or intramolecular cyclisations[86], or intramolecular C–H arylations to yield air-stable porphyrin radicals.[87]

1.3.4.1.2 Nickel- and rhodium-mediated reactions

Other metal catalysts can also be employed. Established examples, although lagging behind in their use in standard organic chemistry, are nickel and rhodium. Nickel catalysts can often be used effectively under mild conditions (Fig. 1.24). A synthetically useful example is the $Ni(OAc)_2$-mediated coupling of meso-bromoporphyrins with (di)carbonyl (doubly activated methylene) compounds (**1.121→1.122**).[88] This approach is quite adaptable and was successfully used to generate aryloxy and amino-porphyrins, *i.e.*, covers the full spectrum of C–C-, C–O-, and C–N-bond formation (see below). Ni-catalysts have also been employed in the generation of directly-linked bisporphyrins through Ullmann homocoupling. Thus, the bromoporphyrin **1.123** gave the meso-meso-linked dimer **1.124**.[89]

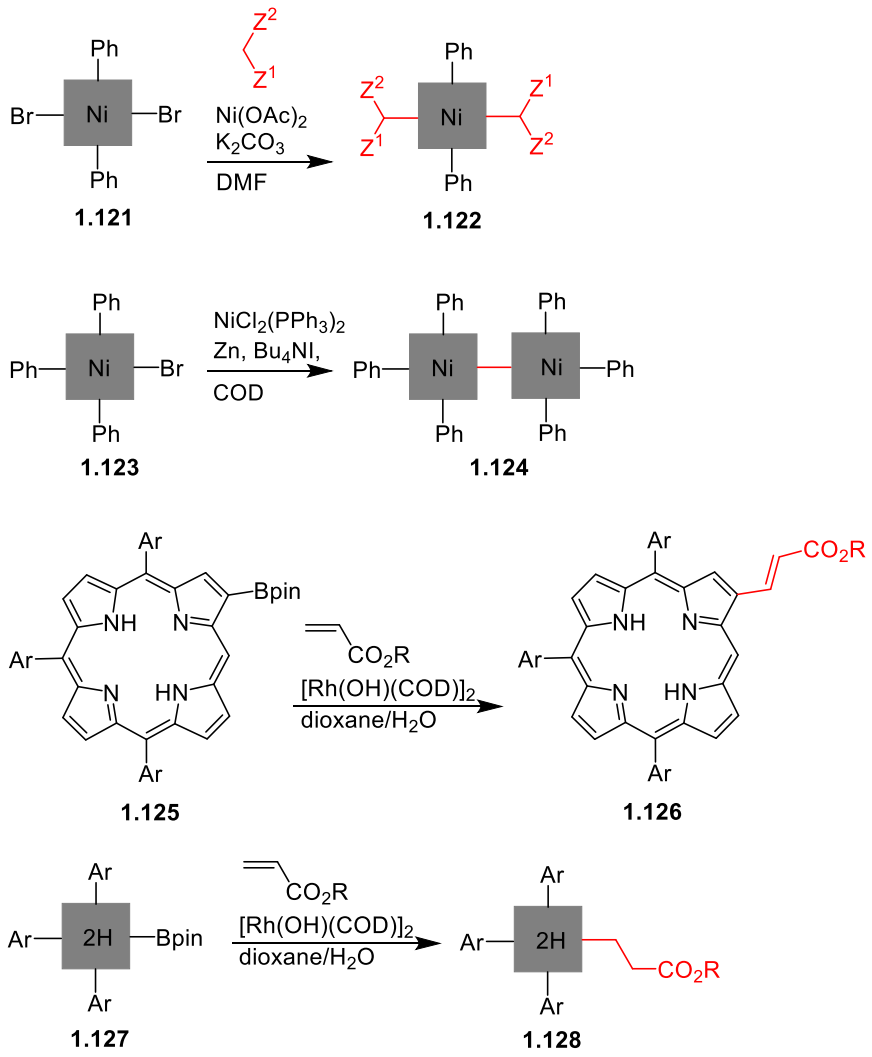

Figure 1.24. Examples of Ni- and Rh-mediated C–C-bond forming reactions.

The positioning of the coupling partner on the porphyrin may also affect the selectivity of the coupling reaction. An intriguing example is the use of borylporphyrins in rhodium-catalysed Heck-type reactions. The β-borylated porphyrin **1.125** is reacted with a vinyl ester under $[Rh(OH)COD]_2$-catalysis to give the vinylated porphyrin **1.126**. However, the positioning of the pinacoleborane unit at the meso-position (**1.127**) resulted in the formation of the 1,4-conjugate addition product **1.128**, presumably due to steric reasons.[90]

1.3.4.2 *C-Het Bond formation*

The use of transition metal-catalysed reactions not only allows the formation of C-C bonds but in recent years we have also seen a parallel development of C-Het bond forming methods, mostly using halogenated porphyrins. Again, these methods derive from advances in the organometallic chemistry of 'small' molecules. A wide range of nucleophiles can now be applied to these reactions,

such as thiols, amines or alcohols, resulting in the corresponding C-S, C-N and C-O bonds.

1.3.4.2.1 Amination and amidation, C–N

Amino groups can have a significant impact on the electronic properties of porphyrins and therefore feature prominently in applications such as dye-sensitised solar cells. Historically they were accessible *via* nitration and reduction or substitution, but the main advance in their use came from the application of the Buchwald-Hartwig reaction (Fig. 1.25). In 2003, Chen and Zhang reported a series of palladium-catalysed amination reactions with bromoporphyrins using Buchwald-Hartwig conditions.[91] This reaction can be used to synthesise aminoporphyrins with a broad variety of alkyl- and arylamines. Various optimisations and adaptations exist, using different strengths of bases (Cs_2CO_3, NaO*t*Bu), different ligands (DPEphos, BINAP, Xantphos) and palladium-catalysts ($Pd(OAc)_2$, $Pd_2(dba)_3$, etc.). Furthermore, optimised reaction conditions do exist for a variety of amines with bromoporphyrins.[92] Normally, both electron-rich and electron-poor derivatives give moderate to high yields in relatively short reaction times (<24 h), but sterically demanding or aliphatic amines require longer reaction times.[93]

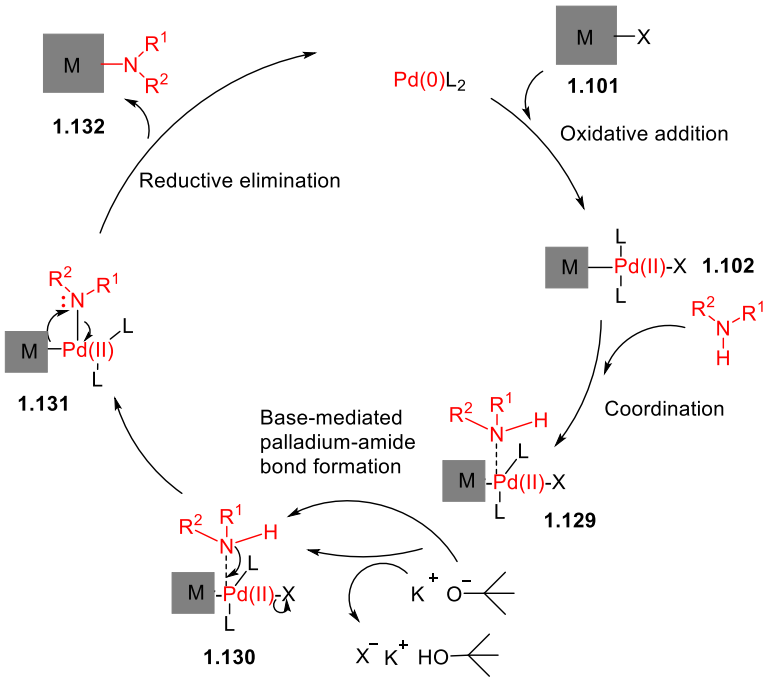

Figure 1.25. Illustration of the Buchwald-Hartwig amination reaction mechanism with porphyrins.

1.4 Multicomponent porphyrin systems and their applications

Molecular electronics are gaining popularity as contemporary inorganic materials are reaching the physical limits of their potential for electronic applications. In particular, inorganic materials are unable to continue the historic trend of continuous miniaturisation.[94]

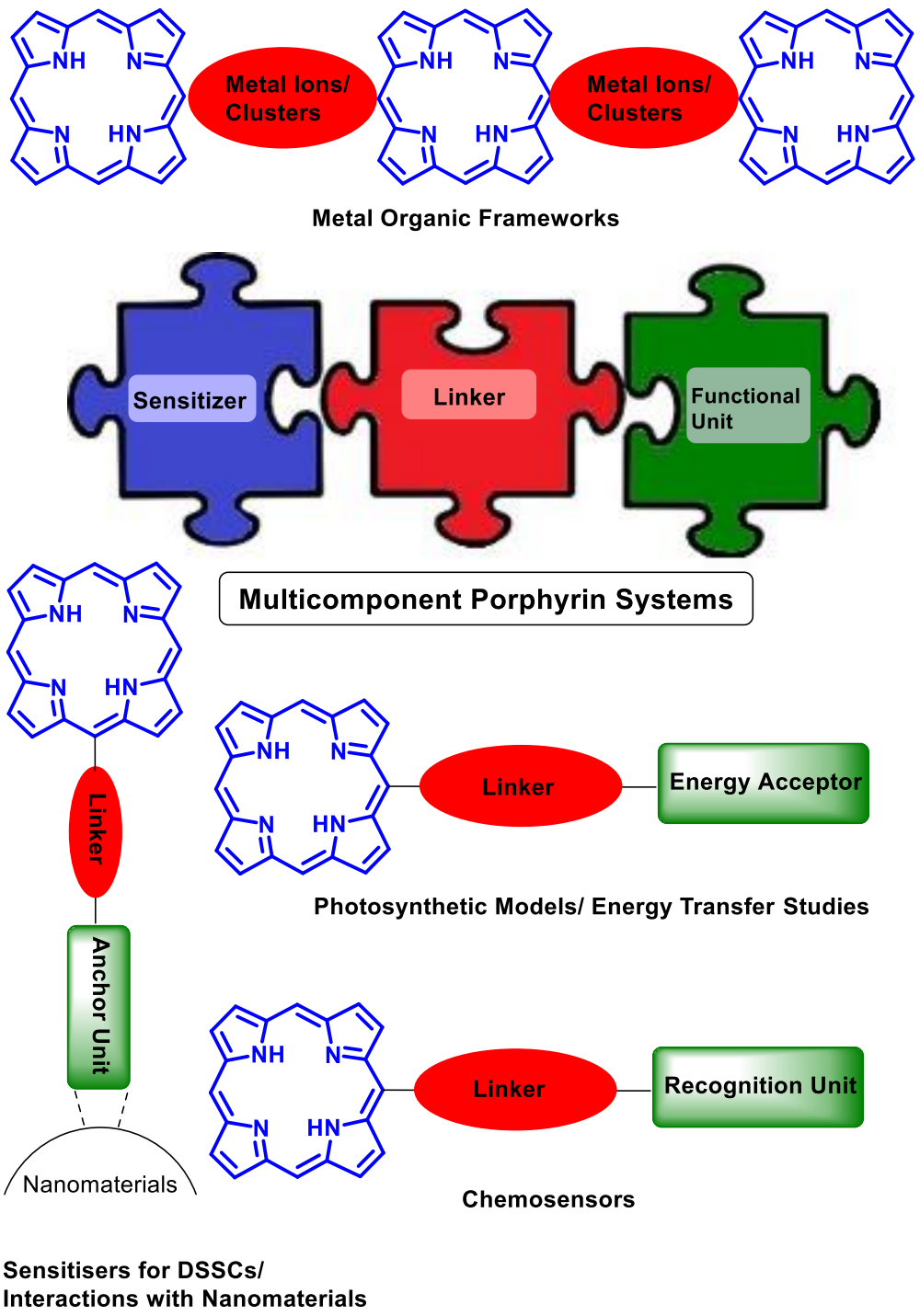

Figure 1.26. Different applications for multicomponent porphyrin systems.

Organic multicomponent systems are a logical next step for electronic applications due to ample exemplars found in nature, such as photosynthetic reaction centres and ion conducting channels, etc.[94]

While these naturally occurring systems are suitable as models, they are far too unstable for direct usage in electronic systems. For example, photosynthetic systems, are multichromophoric structures that are continuously decaying in nature and must be replenished by the organism. This frailty of naturally occurring molecules has inspired the study of synthetic multicomponent systems that share the same characteristics as their natural counterparts, but do not decay and thus can be used within electronic components. While monomeric structures alone can be used as basic models for photosynthetic systems, multicomponent structures are necessary to accurately imitate them.[95] As such, large stable aromatic systems with tunable electronic properties are a valuable and desired material for these applications. Porphyrins exhibit reversible oxidation and reduction properties while also having rich electrochemical properties. Moreover, due to constant improvements and development for synthetic procedures, it is now possible to precisely engineer and architect custom molecular designs of these systems.[7]

Therefore, such multicomponent systems have been extensively employed in various applications over the years. Different specific criteria apply to the sensitisers depending on the applications they are used for. These criteria include: certain electron donor and acceptor units to anchor groups for interactions with nanomaterials, defined molecular arrangement of functional groups on the porphyrin core, specific electronic properties such as isolator systems or fully conjugated systems.

One classical example for the usage of multicomponent porphyrin systems would be in photosynthetic models due to their similarity with chlorophylls. In photosynthesis the antenna molecules are arranged in a spatially defined manner.[96] To accurately mimic these naturally occurring systems synthetically designed systems should also have a defined geometry and spartial arrangement with a specific orientation of the different parts of the multicomponent porphyrin systems. This can be achieved through the employment of rigid linker units. The first systems utilizing small molecules for artificial photosynthesis were designed already in 1980s. Since then a variety of different components and multiporphryin systems has been reported.[97] The first model containing porphyrins was reported in 1984 and consisted of a single porphyrin **1.133** that was linked to an acceptor

molecule through a bicyclooctane (BCO) linker.[98] Other mono porphyrin linked systems reported consisted of a zinc porphyrin as electron donor which was connected *via* a rigid phenylene-ethynylene-phenylene (PEP)-BCO linker to different anilino-substituted multicyanobutadienes or extended tetracyanoquinodimethane analogues (Fig. 1.27, **1.134)**.[99]

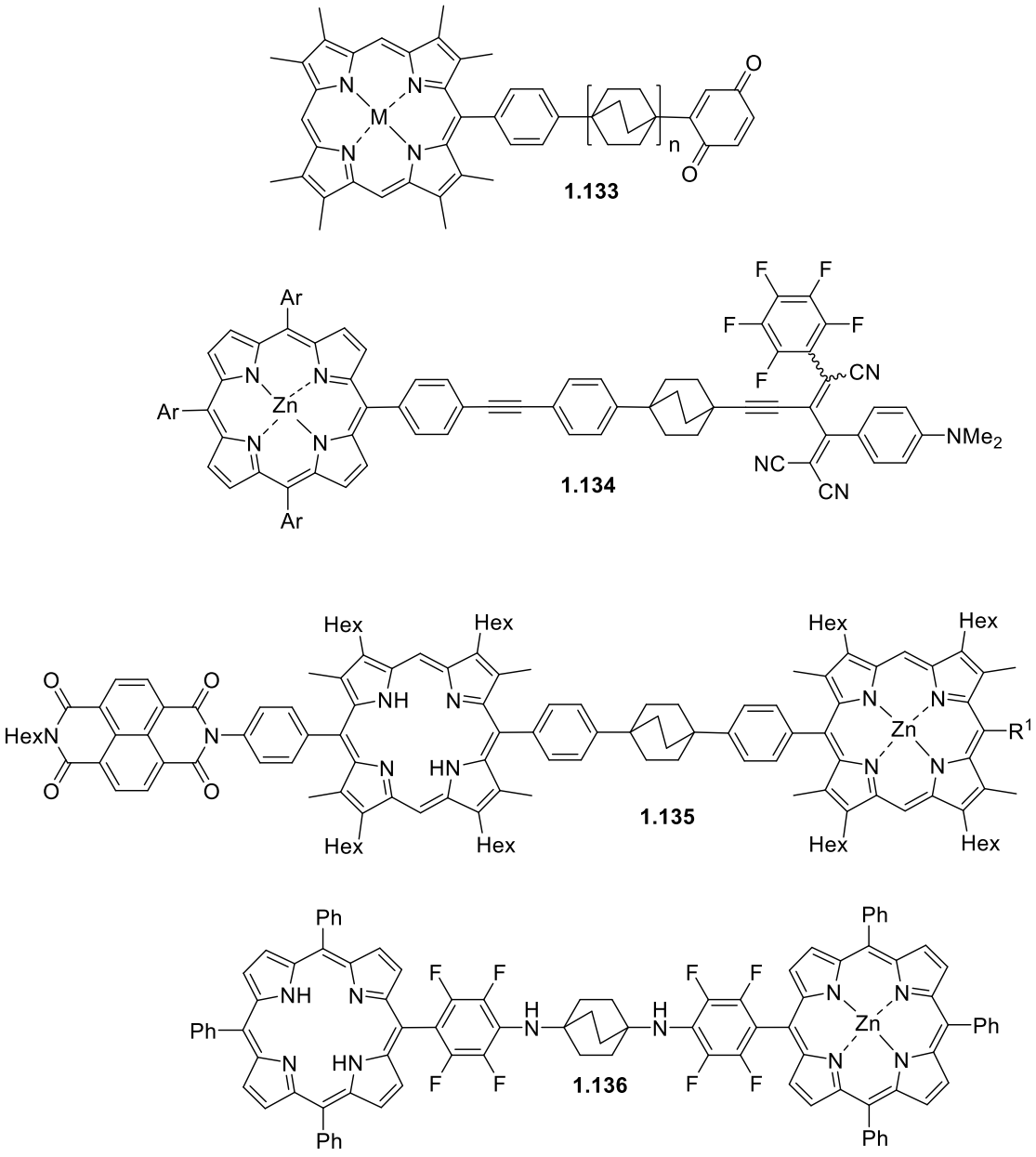

Figure 1.27. Examples of different photosynthetic models utilising multicomponent porphyrins.

Later on, systems with two porphyrin units were investigated. One example are triad systems with a free base porphyrin which is connected through different aromatic linkers to a Zinc porphyrin (Fig. 1.27, **1.135** and **1.136**).[100]

Another application for multicomponent porphyrins is as chemosensors. The detection of for example environmental pollutants is still of utter interest and has resulted in the devolpment and design of organic chemosensors due to their low cost and ease of manipulation. The selective detection of hazardous molecules can be either achieved through supramolecular interactions or through the formation of covalent bonds.[101] One example was reported by Crossley, Fukuzumi et al. utilise a free base porphyrin which is linked to two acridinium units *via* an aromatic linker unit, which acts as fluorescence sensor for superoxides (Fig. 1.28, **1.137**).[102]

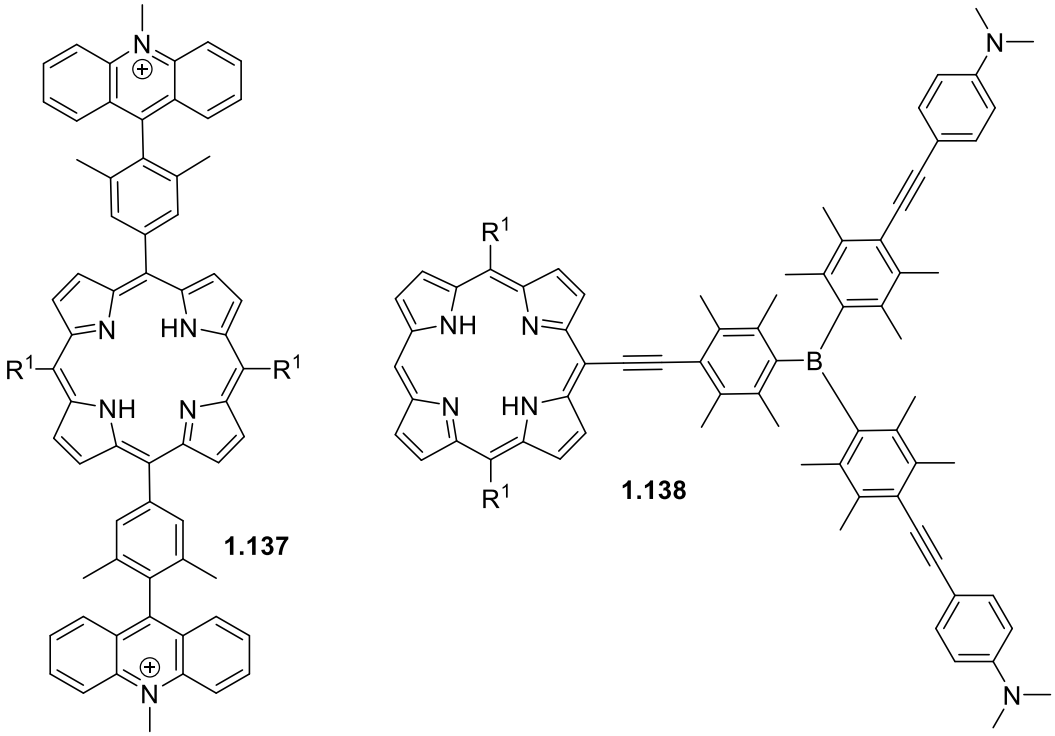

Figure 1.28. Selective examples of multicomponent porphyrin chemosensors.

Initially, the fluorescence is quenched by photoinduced electron transfer to the acridinium units. However, upon addition of potassium superoxide this process is inhibited and the porphryn exhibits fluorescence. Another example represents a porphyrin connected through a linker to a triarylborane unit (Fig. 1.28, **1.138**).[103] Due to the linker units the two systems are electronically coupled and energy transfer from the exhited triarylborane moiety occurs. Once a flourine ion binds to the boron center this connection gets disturbed resulting in the formation of two emission bands rather than one.

A variety of porphyrins with so-called anchor units has been reported in literature. These molecules are used for various of applications and the anchor unit which is most commonly covalently attached to the porprhyin *via* a spacer unit is used to attached the porprhyin moiety to a phletora of nanomaterials. This finds not only application in Dye sensitised solar cells (DSSCs) but also in the functionalisation of nanocarrier, such as gold nanoparticles, for drug delivery[104] or as antibacterial nanotherapeutic agents.[105] Besides this a multitude of different covalently attached anchor groups on porphryins have been used to achieve functionalization with graphene.[106] An application that has recently gained much attention is the incorporation of porprhyins with anchor groups into hydrogels.[107]

Another well-known utilization of porphyrins with anchor groups are metal-organic frameworks (MOFs). Porphyrins with specific linker/anchor units such as pyridine groups or carboxylic-acids moieties have been widely incorporated in metal-organic frameworks (MOFs).[108] Herein the porphyrins are arranged in a well-structured assembley with an metal ion or cluster in between the porphyrin molecules (Fig 1.26). These networks can then be used for a wide range of applications such as for optoelectronic devices or for the incorporation of guest molecules.[109]

2 Synthesis of unsymmetrical push-pull porphyrins

2.1 Introduction to DSSCs

2.1.1 History of Dye-sensitised solar cells (DSSCs)

Challenges for the future involve besides others the ever-growing demand for energy. The human need for this critical resource has become more and more evident in the last decades.[110] However, the current technologies seem to be unable to solve this problem. Fossil fuels, which still are one of the major sources of energy these days, have played a substantial role in the increase of greenhouse emissions, causing yet another challenge for modern humanity.[110] Therefore, the focus in research has shifted towards the exploration of sustainable energy to target these issues. One alternative is the conversion of solar energy into electricity. To compete with classical and well-tried fossil energy production the perfect modern photovoltaic devices need to be cheap and have to absorb light in a broad region of the visible spectra in order to facilitate a maximum efficiency and conversion of sunlight into energy. Like in many research areas of interest, natural occurring systems often provide superior examples and challenge researcher to mimic their processes with similar compounds. One example are dye-sensitised solar cells (DSSCs) which try to mimic naturally occurring systems for photosynthesis.[111]

DSSCs are photovoltaic devices which consist of an electrode, an electrolyte and a dye-sensitised photoanode. The efficiency of these systems strongly depends on the photoactive component, *i.e*. the sensitiser dye. The first concept of dye-sensitised solar cells was published by Grätzel and O'Regan in 1991 (Figure 2.1).[112]

Porphyrins have always been recognised by the research community as potential sensitisers[113] due to their strong absorption bands in the visible region, tunable electronic properties and the diverse ways they can be modified. Thus, it is astonishing that their application in DSSCs is only coming to the fore in recent years. For a long time, ruthenium sensitisers were the dyes of choice for DSSCs owing to their favourable power conversion efficiency (PCE) of >11%.[114]

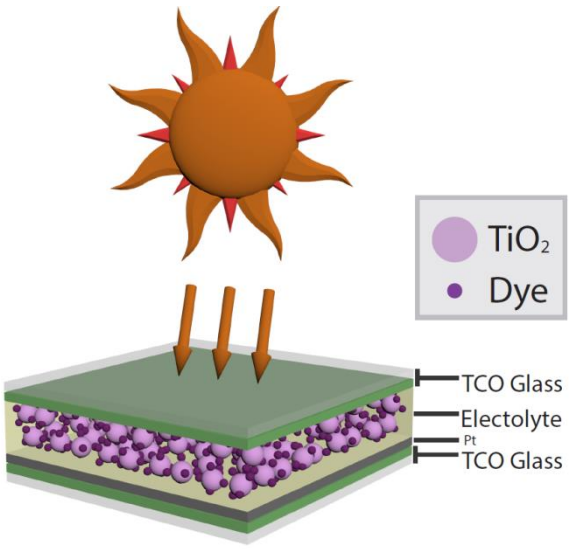

Figure 2.1. Basic principle of a DSSC.

Porphyrins gained popularity as sensitisers in DSSC with the evolution of the "push-pull" porphyrin systems. Pioneered by Suslick's and Therien's groups,[115] *push-pull* porphyrins are donor-π-acceptor systems (D–A) where electrons are transferred from an electron-donating group through a π-spacer to an electron-withdrawing group and have a strong intramolecular dipole moment (Fig. 2.1). Initially developed for use in nonlinear optics (NLO),[9a] they are currently under intense scrutiny as light-harvesting dyes in dye-sensitised solar cells due to their broad and strong absorption properties.[116] Here, carboxylic acid groups often feature as anchoring acceptor units while a variety of different donor units have been explored.[117] Some porphyrins have historically offered poor light harvesting with wavelengths at approximately 500 nm and Q bands of above 600 nm. The "push-pull" system helped overcome poor light absorption of such compounds at these desired wavelengths, making porphyrins a notable alternative to ruthenium-based sensitisers. Grätzel *et al.* made a significant contribution to the advancement of porphyrins as sensitisers for DSSCs (Figure 2.2, **2.1** and **2.2**). In 2005, they reported a η-value of 5.6%[118] and two years later a η-value of 7%.[119] This increase in efficiency of porphyrin sensitisers inspired many other researchers to invest in this field[120] with a large variety of "push-pull" porphyrin systems being published. The most remarkable performance to date was again accomplished by Grätzel reaching an exceptionally high η-value of 13% (Figure 2.2, **2.2**).[116b, 121]

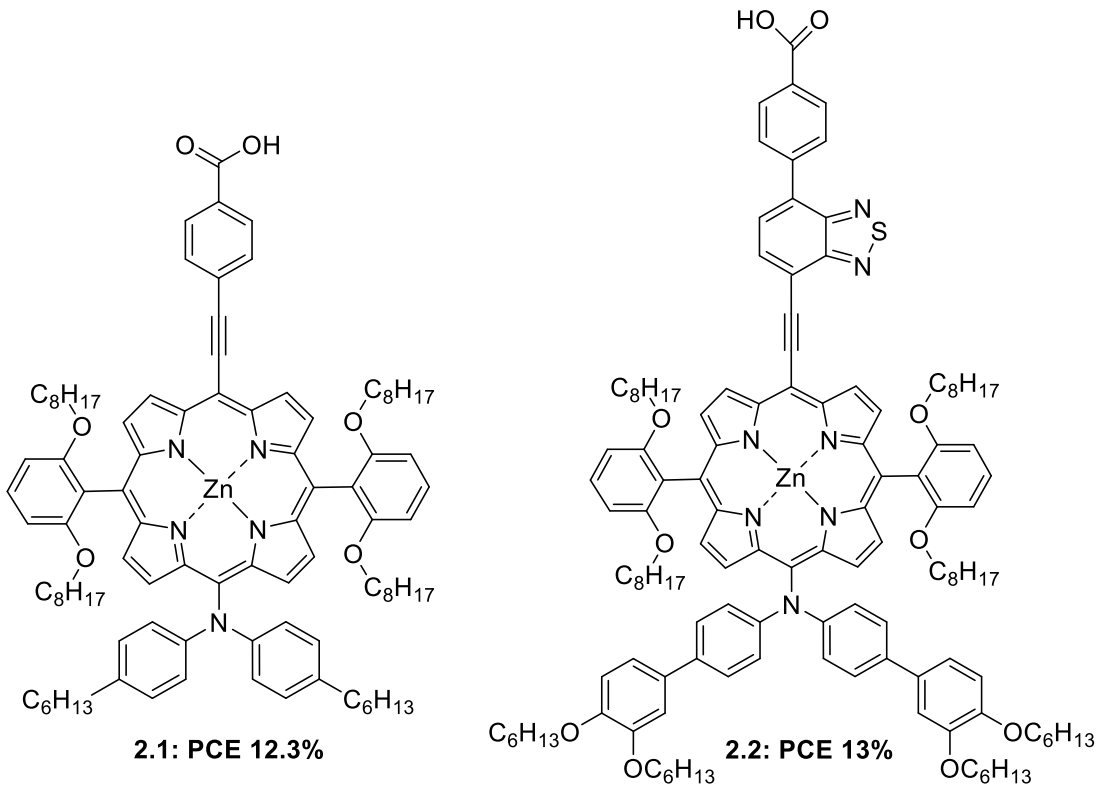

Figure 2.2. State of the art sensitisers in DSSCs: porphyrin **2.1** and **2.2**.

2.1.2 Optical Properties of DSSCs

A DSSC consists of a transparent conducting oxide, a nanoparticle photoanode (*e.g.*, TiO_2) which is covered with a monolayer of the sensitising dye, conducting electrolyte and a counter electrode (Fig. 2.1).[122] In a DSSC, a photon is absorbed by the sensitiser (S) which results in the formation of the excited state of the dye (S*). The resulting electron from the valence band of the excited dye (S*) is injected into the conduction band (CB) of the metal oxide and subsequently moves to the counter electrode. Meanwhile, the excited dye (S*) is reduced by the electrolyte and the cycle is completed when the electrolyte is regenerated by the electron from the counter electrode (Figure 2.3). The theoretical maximum power-conversion efficiency of such systems is called the “Shockley-Queisser limit” and is approximately 32%.[123]

For fast electron injection, a potential difference between the lowest unoccupied molecular orbital of the dye sensitiser and the CB of the metal oxide is essential.[124] In order to improve the power-conversion efficiencies, various research has been carried out to understand the chemistry and device fabrication of DSSCs.[124-125]

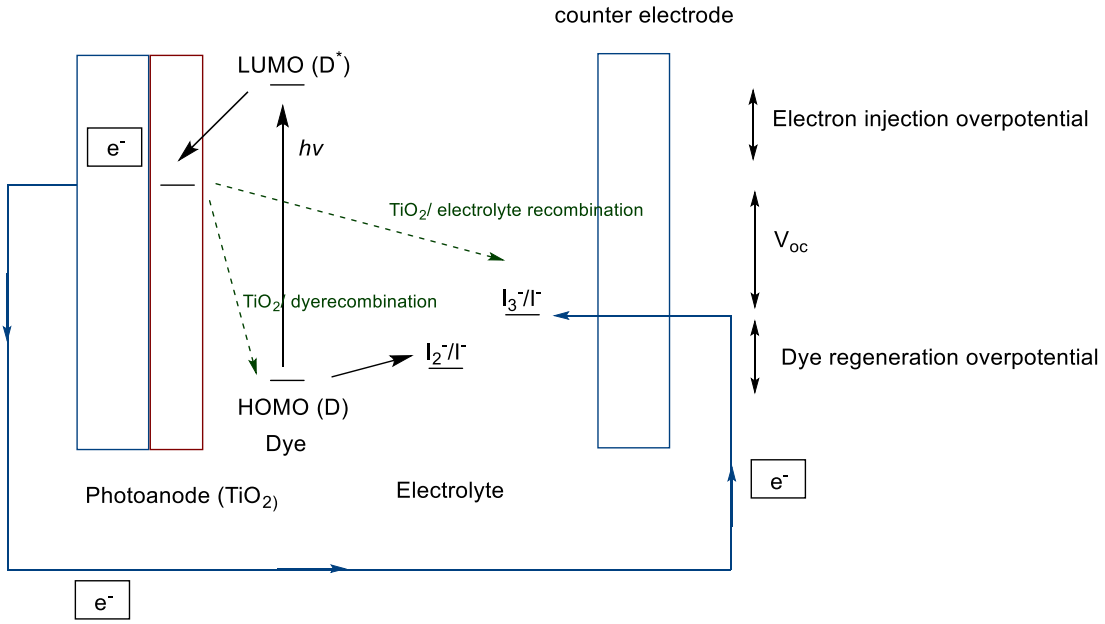

Figure 2.3. Schematic illustration of a DSSC.

In addition, to optimise the dye sensitiser characteristics (discussed later in Section 1.3), various improvements to the other features of DSSCs were investigated.[116c, 126] One method to raise the efficiency of DSSCs involves the use of new redox couples instead of the well-known iodide electrolyte. Even though other redox couples were considered somewhat inefficient in previous studies, new results have proven somewhat more optimistic.[116c, 126e, 127] Researchers have overcome earlier problems associated with alternative redox couples such as high recombination rates and poor performance. They have shown an increase in power-conversion efficiencies for ferrocene Fc/Fc^{+}[126e, 127d],Cu^{+}/Cu^{2+}[116c, 127a-c], all-organic electrolytes[126d, 128] and cobalt Co^{2+}/Co^{3+} systems.[116c, 127a-c] The reason for this improvement in performance was the insulating technique made popular by Grätzel[127a] with his famous donor-π-acceptor dye **2.1** (Figure 2.2) increasing the voltage by 16% compared to iodine-based redox couple. Hereby, the $Co^{2+}$and Co^{3+} ions are surrounded by ligands with bulky groups that operate as insulating spacers and therefore, slow down the recombination process between the electrolyte and the TiO_2.[127a]

Other attempts to improve the performance of DSSCs are the use of solid hole conductors, which can create high voltages,[126c] surface-treatment of the oxide to prevent recombination[126b] or the scattering of light with small titania particles to increase the path length within the cell.[116c, 122, 126a, 129]

2.1.3 Push-Pull Porphyrin Systems as Dye Sensitisers

Contemporary push-pull porphyrins for DSSCs bear a nitrogen-based electron donor and a carboxylic group as an electron acceptor (Figure 2.4). Porphyrins have proven to be very suitable for the π-spacer moiety. In recent years, research has focused on these systems due to their broad and intense absorption properties. In addition, the intramolecular charge transfer (ICT) characteristic of these molecules favours a fast and efficient electron injection.[130] Highlights of such systems with different donor units are detailed below.

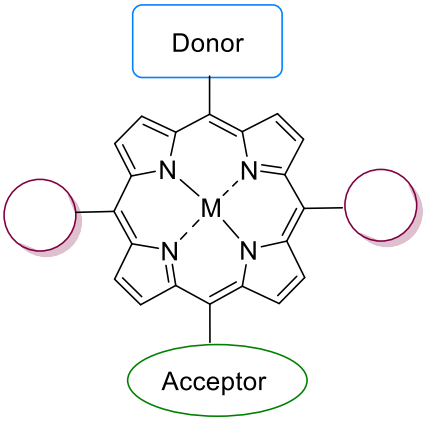

Figure 2.4. Schematic push-pull porphyrin.

2.1.3.1 meso-Diarylamino Porphyrins

meso-Diarylamino porphyrins have gained a lot of attention due to the pioneering work of Grätzel's group. In 2010, Grätzel and co-workers produced the first DSSC sensitised with a porphyrin with a *η*-value of over 10% (Figure 2.5, **2.4**).[131] Their acceptor unit normally features a carboxylic functionality. Modification of the electron acceptor caused a broadening of the absorption in the visible spectrum and lead to the increased PCE.[23,24] Another approach to increase the light-harvesting ability of porphyrins is to introduce several diarylamino groups. Imahori *et al.* designed a series of zinc porphyrins with diarylamino groups at the meso-position (Figure 2.5, **2.3**).[120e] The replacement of one carboxyphenyl group with a carboxyphenylethynyl group and one carboxyphenyl group with a bulkier mesityl group (Figure 2.5, **2.5**) lead to an enhancement of the absorption properties compared to **2.3** (Figure 2.5).[120f]

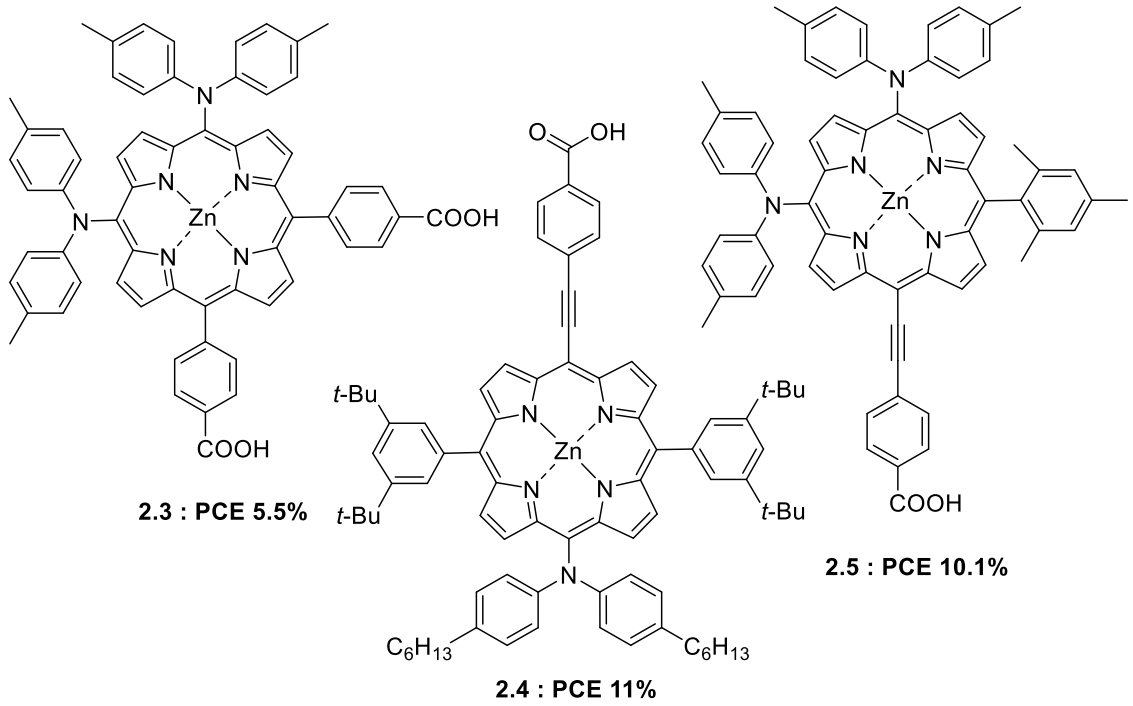

Figure 2.5. Selected examples of meso-Diarylamino porphyrins: **2.3, 2.4** and **2.5**.

2.1.3.2 *Dialkylaminophenylethynyl Porphyrins*

Another moiety which has been used quite frequently for push-pull porphyrins is the dialkylaminophenylethynyl group. The absorption spectrum of **2.6** (Figure 2.6), which was synthesised by Lin and Diau *et al.,* displayed a broadening and red-shift in comparison to that of compound **2.4**. Further modifications led to **2.7** in which the alkoxy chains should lessen the dye aggregation on TiO_2 and the charge recombination (CR) of electrons in the CB of TiO_2 and I_3^- of the electrolyte.[120f] The *η*-value of **2.6** amounted to 9.34% and the *η*-value of **2.7** to 10.2%. Pizotti *et al.* synthesised tetra-substituted bis-(3,5-*di-tert*-butylphenyl)porphyrins with a dimethylaminophenylethynyl and a carboxyphenylethynyl group at the *β*-position.[120d] The absorption spectra of these compounds were less red-shifted and broadened compared to the spectra of **2.6** and **2.7**. The *η*-value for DSSCs with these sensitisers revealed a slightly higher value compared to **2.6**.

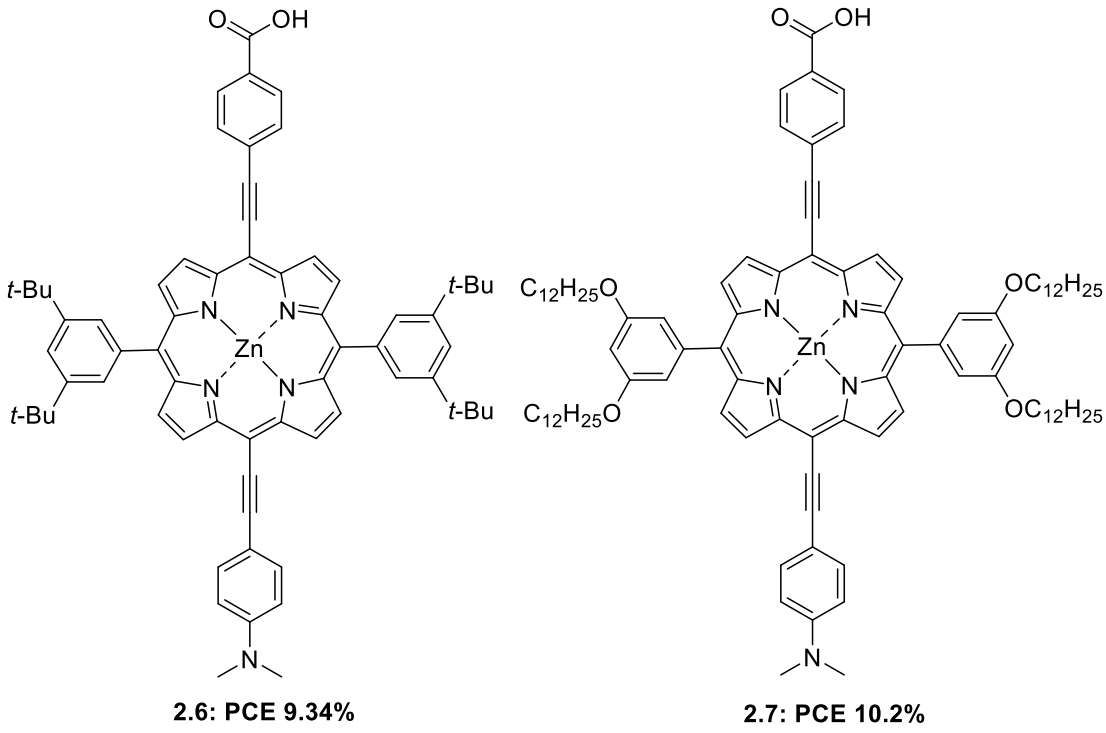

Figure 2.6. Selected examples of ialkylaminophenylethynyl porphyrins: **2.6** and **2.7**.

2.1.3.3 Triarylamine-substituted Porphyrins

Push-pull porphyrins with triarylamine moieties have been reported by Kim *et al.* [120c] and Hung *et al.*[120a, 120b] Porphyrins with multiple anchoring groups, such as **8** or **2.9** (Figure 2.7), are more efficient when it comes to photo-stability relative to porphyrins with just one anchoring group. Overall push-pull porphyrins with triarylalkyl moieties show lower cell performances due to their light-harvesting ability.[117]

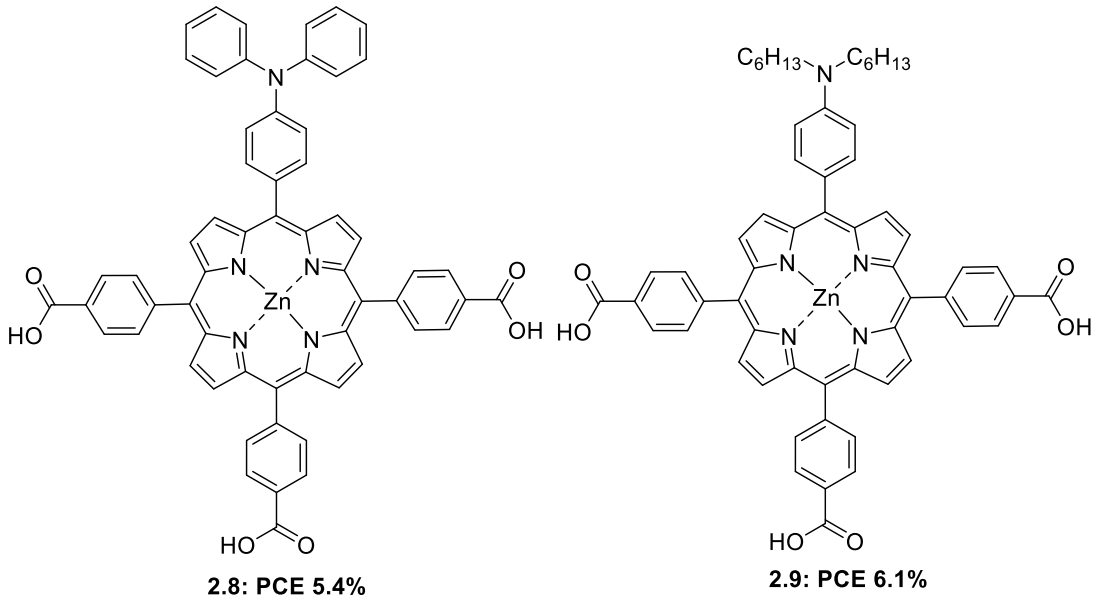

Figure 2.7. Selected examples of triarylamine-substituted porphyrins: **2.8** and **2.9**.

2.1.4 Dipole Moment of Push-Pull Porphyrins

Grätzel's successful series of 5,15-disubstituted push-pull porphyrins[116b, 116c] triggered the synthesis of numerous variations of these donor-acceptor systems. Nearly all of the published work in this field involves 5,15-disubstituted porphyrins where the dipole moment is oriented along the meso-meso axis of the porphyrin. Sessler *et al.,* however, published a series of porphyrin systems where the altered dipole moment runs along the meso-*β* axis.[56, 132] Even though they proved to have a much lower efficiency than the systems Grätzel developed, they still show that a change in the dipole moment can lead to an altering of the solar energy conversion. While 5,15-disubstituted porphyrins have been heavily studied for applications in DSSCs, their 5,10-disubstituted counterparts remained nearly disregarded. This might be due to their difficult synthesis, and therefore, the 5,10-disubstituted counterparts - with the dipole moment along the β-β axis (Figure 2.8) are only now emerging as candidates in DSSC studies.[133] Furthermore, this kind of dipole orientation has proven to enhance many electronic properties of porphyrins such as the non-linear absorption response. Previous work has shown that 5,10-disubstituted porphyrins exhibit a unique reverse saturable absorption (RSA) to saturable absorption (SA) switch under ns irradiation.[134] This is a feature which is very beneficial in the field of NLO and nonexistent in 5,15-disubstituted systems.[135]

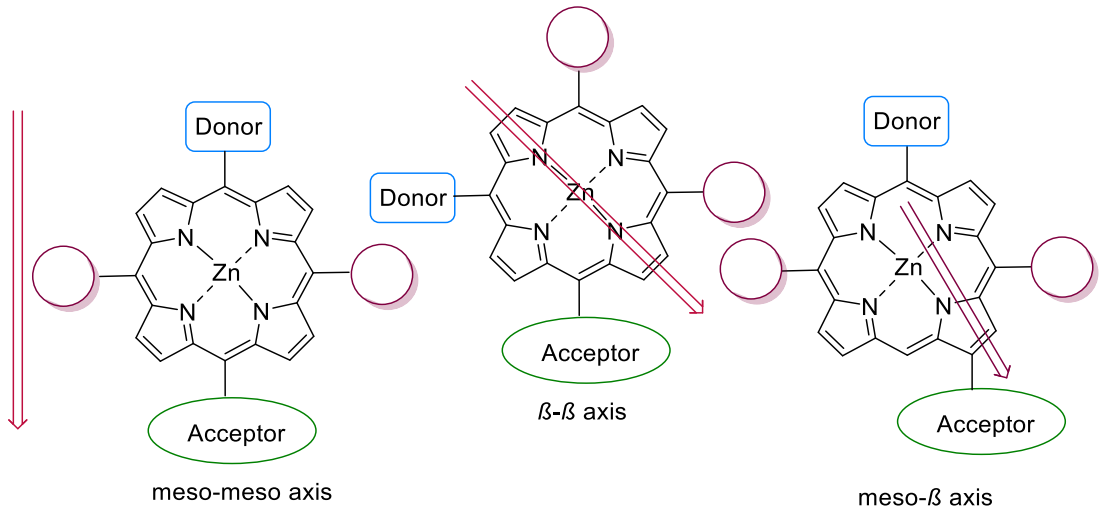

Figure 2.8. Dipole moment orientations in different push-pull porphyrins.

2.2 Objectives

Even though the number of renewable energy technologies is growing, its percentage of the global final energy consumption was estimated at 18% in 2018. To overcome humanity's energy crisis major improvements in this sector are necessary. One of the most promising alternatives besides hydropower is the generation of electricity by converting solar energy. Although this seems to be a very promising solution for the worldwide energy shortage, the full potential of this method has still to be trapped. The rising demand of suitable dyes for DSSCs and other applications such as for electron transfer applications, photosensitisers in PDT just to name a few, inspired us to investigate and compare different synthetic strategies towards unsymmetrically substituted push-pull porphyrins. To expand on the previously mentioned examples of 5,15-type derivatives, these methods were not only utilised on 5,15-disubstituted porphyrins but also on 5,10-disubstituted push-pull porphyrins.

We aimed to synthesise a library of 5,10-disubstituted and 5,15-disubstituted push-pull porphyrins in an attempt to fine-tune the light harvesting properties and maximise the solar energy conversion of these compounds (Figure 2.9). Previous work pioneered by our group gives access to these formerly esoteric compounds through the development of simple and rational syntheses *via* stepwise functionalisation (Chapter 1.3) and will be used for such synthetic protocols.[136] These advancements replaced more cumbersome mixed condensation reactions[136] and made the synthesis of almost every unsymmetrically meso-

substituted porphyrin possible. Our methodologies combine well-known synthetic tools, such as condensation reactions or transition metal catalysed reactions, with strategic planning resulting in a stepwise functionalisation of these precious promising systems. Notably, our step-wise approach enables researchers to easily fine-tune optical and electronic properties of these molecules by synthesising complicated donor or acceptor units separately and introducing them in a one-step reaction to the porphyrin rather than building them on the porphyrin core.

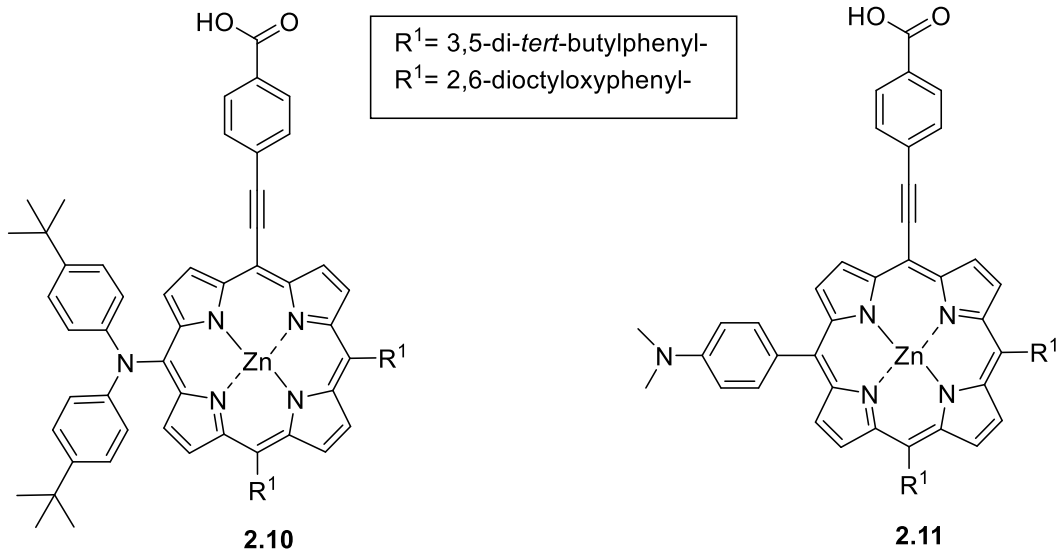

Figure 2.9. Target compounds **2.10** and **2.11**.

The compounds chosen as examples for this study are based on the most prominent porphyrins used in DSSC studies at the onset of this work and an investigation was undertaken in order to compare synthetic strategies and optimisations with a special focus on comparing the synthesis of 5,15- and 5,10-disubstituted push-porphyrins.

2.3 Discussion and Results

Historically, porphyrins have been synthesised through mixed condensation reactions, which are tedious and cumbersome. Senge *et al.* pioneered rational synthetic methods to synthesise unsymmetrically substituted porphyrins.[136] To achieve the desired targets in this work the 5,10-disubstituted porphyrins were functionalised in a step-wise manner implementing halogenation reactions, metal

insertions, and metal-catalysed reactions such as Buchwald-Hartwig amination[137] and Sonogashira cross-coupling reactions.[138] Another approach to introduce a meso-substituent are organolithium reactions which have been also intensively studied by our group.[50-54] Scheme 2.1 and 2.2 show the retrosynthesis of the target molecules.

2.3.1 Overview of the Buchwald-Hartwig pathway

In order to investigate different series of push-pull porphyrins, two distinctive approaches towards these systems were designed. As mentioned above the first approach, here called the Buchwald-Hartwig pathway (Scheme 2.1), involved the synthesis of the 5,10- or 5,15-disubstituted[139] starting material followed by monobromination and metal insertion.

In the next step, the electron donor unit was installed through a Buchwald-Hartwig amination reaction, which unfortunately proved to be plagued with numerous challenges and had to be subjected to various optimisations. The following step involved another bromination prior to the attachment of the electron acceptor unit *via* Sonogashira cross-coupling reaction. By removing the silyl-deprotection step, which has been used in previously reported approaches and had also been investigated in our group in earlier studies[140], and introducing the acceptor group as the ester both, the yield and purification, of this late stage compound, were improved. The one-step introduction for both the donor and acceptor groups allows for complex groups to be synthesised separately, rather than built on the porphyrin core – allowing for a more rational and high-yielding synthesis of diverse electronic systems.

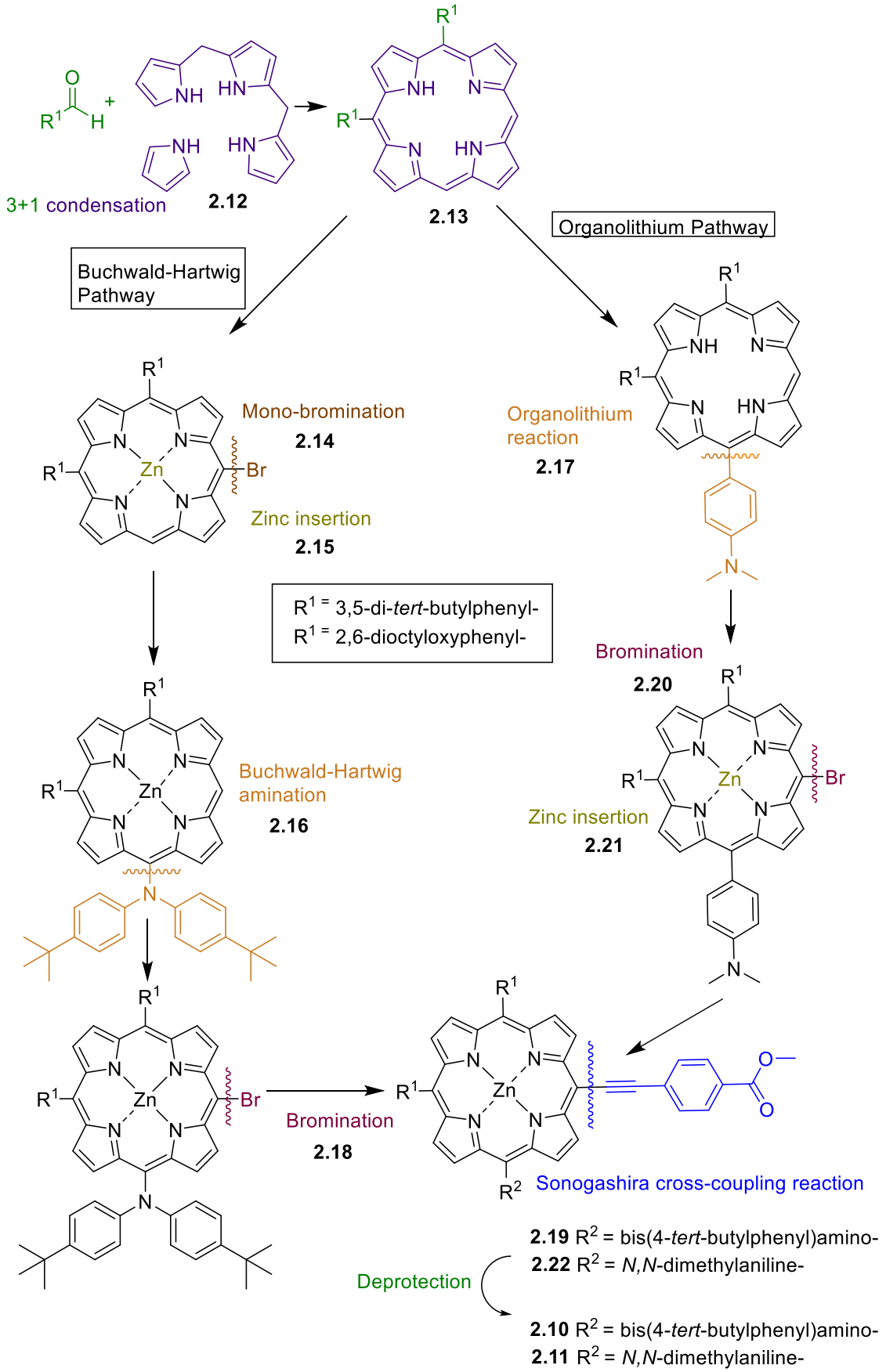

Scheme 2.1 Buchwald-Hartwig pathway and organolithium pathway.

2.3.2 Overview of the Organolithium Pathway

Besides the Buchwald-Hartwig amination, organolithium reactions were employed to vary the donor unit. Organolithium reactions have proven to be a very advantageous method to attach various alkyl or aryl moieties to the porphyrin *via* a nucleophilic reaction without any further modifications of the porphyrins, making this a widely used tool in porphyrin chemistry.[7, 47, 61, 74b, 130c, 51] In addition, this approach proved to be less dependent on substituent effects than the Buchwald-Hartwig amination, making long optimisations redundant. Furthermore, with this method, it was possible to synthesise aminated porphyrins **2.18** in yields comparable to the other amination reaction (e.g., **2.16**), but in much shorter time (Scheme 2.1). Hence, this type of reaction provides an advantageous way of introducing a donor-unit to the 5,10-disubstituted porphyrins compared to the Buchwald-Hartwig amination.

2.3.3 Synthesis of 5,10-Type Precursors *via* Condensation Reaction

This work is focused on 5,10-disubstituted porphyrins which can be synthesised in a number of ways, however, they are all laborious (Chapter 1.2). The condensation methodology [3+1][136] was employed to obtain core 5,10-type structures as it is cost-effective compared to total synthesis and provides several hundred milligrams of starting material.

Recent advances by our group have made 5,10-disubstituted porphyrin synthesis practical *via* a so-called "[3+1]" approach.[9a, 30, 136, 141] This involves the condensation of unsubstituted tripyrrane with pyrrole and the desired aldehyde. Even though the monosubstituted species is formed as a side product, the target compound can be easily separated due to large differences in solubility.[7] Thus the method provides a very fast and cost-effective way of synthesising numerous different 5,10-disubstituted porphyrins.

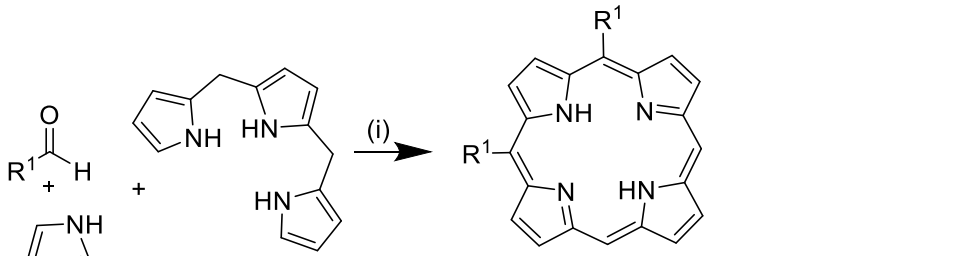

2.12

2.13a R^1 = 3,5-di-*tert*-butylphenyl- (5-7%)
2.13b R^1 = 2.6-dioctyloxyphenyl- (4-7%)

Scheme 2.2. Synthesis of 5,10-disubstituted porphyrins **2.13a** and **2.13b**: (i) (a) TFA, DCM, rt, 18 h (b) DDQ, rt, 1 h.

To obtain the starting material for the future step-wise functionalisation, tripyrrane, pyrrole and the corresponding aldehyde were condensed using TFA as a catalyst. 2,5-Bis(hydroxymethyl)pyrrole[131] and tripyrrane[142] were synthesised according to literature procedures. 5,10-Bis(3,5-di-*tert*-butylphenyl)porphyrin (**2.13a**) and 5,10-bis(2,6-dioctyloxyphenyl)porphyrin (**2.13b**) were obtained using a modified literature procedure in 4-7% yield from the tripyrrane and the corresponding aldehyde (Scheme 2.2).[136, 143]

Numerous different reaction conditions were attempted for each of the two porphyrins. The reaction time, the amount of catalyst and the scale of the reaction were varied according to the different chemical properties of the aldehydes to afford the optimum conditions (Table 2.1). The low yields observed compared to

5,15-disubstituted porphyrins are as a result of polymerisation of about 90% of the tripyrrane.[136] Such behaviour, however, is characteristic for this kind of reaction.

Table 2.1: Optimised reaction conditions for 5,10-disubstituted porphyrins.

Porphyrin	Scale [mg]	Catalyst (TFA)	Time [h]	DCM [L]	Yield [%]
5,10-Bis(3,5-di-*tert*-butylphenyl)porphyrin	920	2.6 mmol (0.63 eq.)	16	1.5	5-7
5,10-Bis(2,6-dioctyloxyphenyl)porphyrin	960	2.6 mmol (0.61 eq.)	16	1	4-7

2.3.4 Synthesis of Brominated and Metallated 5,10-disubstituted Porphyrins

Having porphyrin **2.13a** and **2.13b** at hand they were both selectively monobrominated according to literature protocols with NBS and pyridine.[144] Porphyrins **2.14a** and **2.14b** were obtained in 65% and 78% yields, respectively.[144]

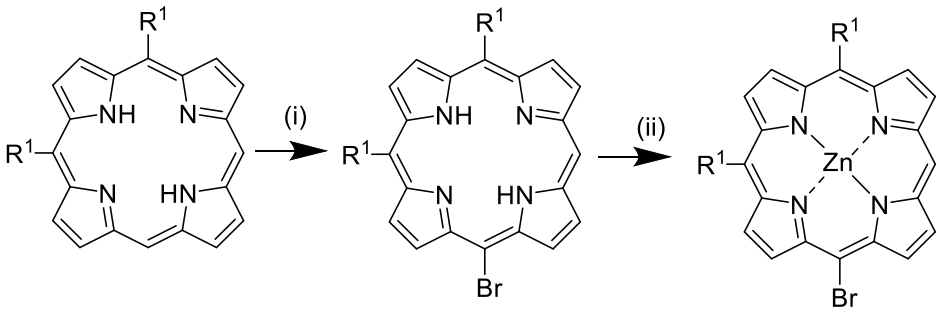

2.13a R^1 = 3,5-di-*tert*-butylphenyl-
2.13b R^1 = 2.6-dioctyloxyphenyl-

2.15a R^1 = 3,5-di-*tert*-butylphenyl- (99%)
2.15b R^1 = 2.6-dioctyloxyphenyl- (97%)

2.14a R^1 = 3,5-di-*tert*-butylphenyl- (57-65%)
2.14b R^1 = 2.6-dioctyloxyphenyl- (50-73%)

Scheme 2.3. Bromination and metallation of 5,10-disubstituted porphyrins **13a** and **13b**: (i) NBS (0.9 eq.), Pyridine (cat.), $CHCl_3$, 0 °C, 1 h. (ii) $Zn(OAc)_2$ (3 eq.), $CHCl_3$, MeOH, rt, 1.5 h.

Despite the fact that only 0.9 eq. of NBS were used and the reaction was performed at 0 °C to direct monobromination, the dibrominated species was still obtained as a side product. Due to their similar polarity, only a mixture of hexane/toluene (3:1, v/v) could separate the two compounds. The zinc insertion

was performed in accordance with the literature at rt for both systems (Scheme 2.3, **2.15a** and **2.15b**).[18]

2.3.5 Synthesis of Aminated Porphyrins *via* Buchwald-Hartwig Amination

To introduce the electron donating group into the porphyrin, a Buchwald-Hartwig amination reaction was chosen (Scheme 2.4). Even though this reaction has been known for a long time[137, 145], it was only recently investigated by Zhang *et al*. in 2003 in relation to porphyrins.[91] This versatile reaction opens the door to a variety of different aminoporphyrins and allows the functionalisation of the porphyrins at meso- and *β*-positions.[146] This functionalisation method was also the method of choice for introducing the electron donor unit in Grätzel's well-known series of zinc porphyrins for dye-sensitised solar cells. Such palladium-catalysed amination reactions are a precious tool in the formation of versatile carbon-nitrogen bonds and they provide access to porphyrins with directly attached arylamino or alkylamino groups.[91] The mechanism is based on a cross-coupling reaction of a brominated porphyrin with an amine. It uses a weak base to minimise the formation of side products and palladium as a catalyst. In this work *N,N*-bis(4-*tert*-butylphenyl)amine was introduced to the porphyrin core (Scheme 2.5). In practice, the reaction was plagued with numerous challenges and initially produced a disappointing yield; thus, numerous optimisation attempts were made. Conditions for optimising the synthesis of 5-bromo-10,15-bis(3,5-di-*tert*-butylphenyl)porphyrinato]zinc(II) (**2.16a**) are shown in Table 2.2. Such reactions are sensitive to water and oxygen, thus, various precautions (e.g., heating of the glassware and starting materials under vacuum) were taken to exclude these factors from the reaction.

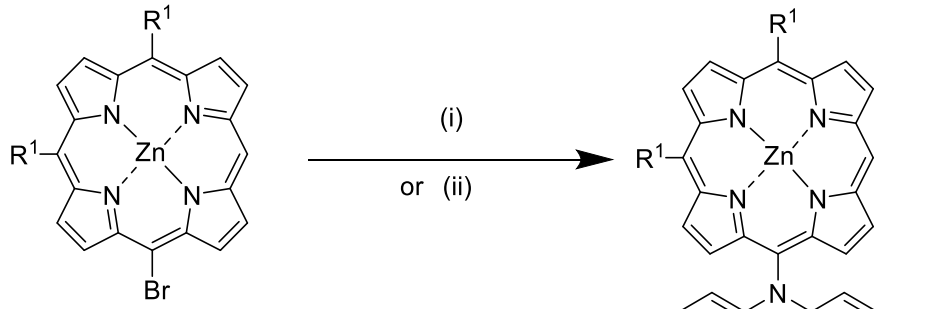

2.15a R^1 = 3,5-di-*tert*-butylphenyl-
2.15b R^1 = 2.6-dioctyloxyphenyl-

2.16a R^1 = 3,5-di-*tert*-butylphenyl- (16-40%)
2.16b R^1 = 2.6-dioctyloxyphenyl- (6-19%)

Scheme 2.4. Buchwald Hartwig amination reaction of porphyrin **2.15a** and **2.15b**: (i) Bench conditions: NaH (for **2.16a**) or Cs_2CO_3 (for **2.16b**), $Pd(OAc)_2$, BINAP, THF, 65 °C, 16-56 h. (ii) MW conditions: Cs_2CO_3, $Pd(OAc)_2$, BINAP, DMF, 160 °C, 6 min.

All reactions were performed under bench conditions at a test scale of 50 mg of porphyrin starting material and loaded with different solvents, catalysts, and bases.

Table 2.2: Optimisation for bench reactions for the synthesis of **2.16a**. Scale of reactions: 50 mg porphyrin.

Reaction	Solvent	Base	Catalyst	Time [h]	Tem perature [°C]	Yield [%]
1	THF	Cs_2CO_3 (2 eq.)	$Pd(OAc)_2$	26	65	27*
2	Toluene	Cs_2CO_3 (2 eq.)	$Pd(OAc)_2$	24	110	39*
3	THF	Cs_2CO_3 (2 eq.)	$Pd(OAc)_2$	30	65	34*
4	Toluene	KO*t*Bu (2 eq.)	$Pd(OAc)_2$	3	110	37*
5	Toluene	KO*t*Bu (2 eq.)	$Pd(dba)_2$	3	110	/
6	Toluene	NaH (4 eq.)	$Pd(OAc)_2$	27	110	78*

* Conversion is estimated, not actual yields since the reactions were on a very small scale, could not be recrystallised and were weighed in a flask

Both reaction 4 and 5 in Table 2.2 by TLC analysis showed complete consumption of starting material after a very short amount of time (3 h); however, reaction 4 yielded only marginal product and only debrominated starting material was obtained from reaction 5. Changing the base to NaH in reaction 6 produced the greatest yield of aminated porphyrin **2.16a**, thus, these conditions were used to upscale the reaction. Performing the reaction with 200 mg of porphyrin afforded its

own problems causing a reduction in the isolated yields (25-40%) of the desired product **2.16a** (Scheme 2.4).

The only disadvantage to this method was the very long reaction times which may be impeding the reaction yield, taking in excess of 27-56 h to afford consumption of all starting material. In an effort to improve reaction times, microwave (MW) assistance was investigated (Table 2.3). Initial attempts using a similar procedure to the bench reaction afforded 16% yield of **2.16a** after 90 min. Altering, the solvent and base *as per* reaction 2 provided compound **2.16a** in 24% yield.

Table 2.3: Optimisation of MW reactions for the synthesis of **2.16a**. Scale of reactions: 50 mg porphyrin.

Reaction	Base	Solvent	Time [min]	Temperature[°C]	Yield [%]
1	NaH	Toluene	90	110	16
2	Cs_2CO_3	DMF	6	160	24

Porphyrin **2.16b** had been previously synthesised within the group using conditions similar to reaction 1 (Table 2.2). Unfortunately, only a yield of 16% was achieved with a considerable amount of debrominated starting material formed as a side product. The formation of dehalogenated side products is a known problem for Buchwald-Hartwig aminations and has been reported before in several papers.[147] In an attempt to improve the yield, MW reactions were attempted under the same conditions as reaction 2 in Table 2.3 and resulted in a 19% yield of compound **2.16b**. Thus, it was decided not to proceed with the MW reaction for the 5,10-substituted porphyrins. The presence of the debrominated starting material was inevitable with such reactions. However, such material could be recycled back into the synthetic pathway affording economic efficiency. Thus, the isolated product was brought forward in the reaction pathway for the addition of the acceptor unit.

2.3.6 Synthesis of Aminated Porphyrins *via* Organolithium Reaction

The second method attempted for the introduction of the donor unit onto the porphyrin core was using organolithium reactions. The meso- and *β*-positions of porphyrins should, in theory, be readily accessible for both electrophilic and nucleophilic substitutions. Furthermore, organolithium reactions have proven to be a very advantageous method to attach various alkyl or aryl moieties to the

porphyrin *via* a nucleophilic reaction without any further modifications of the porphyrins, making them a powerful tool.[50, 52-54, 148]

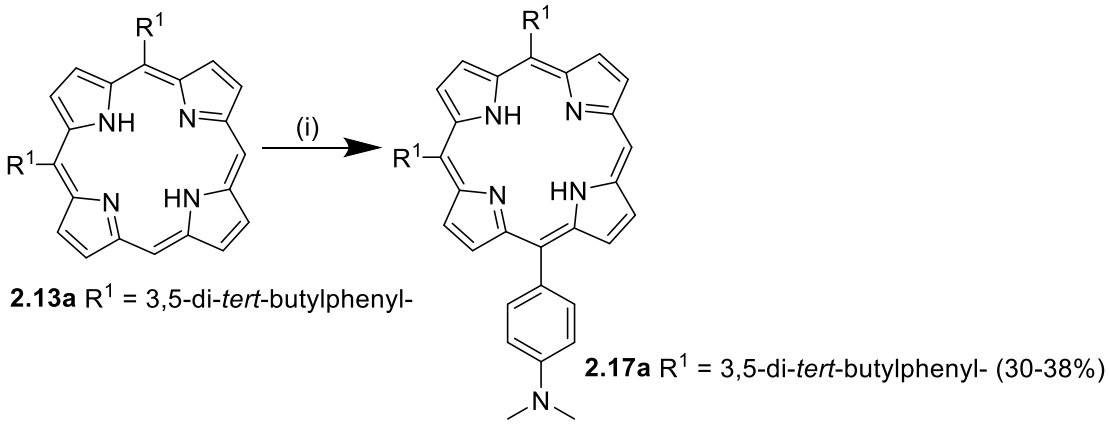

Scheme 2.5. Organolithium reaction of porphyrin **2.13a**: (i) (a) 4-Bromo-4-*N,N*-dimethylaniline, *n*-BuLi, Et_2O, 0 °C, 1 h, (b) rt, 1 h, (c) THF, rt, 2 h, (d) sat. NH_4Cl, rt, 20 min, (e) DDQ, rt, 1 h.

To utilise this methodology an *in situ* generated organolithium reagent has to be synthesised first. This is achieved by adding *n*-BuLi dropwise over an hour to the desired halogenated substituent. A solution of the porphyrin is then added to the mixture to form the substituted porphyrin. More specifically, to synthesise porphyrin **2.17a** (Scheme 2.5), firstly the organolithium reagent had to be prepared *via* a halogen-metal-exchange reaction. Therefore, *n*-BuLi was added dropwise to 4-bromo-4-*N,N*-dimethylaniline in dry diethyl ether at 0 °C. The reaction was stirred for 1 h at rt before the porphyrin was added. After 2 h the porphyrin was hydrolysed, followed by oxidation with DDQ. The first attempt of this reaction resulted in trace amounts of the desired substituted compound, hence optimised conditions were explored. One explanation for this unsuccessful attempt was a lack of lithium reagent formation. The halogen-lithium exchange reaction was stirred for 1 h at 0 °C while *n*-BuLi was added. After a careful review of the literature,[149] it was decided to let the reaction stir for another hour at rt, to complete the conversion. In addition, all starting materials were dried under vacuum prior to the reaction and the porphyrin was stirred for 2 h with the organolithium reagent instead of the 1 h suggested by the literature,[149] resulting in a yield of 30-38% of porphyrin **2.17a**.

Since the Buchwald-Hartwig reactions proved to be quite time-consuming and the observed yields did not legitimate such long reaction times, organolithium

reactions were explored as an efficient alternative. Indeed, it was possible to synthesise aminated porphyrins in the same yield as with the Buchwald-Hartwig amination in much shorter time. In addition to this, fewer optimisations had to be explored and the few optimisations made could be directly applied to various porphyrin systems without further changes. Hence, this type of reaction provides a superior way of introducing a donor-unit to the 5,10-disubstituted porphyrins compared to the Buchwald-Hartwig amination.

2.3.7 Attachment of the donor unit *via* Sonogashira cross-coupling Reaction

Sonogashira cross-coupling reactions are well established especially with regard to their advantages in C-C bond formation with porphyrin scaffolds (Chapter 1.3).[150] This high yielding reaction was chosen to introduce the carboxylic acid group to the porphyrins in this project. It is a palladium- and copper-catalysed cross-coupling reaction which involves the oxidative addition of the halogenated porphyrin to the palladium catalyst. At the same time, a copperorgano species with the alkyne is formed in the second catalytic cycle. In the next step, a transmetallation takes place which leads to the halide-elimination followed by the final reductive elimination. Before the Sonogashira cross-coupling reaction was performed the porphyrins were brominated on the meso-position according to literature procedure.[116b] This time cooling to 0 °C was unnecessary since the bromination occurred selectively (Scheme 2.6, **2.18a**).

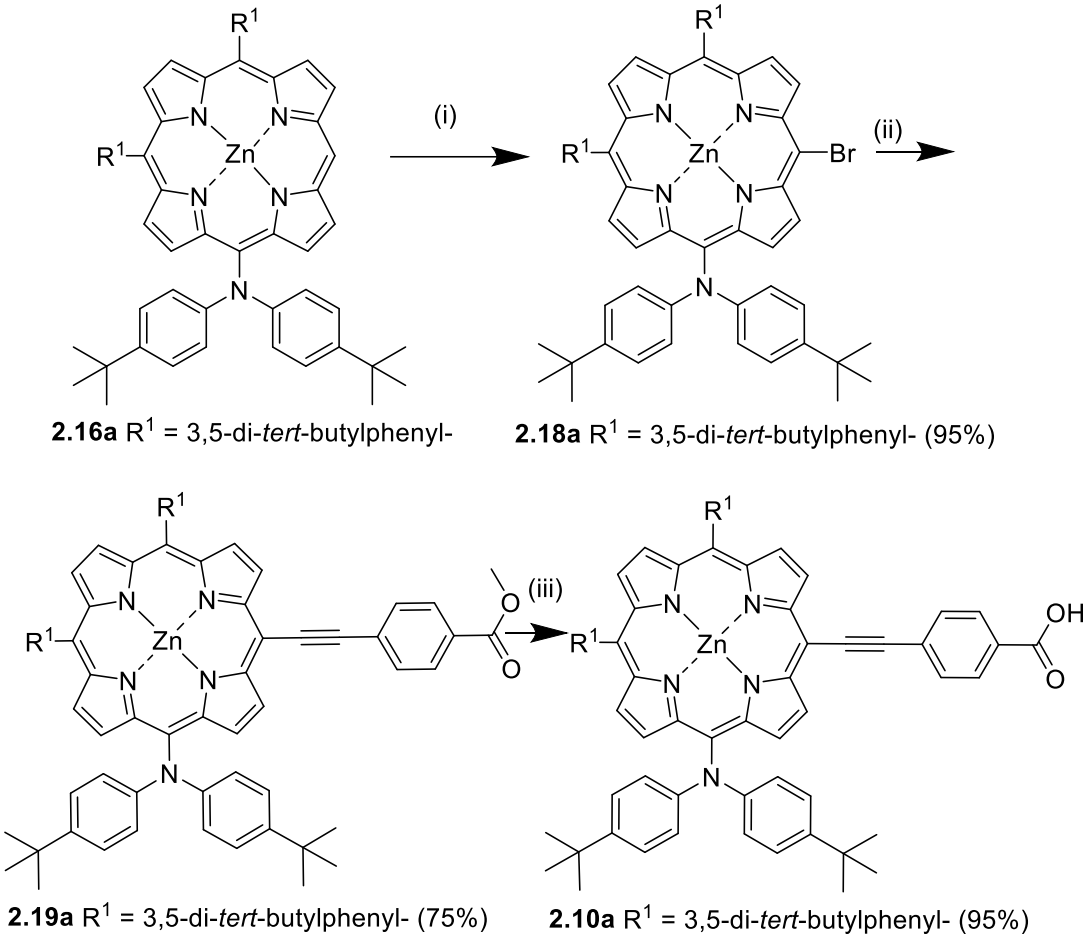

Scheme 2.6. Sonogashira cross-coupling reaction of porphyrin **2.18a**: (i) NBS, pyridine, $CHCl_3$, rt, 1 h. (ii) methyl-4-ethynylbenzoate, $PdCl_2(PPh_3)_2$, CuI, DMF, 120 °C, 16 h. (iii) NaOH, MeOH, THF, 65 °C, 16 h.

Under Sonogashira conditions compound, **2.19a** was afforded in a good yield of 75% and subsequent deprotection of **2.19a** with excess of NaOH and MeOH produced the final target porphyrin **2.10a** in quantitative yield. The second donor scaffold **2.17a**, obtained *via* an organolithium reaction, was metallated to avoid Cu or Pd insertion into the porphyrin core and then brominated (Scheme 2.7, **2.20a** and **2.21a**) prior to further manipulation. This reaction was performed without any difficulty and resulted quantitative in product **2.22a**. The next step was again a Sonogashira cross-coupling reaction to install the acceptor unit followed by deprotection to yield the final target porphyrin **2.11a** in 84% (Scheme 2.7).

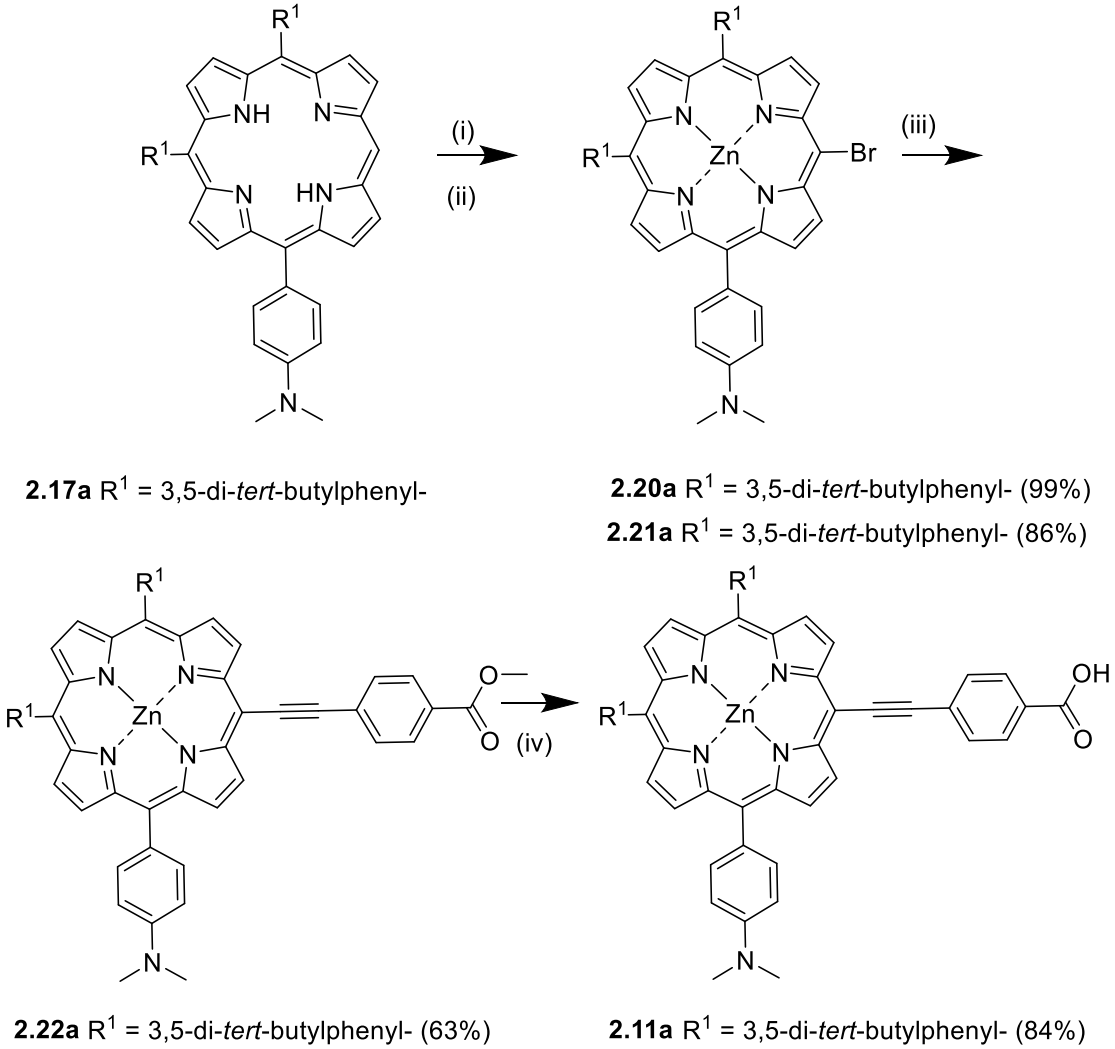

2.17a R^1 = 3,5-di-*tert*-butylphenyl-

2.20a R^1 = 3,5-di-*tert*-butylphenyl- (99%)

2.21a R^1 = 3,5-di-*tert*-butylphenyl- (86%)

2.22a R^1 = 3,5-di-*tert*-butylphenyl- (63%)

2.11a R^1 = 3,5-di-*tert*-butylphenyl- (84%)

Scheme 2.7. Sonogashira cross-coupling reaction and deprotection of porphyrin **2.21a**: (i) NBS, Pyridine,$CHCl_3$, rt, 1 h. (ii) $Zn(OAc)_2$, $CHCl_3$, MeOH, rt, 1.5 h. (iii) Methyl-4-ethynylbenzoate, $PdCl_2(PPh_3)_2$, CuI, DMF, 120 °C, 16 h. (iv) NaOH, MeOH, THF, 65 °C, 16 h.

2.3.8 Synthesis of 5,15-A_2BC D–A-systems

2.3.8.1 Buchwald-Hartwig versus organolithium pathway.

The 5,15 counterparts to **2.10a** were synthesised using the same methods described above (Scheme 2.8). For the Buchwald-Hartwig pathway, the 5,15-disubstituted starting materials were mono-brominated giving compounds **2.24a**. Even though the formation of dibrominated side product was tried to be minimised, it could not completely be avoided.

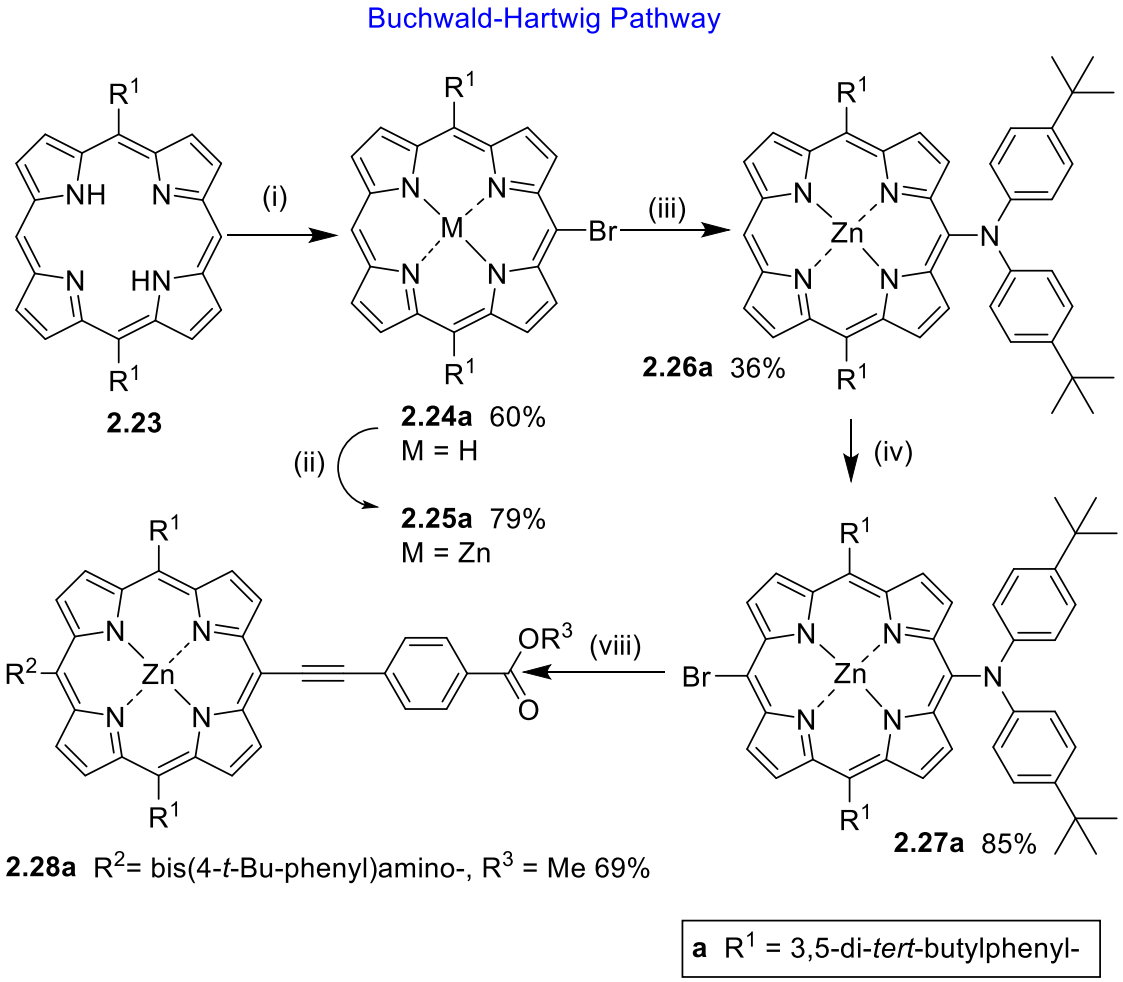

Scheme 2.8. Synthesis of A_2BC 5,15-disubstituted porphyrins *via* Buchwald-Hartwig amination and Sonogashira cross-coupling reactions. (i) NBS, pyridine, $CHCl_3$, 0 °C, 1 h. (ii) $Zn(OAc)_2$, $CHCl_3$, MeOH, rt, 1.5 h. (iii) *Bench conditions:* Cs_2CO_3, $Pd(OAc)_2$, *N,N*-bis(4-*tert*-butylphenyl)amine, BINAP, THF, 65 °C, 16 h; *MW conditions:* Cs_2CO_3, $Pd(OAc)_2$, BINAP, DMF, 160 °C, 6 min. (iv) NBS, pyridine, $CHCl_3$, rt, 1h. (viii) methyl-4- ethynylbenzoate, $PdCl_2(PPh_3)_2$, CuI, DMF, 120 °C, 16 h.

Preceding the Buchwald-Hartwig amination, zinc was inserted into the core of the porphyrin to avoid metal insertion during the Pd-catalysed reaction and resulted in compound **2.25a** in 79%. In the next step, the previously applied reaction conditions for the Buchwald-Hartwig amination were used to form compound **2.26a**, again debrominated starting material was obtained as unwanted side-product. Thus, compound **2.25a** was subjected to MW reactions in an attempt to optimise the reaction further. The porphyrin was heated to 160 °C for 4 min using Cs_2CO_3, $Pd(OAc)_2$ and BINAP in dry DMF giving **2.26a** in 36%.

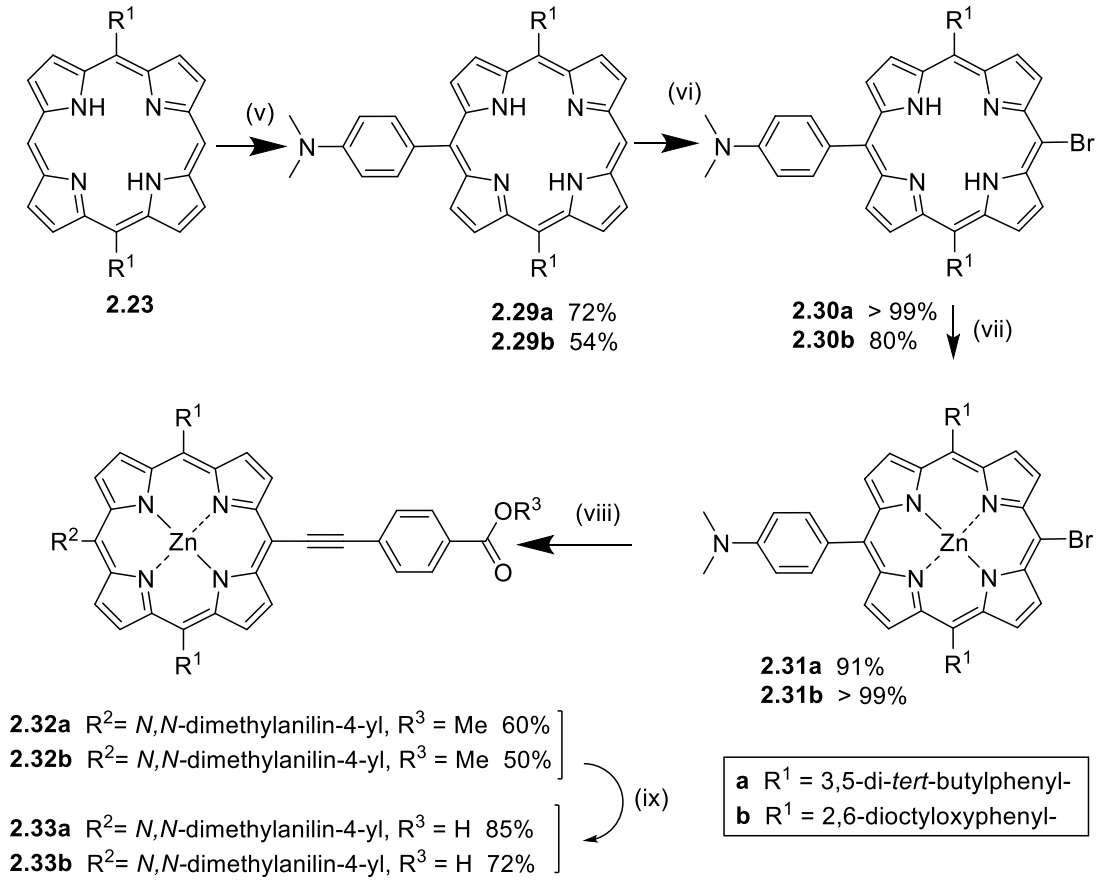

Scheme 2.9. Synthesis of A_2BC 5,15-disubstituted porphyrins *via* organolithium reaction and Sonogashira cross-coupling reactions. (v) (a) 4-Bromo-4-*N,N*-dimethylaniline, *n*-BuLi, Et_2O, 0 °C, 1 h, (b) rt, 2 h, (c) THF, rt, 2-3 h, (d) sat. NH_4Cl, rt, 20min, (e) DDQ, rt, 1 h. (vi) NBS, pyridine, $CHCl_3$, rt, 1 h. (vii) $Zn(OAc)_2$, $CHCl_3$, MeOH, rt, 1.5 h. (viii) methyl-4-ethynylbenzoate, $PdCl_2(PPh_3)_2$, CuI, DMF, 120 °C, 16 h. (ix) NaOH, MeOH, THF, 65 °C, 16 h.

The MW conditions resulted in the same yield for this compound than bench reaction, although in much shorter time. Sonogashira cross-coupling reaction gave porphyrin **2.28a** in high yield. No further optimisations were undertaken for the organolithium pathway since adopting the previously used conditions gave **2.29a** and **2.29b** in 72 and 54%, respectively. Subsequent bromination and metallation of **2.29a** and **2.29b** progressed without difficulties in high yields as well as the Sonogashira cross-coupling reaction and the subsequent deprotection which lead to the final targets **2.33a** and **2.33b** in 85% and 72% (Scheme 2.9).

2.4 Comparision of different synthetic pathways

Both established pathways have their individual strengths. The amination in the organolithium pathway works readily and in good yields for both 5,10-disubstituted and 5,15-disubstituted porphyrins. Another advantage is that bromination is used when three of the four meso positions on the porphyrin core are already occupied. This significantly minimises the loss of compound due to unwanted dibromination. Thanks to optimisations of the Buchwald-Hartwig amination step we were able to find the most promising reaction conditions for these porphyrins. Additionally, the reaction time can be significantly shortened by applying MW conditions. Yields of around 45% were achieved with reaction times of 4-6 min which may provide a synthetic benefit considering DSSC device production. Furthermore, changing the sequence of our synthesis, compared to Grätzel and Imahori[116b, 121, 133, 151] resulted in some practical advantages and simplifications outlined above.

2.5 Conclusions and Future Work

To conclude, two different methodologies towards the functionalisation of 5,10- and 5,15-disubstituted *push-pull* porphyrins related to **2.1-2.3,** which have been used extensively in recent studies on DSSCs, were developed. Due to their prominent feature in current research as sensitisers for DSSCs, a comparative investigation was undertaken to focus on synthetic optimisation and comparison of widely used methods for porphyrin chemistry. These strategies proved that the step-wise functionalisation of porphyrins is a superb synthetic route and can be easily adapted to other porphyrin systems and therefore allows access to a library of various unsymmetrically substituted “push-pull” porphyrins. The methods of choice included selective brominations, organolithium reactions as well as Pd-catalysed cross-coupling reactions. This allowed us to achieve the desired functionality step-wise in a very controlled and strategic manner. This approach has many advantages; however, its superiority to other comparable approaches lies in its modality. It enables researchers to incorporate modified donor and acceptor units or exchange the functional groups at any time of the synthesis with hardly any effort. Furthermore, complicated donor and acceptor units could be built separately and then introduced to the porphyrin step-wise rather than building them on the porphyrin. In addition, the introduction of the carboxylic ester in one-

step instead of a two-step built on synthesis as previously reported resulted in a simplification of the synthesis due to easier purification. Moreover, the sequence of the functionalisation steps was altered. More functional group tolerance was achieved by introducing the tertiary amine prior to the carboxylic acid. The desired target compounds were obtained in moderate to good yields. Condensation reaction for 5,10-disubstituted porphyrins, the Buchwald-Hartwig amination reaction, as well as the organolithium reaction was optimised and applied to yield the desired target compounds in moderate to good yields. Besides this MW conditions were explored for the Buchwald-Hartwig amination reaction which resulted in an impressive reduction of the reaction time to just 4 min. Overall, it can be said that the organolithium reaction is a feasible alternative to the Buchwald-Hartwig amination. Future work includes the tesing of the synthesised sensitisers in DSSCs and the comparison of the efficiency of the 5,15-disusbtituted and 5,10-disubstituted porphyrins as well as further fine-tuning of the electronic properties of the push-pull porphyrins.

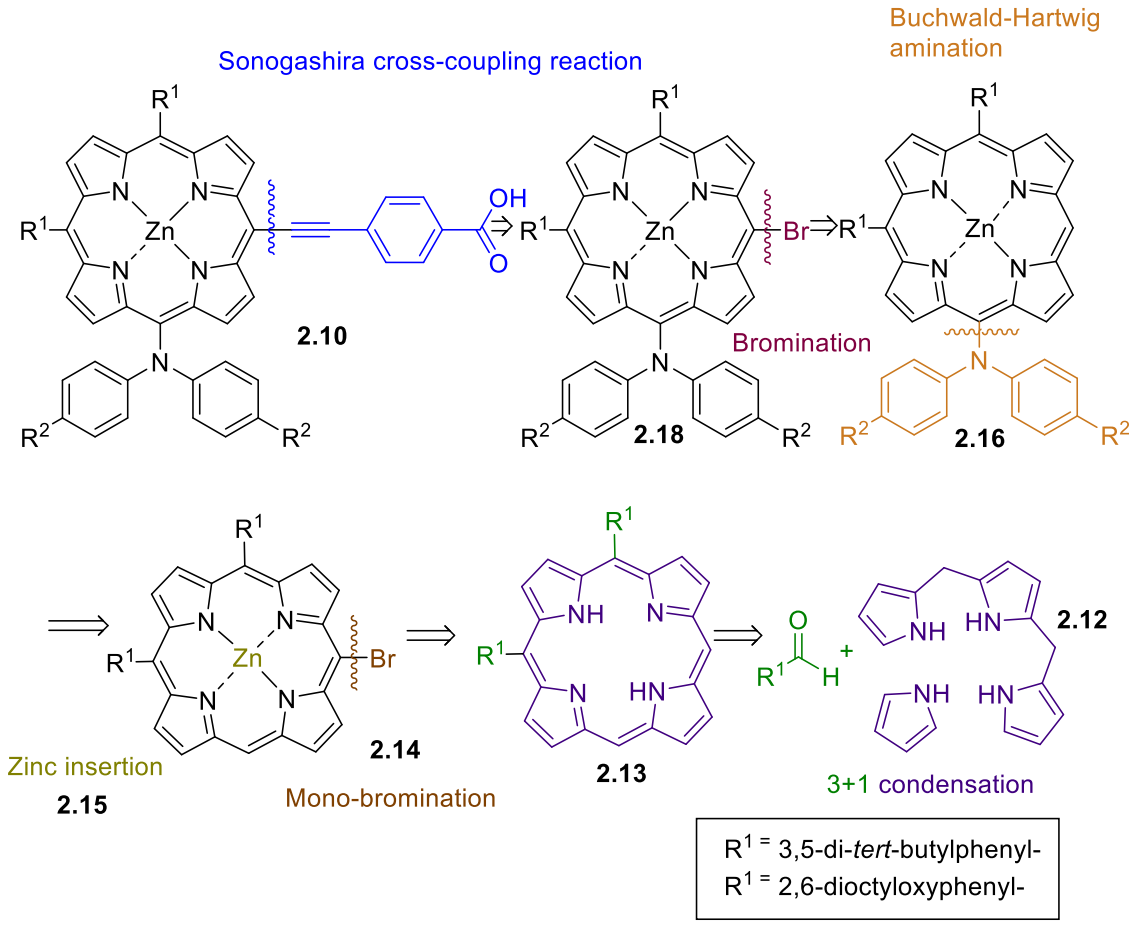

Scheme 2.10. Retrosynthesis of target sensitiser **2.10** *via* Buchwald-Hartwig amination.

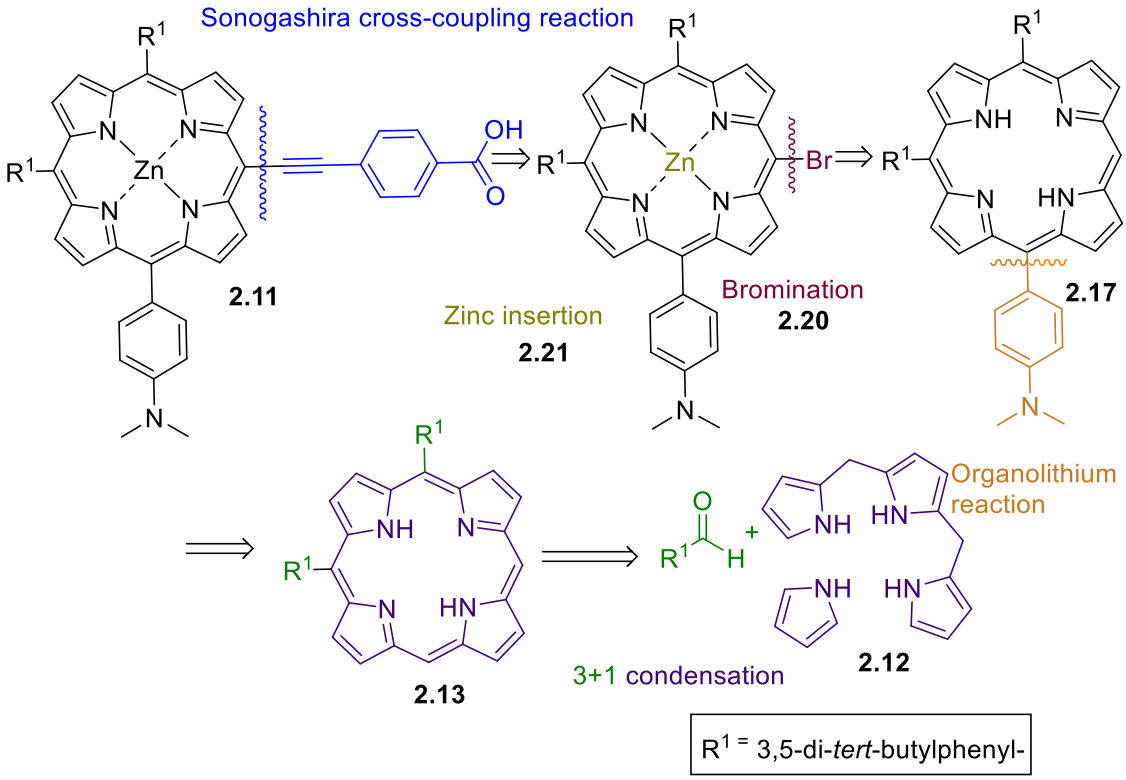

Scheme 2.11. Retrosynthesis of target sensitiser **2.11** *via* organolithium reaction.

3 Connecting two systems – Cubanes and Porphyrins

3.1 Cubane – a forgotten linker system with great potential

The goal of this chapter is to describe how to connect a porphyrin with a cubane molecule. Cubanes are perfectly shaped cubes made out of carbon atoms. Despite their simple shape and discovery several decades ago, they pose multiple synthetic challenges[152] and limited synthetic tools are available that can modify this molecule. This is unfortunate, as cubanes are widely used as bioisosteres in the pharma industry for medical drug development, molecular electronics and material science.[153]

3.1.1 Synthesis of cubane

The cubane system was historically considered impossible to synthesise due to its 90° arrangement of carbon atoms and the high degree of strain this causes.[154] Therefore, its eventual discovery in 1964 by Phillip E. Eaton and Thomas W. Cole marked a significant achievement for the field. This very simple looking structure only consists of eight methane units which are arranged in a perfect cube.[155] Their synthesis involves two cycloadditions, a diastereoselective Diels-Alder reaction, [2+2] photocyclisation followed by a double ring contraction under Favorskii conditions.[156]

Surprisingly, the original approach developed in 1964 is still the basis of most cubane synthesis methods; only slight modifications have been introduced in the last fifty years.[157] Chapman *et al.,* for example, improved the synthesis of cubanes by implementing the ethynyl ketal of cyclopentanone as a different starting material.[157a] This resulted in intermediates that were easier to handle as well as higher yields of the overall reactions. Another modification was introduced by Tsanaksidis *et al.* in 1997.[157b] They exchanged some of the more corrosive and costly reagents while also amending the purification process of some key intermediates. Furthermore, this allowed the synthesis of cubanes on multi-gram scales in only five steps, making them a viable starting material for further studies.[157c, 158]

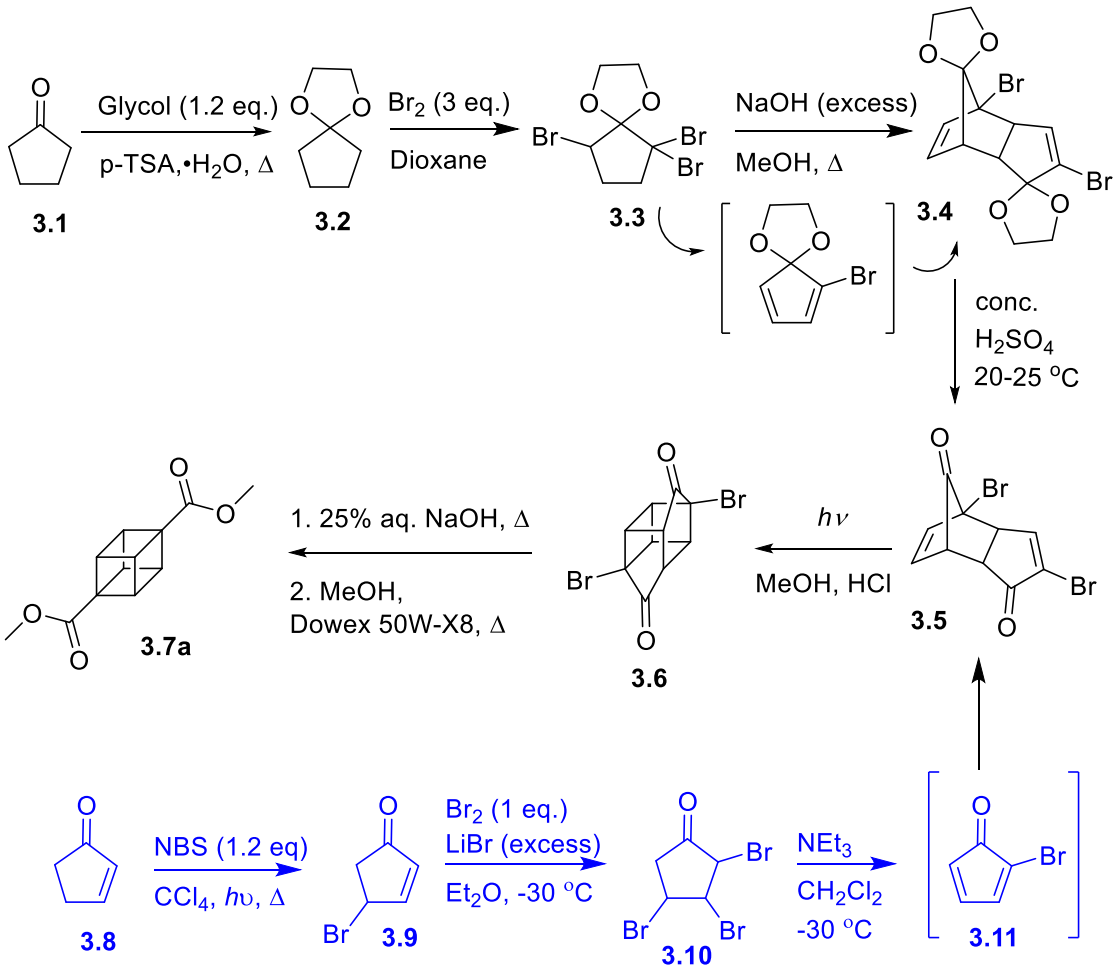

Scheme 3.1. Reported Tsanaktsidis method (black) and original Eaton synthesis (blue) towards the synthesis of dimethyl cubane 1,4-dicarboxylate **3.7a**.

The method developed by Tsanaktsidis starts with the bromination of compound **3.2** resulting in the tribromo-derivative **3.3**. The next step involves an endo-selective [4π+2π] Diels-Alder dimerization (Scheme 3.1). This compound is obtained through a treatment with an excess of NaOH, followed by refluxing in MeOH. The resulting bisethylene ketal is converted into the diketone through stirring in concentrated sulphuric acid. The next step involves a [2π+2π] photocyclisation, as first proposed by Eaton.[156] To obtain the final cubane molecule the caged dione **3.6** is heated in NaOH, which results in a double Favorskii reaction and gives the diacid. One optimisation for the purification of the final product was done through functional group interconversion to the dimethyl cubane-1,4-dicarboxylate followed by sublimation.[157b] The yields obtained for the modified procedure are 42-47% for the synthesis of 5 ->7 whereas Eaton and

Chapman reported around 20% for the same sequence, showing an overall yield of about 25% can be achieved for the whole synthesis.[157b] The resulting diester has been proven to be a very valuable entry point for various functionalisations of the cubane molecule and the optimisation of this reaction sequence has given researchers access to this esoteric molecule.

3.1.2 Cubane-its properties and possible applications

Although few synthetic investigations have been undertaken, the properties of this molecule are quite well known.[159] Cubane's unique geometry results in C-C bonds which are forced to have more p-character while the C-H bonds adopt more s character in order to allow the ring strain. Despite significant ring strain, this molecule has a very high thermal stability with thermal rearrangements occurring only around 200 °C.[160] Furthermore, the physical properties exhibit significant variance compared to other hydrocarbons. This is most likely due to its unique structure. The carbon-carbon distance of cubanes is 1.571 Å.[161] This is slightly longer compared to other unstrained hydrocarbons such as alkanes (1.54 Å) or in cyclobutane (1.55 Å).[161] In addition, the cubane has a relatively high density of 1.29 g/cm^3 [159b] and a strain energy of 161.5 kcal/mol.[162] Due to its high hydrocarbon density, strain energy and kinetic stability, this molecule has been used for fuel as well as a source of combustion.[163] Besides this they are also used in medicinal chemistry as biosisosteres.[164] Most of these small scaffold systems used today contain conjugated groups such as arenes, alkenes or aromatic heterocycles.[165] Not only would the cubane system guarantee a precisely known substitution pattern due to its rigidity, but it is also more favourable in terms of toxicity compared to many other systems used. Besides that, the distance across the cubane of 2.72 Å is comparable to the distance of a benzene linker of 2.79 Å, making it a desirable target as a nontoxic alternative for this bioisostere.[161, 166]

In 1971 the first drug containing a cubane-scaffold was developed. This compound exhibited antiviral properties, in particular against the influenza virus.[167] Other examples followed later on, such as dipivalylcubanes with anti-HIV activity and diphenylcubanes for anti-cancer treatment.[167] The cubane scaffold in these drugs allows easier crossing of cell membranes due to their higher lipophilicity as well as lower toxicity. In addition, certain 1,4-disubstituted cubanes can be used to relax

aortas and remove calcium channel blocking.[168] Furthermore, research by Cheng *et al.* has shown that N-cubylmethyl substituted morphinoids show higher activity at the *μ* and *κ* opioid receptors than morphine.[169]

Besides medical applications, cubanes can be used as electronic resistors. Since they are nonconjugated hydrocarbon linkers, they act as an insulator and do not allow electronic communication through the cubane scaffold.

3.1.3 Cubane functionalisation chemistry

Despite their discovery over 50 years ago, cubanes are still a relatively immature field, with little exploration into synthetic functionalisation. The few methods that have been developed for adding functional groups to the cubane include classic carbonyl chemistry. One example is the transformation of a carboxylic acid group **3.12** into iodine **3.13** (Fig. 3.2).

This can be achieved *via* hypervalent iodine oxidative decarboxylation process.[170] For this reaction $PhI(OAc)_2$-CCl_4-I_2 and irradiation are needed. In another reaction type, a phenyl-substituted cubane **3.15** can be obtained from a fluorocubane **3.16**. The cubane is reacted with benzene and boron trifluoride in toluene. The desired cubane can be obtained in yields of up to 40%.[171]

Besides this, Wlochal *et al.* prepared a series of substituted cubane molecules with functional handles for use in medicinal chemistry.[172] Their synthesis starts from the commercially available cubane-1,4-dimethyl ester **3.7** and results in various different cubane molecules. Their building blocks contain, among others, pyridine **3.18**, imidazole **3.17**, thiazole **3.16** and benzimidazol units **3.19**.

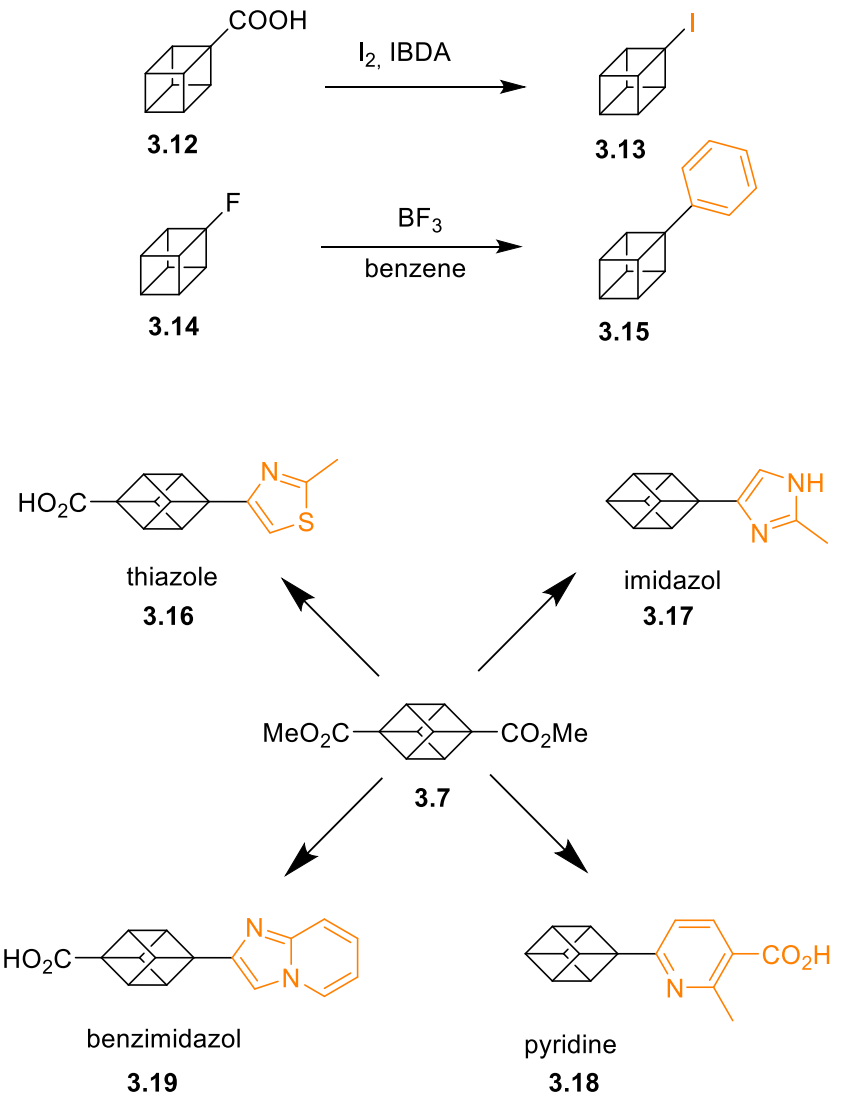

Scheme 3.2. Selected examples of cubane carbonyl chemistry.

Cross-coupling reactions are a major branch in synthetic organic chemistry. Despite their prominence in synthetic porphyrin chemistry, cross-coupling reactions have been somewhat overlooked as a tool for cubane chemistry.

The first cubane-aryl system was reported by Moriarty and Khosrowshahi in 1989. They described a radical functionalisation of the cubane carboxylic acid **3.20** utilising [Pd(OAc)$_4$] and benzene (Scheme 3.3).[173] Unfortunately, this method lacks versatility since it is applicable for a limited number of aryl groups. Ten years later Eaton's group reported a method for synthesising phenyl substituted cubanes **3.23** from the highly reactive cubane-1,4diyl diradical. However, this approach is limited due to the harsh reaction conditions and missing functional group tolerance.[174]

In addition, Plunket *et al*.[175] investigated the use of palladium cross-coupling reactions for cubanes, synthesizing a series of activated cubane molecules *via* organolithium reaction. Through this method, boron, phosphorous, tin, silicon, sulphur and alkyl groups were introduced to the cubane scaffold **3.25**. These molecules were then subjected to cross-coupling reactions such as Suzuki, Negishi and Stille reactions (Scheme 3.2, **3.25**). Unfortunately, this initial approaches with the electrophilic cubanes and halogenated phenyl groups failed due to the instability of the cubane core.[175-176] While the use of palladium catalysts proved unsuccessful, the introduction of redox-active esters to the cubane molecule **3.26** showed more promising results. Recently, the Baran group reported a method involving redox active esters which they later expanded to the synthesis of aryl-cubanes **3.27**.

They managed to couple phenyl groups to the cubane through the use of the organozinc or organomagnesium species in the presence of $Fe(acac)_3$ and dppBz ligand, achieving a 25% yield.[177]

Furthermore, alkyl boronic esters **3.28** can be synthesised with the aid of redox-active esters as well. Li *et al.* showed that through the use of $NiCl•6H_2O$ and a Grignard reagent such as $MgBr_2•OEt_2$, the redox-active cubane ester **3.26** can be coupled with the lithiated bis(pinacolato)diboron. The boronic acid can then be obtained through reaction with boron trichloride.[178]

Pd cross-coupling reactions were finally achieved through the insertion of a linker between the cubane scaffold and the coupling group. This was introduced by the Senge group, resulting in the first stable cubane linked compounds **3.30** in the presence of a palladium catalyst. Furthermore, direct coupling on the cubane scaffold **3.28** was reported by the same group through SET reactions utilising Ni catalysts.[179]

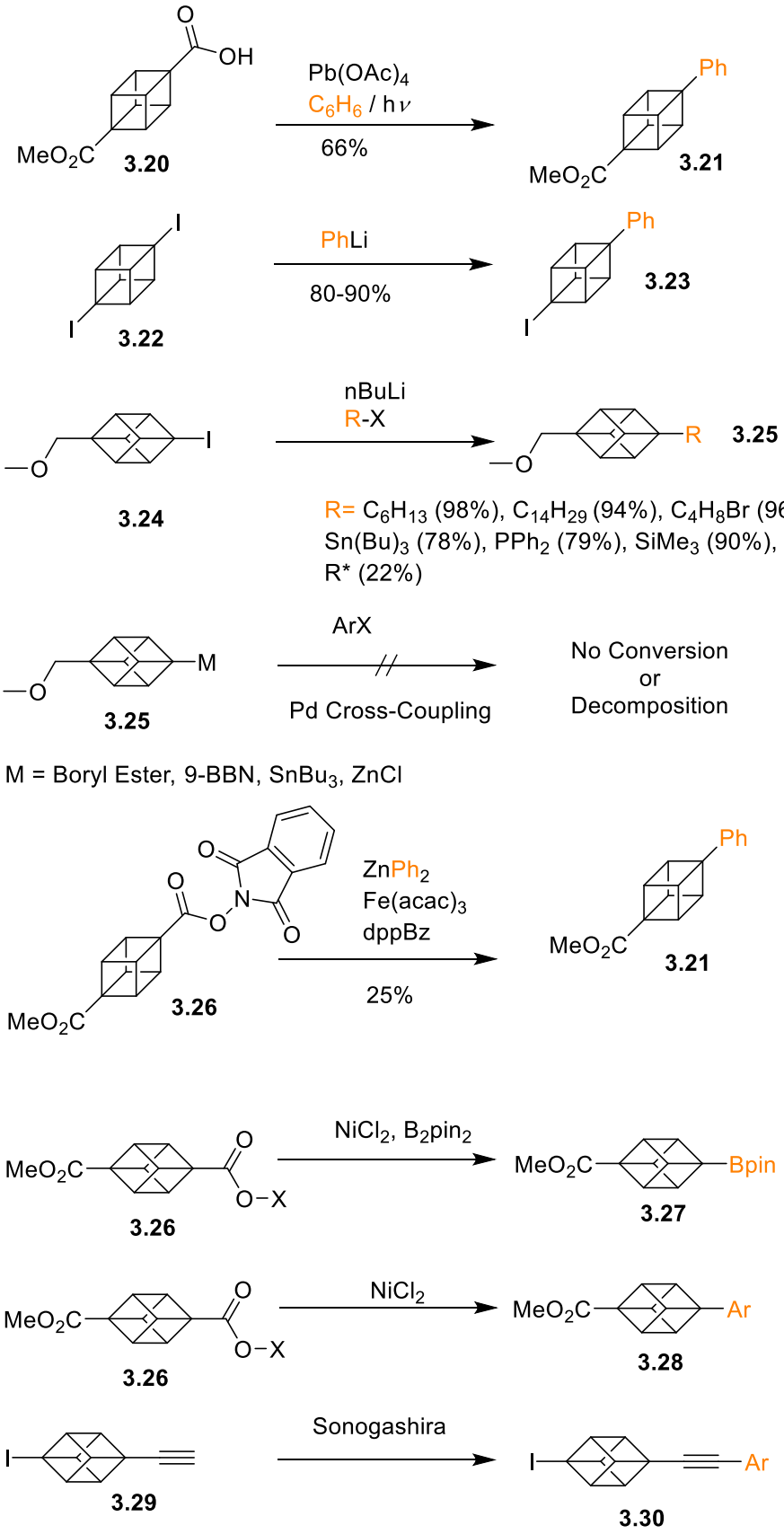

Scheme 3.3. Previous work on cubane coupling reactions.

3.1.4 Linking cubanes and porphyrins directly

The synthesis of directly linked cubane-aryl systems is still a largely unexplored topic in the field of organic synthesis, with the linking of a porphyrin directly to a cubane scaffold remaining entirely un-investigated. This poses an opportunity in the search for new linker systems as the highly strained cubane molecule seemingly has many interesting features as a porphyrin substituent[7, 180] Alkane linkers have been used widely, but this entails using flexible linker, this undesirable characteristic is not shared by the rigid cubane system. [181] Furthermore, due to it being an isolator, cubane bridged porphyrin systems could be interesting targets for electron transfer studies and in the area of organic circuitry. This type of alpiphatically linked bisporphyrins could bear potential as interesting compounds for light harvesting studies since they have never been investigated before.[182]

3.2 Objectives

The primary objective of this study is to gain deeper insights into cubane coupling chemistry, with a special focus on the synthesis of directly linked cubane-porphyrin systems and multi-porphyrin arrays where cubane is the scaffold linker. The ambition of this study is to overcome synthetic challenges associated with the cubane molecule, thus opening up doors for its renaisance. The exploration of electronic properties of such systems is a secondary interest of this study. While models which explore the photosynthetic reaction centre often consist of fullerene, carbon nanostructures[183] or molecular wires[184] as scaffolds for porphyrin systems, truly isolated systems have remained largely un-investigated [100, 185] Therefore, ridgidly, aliphatically linked porphyrin systems are an important class to be examined. The improvement of suitable coupling chemistry for cubane molecules could overcome the lack of available small, rigid and defined sub-units and linkers, thus making compounds which incorporate electronically isolated porphyrin units in a defined geometry and space viable for the first time.

3.3 Synthesis of Starting Materials

Before an investigation into different coupling reactions could be undertaken, various porphyrin starting materials required synthesising. The main 5,15-porphyrin used for these investigations was 5,15-dihexylporphyrin **3.33** due to its superior solubility. Previous work in our group on cubane coupling has shown that

aryl substituted porphyrins tend to become very insoluble after a cubane molecule has been attached. Therefore, in the first step, the 5,15-dihexyl precursors were synthesised according to literature procedure (Scheme 3.4).[23] Initial reactions were based on a scale of 1.2 g DPM **3.31** which resulted in a yield of 26% for compound **3.33**. It was suspected that the general yields for cubane coupling reactions might be quite low and therefore a large amount of this material would be needed. Considering this, as well as keeping in mind the three subsequent functionalisation reactions, it was decided to upscale the condensation reaction in order to obtain more porphyrin material **3.33** in a short amount of time. Therefore, a test reaction was set up utilising 2.4 g of DPM **3.31** under the same reaction conditions as previously. This reaction resulted in a yield of 24% for compound 3.33, which is nearly identical to the reaction carried out on the smaller scale. Hence, it was decided to continue the condensation reactions on the large scale.

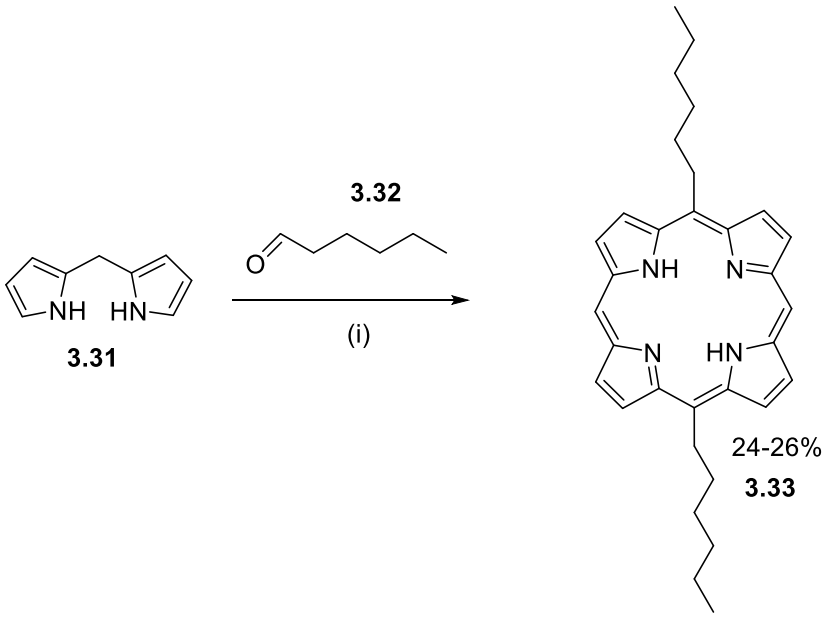

Scheme 3.4. Synthesis of 5,15-dihexylporphyrin precursor **3.33**: (a) (i) DPM **3.31** (1 eq.), heptanal **3.32** (1.02 eq.), TFA (0.22 eq.), DCM, rt, 18 h. (ii) DDQ, rt, 18 h.

In the following step, a phenyl group was attached selectively through an organolithium reaction (Scheme 3.5). This type of reaction is a well-established tool in porphyrin chemistry and can be used for a plethora of different aryl- and alkyl substrates.[50-53, 148-149] A test reaction of the organolithium reaction was performed on a scale of 150 mg of porphyrin **3.33**. The desired target porphyrin **3.34** was obtained in a yield of 70% (Table 3.1, entry 1). Again, the aim of this procedure was the quick large scale generation of starting material, therefore, the

reaction was scaled up and 200 mg of porphyrin **3.33** was used. The same reaction conditions were applied and the phenyl substituted-porphyrin **3.34** was obtained in 67% yield (Table 3.1, entry 2). Since a small upscale did not change the yield drastically it was decided to further upscale the reaction. This time 300 mg of porphyrin **3.33** was used under the same reaction conditions, which resulted in a slightly lower yield of 63% (Table 3.1, entry 3). Considering the overall amount of porphyrin obtained during this reaction it was deemed a good compromise and subsequent reactions were performed at a scale of 300 mg porphyrin **3.33** from then on (Table 3.1, entry 3).

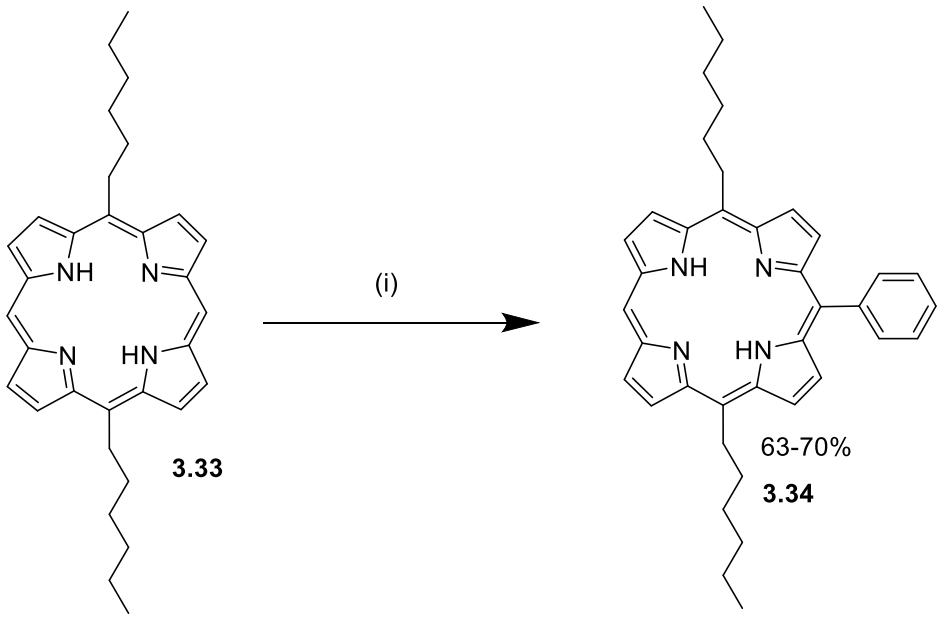

Scheme 3.5. Phenylation of **3.33** *via* organolithium reaction: (i) (a) PhLi (7 eq.), THF, 0 °C. (b) rt, 30 min. (c) H_2O, 20 min, rt; (d) DDQ (5 eq.), rt, 1 h.

Table 3.1. Otimisation of Organolithium reaction for the synthesis of porphyrin 3.34:

Entry	Porphyrin 3.33 [mmol]	Yield [%]
1	0.313	70
2	0.418	67
3	0.627	63

In the next step, porphyrin **3.34** was iodinated (Scheme 3.6). In a first attempt, 0.9 eq. of iodine and 1.08 eq. of (bis(trifluoroacetoxy)iodo)benzene (PIFA) were dissolved in $CHCl_3$ and stirred at rt (Table 3.2, entry 1). However, the desired porphyrin was not obtained. Instead, the porphyrin had degraded. Therefore another procedure was attempted.[186] The reaction was repeated but this time pyridine was added to the reaction (Table 3.2, entry 2,3). This resulted in the desired porphyrin **3.35** in 73-75% yield. The reaction was upscaled without any issues, up to 500 mg of porphyrin while retaining 94% of the desired iodo-porphyrin **3.35** (Table 3.2, entry 3).

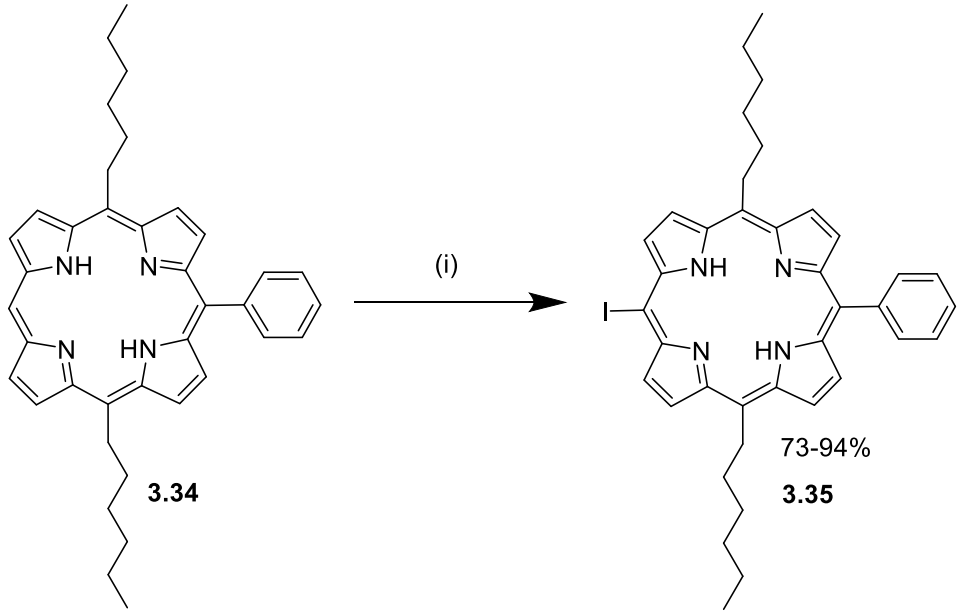

Scheme 3.6. Synthesis of iodo-substituted porphyrin **3.35**: (c) iodine (0.9 eq), PIFA (1.08 eq.), pyridine (34 eq.), $CHCl_3$, rt, 16 h.

Table 3.2. Optimisation of the iodination reaction of **3.34**:

Entry	Porphyrin 3.34 [mmol]	Optimisation	Yield [%]
1	0.076	-	degradation
2	0.094	Pyridine (34 eq.)	73
3	0.451	Pyridine (34 eq.)	75
4	0.901	Pyridine (34 eq.)	94

The last step of the synthesis for the starting material was a simple nickel insertion, which proceeded without difficulties in nearly quantitative yield.

3.4 Coupling of a cubane and a porphyrin-organolithium approach

The first approach to link a cubane with a porphyrin directly was based on the method Fujimoto *et al.* reported in 2015 for porphyrinborylanes.[187] They reported the synthesis of various coupling products through the use of a porphyrinyllithium species. Since the Senge group has a long history of working with organolithium reactions, it was decided to use this approach as a starting point for linking cubanes with a porphyrin.

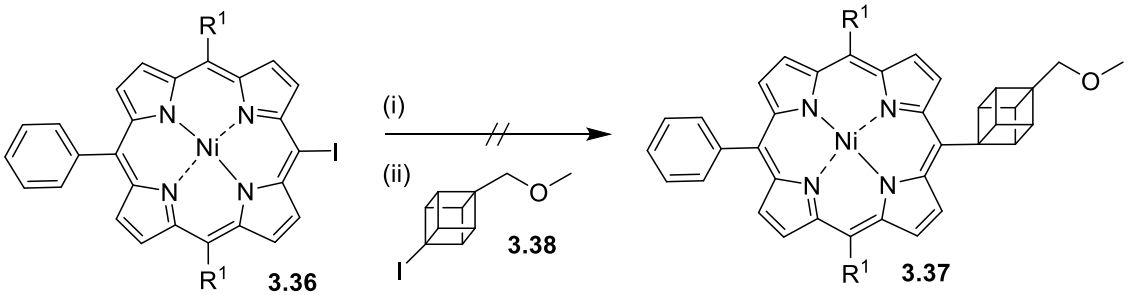

3.36a R^1= hexyl
3.36b R^1= phenyl

Scheme 3.7. Synthesis of directly linked cubane-porphyrin **3.37** through organolithium reaction: (i) *n*-BuLi (1-2.25 eq.), THF, -98 °C, 30-40 min. (ii) cubane **3.38** (1-1.5 eq.), THF, rt, 30 min.

For the first reaction, porphyrin **3.36a** was dissolved in dry THF and cooled to -98 °C (Table 3.3, entry 1). In the next step *n*-BuLi (1.6 M) was added dropwise to the reaction. After the addition, the reaction was stirred for 40 min at -98 °C. The cubane was dissolved in dry THF and was added dropwise to the reaction. After completion and workup, only dehalogenated and butylated starting material was obtained. Therefore, the reaction conditions were altered slightly and only 1 eq. of porphyrin **3.36a** was used instead of 1.5 eq and 1 eq. of n-BuLi instead of 2.25 eq. The next reaction (Table 3.3, entry 2) was set up in a similar manner, likewise only dehalogenated and butylated starting material was obtained.

Table 3.3. Synthesis of directly linked cubane-porphyrin **3.37**.

Entry	Cubane 3.38	Porphyrin 3.36	*n*-BuLi [1.6M]	Temp. [°C]	Time [min.]	THF [mL]	Outcome
1	0.066 mmol, 1 eq.	**3.36a** 0.1 mmol, 1.5 eq.	0.09 mL, 2.25 eq.	-98	1) 40 2) 30	1) 2 2) 0.1	dehalogenated, butylated
2	0.099 mmol, 1eq.	**3.36a** 0.1 mmol, 1eq.	0.06 mL, 1eq.)	-98	1) 40 2) 30	-	dehalogenated, butylated
3[#]	0.051 mmol, 1eq.	**3.36b** 0.05 mmol, 1 eq.	0.02 mL, 1 eq.	-85	1) 40 2) 30	1)1.5 2) 1	dehalogenated, butylated
4[#]	0.051 mmol, 1eq.	**3.36b** 0.051 mmol, 1 eq.	0.02 mL, 1 eq.	-85	1) 40 2) 30	1)1.5 2) 1	dehalogenated, butylated
5[#]	0.150 mmol, 1.5 eq.	**3.36a** 0.1 mmol, 1 eq.	0.09 mL, 1.5 eq.	-98	1) 30 2) 120	1) 2 2) 0.21	dehalogenated, butylated, dimer
6[#]	0.150 mmol, 1.5 eq.	**3.36a** 0.1 mmol, 1 eq.	0.09 mL 1.5 eq.	(-100) – (-110)	1) 30; 2) 120	1) 2 2) 0.21	dehalogenated, butylated, dimer

[#] *n* BuLi was diluted in dry ether.

Since Fujimoto *et al*.[187] used porphyrins with solely aromatic substituents, the porphyrin was changed and [5-iodo, 10,15,20-triphenyl porphyrinato]nickel (II) **3.36b** was used. In this iteration, the reaction temperature was altered so that the first step of the reaction was performed at -85 °C, the results again only yielded dehalogenated and butylated starting material (Table 3.3, entry 3). The reaction was repeated but with the same outcome (Table 3.3, entry 4). For entry 5 the equivalents of *n*-BuLi, as well as the equivalents of cubane, were altered. Since the utilisation of porphyrins with only aromatic substituents did not show any improvements of the reaction outcome the dihexyl-substituted porphyrin **3.36a** from the first attempts was used again. Apart from the two components, the reaction time for the second step was prolonged and the reaction was stirred for 2 h instead of 30 min (Table 3.3, entry 5). In this iteration, the dehalogenated and butylated starting material were complemented by the directly linked porphyrin dimer. This result is notable as in the previous reported literature[52, 58] only the free-base directly linked porphyrin dimer was synthesised, not the metallated porphyrin dimer. While the porphyrin dimer was obtained as an interesting side-product under these reaction conditions, the actual target compound, the cubane-linked porphyrin was not observed. Following this setback, it was decided to try

lower reaction temperatures to see if this would favour the formation of the porphyrinyllithium species. For this reaction 1,5 eq.of cubane and 1,5 eq. of *n*-BuLi were used compared to 1 eq. of porphyrin **3.36a** (Table 3.3, entry 6). The reaction was set up as in previous attempts; however, the reaction mixture during the first step of the porphyrinyllithium formation was cooled to -100 – (-110) °C. Again, the second step of the reaction was stirred for 2 h instead of 30 min. After purification, the dehalogenated starting material, the butylated starting material as well as porphyrin dimer were obtained.

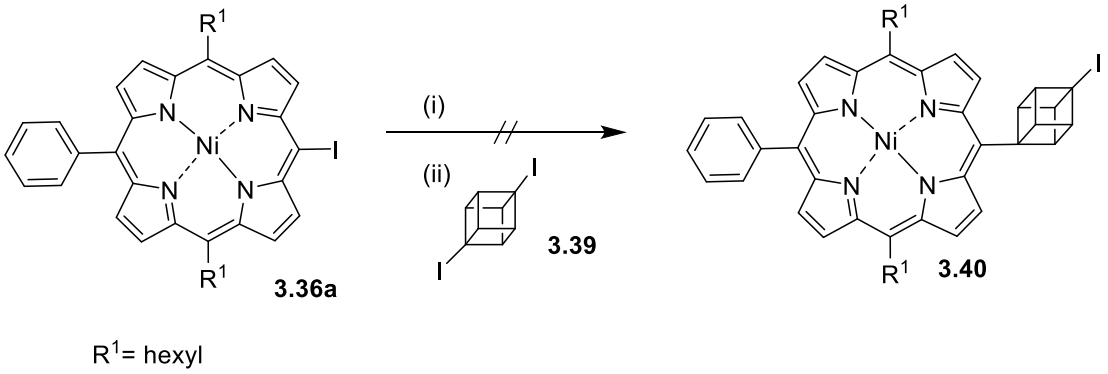

Scheme 3.8. Synthesis of directly linked cubane-porphyrin **3.40:** (i) *n*-BuLi, THF, -98 °C. (ii) THF, rt, 1 h.

After these drawbacks, the approach was changed slightly. Eaton *et al.* reported a method to link a cubane directly with a phenyl group through the usage of PhLi.[188] This was deemed a good alternative approach to the previous attempts. The cubane was changed to the di-iodo cubane, which allowed similar reaction conditions to the ones reported by Eaton *et al*. (Scheme 3.8).[188] For the first attempt (Table 3.4, entry 7), 3 eq. porphyrin **3.36a** were used to generate the porphyrinyllithium as described before. In the second step, the porphyrinyllithium was added to the cubane **3.39** (1eq.). After 1 h of stirring at rt another 1 eq. of the porphyrinyllithium was added to the reaction and stirred for further 45 min. This reaction resulted again in dehalogenated porphyrin, butylated porphyrin and a small fraction of dimer.

Table 3.4. Synthesis of cubane-porphyrin **3.40** through organolithium approach:

Entry	Cubane 3.39	Porphyrin 3.36a	*n*-BuLi [1.6M]	Temp. [°C]	Time [min.]	THF [mL]	Outcome
7	0.067m mol, 1eq.	0.201 mmol, 3 eq.	0.18 mL, 4.5 eq.	(-100) – (-110)	1) 30 2) 105	1) 2 2) 0.5	dehalogenated, butylated
8	0.034 mmol, 1eq.	0.1 mmol, 3 eq.	0.18 mL, 4.5 eq.	(-100) – (-110)	1) 30 2) 16 h	1) 2 2) 0.5	dehalogenated, butylated

For the next attempt (Table 3.4, entry 8), the reaction was scaled down using only 74 mg of porphyrin **3.36a** (3 eq.). Again, the first step was completed as described before. This time the reaction was stirred for 16 h after the second addition of porphyrinyllithium. TLC and Mass spectrometry confirmed that only dehalogenated porphyrin and butylated porphyrin was formed. Since the reaction temperature, the reaction time, the concentration and the method for the addition of the cubane to the porphyrin were altered without any success it was decided to change strategy and move towards palladium catalysed coupling reactions.

3.5 Coupling of cubane and porphyrins utilising SET

After several unfruitful attempts of coupling porphyrins *via* organolithium reaction directly to a cubane, the initial approach was revised. The use of redox-active esters was deemed a noteworthy approach and has been successfully used before.[189] Furthermore, concurrent research on this topic within the Senge group gave very promising results for coupling aryl compounds efficiently to cubanes. After thorough optimisation and investigation of the reaction conditions in this line of research,[179] the optimised reaction conditions were adapted and coupling between porphyrin and cubanes were attempted. This type of coupling reaction required a three step-reaction, starting with the formation of a porphyrin Grignard, followed by metal exchange[190] to the Zn species and finally the cross-coupling reaction with the cubane species. Due to all these reaction steps, which had to be performed *in-situ* since the various porphyrin species were not stable and could

not be isolated, the optimisation process posed a difficult task. Not only was there a plethora of different reaction conditions which could be optimised, but also the conversion of the porphyrin to the different active species could only be monitored, analysed and quantified by TLC analysis. For the ease of discussion, the individual optimisation attempts for the different reaction steps will be elaborated one after another, even though they have been performed simultaneously since the respective porphyrin species was used for the next step in the synthesis.

3.5.1 Formation of the porphyrin Grignard species

As mentioned above for the cubane cross-coupling reaction a porphyrin Grignard had to be synthesised first. This was achieved following the literature procedure.[1] Therefore, the iodo porphyrin **3.36a** was dissolved in dry THF and cooled to -40 °C. 1-1.5 eq. of *i*PrMgCl•LiCl was added dropwise (Scheme 3.9). The reaction was monitored by TLC. The progress of the reaction was judged by the consumption of the starting material during the Grignard species formation. Since the porphyrin Grignard **3.41a** was expected to lack stability, it was crucial that all the starting material was consumed in a relatively short time window. However, upon monitoring the Grignard formation using the conditions entry 1, Table 3.5 *via* TLC it became obvious that there was still starting material left after 2 h. Therefore, the first step of the reaction cycle in Table 3.5 was left to stir for 21 h instead of 2 h (Table 3.5, entry 2). Unfortunately, even stirring overnight did not lead to a complete conversion. The following metal exchange to **3.42a** was also performed at a lower temperature (-20 °C) to avoid possible degradation. Since difficulties were expected during the second coupling step with the cubane, it was crucial to minimise the loss of material in the first step and the strategy used had to be revised.

Table 3.5. Optimisation for porphyrin Grignard species **3.42a**:

Entry	*i*PrMgCl*LiCl	Porphyrin 3.36a	$ZnCl_2$	Temp [°C]	Time	THF [mL]	Observation
1	0.15 mmol 1.5 eq.	0.1 mmol 1 eq.	1.5 eq.	1) 40 2) rt	1) 2 h 2) 30 min	2	Starting material was still present
2	0.1 mmol 1 eq.	0.1 mmol, 1 eq.	1 eq.	1) -40 2) -20	1) 21 h 2) 3 h	2	Starting material was still present

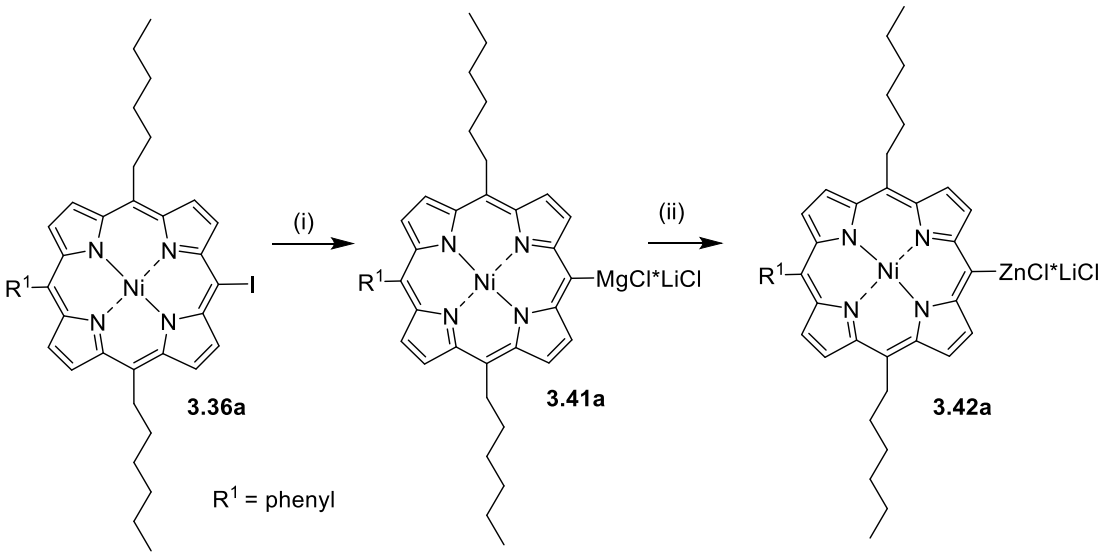

Scheme 3.9. Synthesis of porphyrin Grignard species **3.42a**: (i) *i*PrMgCl*LiC (1.5 eq.), THF, -40 °C, 2 h. (ii) ZnCl (1.5 eq.), THF, rt, 30 min..

After a revision of the literature, it was noticed that the porphyrins reported in the literature[1] for this reaction type had always aryl substitution. The porphyrin systems used in this investigation, however, were bearing long alkyl chains to improve solubility. It was decided to change the porphyrin system to see if the substitution pattern on the porphyrin can influence the conversion of the iodo porphyrin into the Grignard species (Scheme 3.10). Therefore [5-iodo-10,15,20-tris(4-methylphenyl)porphyrinato]nickel(II) **3.36c** was subjected to the same reaction conditions (Table 3.6, entry 3). The porphyrin was again dissolved in dry THF and cooled. The Grignard reagent was added dropwise and after stirring for 3.5 h all of the starting material was consumed. Therefore, aryl-substituted porphyrins were deemed the better choice of starting material. Following these results [5-iodo-15-phenyl-10,20-bis-(4-methylphenyl)porphyrinato]nickel(II) **3.36d** was synthesised and used in the following reactions (Table 3.6, entry 4 and 5). The side products that were identified after the cubane coupling for entry 4 were traces of the starting material, dehalogenated porphyrin and porphyrin substituted with an isopropyl group. This was rather interesting since it was the first time this porphyrin was observed during this reaction and no addition like this was mentioned in Osuka's paper.[1] Mass spectrometry and NMR spectroscopy confirmed the formation of this porphyrin. This addition most likely happens before the cubane cross-coupling, since two porphyrins were observed on the TLC while monitoring the Grignard reaction. Following this outcome, it was decided to add the Grignard reagent dropwise over 15-30 min to the porphyrin and additionally to

perform the metal exchange at - 40 °C to hopefully slow down the undesired addition reaction and therefore minimise the side-product formation (Table 3.6, entry 5).

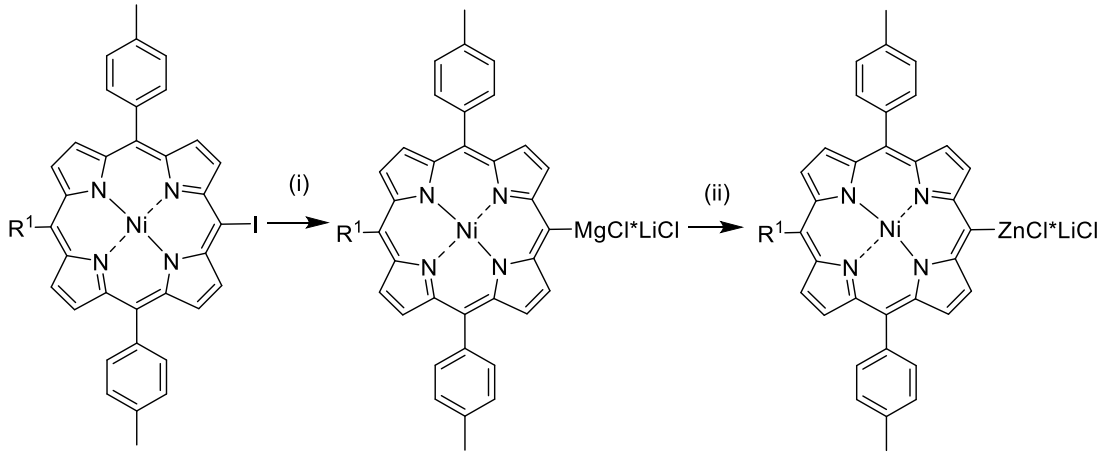

3.36c R^1= 4-Me-C_6H_4
3.36d R^1= phenyl

3.41c R^1=4-Me-C_6H_4
3.41d R^1= phenyl

3.42c R^1= 4-Me-C_6H_4
3.42d R^1= phenyl

Scheme 3.10. Synthesis of porphyrin Grignard species **3.42**: (i) iPrMgCl*LiC (0.9-1.1 eq.), THF, -40 °C, 2-3.5 h. (ii) ZnCl (1 eq.), THF, rt - -40 °C, 0.5-1 h.

Even though the formation of the side-product could not be avoided completely, TLC analysis for the Grignard formation showed that the band which was associated with the side product had decreased compared to entry 4, Table 3.6. After the cubane-coupling step, the side product was isolated and only 8% conversion of the starting material to the side product was observed. This was considered low enough and these reaction conditions were used for the cubane coupling reactions henceforth.

Table 3.6. Optimisation of porphyrin Grignard species formation:

Entry	*i*PrMgCl*LiCl	Porphyrin	$ZnCl_2$	Temp [°C]	Time	THF [mL]	Observation
3	0.09 mmol 0.9 eq.	**3.36c** 0.1 mmol, 1 eq.	1 eq.	1) - 40 2) rt	1) 3.5 h 2) 30 min	3	Full consumption of starting material
4	0.11 mmol 1.1 eq.	**3.36d** 0.1 mmol, 1 eq.	1 eq.	1) - 40 2) rt	1) 2 h 2) 30 min	2	Large amount of side product
5	0.165 mmol 1.1 eq.	**3.36d** 0.15 mmol, 1 eq.	1 eq.	1) - 40 2) - 40	1) 3 h 2) 1 h	3	Only 8% side product

3.5.2 Cubane cross-coupling reaction

Besides the Grignard reaction, the cubane cross-coupling step had to be optimised (Scheme 3.11). This attempt proved to be rather difficult since various side products were obtained during this reaction. Furthermore, the porphyrin Zn*Cl species **3.42** had to be used *in-situ* from the previous reaction and therefore the amount of actual porphyrin species could only be assumed and might have varied slightly. Previous optimisations discovered by the Senge group for small aromatic molecules showed that the coupling reaction worked well with 1 eq. $NiCl_2$*glyme and 1 eq. dtBBPy in relative concentrated reaction conditions.[179] Therefore, these conditions were deemed a good starting point towards the investigation of directly linked cubane-porphyrin systems.

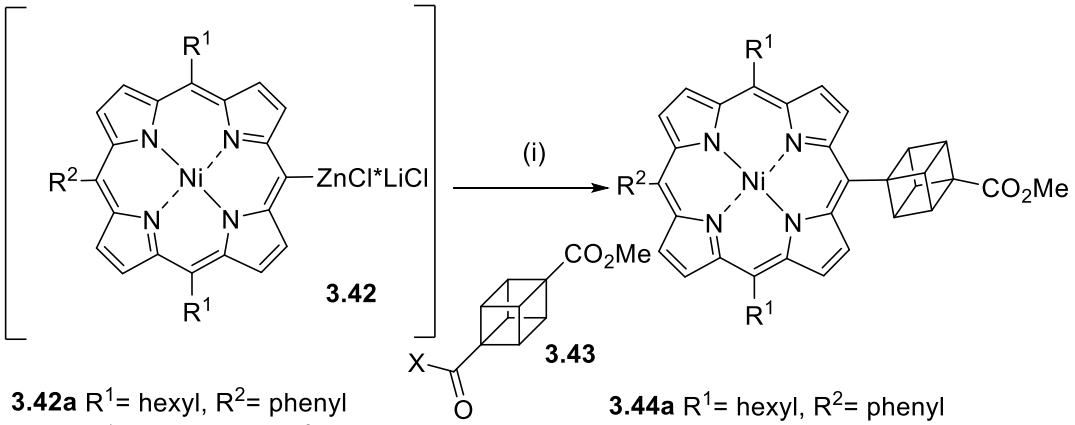

3.42a R^1= hexyl, R^2= phenyl
3.42c R^1= 4-Me-C_6H_4, R^2= 4-Me-C_6H_4
3.42d R^1= 4-Me-C_6H_4, R^2= phenyl

3.44a R^1= hexyl, R^2= phenyl
3.44c R^1= 4-Me-C_6H_4, R^2= 4-Me-C_6H_4
3.44d R^1= 4-Me-C_6H_4, R^2= phenyl

Scheme 3.11. Cubane cross-coupling reaction: (i) $NiCl_2$ (0.2 eq.), dtbbpy (0.4 eq.), cubane (1 eq.), THF/DMF (2:1).

Entry 6 and 7 used the same amounts of cubane **3.43**, porphyrin **3.42a** and catalysts. However, they were performed at different temperatures (Table 3.7). Notably, both reactions were succesful at 40 °C as at 70 °C showing the formation of possible cubane-porphyrins **3.44a**. However, due to the small amount formed it was not possible to isolate and purify the compounds. Therefore, reaction 6 was set up again on a larger scale (entry 8). This time it was possible to isolate the porphyrin-cubane **3.44a** and confirm its formation through NMR analysis. Since side products were abundant, it was assumed that the reaction temperature might be too high, possibly resulting in degradation of the porphyrin species.

Therefore, the next reaction was set up at rt (Table 3.7, entry 9). In addition, the reaction scale was further increased in order to make the workup and purification process easier. The reaction was stopped after 18 h but unfortunately, no product **3.44a** formation was observed. Following this set back we decided to take a closer look at the reaction concentration (Table 3.7, entry 10 and 11). Two reactions were set up under the same conditions but one reaction was more concentrated (Table 3.7, entry 10) than the other (Table 3.7, entry 11). Strangely, again no formation of the target compound was observed. Since there was suddenly, no cubane-porphyrin formation in three subsequent reactions it was decided to take a closer look at the Grignard reagent and it was confirmed that the Grignard reagent had degraded. Thus, a new Grignard reagent was prepared. Entry 12 resulted then again in the formation of the desired porphyrin **3.44a**, however, purification proved to be unsuccessful. At this stage, it was decided to vary the catalyst loading to see if similar or better results could be obtained with a lower loading (Table 3.7, entry 13). Therefore only 0.2 eq $NiCl_2$*glyme and 0.4 eq. dtBBPy were used. After completion of the reaction the cubane-porphyrin **3.44a** was isolated in 8% yield. This showed that the higher catalyst loading does not affect the coupling reaction hugely since a very comparable yield of 10% was achieved with 1 eq. and 2 eq. for the $NiCl_2$*glyme and dtBBPy respectively in entry 8. Bearing this in mind the lower catalyst loading was henceforth used.

Table 3.7. Optimisation for cubane cross-coupling:

#	Cond. 3.42 [#]	Comp. 3.43	Porph. 3.42a	$NiCl_2$* glyme [eq.]	dtBBPy [eq.]	Temp. [°C]	Time [h]	Solvent [mL]	Result 3.44
6	1	1 eq. 0.025 mmol	2 eq., 0.05 mmol	1	2	40	18	THF:2 DMF:1	Product Yield: N.D
7	1	1 eq. 0.025 mmol	2 eq., 0.05 mmol	1	2	75	18	THF:2 DMF:1	Product Yield: not pure
8	1	1 eq. 0.05 mmol	2 eq., 0.1 mmol	1	2	40	18	THF:2 DMF:1	Product Yield: 10%

9	**1**	**1 eq. 0.125 mmol**	**2 eq., 0.250 mmol**	**1**	**2**	**25**	**18**	**THF:5 DMF:2.5**	**No product**
10	1	1 eq. 0.03 mmol	2 eq., 0.07 mmol	1	2	40	18	THF:2.5 DMF:1	No product
11	1	1 eq. 0.03 mmol	2 eq., 0.07 mmol	1	2	40	18	THF:2.5 DMF:5	No product
12	1	1 eq. 0.05 mmol	2 eq., 0.1 mmol	1	2	40	18	THF:2 DMF:1	Product Yield: not pure
13	2	1 eq. 0.1 mmol	1 eq., 0.1 mmol	0.2	0.4	40	18	THF:2 DMF:1	Product Yield: 8%
14	3	1 eq. 0.1 mmol	**3.42c** 1 eq., 0.1 mmol	0.2	0.4	25	16	THF:3 DMF:1.5	Product Yield: 6%
15	4	1 eq. 0.1 mmol	**3.42d** 1 eq., 0.1 mmol	0.2	0.4	65	16	THF:2 DMF:1.4	No product
16	4	1 eq. 0.1 mmol	**3.42d** 1 eq., 0.1 mmol	0.2	0.4	65	16	THF:2 DMF:5	No product
17	5	1 eq. 0.15 mmol	**3.42d** 1 eq., 0.15 mmol	0.2	0.4	rt	41	THF:3.2 DMF:2.1	Product Yield: 9%
18	5	1 eq. 0.1 mmol	**3.42d** 1 eq., 0.1 mmol	0.2	0.4	-40	23.5	THF:2 DMF:1.4	Product Yield: 12%

At this stage of the investigations into the cubane cross-coupling, it was shown that the formation of the porphyrin Grignard in the first step of the reaction cycle occurred much faster for aryl-substituted porphyrins than alkyl-substituted porphyrins.

Therefore, the porphyrin system was changed at this stage. This time the reaction was stirred for 16 h at room temperature and the target compound **3.44c** was obtained in 6% yield (Table 3.7 entry 14). Due to the ease of synthesis, the porphyrin was changed to the porphyrin **3.42d** for the following optimisation attempts. The usual procedure was followed for the Grignard formation and the metal exchange (Table 3.6, entry 4). The cubane **3.43** was then dissolved different amounts of dry DMF (Table 3.7, entry 15 and entry 16) to observe the impact of the concentration on the reaction. Both reactions were heated to 65 °C and stirred for 16 h. While the concentration did not seem to play a significant role, no product

formation was observed. The side products for these reactions were identified as traces of the starting material, dehalogenated porphyrin and the porphyrin with the isopropyl group attached to it. To avoid or minimise this side product the Grignard reaction conditions were altered as mentioned in the chapter above. Furthermore, the reaction temperature for the cubane cross-coupling was decreased to avoid decomposition of the Grignard porphyrin. The following cubane cross-coupling was performed at rt instead of 65 °C (entry 17) The cubane suspension was cooled to - 40 °C and the porphyrin **3.42d** was added. The reaction was then stirred at rt for 41 h (entry 17). Another reaction was set up adopting the above-mentioned changes. The Grignard reagent was added dropwise over 30 min to the porphyrin **3.42d** and the metal exchange was done at -40 °C. For this reaction, the cubane solution was also cooled to - 40 °C, the porphyrin was added and the reaction was stirred at - 40 °C for 23.5 h (entry 18). TLC analysis showed that in both cases (entry 17 and 18) the first two fractions were the dehalogenated porphyrin and the porphyrin with the isopropyl group. Since the polarity of the cubane coupled products **3.44** and the porphyrins which occur as side products are normally very different, the porphyrin fractions were washed off the silica filtration with a mixture of DCM: hexane = 1:1. Afterwards, the remaining fractions were eluted off the plug using pure MeOH. This fraction was then put on a prep TLC using DCM/hexane = 1:1 and DCM/hexane = 2:1 in both cases. For entry 17 the target compound **3.44d** was obtained in 9% yield whereas for entry 18 a yield of 12% was achieved. Since all of the attempted optimisation procedures did not really result in a notable increase in the yield obtained, it was decided to try a different type of coupling reaction. Therefore Fe-catalysed C-C coupling was attempted following a procedure published by Phil Baran and his group (Scheme 3.12).[177]

To implement this new methodology, the iodoporphyrin (1 eq.) was dried under vacuum for 1 h before 2 mL of dry THF was added. The reaction was cooled to -40 °C and the turbo Grignard (1 eq.) was added dropwise. In the next step $ZnCl_2$ (0.5 eq.) in THF was added to the reaction mixture (**3.42d**, Scheme 3.12). The reaction was stirred for 1 h while slowly warming up to -20 °C. Meanwhile, the cubane coupling reaction was set up. The cubane **3.43** (1 eq.), dppBz (0.48 eq.) and $Fe(acac)_3$ (0.4 eq.) were added to a vial and 1 mL of dry THF was added.

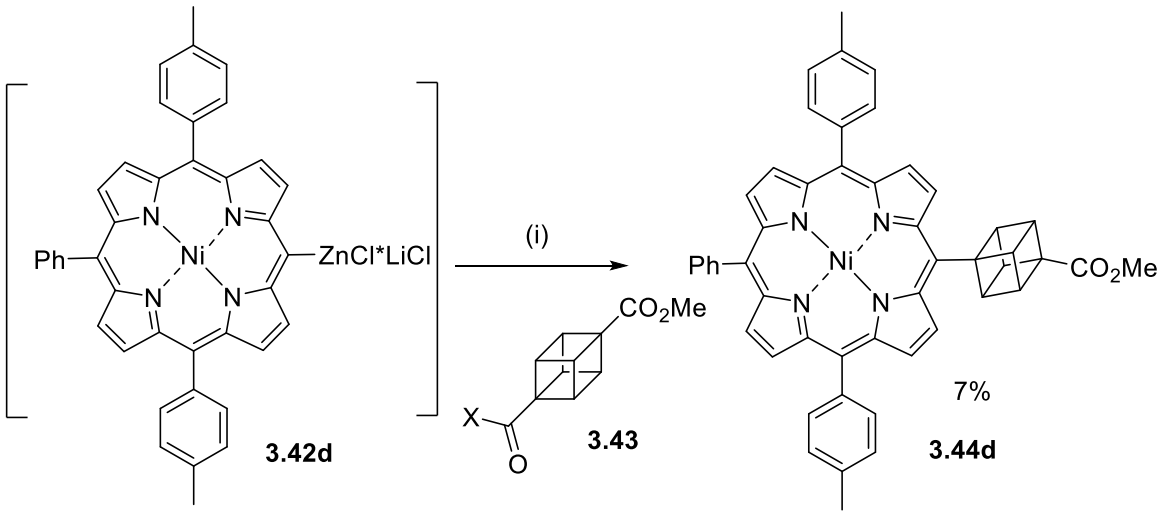

Scheme 3.12. Fe-catalysed coupling reaction: (i) porphyrin **3.42d** (1 eq.), iPrMgCl*LiC (1 eq.), THF, -40 °C. (ii) $ZnCl_2$ (0.5 eq.), THF, -20 °C, 1 h. (iii) cubane **3.43** (1 eq.), Fe(acac) (0.4 eq.), $dppB_2$ (0.48 eq.), THF/toluene, -20 °C - rt, 16 h.

Due to solubility issues, another 0.5 mL dry toluene had to be added. Once the metal-exchange reaction was stirred for 1 h the cubane reaction was cooled to -20 °C and the porphyrin solution was added to the cubane mixture. The reaction was stirred at the same temperature for 1h and TLC analysis was done. Since no change was observed the reaction was warmed to rt and stirred overnight. After purification, the target compound **3.44d** was isolated in 7% yield. Since this reaction gave similar results compared to the Ni-catalysed reaction, no further optimisations were attempted.

3.6 Conclusion

Organolithium reactions, as well as Ni- and Fe-catalysed cross-coupling reactions, have been utilised to attempt the synthesis of directly linked cubane-porphyrin systems. Although various different reaction conditions have been investigated such as the reaction temperature, reaction time, concentration and the method for the addition of the cubane to the porphyrin, the organolithium approach proofed to be unsuccessful. Despite this setback, the directly linked metallated porphyrin dimer was formed. The formation of this compound through direct organolithium reaction has previously been reported as impossible.[52, 58]

This work reports the first known synthesis of a directly linked cubane-porphyrin system. This is achieved through the utilisation of Ni-catalysed single electron transfer cross-coupling reaction. In the course of this investigation, several different reaction conditions have been varied to obtain three different cubane-linked porphyrins in yields from 6-12%. Every single reaction step of the three-step synthesis process was optimised. Through variation of the reaction temperature, reaction time and porphyrin systems used, the formation of the Grignard porphyrin was optimised, the reaction time was reduced and the side product formation minimised. Furthermore, the reaction temperature of the subsequent metal exchange was reduced to ensure maximum stability of the active porphyrin species and avoid degradation.

A thorough investigation of the final coupling step with the cubane redox-ester resulted in variations of the reaction time, reaction temperature, eq. of porphyrin and cubane used, reaction concentration and addition procedure. This reaction type proved to be very sensitive to any alteration at any step of the synthesis and small changes led to very different results. However, the best results were obtained at low catalyst loading at –40 °C for 23.5 h. Furthermore, a Fe-catalysed reaction with $Fe(acac)_3$ and dppBz was attempted, which resulted in lower yields than the Ni-catalysed coupling and was therefore disregarded.

Even though directly linked cubane-porphryins were obtained, future work include further optimisation of the reaction conditions to obtain higher yields. Recent advances in linker chemistry also open the door to other functionalisation reactions, such as the nickel catalysed coupling with boronic esters[191], which could be adapted for cubanes and used to obtain directly linked cubane-porphyrins in the future.

4 Porphyrins as building blocks and their interactions with nanomaterials

The concept of building blocks is well known in natural systems. Proteins, nucleic acid and natural products are constructed of smaller units such as amino acids, nucleotides or carbohydrates. Recently this strategy has been also adopted by synthetic chemists for applications in bioorganic chemistry or material chemistry.[192] The benefit of this approach is the possibility of constructing complex larger systems from simple easily available building blocks, as well as combining various materials with different functionalities. The ongoing interest in mimicking photosynthetic processes justifies the approach of molecular building blocks even more. Furthermore, functionalised nanomaterials with defined shapes and sizes are gaining more and more popularity for applications such as electronics, light-energy conversion and photonics. Porphyrins represent very promising photonics materials for such applications due to their strong absorption bands in the visible region, tunable electronic properties and scope of possible modifications. The use of porphyrins as building blocks, however, is hardly a new approach. These versatile systems have been used for a long time dating back to porphyrin dimers, picket fence porphyrins, artificial enzymes or light-harvesting arrays.[193] Materials exhibiting strong absorption in the infrared region are especially of interest. Even though there are many porphyrin-based nanomaterials, current studies target composite 2D and 3D materials. One example is the use of suitably functionalised porphyrins as tectons in SMOFs, MOFs, DSSCs and for binding to surfaces.[194] Such applications require porphyrin building blocks where:

(1) tailored functionalisation of the porphyrin core can be used to optimise key performance for different applications and

(2) suitable functional groups can direct their spatial arrangement in a given environment or facilitate the assembly to nano-networks of these compounds.

Porphyrin tectons can be described as building blocks on a molecular level.[195] These building blocks interact with reciprocal counterparts in a specific manner to form molecule-substrate or -surface interactions. Interactions are based on different means such as ionic self-assembly, re-precipitation or coordination polymerisation. Notably, the use of weak binding forces offers a facile approach, *e.g.*, to 3D supramolecular networks stabilised by hydrogen bonding or electrostatic forces.[196] Very dense packing can be achieved by porphyrins with

unreactive meso-substituents (e.g., phenyl-groups) or porphyrin itself due to van der Waals interactions. Introducing functional groups to the porphyrin such as pyridyl, alkoxy or carboxyphenyl helps to fine-tune the strength, selectivity and direction of these intermolecular interactions. Thus, porphyrins provide valuable tools to form molecular constructs such as porous networks, aggregates or closed-packed arrays.[197]

4.1 Objectives

In this chapter different interactions of porphyrins with nanomaterials are investigated. Various porphyrin systems are synthesised bearing a variety of functional groups, which can interact with nanomaterials in a specific and defined manner through intermolecular non-covalent interactions or covalent interactions.

This includes *π*-*π* interactions between porphyrins and nanomaterials with additional directional carboxylic acid groups, which represent an interesting class of molecular tectons. Synthetic methodologies for porphyrin-based supramolecular tectons for surface studies are investigated. The study aims to generate porphyrins with directional anchoring groups of different length with a special focus on organometallic coupling reactions for the introduction of benzoic acid moieties as anchor groups

In addition to the use as building blocks and tectons, porphyrins also exhibit various beneficial properties as electron-donor materials in combination with carbon-based nanomaterials. Especially the investigation of such molecular carbon-based hybrid materials with organic sensitisers have gained attention due to their potential use in optoelectronic applications.[198] Furthermore, research has shown that grapheneporphyrin hybrids show also promising results as sensitisers in DSSCs. These type of molecules exhibit even better charge injection efficiencies than solely the porphyrin itself. In addition, aggregation, which is one of the big challenges in DSSCs, was averted which lead to a better regeneration process of the porphyrin sensitiser as well as a decline in the recombination losses.[199] Therefore, detailed investigation into charge transfer processes between nanocarbon materials and sensitisers for DSSCs is of utter interest. Since synthetic optimisations of state-of-the-art type push-pull porphyrins have been investigated in chapter 2, interactions of these molecules between fullerene C_{60} and graphene carboxylate are further explored in this section.

Metal-organic frameworks resemble another well-known application of porphyrins when it comes to interactions with other nanomaterials. Pyridine-substituted porphyrins have been widely used for MOF systems due to their favourable interaction with other molecules.[200] We are especially interested in molecules with a certain length of linker system. Thus, the synthesis of molecules which possess a defined spatial arrangement and distance between the porphyrin core and the pyridine linker units is attempted. Furthermore, the insertion of Pd into the porphyrin core results in a heavy atom effect once the porphyrin is excited, which is beneficial for the applications in light-harvesting and energy migration.[201]

Besides spacial arrangement and intermolecular interactions, also electron transfer between covalently linked porphyrins and an electrode is explored. Sheridan *et al.* have reported a method of an anodic attachment of 5,10,15,20-tetraethynyl-porphyrin to an electrode.[202] This was the first reported covalently linked porphyrin monolayer to an electrode. As the results obtained were rather promising, we are interested in synthesising porphyrins with only one ethynyl linker to allow a more rational attachment to the electrode. These meso-substituted porphyrins would then be attached to carbon surfaces in order to make chemically modified electrodes with covalently-bonded monolayers of different metalloporphyrins.

4.2 *m*-Benzoic acid porphyrins as molecular tectons for surface studies

Notably, carboxyphenylporphyrins are key components of some of the earliest mesoporous porphyrin-based MOFs[203] and have been widely used in surface chemistry as chemosensors, coordination polymers and catalysts.[204] Other applications of carboxylic acid porphyrins include use in photodynamic therapy[205] or DSSCs,[9c, 116b, 140] and they present a suitable means to create molecular tectons.

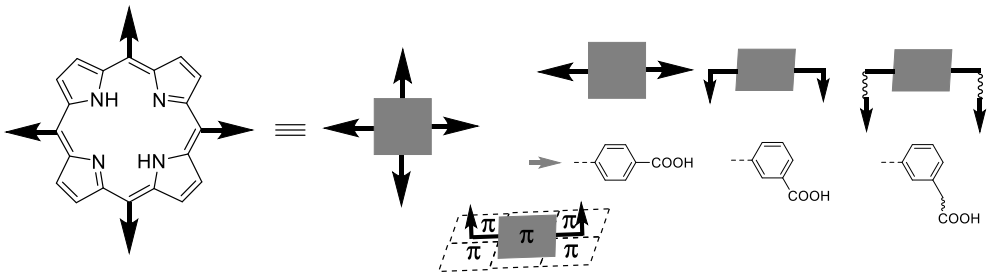

Figure 4.1. Illustration of porphyrin carboxylic acids as directional tectons.

In the context of exploratory studies on the use of surface-bound porphyrins as biosensors, we were interested in providing porphyrins with unique optical properties capable of binding to surface materials in a directional manner. One possible avenue would be the attachment of porphyrins *via π-π*-interactions to a graphene surface and then using COOH groups for the attachment of bioconjugates. This requires the COOH anchors to point towards one side of the system away from the porphyrin plane, similar to the orientation utilised by Collman in his picket-fence porphyrins as models for oxygen binding heme proteins.[193a] A simple means to achieved different directionalities and spacings are provided by using meso-benzoic acid residues as directional anchor groups (Figure 4.1). Various syntheses have been reported to generate porphyrins with different aryl-carboxylic acid groups in the past and range from Sonogashira[124, 134, 206] and Suzuki[207] couplings to nucleophilic substitution reactions.[208] Herein, we give a brief account of synthetic studies aimed to synthesise porphyrins with directional anchoring groups.

4.2.1 Synthesis of A_4 type tetracarboxylic acid porphyrin

Our first target compound was the tetrasubstituted *m*-benzoic acid porphyrin **4.3** which was deemed to be a good starting point for our synthetic studies due to its ease of synthesis. Furthermore, it provides a very useful reference for comparison with other more complex carboxylic acid porphyrins. Therefore, our investigations began with the synthesis of tetrasubstituted porphyrin **4.1** using standard condensation procedures.[209] Further modification included the insertion of nickel into the porphyrin core *via* reaction with $Ni(acac)_2$ to give **4.2** with a yield of 94% (Scheme 4.1). Next, the acid was generated by deprotection of the carboxylic ester under standard base hydrolysis conditions. The reaction required a large excess of base and long reaction times until the starting material was completely consumed. After acidification and extraction, the free carboxylic acid **4.3** was obtained in a yield of 81% after recrystallisation (Scheme 4.1).

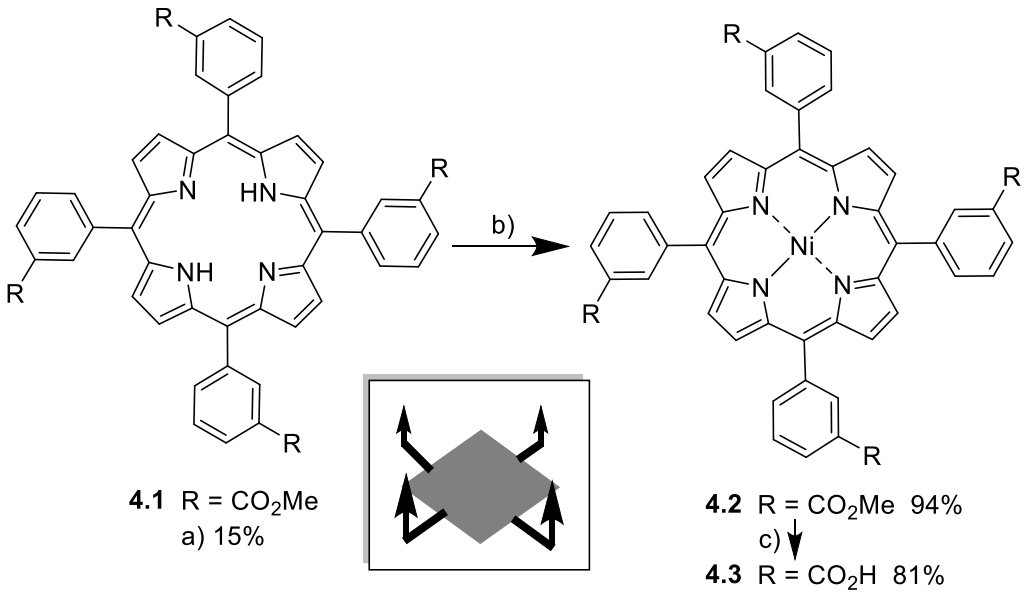

Scheme 4.1. Synthesis of simple, A_4-type *m*-benzoic acid porphyrins: a) (i) 3-Carbomethoxybenzaldehyde, pyrrole, DCM, BF_3 etherate, rt, 16 h. (ii) DDQ, rt, 1 h. b) $Ni(II)(acac)_2$ (2.5 equiv.), toluene, 120 °C, 18 h. c) KOH (400 equiv.) in H_2O, THF/MeOH (1:1), 66 °C, 72 h.

4.2.2 Synthesis of porphyrin dimers with *m*-benzoic anchor groups

While A_4-type systems are easily accessible, they are not that interesting, nor unique. In light of current reports on the use of *π*–conjugated and triply-fused systems and related materials for the solubilisation of and aggregation with carbon nanotubes[210] we aimed to access related species capable of further

bioconjugation and for the use as supramolecular tectons as illustrated in Figure 4.1. For these reasons, we decided to synthesise bis-carboxylic acid porphyrin dimers, namely the ethyne-bridged dimer 4.**6f** (Scheme 4.2). Such compounds are of interest in photonics as two-photon absorbers[9a] and subsequent studies on this will be reported elsewhere.

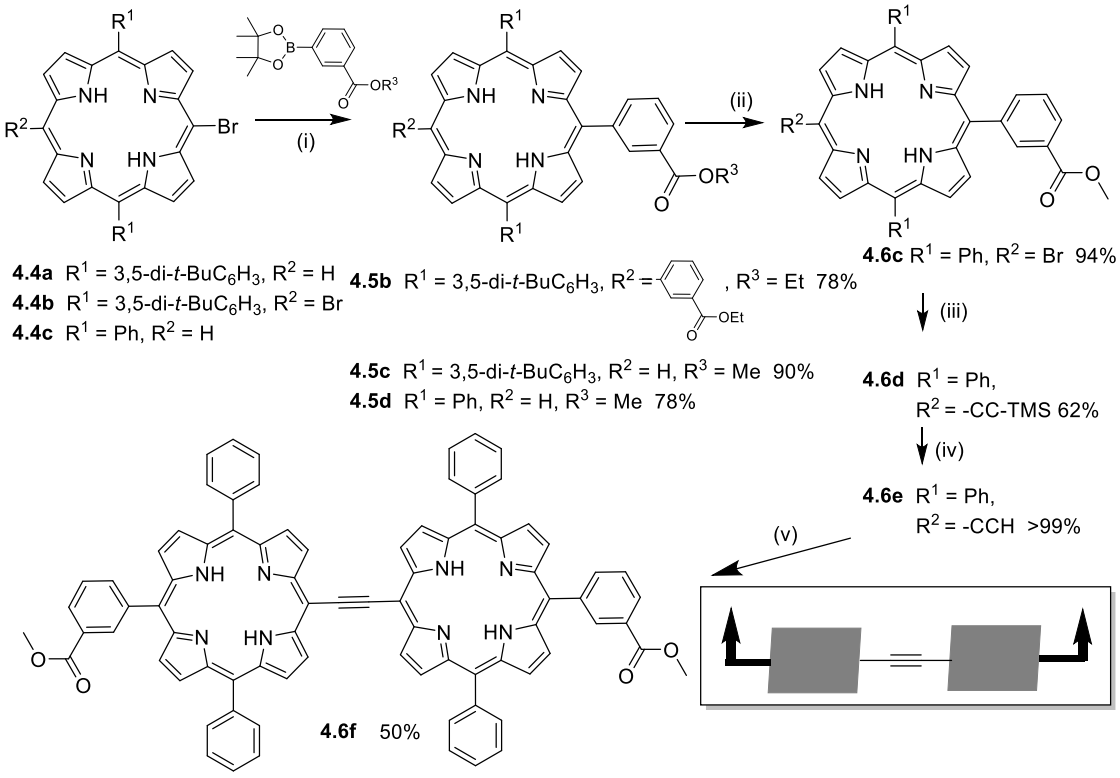

Scheme 4.2. Synthesis of a bisporphyrin with two *m*-benzoic acid residues: (i) $Pd(PPh_3)_4$ (20 mol%), K_3PO_4 (10 equiv.), THF, 66 °C, 18 h. (ii) NBS (1 equiv.), $CHCl_3$, pyridine, rt, 2 h. (iii) CuI (20 mol%), $PdCl_2(PPh_3)_2$ (10 mol%) THF/TEA (3:1, v/v), 66 °C, 18 h. (iv) TBAF, THF. (v) $AsPh_3$ (1.1 equiv.), $Pd_2(dba)_3$ (15 mol%), THF/TEA (3:1, v/v), 66 °C 18 h.

The starting materials for this project were obtained through simple condensation from either benzaldehyde or 3,5-bis-*tert*-butylbenzaldehyde. In order to attach the benzoic acid to the porphyrin, the macrocycle was first functionalised *via* bromination to yield porphyrin 4.4. Therefore, 0.8 eq. of NBS and 1 eq. of porphyrin were dissolved in $CHCl_3$ and pyridine was added in catalytic amounts. The reaction was stirred at 0 °C. To force the reaction to completion another 0.3 eq. of NBS were added. Due to the similar polarity of the mono and di-brominated side product, purification of this type of porphyrin is rather difficult. However, a mixture of toluene: hexane= 1:3 showed promising results on the TLC and was therefore used. For the synthesis of the dimer starting material **4.4a** was subjected

to Suzuki conditions with a boronate ester either containing an ethyl group at the ester to yield porphyrin **4.5a** in 74% or with a methyl group to yield **4.5c** in 90%. Besides mono substituted m-benzoic acid porphyrins also di-substituted acids can be synthesised by utilising di-brominated starting material **4.4b** instead of the mono-brominated porphyrin species **4.4a/4.4c**. Compounds such as **4.5c/d** can be used as starting materials for Pd-catalysed cross-coupling reactions to yield bisporphyrin carboxylic acids with different linker units. This is exemplified by sequence **4.5d** to **4.6f** (Scheme 4.2) which gives the target **4.6f** in an overall yield of 29%. Compound **4.5d** was readily brominated with NBS. Since every position except one was already occupied by a substrate, an excess of NBS could be used and the reaction was stirred at rt instead of at 0 °C. The desired target compound **4.6c** was obtained in nearly quantitative yields. The next step involved the introduction of a linker unit. In this case, an ethynyl group was chosen but also the introduction of large linkers such as a phenyl group would be possible. The target **4.6d** was obtained in 62% using Sonogashira-reaction conditions. To obtain the dimer this compound was then subsequently deprotected with TBAF giving compound **4.6e** in quantitative yield. The final step involved the coupling of the two porphyrin units to obtain the dimer. Therefore, compound **4.6c** and deprotected compound **4.6e** were subjected to copper-free Sonogoashira cross-coupling conditions. The final porphyrin dimer was obtained in 50% yield (Scheme 4.2). Furthermore, metal insertion into the dimer was attempted. Thus, 60 mg of the porphyrin dimer **4.6f** was dissolved in toluene and $Ni(acac)_2$ was added in 4 eq excess. The reaction was then heated to 100 °C for 18 h. However, the metal insertion proved unsuccessful, probably due to solubility issues of the starting material. Therefore, in the next attempt DMF was used with 5 eq $Ni(acac)_2$ which should circumvent the solubility issues of the starting material. The reaction was stirred again for 18 h but this time at 125 °C. Another 2 eq of $Ni(acac)_2$ was added since the reaction had still not gone to completion. Unfortunately, again only starting material was obtained and the metal insertion was abandoned.

4.3 Charge transfer interactions of porphyrins and nanomaterials

Besides, for potential use as biosensors porphyrins can also be utilised for nanocarbon-based hybrid materials. Carbon-based nanomaterials have gained a

lot of attention due to their structural and electronic properties as well as high electrical conductivity.[211] This makes them promising candidates for future electronic and energy applications. Different types of such nanomaterials exist, such as fullerenes or graphene. Combining nanocarbon materials with other electron-rich molecules with interesting optical and electronic properties can result in new promising multifunctional hybrid materials with great potential as optoelectronic or energy conversion devices. In these hybrid materials, porphyrins can be used as efficient electron donor systems, while fullerene or graphene act as electron acceptors.[212] These two molecules can be linked through two different methods: covalent or noncovalent binding. The latter normally occurs through intermolecular interactions as mentioned earlier.[213] Usually, noncovalent interactions do not interfere with the π-electronic structure of graphene and are therefore favourable over covalent linkage.[198a, 214] Multiple investigations of charge transfer processes between these type of materials have been done.[215] Kiessling *et al.* investigated the incorporation of graphene-porphyrin nanohybrid materials into DSSCs.[199] They found that the electron injection occurs either from the porphyrin directly into the conduction band of the TiO_2 or through the graphene as an indirect conducting mediator. These graphene-porphyrin hybrids exhibited even better charge injection efficiencies than the porphyrin itself. In addition, aggregation, which is one of the biggest challenges in DSSCs, was averted which lead to a better regeneration process of the porphyrin sensitiser as well as a decline in the recombination losses.

4.3.1 Charge transfer interactions between C_{60}/ GC and porphyrins

For this analysis, steady-state spectroscopy, as well as transient absorption spectroscopy, was used to investigate the charge transfer interaction between two push-pull porphyrins and fullerene (C_{60}) or graphene carboxylate (GCO). This work was carried out in collaboration with Pinar Arpaçay from the research group of Prof. W. Blau (physics, TCD).

The interaction of the two porphyrins **2.33a** and **4.7** (Fig 4.2) with the nanomaterials was investigated in NMP (*N*-methyl-2-pyrrolidone) for the addition of C_{60} as well as a mixture of THF: H_2O (1:1, v/v) for GCO. Figure 4.2 and Figure 4.3 show the absorption spectra of the two porphyrins upon addition of C_{60}. At the beginning of the measurements, the Soret bands for both of the porphyrins are

clearly visible. Once C_{60} is added to the solution the Soret band of the porphyrins decreases and a broad signal with a hypochromical shift arises, which refers to the absorption of the C_{60}. This confirms the formation of the porphyrin nanohybrid material, as the absorption spectra contain characteristics of both individual components.[216] Furthermore, the overall absorption increases due to the absorption of both, the porphyrin and nanocarbon material, in the same region.

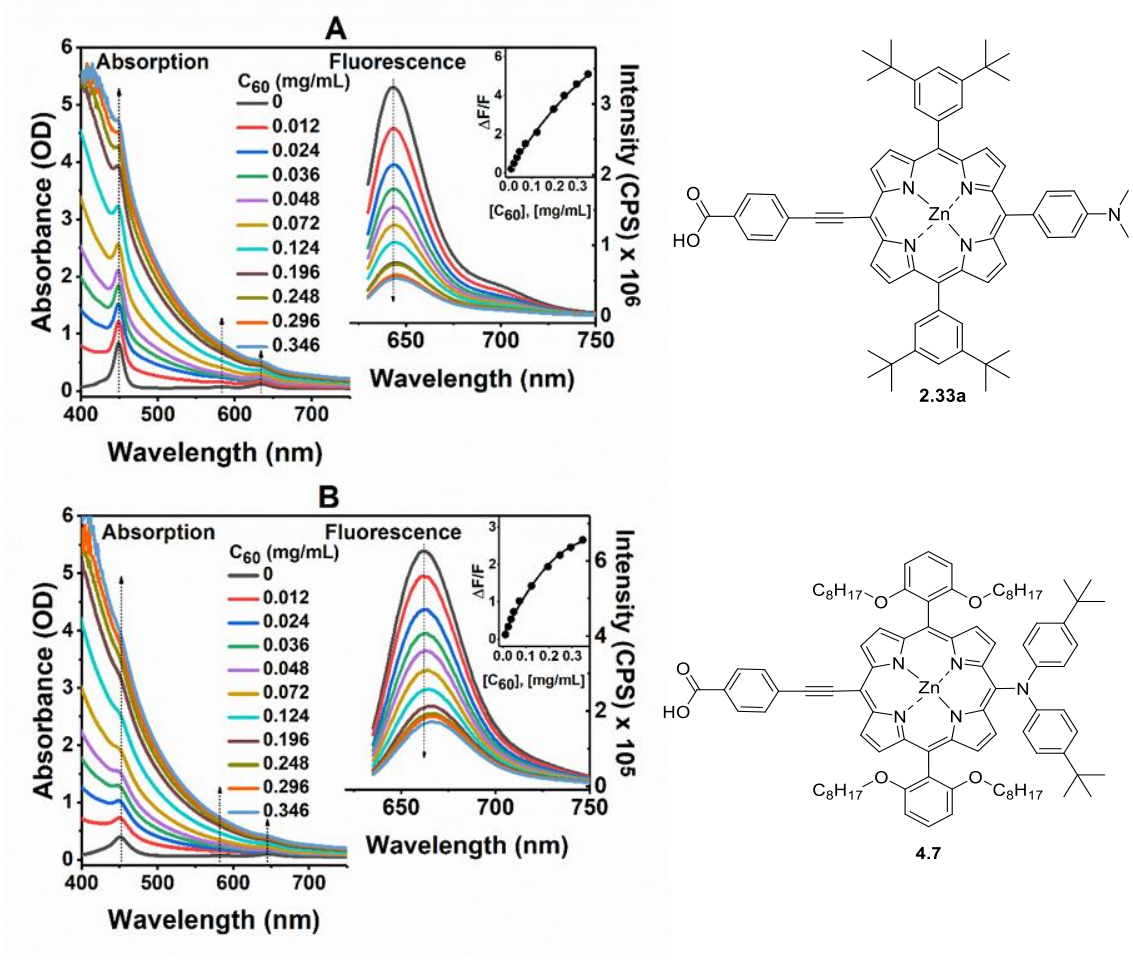

Figure 4.2. Steady-state absorption (left) and emission spectra (λ_{Ex} = 625 nm) (right) of (**A**) **2.33a** and (**B**) **4.7** recorded in NMP at different C_{60} concentrations (in mg/mL) as indicated. The Stern-Volmer plots are shown as a function of the C_{60} concentration of each porphyrin in the insets.

To further evaluate the non-covalent interactions of the porphyrins with C_{60}, fluorescence spectra were recorded. These are shown in the right insertion of Figure 4.2 and 4.3. For these spectra the porphyrins were excited at 625 nm. It is clearly visible that upon addition of C_{60} to the porphyrin solution the emission of the porphyrins is quenched, which correlates with the formation of the hybrid

materials.[217] In addition, a slight red shift is observed. The red-shift corresponds to the degree of complexation or interaction of the porphyrins with the nanomaterials, a larger redshift resembles stronger interactions.

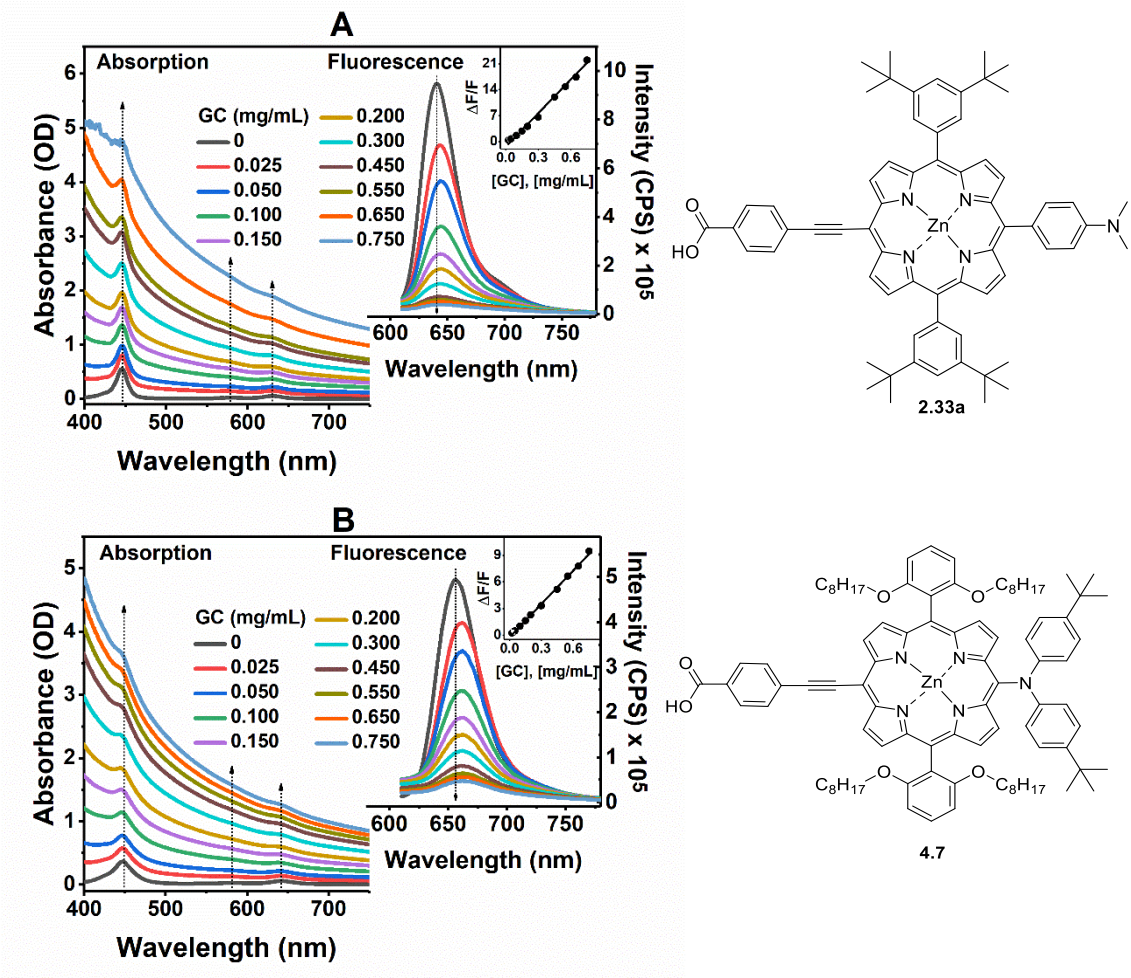

Figure 4.3. Absorption (left) and fluorescence after excitation at 600 nm (right) of (A) **2.33a** and (B) 4.7 recorded in THF: H_2O (1:1, v/v) at different GCO concentrations (in mg/mL) as indicated. Insets show the respective Stern-Volmer plots.

The same studies were performed for the interaction of the two porphyrins with graphene carboxylate (see Fig. 4.3). Here, similar trends can be observed as for C_{60}. Concurrently, the absorption spectra characteristics of both the porphyrins and the nanocarbon material are visible. As in the previous study, the peak of the Soret band of the porphyrins decreases with increasing addition of GCO, while the absorption of the nanomaterial becomes more prominent. The overall absorption increments are due to the absorption of both materials in the same region. The fluorescence spectra show, once again, quenching with increased concentration of

GCO. This time, however, a slightly larger red-shift can be seen for porphyrin **2.33a** as well as **4.7**. This implies that the interactions between porphyrin/GCO hybrids are slightly stronger than for the porphyrin/C_{60} hybrids

Some more conclusions about the nature of interactions can be drawn from the Stern-Volmer plots. These are shown in the right corner of each fluorescence spectra (Fig. 4.2 and Fig. 4.3). For the porphyrin/C_{60} hybrids a curved progression is observed. This resembles a combination of diffusion-controlled (dynamic) and static mechanisms for the deactivation of the excited-state.[218] On the other hand, the Stern-Volmer plot for the porphyrin/GCO hybrids is linear and passes through the origin. This solely correlates to a static mechanism during the quenching process. Since both of these processes can occur from either electron or energy transfer from the excited porphyrin to the nanocarbon material, further studies were necessary to elaborate the exact charge transfer process.

Furthermore, nanosecond- (ns) and femtosecond- (fs) transient absorption (TA) were performed by Pinar Arpaçay for both porphyrins as well as the four different porphyrin/nanocarbon hybrids. fs-TA spectra for the porphyrins show a strong negative absorption band, which can be accredited to the ground state bleach (GSB) of the Soret band. GSB refers to the depletion of the ground state due to the transfer of electrons to a higher excited state. After the band of the GSB, a broad excited state absorption (ESA) band is visible. This can be attributed to the formation of long-lived triplet states through intersystem crossing.[215a] Once the C_{60} is added to the porphyrin, changes occur in the GSB recovery and ESA decay. For both porphyrin hybrids, both processes occur at a faster rate. When GCO is added, GSB recovery is again faster compared to the porphyrins on their own; however, the ESA shows a rise in the signal. The faster GSB recovery for both hybrid systems suggests electron transfer from the porphyrin to the nanocarbon material. The GSB recovery happens even faster for the GCO hybrids than for those with C_{60}. This implies stronger interactions of the GCO material with the porphyrins and faster electron transfer compared to C_{60}. The ESA of C_{60} decays faster than that of the GCO hybrids. This indicates better charge separation between the porphyrins and GCO material. Further investigations of the kinetics showed that in the case of the porphyrin/C_{60} hybrids, a long distance diffusing-controlled quenching process occurs, while for the porphyrin/GCO hybrids only static electron transfer is observed.

4.4 Porphyrin-based Metal-Organic Frameworks

As previously mentioned, another application for interactions of porphyrins with nanomaterials are metal-organic frameworks (MOFs). MOFs are hybrid materials between inorganic connectors and organic linker systems. Since the first synthesis of MOFs in 1990, these types of porous coordination polymers have gained a lot of attention.[219] Depending on the type of organic linkers and connectors used, the physical and chemical properties of the material can be varied and modified very easily. Some of their remarkable properties include high porosity and high surface area, as well as chemical and thermal stability. This gives the materials a flexibility, which more traditional porous materials, such as mesoporous silicon and activated carbons, are lacking. This flexibility combined with their high degree of organisation makes them promising candidates for various applications such as gas storage, sensing, catalysis and drug delivery.[220] Furthermore, key properties such as pore size, structure and specific functionality can be fine-tuned through the selection of appropriate metal nodes and organic linker molecules.[220] In general, MOFs can be categorised into two classes, namely polycrystalline films and surface-mounted MOFs (SURMOF).[221]

Recently, porphyrins have been used as organic linkers in MOF and SURMOF materials. This comes without much surprise considering the wide range of properties and applications for porphyrins. Some early porphyrin-based MOFs feature a 5,10,15,20-tetra(-4-pyridyl)porphyrin or 5,10,15,20-tetrakis(2,6-dihydroxyphenyl)porphyrins.[222] Since then, multiple investigations have been undertaken to integrate porphyrins into this type of material. In 2011 Lee *et al*. synthesised a MOF which incorporated both BODIPY and porphyrin moieties.[223] The group more recently reported a MOF system featuring [5,15-diphenyl-10,20-bis(4-pyridylacetyl)porphyrinato]zinc(II). They were able to show long-range energy migration in a porphyrin-based MOF, mimicking the process of chlorophylls in photosynthesis. This is promising for applications in light-harvesting and energy transport.[200] For such systems, it is crucial to have a good excited-state transport length to photon absorption length ratio in order to work effectively. The absorption length describes the distance light must travel through a material to have most of its photons absorbed. This correlates directly with the thickness a light absorbing material must have to absorb most of the photons. Excited-state diffusion length describes the average length a carrier can travel before recombination. The higher

the ratio of excited-state transport length to photon absorption length, the more efficiently the energy of the light is absorbed and the resulting excited states are used to drive reactions. Since organic materials tend to have short absorption lengths, they represent promising materials for photon harvesting materials. Therefore, research has focused on enhancing the excited-state transport length. This was achieved by delocalising the excitation over several molecules. This so-called coherent transport mechanism has been employed in systems such as nanotubes[224], nanofibers[225] and conjugated polymer wires ingrained in a crystal[226].

4.4.1 Synthesis of pyridine-substituted porphyrins

In this part of the chapter, pyridine-substituted porphyrins were synthesised for implementation into the surface-anchored metal-organic framework (SURMOF). The synthesis of this project started with Pd insertion into diphenyl porphyrin **4.8**. Pd has shown to be a valuable metal for such systems, as it promotes a high intersystem-crossing rate, leading to the absorbed photons being efficiently translated into triplet exciton states.[201, 227] Therefore, **4.8** was dissolved in toluene in a MW vial with 5 eq. of $Pd(OAc)_2$. The reaction was heated for 45 min at 120 °C in the MW. This reaction step proceeded without difficulties to completion and after purification and crystallisation from MeOH, the desired porphyrin **4.9** was obtained in 69% yield (Scheme 4.3).

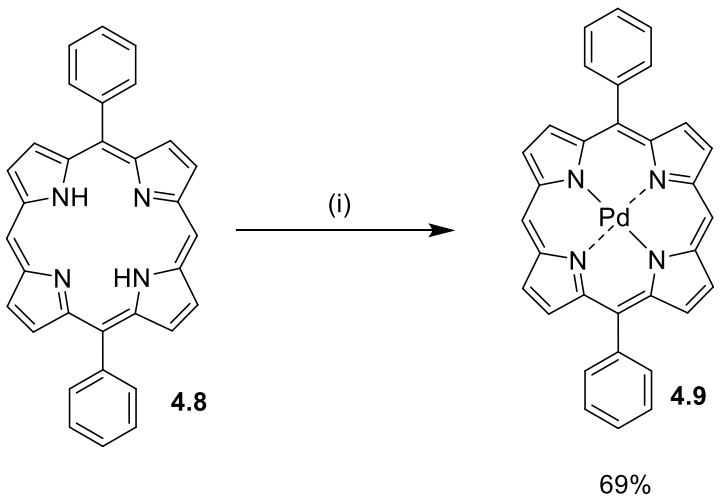

Scheme 4.3. Synthesis of [5,15-diphenylporphyrinato]palladium(II) **4.9**: (i) $Pd(OAc)_2$ (5 eq.), toluene, MW: 120 °C, 45 min.

The next step involved dibromination of **4.9** with NBS, followed by a Sonogashira cross-coupling reaction with 4-ethynylpyridine (Scheme 4.4). The cross-coupling

reaction was attempted in the MW using 3 eq. of 4-ethynylpyridine, $Pd(PPh_3)_4$ (0.16 eq.), CuI (0.16 eq.) and TEA. The reaction was irradiated first for 45 min at 45 °C. Since starting material was still present, the reaction was heated again at 75 °C for 60 min. Even though at this point all of the starting material was consumed, the target compound **4.11** was not obtained.

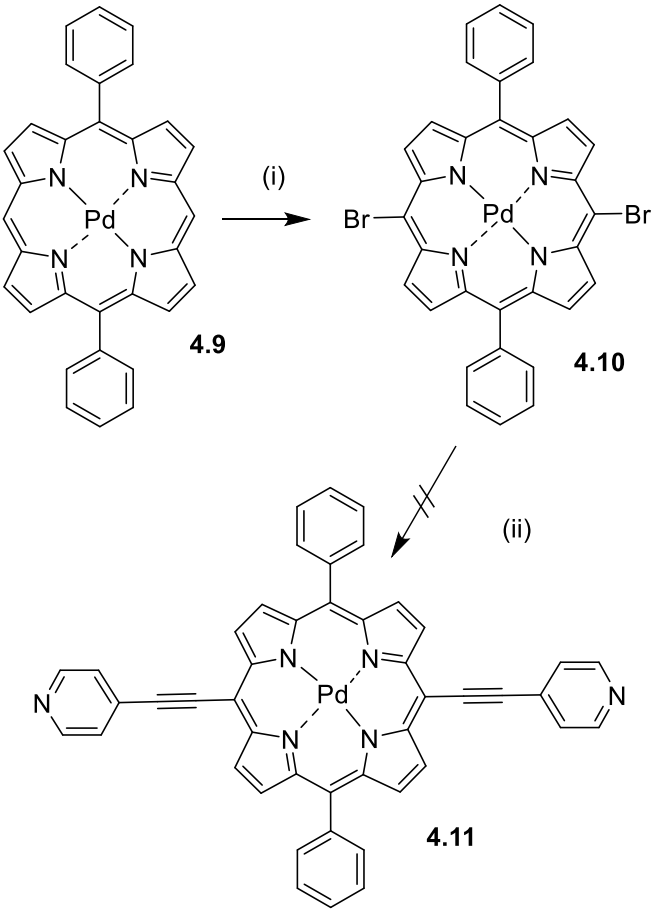

Scheme 4.4. Synthesis of (5,15-diphenyl-10,20-bis-[(4-pyridyl)ethynylporphyrinato)palladium(II) **4.11** *via* Sonogashira-cross coupling: (i) NBS (2.2 eq.), pyridine (cat.), $CHCl_3$, rt. (ii) 4-Ethynylpyridine (3 eq.), $Pd(PPh_3)_4$ (0.16 eq.), CuI (0.16 eq.), TEA, dry THF, MW 70-75 °C, 60 min-4 h.

Therefore, the reaction was set up a second time at 70 °C for 4h. Again, all of the starting material was consumed but porphyrin **4.11** could not be purified. Several attempts at purification *via* column chromatography were performed with various solvent mixtures on either silica gel or ALOX (silica: DCM+1-5% MeOH, $CHCl_3$, THF; ALOX: THF, $CHCl_3$, DCM). Following further review of the literature, the decision was made to synthesise the pyridine-substituted porphyrin as the free base first, as this had been reported several times.[2] The dibrominated porphyrin

4.12 was synthesised as starting material for the coupling reaction (Scheme 4.5), with the reaction first attempted in the MW (Table 4.1). The reaction in THF was heated for 2 h at 40 °C.

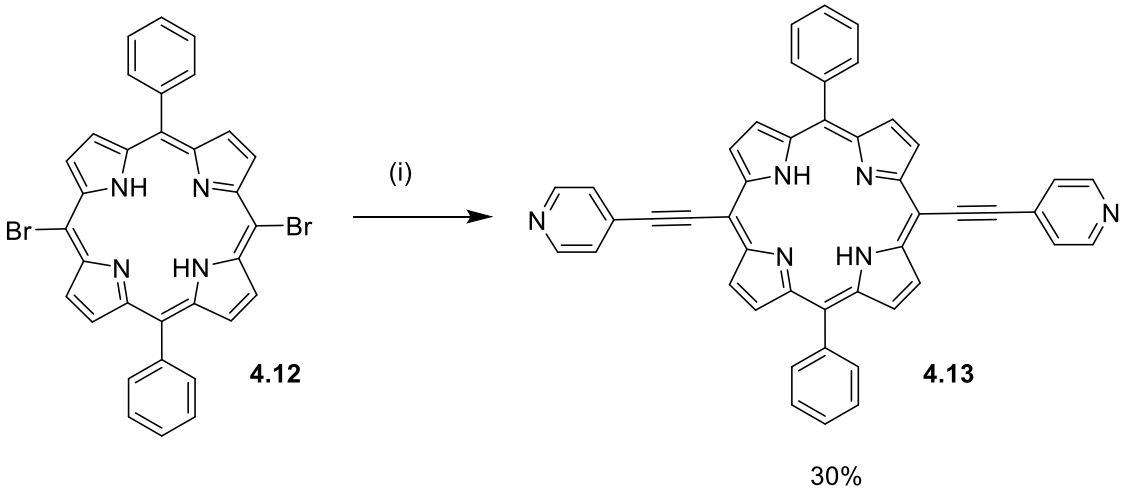

Scheme 4.5. Synthesis of 5,15-diphenyl-10,20-bis-[(4-pyridyl)ethynylporphyrin **4.13** *via* Sonogashira cross-coupling: (i) 4-Ethynylpyridine (3 eq.), $Pd_2(dba)_3$ (0.3 eq.), $AsPh_3$ (2.4 eq.), TEA, dry THF, 75 °C, 60 min.

As a large amount of starting material remained, the reaction was heated for a further 4 h at 70 °C in the MW. Another reaction was set up on the same scale and heated in the MW for 4 h at 100 °C. However, the target compound **4.13** was not formed. A third reaction was set up with 8 mL of dry DMF. On this occasion, all of the starting material was consumed after 20 min at 160 °C, however, no coupled product was observed. The same reaction was then attempted under bench conditions which resulted in a 30% yield of **4.13** (Scheme 4.5). Following these results, synthesis was continued under bench conditions as MW irradiation may have been too harsh, leading only to dehalogenation of the starting material **4.12**. As **4.13** is quite polar, MeOH was necessary to remove it from the ALOX column. Therefore, it was crucial to wash the crude solid immediately after the reaction with MeOH to remove major impurities, which would otherwise co-elute with the target compound.

Table 4.1. Optimisation of Sonogashira cross-coupling reaction conditions for porphyrin **4.13**:

Entry	Solvent	Temperature [°C]	Reaction Time [min]	Outcome
1	THF	MW (i) 40; (ii) 70	(i) 120; (ii) 240	No product formation
2	DMF	MW 160	20	No product formation
3	THF	75	60	30%

The final step involved Pd insertion into the porphyrin (Scheme 4.6). Thus, **4.13** was dissolved in toluene with 5 eq. $Pd(OAc)_2$ and heated in the MW for 45 min at 120 °C. Unfortunately, as soon as the insertion of Pd was attempted, the porphyrin formed networks and precipitated out of solution due to the interaction between the pyridine units and Pd. Thus, metallation with lower eq. of Pd was attempted in the hopes of circumventing this issue. The number of equivalents of Pd were reduced to 2.5 eq., however, the compound again precipitated out of solution. Even with just 0.5 eq. Pd networks of porphyrin **4.13** were formed. The same outcome was obtained upon use of $CHCl_3$ in the place of toluene.

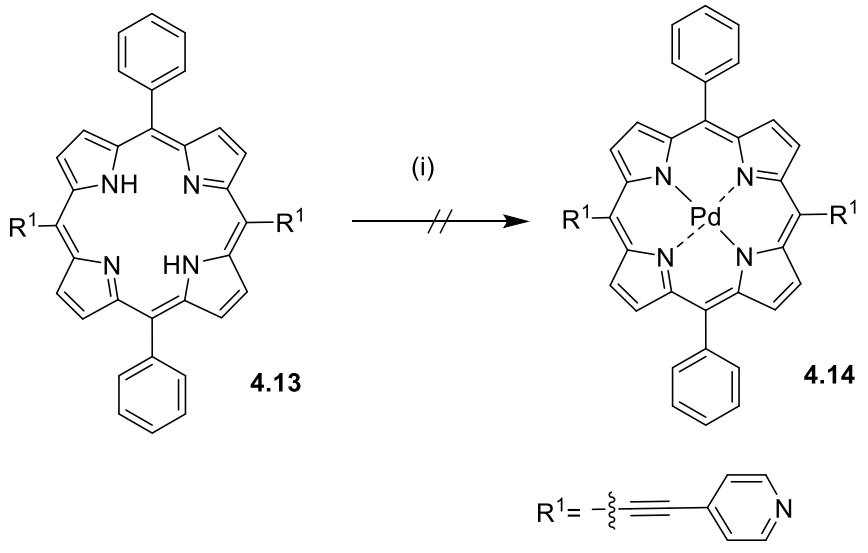

Scheme 4.6. Attempted synthesis of (5,15-diphenyl-10,20-bis-[(4-pyridyl)ethynyl]porphyrinato)palladium(II) **4.14**: (i) $Pd(OAc)_2$ (5 eq.), toluene, MW 120 °C, 45 min.

Therefore, the synthetic route had to be revised. The Pd was again inserted prior to the coupling reaction to minimise the interactions between the pyridine units and

Pd. Since purification proved to be very difficult once Pd was inserted into the porphyrin core, the metal insertion was held off until the just before the cross-coupling reaction (Scheme 4.7).

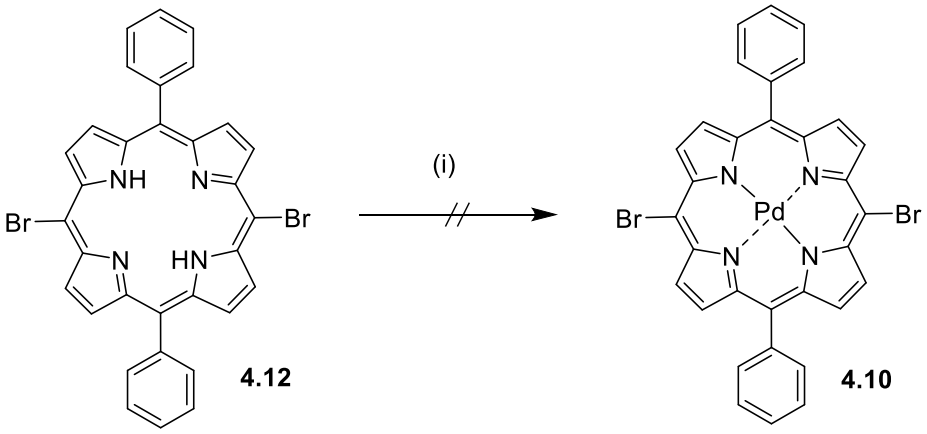

Scheme 4.7. Attempted palladium insertion into 5,15-dibromo-10,20-diphenylporphyrin **4.12**: (i) $Pd(OAc)_2$ (2 eq.), toluene, MW: 120 °C, 60 min.

The same procedure as previously described for the Pd insertion was followed (Scheme 4.7). The brominated porphyrin **4.12** was dissolved in toluene, $Pd(OAc)_2$ was added and the reaction was subjected to MW irradiation at 120 °C for 60 min. Unfortunately, this reaction resulted in a mixture of dibrominated, monobrominated and debrominated species. At this point, it was suspected that heating the reaction might lead to the debromination process. Therefore, porphyrin **4.12** was dissolved in $CHCl_3$ with 5 eq. $Pd(OAc)_2$ and was stirred at room temperature for 18 h (Scheme 4.8). The solvent was removed and filtration through silica was carried out immediately afterwards to remove the excess Pd from the reaction mixture. After purification, the target compound **4.10** was obtained in 66% yield. This demonstrated that Pd insertion can be achieved as long as no heat is applied during the reaction. An attempt to upscale, however, resulted in only 34% of the desired metal porphyrin **4.10**, mainly due to solubility issues. Therefore, this reaction should not be performed on a scale larger than 100 mg of porphyrin.

Having the Pd porphyrin **4.10** at hand, another attempt to couple the porphyrin with the two ethynylpyridine groups was undertaken (Scheme 4.9).

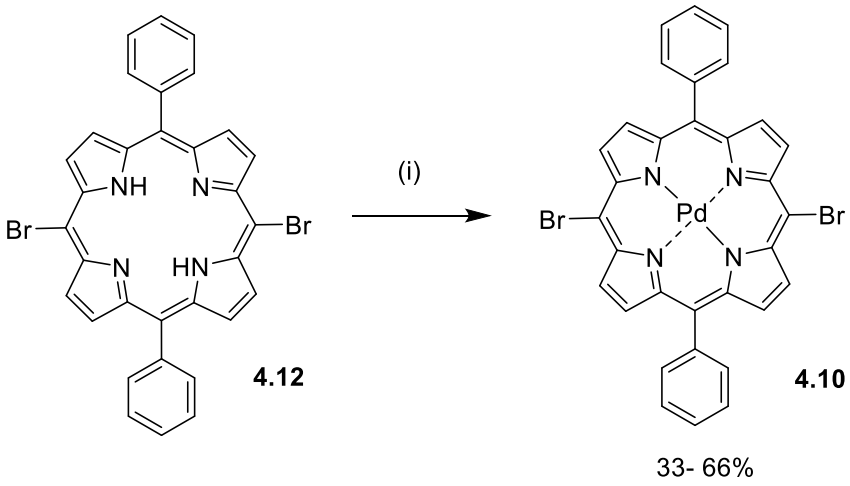

Scheme 4.8. Optimised palladium insertion into 5,15-dibromo-10,20-diphenylporphyrin **4.12**: (i) $Pd(OAc)_2$ (2 eq.), $CHCl_3$/MeOH, rt, 16 h.

Porphyrin **4.10**, 4-ethynylpyridine, $Pd(PPh_3)_4$ and CuI were dried for 3 h under vacuum. After the addition of dry THF and TEA, the reaction was heated to 75 °C for 1 h. Upon completion of purification, however, only 15 mg of porphyrin **4.11** (18%) was obtained. This low yield resulted most likely from loss of product during purification. The reaction was repeated with 99 mg of porphyrin, however more base and solvent was necessary to ensure that all of the starting material was in solution. Work-up followed the same procedure as previously described, leading to collection of the desired Pd porphyrin **4.11** in 52% yield.

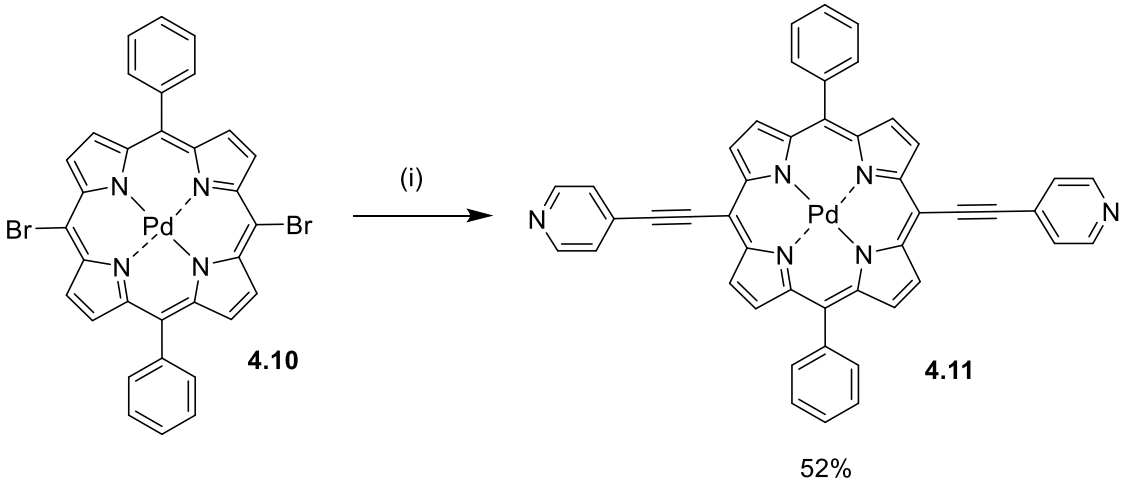

Scheme 4.9. Synthesis of (5,15-diphenyl-10,20-bis-[(4-pyridyl)ethynylporphyrinato)palladium(II) **4.11** *via* Sonogashira cross-coupling: (i) 4-ethynylpyridine (3 eq.), $Pd(PPh_3)_4$ (0.16 eq.), CuI (0.16 eq.), TEA, dry THF, 75 °C, 1 h.

4.5 Covalent attachment of ethynyl-porphyrins to electrode surfaces

The modification of electrodes with porphyrins has gained recent attention. Such modified electrodes can be used, for example, as electrocatalysts for chemical and photochemical reactions or for analytical applications.[228] Porphyrin layers, which are produced through non-covalent interactions, are well known, however, they tend to be rather fragile.[229] More recent work has focus on the generation of covalently linked porphyrin monolayers. These systems have the benefit of being more robust and easier to manipulate.[230] Strategies used for both types of systems include electropolymerisation[229, 231], self-assembly[232], thermolysis[233], click chemistry[234] or covalent linkage[235]. Terminal alkynes, in general, represent a very useful handle for a plethora of reactions. For example, they can be used as linkers for electron transfer systems between redox-active molecules and electrodes.[236] Sheridan *et al.* published a method of linking porphyrins covalently to electrode surfaces such as glassy carbon, platinum or gold.[202] They managed to generate an ethynyl radical through a one-electron oxidation resulting in the loss of the terminal proton. The radical then reacts readily with the electrode, resulting in a porphyrin monolayer on the electrode.

4.5.1 Synthesis of metalloporphyrins with a terminal alkynyl group

For the synthesis of the porphyrin with the desired ethynyl handle, a well-known approach was applied. Thereby, an organolithium reaction was chosen as starting point. The reaction of such unprotected ethynyl-substituted porphyrins has been reported by Feng and Senge in 2001.[149] This has proven to be a straightforward approach as the unprotected triple bond can be introduced in one reaction, rather than having to use several functionalisation steps. The unsubstituted 5,15-diphenylporphyrin **4.8** was subjected to the organolithium reaction conditions without prior activation through bromination (Scheme 4.10). Another advantage of this reaction lies in the selective formation of the monosubstituted species. For other coupling reactions, the mono-halogenated precursor would be required, which always results in loss of material due to the formation of the dihalogenated porphyrin. However, utilising this reaction just one substituent can be selectively introduced without prior functionalisation.

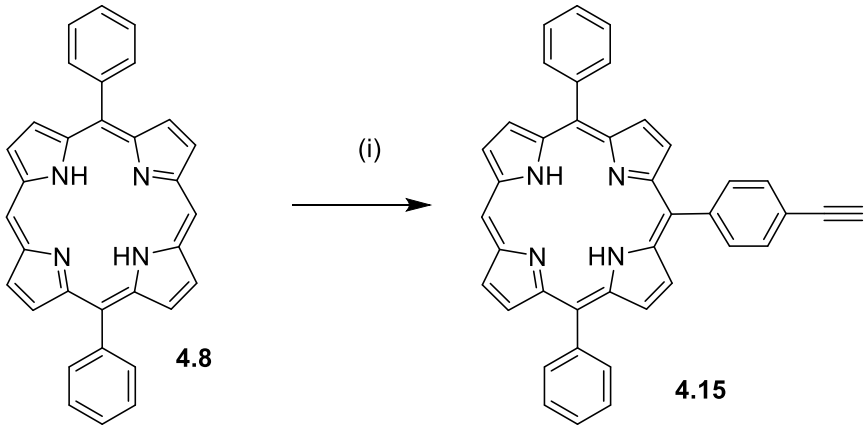

Scheme 4.10. Synthesis of ethynyl-substituted porphyrin 4.15 *via* organolithium reaction: (i) (a) 4-Bromo-ethynylbenzene (11 eq.), *n*-BuLi (23 eq.), dry ether, -40 °C; (b) dry THF, rt, 1 h; (c) H_2O, rt, 30 min; (d) DDQ, rt, 1 h.

The organolithium species is formed *in-situ via* metal-exchange through the addition of *n*-BuLi to 4-bromo-ethynylbenzene (Scheme 4.10). After addition of *n*-BuLi at -40 °C, dry THF was added dropwise until a white suspension of the aryllithium formed, followed by the addition of the porphyrin solution. After hydrolysis and oxidation, the desired porphyrin **4.16** was obtained in 68% yield.

The next step involved the metal insertion. Two different metal complexes were targeted, namely the Ni and Co porphyrin species. For the Ni insertion, **4.15** was dissolved in toluene with $Ni(acac)_2$ and heated to 120 °C until all of the starting material was consumed (Scheme 4.11). This metal insertion proceeded readily and without any difficulties. Due to similar polarities, difficulties during separation of the free-base porphyrin **4.15** from the starting material **4.16** occurred. Therefore, a mixture of both porphyrins was subjected to the Ni-insertion in the hope that the metal would increase the difference in polarity between the two porphyrins. Indeed, separation proceeded without any difficulties after the metal insertion. However, due to the fact that a mixture of porphyrins was used in the reaction, the yields of the isolated Ni-porphyrin **4.16** appeared lower than usually expected.

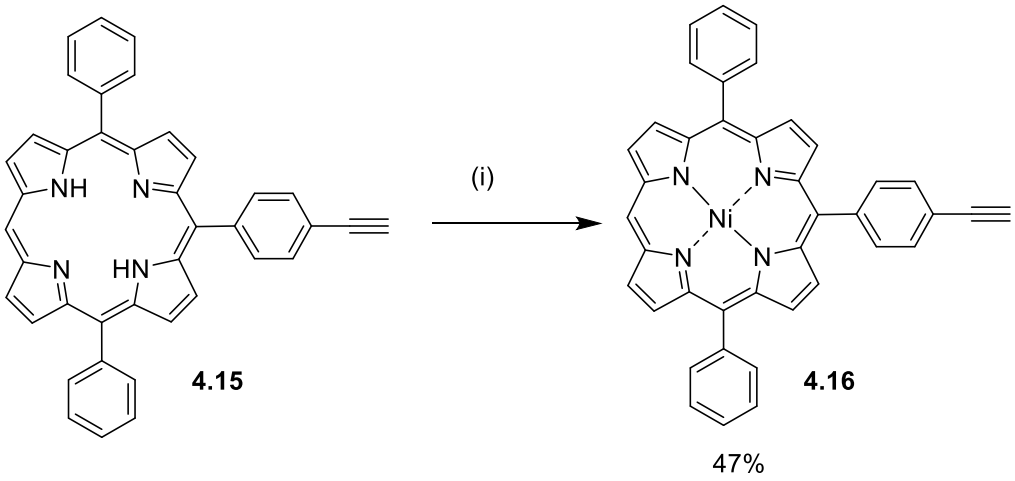

Scheme 4.11. Ni insertion into the free-base porphyrin **4.15**: (i) $Ni(acac)_2$ (1.2 eq.), toluene, 120 °C, 3 h.

The same procedure was used for the attempted Co insertion (Scheme 4.12). The free base porphyrin **4.15** was dissolved in $CHCl_3$ together with $Co(OAc)_2$ and heated to 75 °C until all of the starting material was consumed. Upon purification, however, the Co porphyrin **4.17** showed strong interactions with silica gel and ALOX, with most of the target material lost during column chromatography. Since this was happening in every reaction attempted, the synthetic pathway had to be revised. The interaction of the porphyrin with ALOX or silica gel seemed to be the main issue.

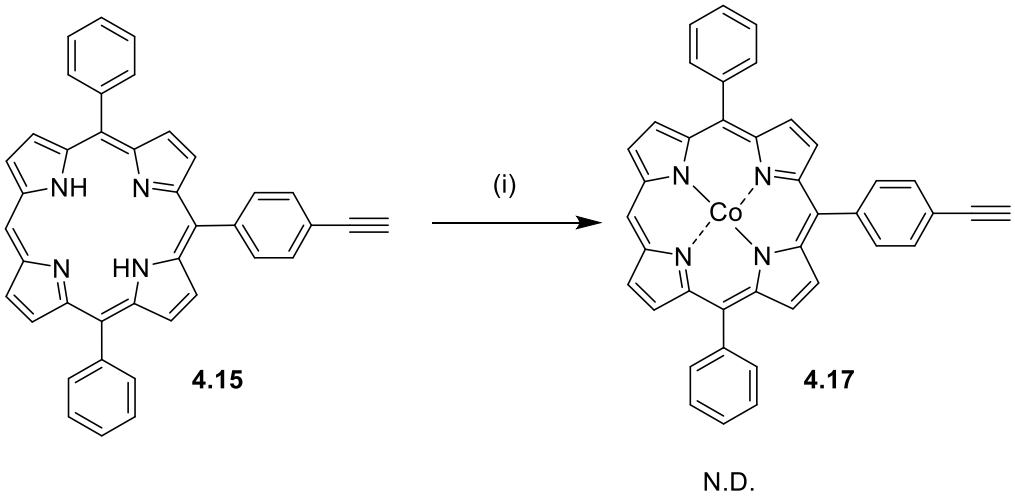

Scheme 4.12. Co insertion into 5-(4-ethynylphenyl)10,20-diphenylporphyrin **4.15**: (i) $Co(OAc)_2$ (5 eq.), $CHCl_3$/MeOH, TEA, 75 °C, 3 h.

Thus, the decision was made to insert the Co into the porphyrin prior to the attachment of the ethynyl group. Furthermore, the TMS-protected triple bond would be attached *via* a Suzuki coupling reaction, which should allow facile purification of the porphyrin at that stage. The final compound would then be obtained through deprotection with TBAF. Due to the fact that it should be possible to purify the protected porphyrin in the previous step, the final target compound would need only be purified through aqueous workup and recrystallisation, avoiding any interaction with silica or ALOX and loss of production thereof.

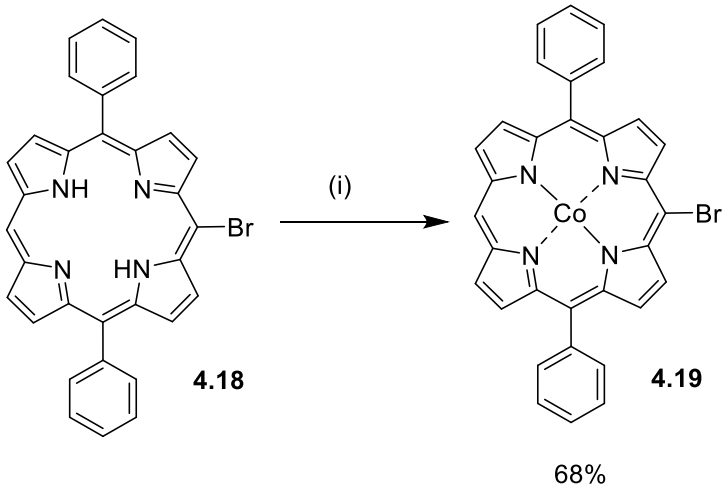

Scheme 4.13. Co insertion into 5-(bromo)-10,20-diphenylporphyrin **4.18**: (i) $Co(OAc)_2$ (5 eq.), $CHCl_3$/MeOH, TEA, 75 °C, 3 h.

The metal was readily inserted into the mono-brominated free base porphyrin **4.18** using the same procedure as before (Scheme 4.13). This time, compound **4.18** was purified with a simple filtration through silica without any problems of the porphyrin interacting with the silica gel. The metal complex **4.19** was obtained in 68% yield. The next step involved the Suzuki coupling of 4-[(trimethylsilyl)ethynyl]phenylboronic acid pinacol ester with the brominated porphyrin **4.19** (Scheme 4.14). Thus, the brominated porphyrin **4.19** was subjected to Suzuki coupling conditions. 50 mg of porphyrin **4.19** were dried with $Pd(PPh_3)_4$, K_3PO_4 and the 4-[(trimethylsilyl)ethynyl]phenylboronic acid pinacol ester. The porphyrin was dissolved in dry THF and the reaction was stirred at 70 °C for 18 h. Again, column chromatography proceeded without any problems and the desired porphyrin **4.20** was obtained in 68% yield (Scheme 4.14). The final step involved a deprotection of the TMS group with TBAF (Scheme 4.15). Therefore, porphyrin **4.20** was dissolved in dry THF and TBAF (4 eq.) was added to the reaction.

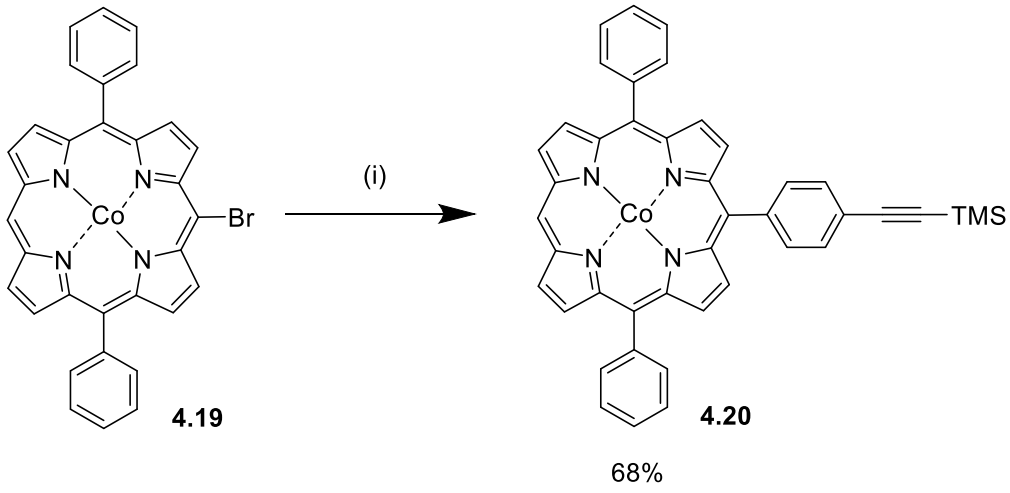

Scheme 4.14. Suzuki cross-coupling reaction with 4-[(trimethylsilyl)ethynyl]phenylboronic acid pinacol ester: (i) 4-[(Trimethylsilyl)ethynyl]phenylboronic acid pinacol ester (2 eq.), $Pd(PPh_3)_4$ (0.22 eq.), K_3PO_4 (10 eq.), dry THF, 70 °C, 18 h.

The reaction mixture was stirred until completion at rt. The crude mixture was then poured in H_2O and extracted with DCM. After an aqueous wash, the target porphyrin **4.17** was collected in 98% yield.

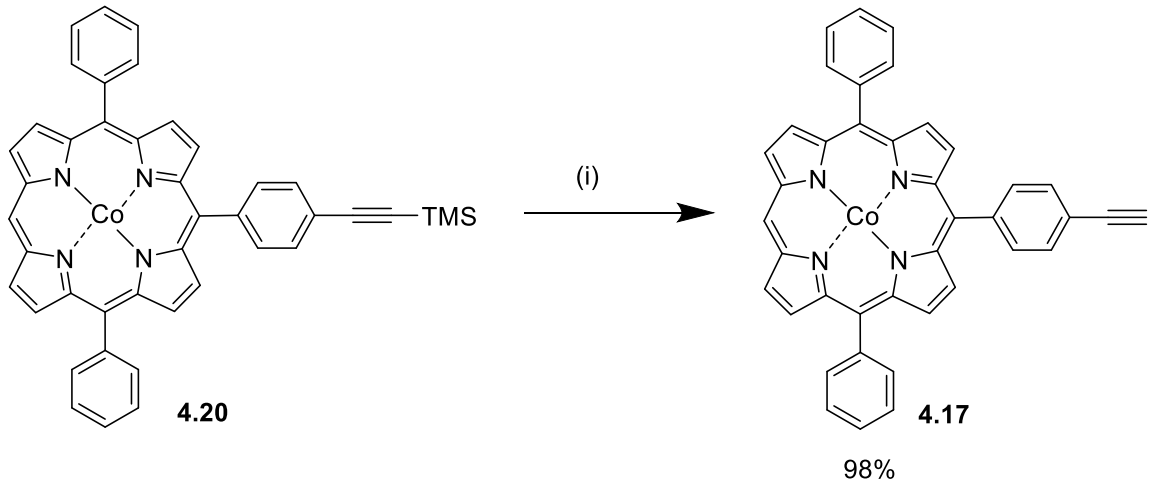

Scheme 4.15. Synthesis of the porphyrin **4.17** *via* TBAF deprotection: (i) TBAF (4 eq.), dry THF, rt.

4.6 Conclusion

The synthesis of a series of different *m*-benzoic acid porphyrins for potential application as supramolecular tectons in surface binding studies was accomplished. The approach was based on a logical and straightforward step-wise

functionalisation of the porphyrin core to achieve the desired performance for surface binding studies. The compounds reported vary from monomeric compounds with one to four carboxylic acid moieties as well as *π*-extended bis-carboxylic acid porphyrin dimers which prominently feature long-wavelength absorbance.

Subsequently, previously synthesised *push-pull* porphyrins were used for the investigation of charge transfer processes with graphene carboxylate and fullerene. Steady-state photoluminescence quenching is observed which confirms that energy and/or electron transfer from the excited porphyrin to the nanomaterial is occurring. Further investigations of the Stern-Volmer plots gave insights into the quenching mechanism. For the porphyrin/GCO hybrids, it was found that the plot shows linear progression which can be correlated to a static quenching mechanism. For the porphyrin/C_{60} hybrids, however, a curvature is observed. This can be associated with a mixture of both static and dynamic quenching. fs-TA and ns-TA further showed that electron transfer without energy transfer is occurring. It also confirmed that a combination of static and diffusion controlled electron quenching is occurring for the porphyrin/C_{60} hybrid while the porphyrin/GCO hybrid is quenched *via* a static mechanism. Analysis of the ESA shows that the ESA of C_{60} decays faster than for the GCO hybrids. This indicates better charge separation between the porphyrins and GCO material.

Furthermore, symmetric porphyrins with pyridine linker units were synthesised for use in MOFs. The pyridine units were attached in a defined spatial arrangement. In addition, the insertion of Pd results in a heavy atom effect. Initial synthetic considerations were based on the Pd insertion into the unsubstituted 5,15-diphenylporphyrin followed by bromination and subsequent Sonogashira cross-coupling reaction. The synthesis of these systems proved to be challenging due to unwanted interactions of Pd with other groups on the porphyrin, namely bromine atoms and the pyridine groups. This resulted in time-consuming and cumbersome purification. The Sonogashira coupling reaction was first attempted in the MW, however, the target compound could not be isolated/purified. Therefore, the synthetic methodology was revisited. The synthesis of the free-base pyridine-substituted porphyrin is a well-known reaction in literature.[2] Besides this, most other metal complexes of this type of porphyrin were synthesised through metal insertion into the free-base pyridine-substituted porphyrin.[237] Thus, it was decided

to synthesise the free-base porphyrin first and insert the Pd afterwards. Initial attempts to insert Pd into the free-base pyridine-substituted porphyrin resulted in the formation of insoluble networks upon Pd insertion. This was due to the interaction between pyridine and Pd. Since it became apparent that the purification of any Pd porphyrin in this study was plagued with numerous challenges, it was decided to insert the Pd into porphyrin core as far into the synthesis as possible. The Pd insertion was therefore attempted with the 5,15-dibromo-10,20-diphenylporphyrin. The same procedure was used as for the 5,15-diphenylporphyrin. However, heating resulted in debromination and gave a mixture of mono-, di-, and de-brominated porphyrin species. Metal insertion at room temperature finally resulted in the desired metalloporphyrin. In the final step, the Sonogashira reaction conditions were optimised and the reaction was only allowed to be heated for 1 h at 75 °C under bench conditions to avoid degradation or the formation of unwanted side products. This gave the target compound in 52% yield. The porphyrin was then sent to our collaborator Dr. Andrey Turshatov in Karlsruhe for the implementation into MOFs and subsequent investigation of their electronic properties.

Finally, ethynylphenyl-substituted metal porphyrins were synthesised for their aniodic covalent attachment to electrodes. Therefore, the free-base porphyrin was synthesised using a well-known organolithium approach.[149] The Ni insertion into the porphyrin proceeded without any complications. The Co insertion, however, resulted in difficulties during the purification process due to the intense interaction of the porphyrin with silica and ALOX and subsequent degradation of the molecule. To minimise the possible interactions of this porphyrin, the decision was made to insert the Co prior to the coupling reaction and to attach the TMS-protected ethynylphenyl linker *via* a Suzuki cross-coupling reaction. This allowed facile and straightforward purification of this molecule. The final step consisted of deprotection of the TMS group with TBAF. Exposure of the final compound to silica gel or ALOX was avoided and purification was done solely through aqueous work-up. This gave the target compound in 98% yield. Both metal complexes were then sent to our collaborator Prof. Geiger in Vermont for their investigations into the covalent attachment of the metalloporphyrins to electrode surfaces.

5 Large π-conjugated porphyrin systems

Porphyrins with peripherally-fused ring systems and conjugated porphyrin arrays are currently being widely investigated due to their unique electronic, optical and electrochemical properties. The synthetic methodologies used to explore annulated, π-extended and bridged systems span a whole range of reactions from 'old' Friedel-Crafts reactions to 'modern' transition metal-catalysed ones.[238] The number of macrocycles with fused substituents (**5.1** or **5.2**) and of porphyrin dimers and arrays prepared through these reactions is ever expanding, as are the types of fused structures (*e.g.*, singly-fused **5.3** *versus* triply fused **5.4**).[239] These structures are complemented by an even larger number of porphyrin arrays of which porphyrin units are linked by bridging linkers (**5.6**) or fused ring systems **5.5**). Some general examples of such systems are shown in Figure 5.1.

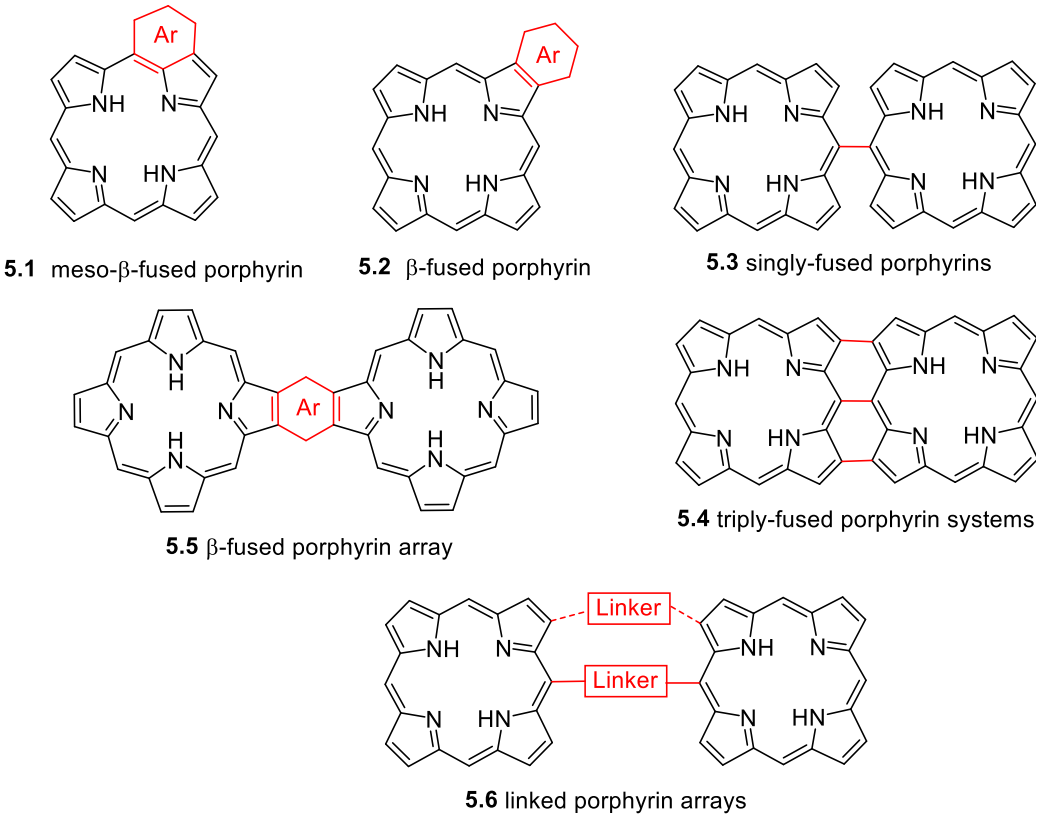

5.1 meso-β-fused porphyrin **5.2** β-fused porphyrin **5.3** singly-fused porphyrins

5.5 β-fused porphyrin array **5.4** triply-fused porphyrin systems

5.6 linked porphyrin arrays

Figure 5.1. Selected types of 'fused'-porphyrin systems.

Researchers have always been interested in understanding the correlation between the structure of porphyrins and their rich photophysical properties.[75, 240] One very effective way of achieving a change of these properties is through π-

extension of the porphyrin macrocycle. This synthetic method normally results in a considerable bathochromic shift of the absorption spectra. The dimension of this shift normally depends on the type of conjugation.[241] Many different methods exist to obtain such systems and some will be discussed later. However, oxidative aromatic coupling has gained most attention recently as it results in the largest bathochromic shift.[241] Although intramolecular oxidative fusing reactions are used quite frequently, the exact mechanism is still not entirely known. It is still not clear if the porphyrin or the other aromatic moiety is attacked first by the oxidant and subsequently forms the electrophilic radical cation.[241] Such fused porphyrin systems exhibit multiple interesting photophysical properties such as red-shifted absorption, short excited-state lifetimes extensive nonlinear optical properties and interesting electronic characteristics.[242] These properties open the pathway to valuable applications such as for conducting molecular wires, semiconductors or dyes for photovoltaic devices and nonlinear optics.

Classic examples of porphyrins with fused, 'extra' ring systems were prepared by intramolecular cyclisation reactions. A case in point is the purpurin family (cyclopenta[*at*]porphyrins **5.7**), in which a five-membered ring system links a meso- and β-position (Fig 5.2). These compounds are easily recognised as being related to the fundamental structure of chlorophylls. Fused six-membered ring systems were initially investigated in the form of benzochlorins **5.8** prepared by intramolecular cyclisation of formylvinylporphyrins.[243] Another example are benzoporphyrins **5.9** (Fig. 5.2), in which benzene residues are fused to both β-positions of one or more pyrrole rings. These are best prepared *via* pericyclic reactions. Related compounds are the naphthoporphyrins **5.10** (where a classic synthesis by Callot used a 2-formylporphyrin for an intramolecular acid-catalysed reaction)[244] and naphthochlorins **5.11** (Fig 5.2).[245] For the latter, the easiest access is given by the treatment of (5,10,15,20-tetraphenyl-2-vinylporphyrinato)nickel(II) with dilute sulfuric acid.[246]

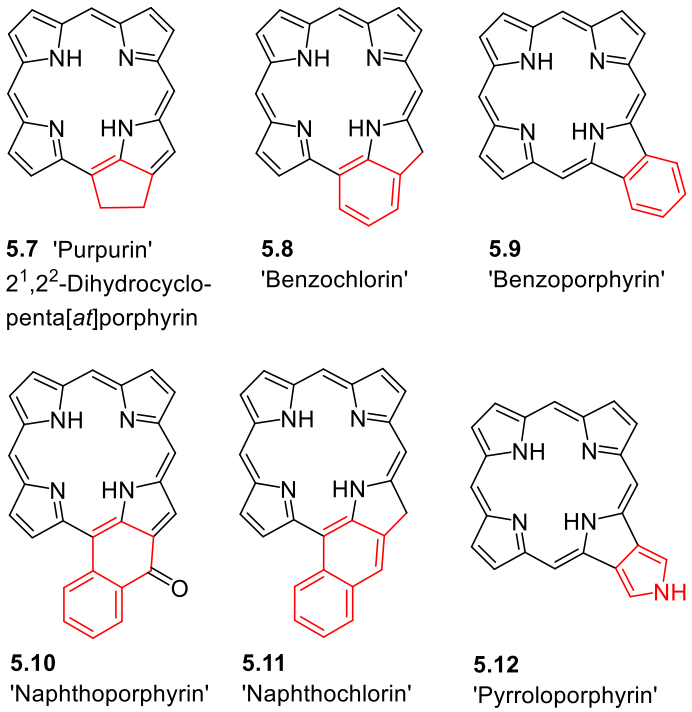

5.7 'Purpurin' $2^1,2^2$-Dihydrocyclo-penta[*at*]porphyrin

5.8 'Benzochlorin'

5.9 'Benzoporphyrin'

5.10 'Naphthoporphyrin'

5.11 'Naphthochlorin'

5.12 'Pyrroloporphyrin'

Figure 5.2. Porphyrins with fused five- or six-membered rings.

Larger aromatic systems and/or porphyrins can also be fused with or linked to porphyrins. An excellent account of this area has been given by Tanaka and Osuka.[247] This area of research started to take off in the late 1990's with the first reports on singly-meso-meso- **5.13** and doubly-meso-β-linked bisporphyrins **5.14**. Porphyrins can also be fused solely at the β-positions and this was elegantly demonstrated by Smith and co-workers using pyrroloporphyrins **5.12**.[248] These are accessible using a 2-nitroporphyrin as the nitroalkene component of a Barton-Zard reaction[249], *i.e.*, utilising the porphyrin as a precursor for a pyrrole. The latter could then be applied to a standard pyrrole condensation reaction to yield directly doubly-β-β-fused bisporphyrins such as **5.15** (Fig. 5.3).

As a 'pyrrole' pyrroloporphyrins can also undergo standard tetramerisation reactions to yield a cross-shaped pentaporphyrin with a central porphyrin appended at all four C_b-C_b units by another porphyrin, *e.g.*, **5.17** .[250] However, in this case, the pyrrole unit(s) had to be positioned farther away to minimise steric hindrance which was achieved by preparing pyrroloporphyrins of type **5.16**, a 2*H*-dihydroisoindoloporphyrin.

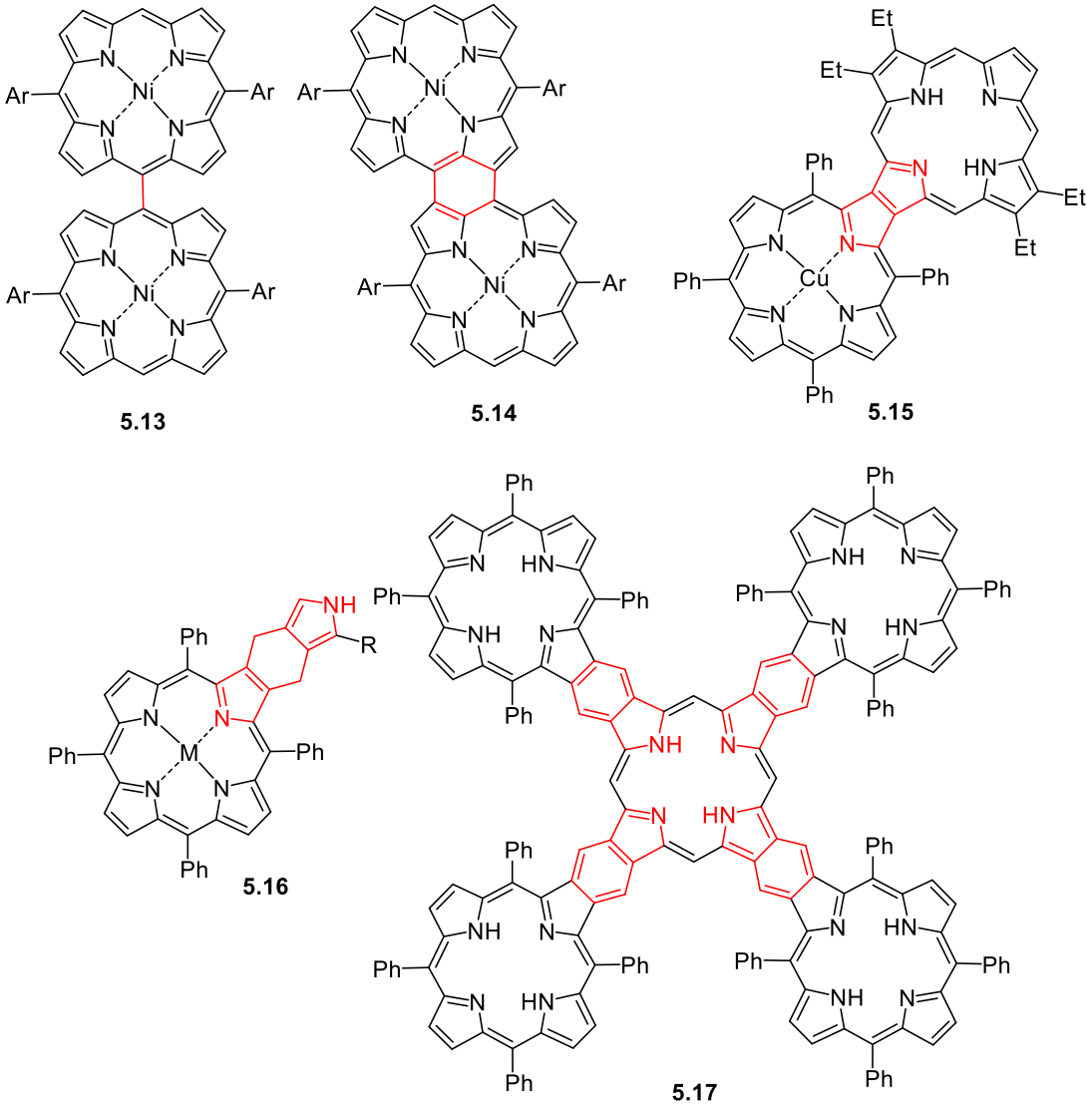

Figure 5.3. Examples of β-fused porphyrin systems.

This required a [4+2] cycloaddition of a 5,10,15,20-tetraarylporphyrin with 1,1-sulfolano[3,4-c]pyrrole[251], acid-catalysed tetramerisation and exhaustive oxidation with DDQ to assure oxidation of both the porphyrinogen and the cyclohexadiene fragments between the porphyrins.

Apart from fusing porphyrins along the β-position, many porphyrins directly-linked at the meso-position have been prepared – ultimately leading to series of bisporphyrins, oligomers and polymers with meso-meso, meso-β or meso-β-β fusions.[247] The key development was Osuka's Ag(I)-promoted coupling of porphyrins **5.18** to yield **5.19**.[252] These singly-linked systems could then be oxidised to the triply-linked systems **5.20**.[253] Notably, the meso-meso-linkage could also be achieved through polymerisation reactions[254], up to the 128mer leading to the preparation of fully conjugated porphyrin tapes.[255]

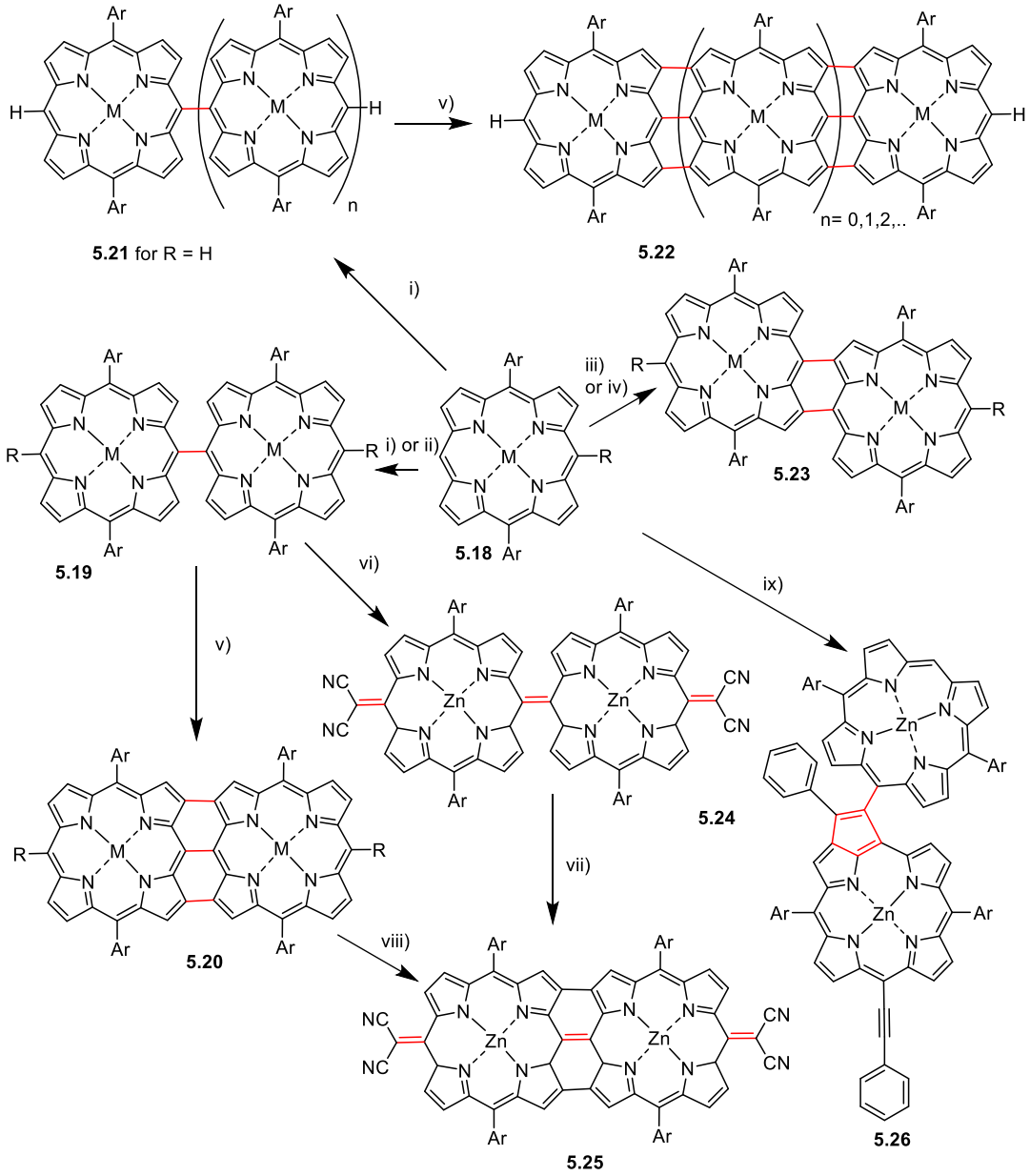

Figure 5.4. Synthesis of selected meso-meso–, meso-β–, and β-β–fused bisporphyrins. Reaction conditions: i) R = Ar, M = Zn(II), Ag(I) promoted coupling; ~20–90%. ii) R = H, M = Ni(II), RLi, THF, –40 °C, DDQ; 60-80%. iii) M = Pd(II), toluene, 5 eq. DDQ, $Sc(OTf)_3$, 5 eq. 50 °C, 12 h; ~70%. iv) 1 eq. $TeCl_4$, DCM, rt; ~30% + oligomers. v) M = Zn(II), toluene, 5 eq. DDQ, 5 eq. $Sc(OTf)_3$, 50 °C, 30 min; ~90%. vi) M = Zn(II), R = Br; a) $NaCH(CN)_2$, $Pd_2(dba)_3$, CuI, PPh_3. vii) DDQ, $Sc(OTf)_3$; ~80%. viii) R = Br; vi); ~80%. ix) R = C≡C-Ph; $AgPF_5$; >30%.

Figure 5.4 highlights some key (but not all!) fusing transformations and illustrates the range and type of accessible compounds. These include the formation of the porphyrin-dehydropurpurin dimer **5.26**[256], an example of the fusion of a meso-substituent onto a β-position, various doubly meso-β–linked bisporphyrins **5.23**[257] and triply meso-meso−, meso-β−, and β-β−linked porphyrins **5.20**. Over the years, many improvements have been made with regards to regioselectivity, oxidant (*i.e.*,

DDQ, $Sc(OT)_3$ – now often used instead of tris(4-bromophenyl)ammoniumyl hexachloroantimonate) and target systems.[247] Depending on the central metal or the meso-substituents, other types of fusions are possible with zinc(II) complexes leading to triply-linked systems and Pd(II) complexes yielding doubly meso-β−linked bisporphyrins.[258] Treatment of porphyrins with meso-hydroxyaryl substituents gave an entry into oxoquinoidal porphyrins **5.24**[259] while planarisation of the porphyrin dimer **5.24** gave the quinoidal porphyrin dimer **5.25**, and so on. Larger 2D structures, for example, a tetrameric fully-fused porphyrin system with a planar cyclooctatetraene core **5.27** (Fig. 5.5), can be prepared in a similar manner.[260] Note, that all of these systems are also accessible *via* step-wise reactions using transition metal-catalysed approaches, or RLi chemistry.[7] As for monomeric porphyrins, these reactions become progressively more involved if one targets unsymmetrically substituted, fused oligoporphyrinoid systems.[261]

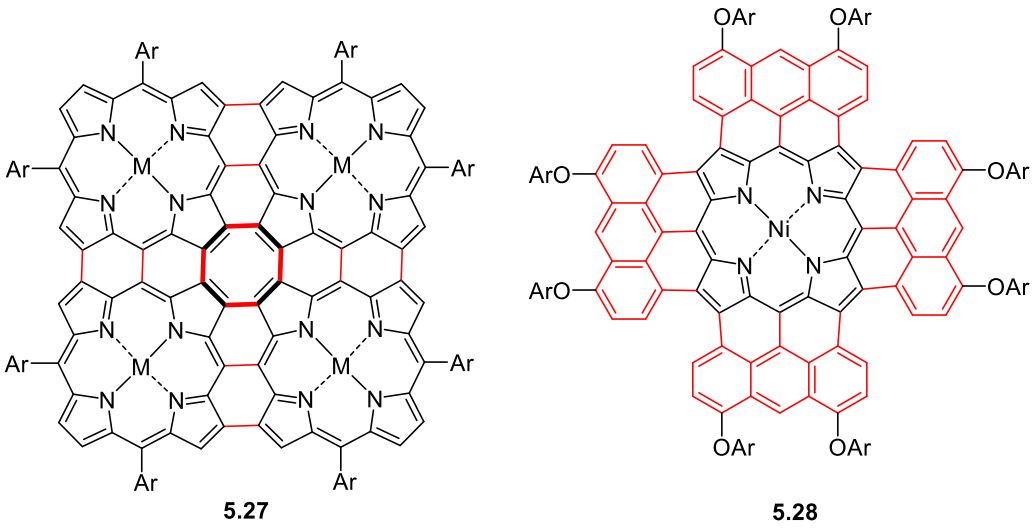

5.27 **5.28**

Figure 5.5. Osuka's fully fused porphyrin tetramer and Anderson's fully fused tetraanthracenylporphyrin.

If porphyrins can be fused to porphyrins, then it is natural to assume the same for other aromatic units (Fig. 5.5). By now many different aromatic and heteroaromatic residues have been fused to porphyrins.[241] Fusing anthracene proved to be one of the more challenging tasks and Anderson's synthesis of anthracenyl-triply fused porphyrins, including the tetraanthracenyl-fused system **5.28**, is a recent highlight in this area.[262] Their syntheses proceeds in a similar manner to the preparation of triply-linked bisporphyrins, *i.e.*, first the substituent is attached by one covalent bond (meso) and this is then followed by oxidative coupling at the remaining

neighbouring (C_b) positions. Later on, Thompson and co-workers reported the fusing of unsubstituted pyrene to the porphyrin through oxidative ring closure with iron(III) chloride and DDQ.[247] Other examples of fused porphyrins included pyrene fused porphyrins or BODIPY fused porphyrins.[241, 263]

5.1 Objectives

Graphene is a well-known molecule which has been used for a wide range of research, gaining extreme popularity due to its exceptional properties. Graphene is a large aromatic molecule, which consists solely of carbon atoms. It is known for its electronic properties, such as acting as a zero-gap semiconductor or for being the strongest material tested so far. Aside from this, graphene also exhibits nonlinear optical behaviour, namely saturable absorption. Graphene has a perfectly hexagonal flat 2D structure. This very ordered structure, however, makes the molecule chemically less active. Therefore, some strategic functionalisations have to be performed to make this material suitable for applications such as sensing, energy storage or electrochemical systems.[264] The remedy of this limitation can be provided for example through doping, which is the replacement of some C-atoms with various other atoms. Another possibility would be to incorporate porphyrins into the graphene structure. A combination of these versatile molecules with the electronic properties of graphene could result in a new area of molecular electronics. While porphyrins have already been attached through thermal annealing to graphene sheets, their positioning is based on coincidence rather than strategic planning.[265] Therefore, this research aims to synthesise porphyrin-graphene nano-bands in which the different components can be precisely arranged. The aforementioned will be achieved through stepwise functionalisation of the porphyrin with graphene precursors through Pd-catalysed coupling reactions, followed by oxidative fusing reactions. This allows for the creation of large conjugated graphene-like systems of different lengths with the strategic incorporation of different porphyrin moieties.

5.2 Synthesis of symmetric tetrasubstituted anthracene pre-cursors

Large conjugated fused porphyrin systems normally tend to have poor solubility. In order to circumvent these issues as much as possible and to guarantee the best

possible solubility for the final target compounds, large alkyloxy chains were installed on all of the starting materials. This not only helps to improve solubility but also adds electron donating groups to the system, which are necessary to fuse the porphyrin-anthracene system.[262b] Therefore, catechol **5.29** was substituted with 1-bromooctane. 1-Bromooctane, 18-crown-6 and potassium carbonate were dissolved in acetone in the presence of catechol and heated to 65 °C for 5 days (Scheme 5.1).[266] However, only a small amount of the starting material was converted into the substituted catechol **5.30**. Therefore the reaction was repeated; however, on this occasion without 18-crown-6 and using DMF as a solvent. The starting material was consumed after heating the reaction at 90 °C for 24 h and the desired compound **5.30** was collected in 85% yield (Scheme 5.1).[267]

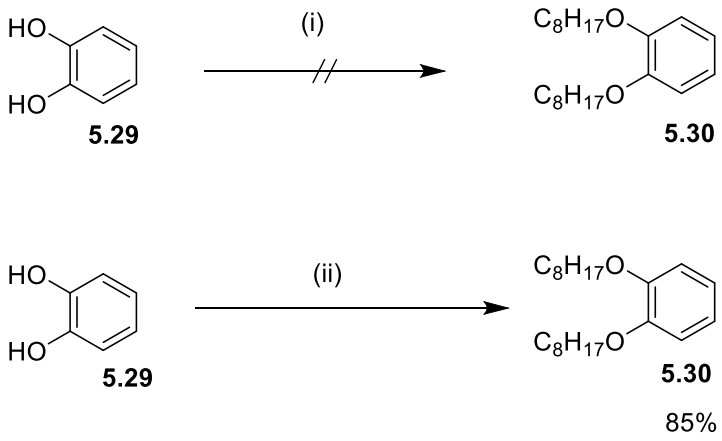

Scheme 5.1. Synthesis of substituted catechol: (i) 18-crown-6 (0.19 eq.),1-bromooctane (3 eq.), potassium carbonate (3 eq.), acetone, 65 °C, 5 days. (ii) 1-bromooctane (4 eq.), potassium carbonate (3 eq.), DMF, 90 °C, 24 h.

The next step involved the conversion of the substituted catechol into the respective anthracene. Thereby a literature procedure was followed[267] but unfortunately, compound **5.31** was only obtained in 8% yield (Scheme 5.2, (i)). In another attempt to synthesise the tetra-substituted anthracene, the hydroxy-substituted anthracene **5.32** was synthesised first to then substitute the hydroxy groups in a following step (Scheme 5.2). The same procedure was used as for the substituted catechol **5.30**, however, after a reaction time of 3 days at 90 °C only black polymers were obtained.

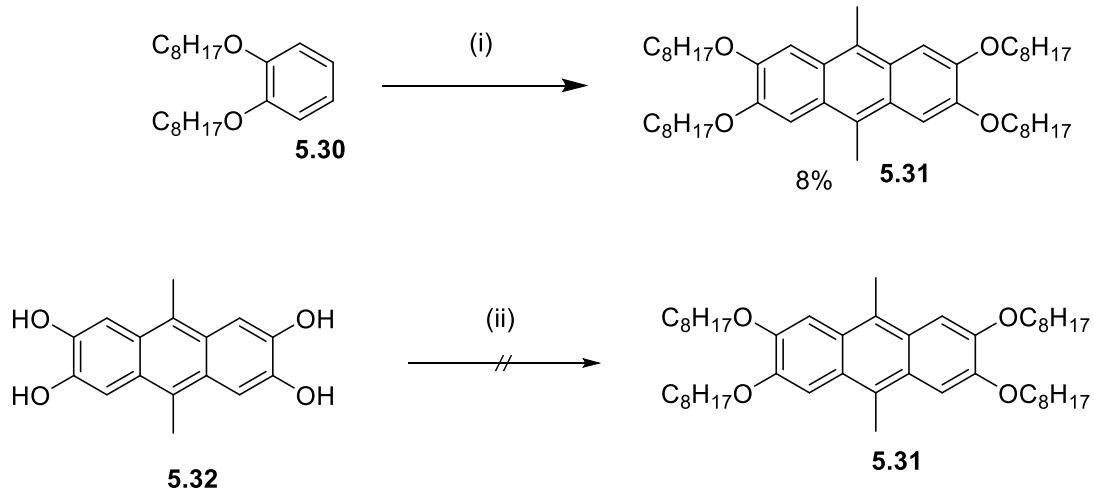

Scheme 5.2. Synthesis of symmetrically substituted anthracenes: (i) 1) acetaldehyde (1.5 eq.), glacial acetic acid, MeOH, 0 °C, 1 h; 2) conc. H_2SO_4, 0 °C, 2 h; 3) 0 °C, 20 h. (ii) 1-bromooctane (4 eq.), potassium carbonate (3 eq.), DMF, 90 °C, 3 days.

Subsequently, the conversion of compound **3** into the anthraquinone **11** was attempted (Scheme 5.3). This, however, resulted only in traces of the target compound **5.33** and mainly ring-opened by-products.

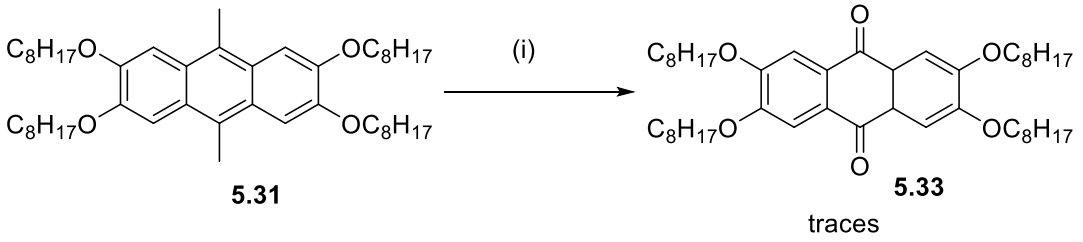

Scheme 5.3. Synthesis of tetra-substituted anthraquinone: (i) potassium dichromate (5.5 eq.), glacial acetic acid, 120 °C, 1 h.

5.3 Synthesis of unsymmetric di-substituted bisanthracene building blocks

Since the synthesis of symmetric anthracene building blocks had proven to be somewhat unfruitful, the decision was made to switch to commercially available anthraflavic acid in order to develop a working synthetic pathway towards the anthracene-substituted porphyrins first, before moving to tetrasubstituted anthracene units. This had the advantage that the route could be shortened by several synthetic steps and the key focus could be placed on the following, synthetically more challenging steps.

Having large quantities of the starting material at hand, the anthraflavic acid was subjected to the substitution reaction (Scheme 5.4). Again, the starting material **5.34** was dissolved in DMF with 4 eq. potassium carbonate and 2 eq. 1-bromooctane. After stirring for 48 h at 90 °C the desired product **5.35** was obtained in 98% yield. This reaction worked very well and was therefore performed with up to 1 g of anthraflavic acid.

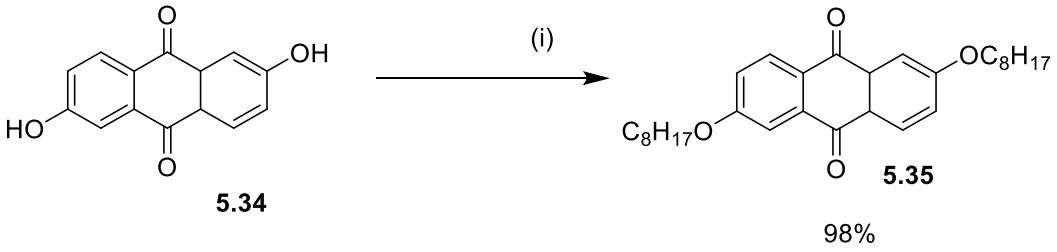

Scheme 5.4. Synthesis of substituted anthraflavic acid: (i) potassium carbonate (4 eq.), 1-bromooctane (2 eq.), DMF, 90 °C, 45 h.

The next challenge involved the synthesis of the bisanthracene building block. It was decided that it would be easier to synthesise bisanthracene building blocks rather than attaching one anthracene unit after another to the porphyrin due to anticipated challenging yields and solubilities. Even though a series of different methods exist to synthesise unsubstituted bisanthracenes[268] not many publications exist for bisanthracene units with long alkyl chains. Initially, the most common procedure to synthesise unsubstituted bisanthracene was explored.[268e]

A dissolving metal oxidation[3] was used for this reaction (Scheme 5.5). The substituted anthraquinone **5.35** (1 eq.), tin powder (7 eq.), and glacial acetic acid (1 mL) was added to a flask followed by heating to 120 °C. Conc. HCl was then added dropwise and the reaction was stirred for 1.5 h.

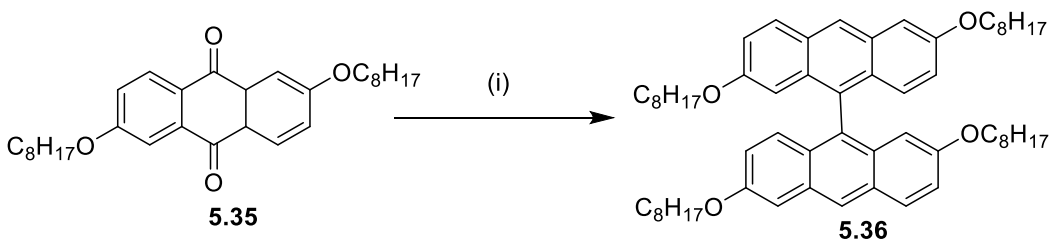

Scheme 5.5. Synthesis of bisanthracene precursor: (i) tin powder (7 eq.), glacial acetic acid, conc. HCl, 120 °C, 1.5 h.

The product was extracted with DCM and washed with sat. NH_4Cl solution and $NaHCO_3$ solution. The crude reaction mixture was recrystallised from hot acetic anhydride, however the compound was not pure enough. Therefore, a prep TLC was carried out with DCM:hexane = 1:3 (v/v), and unfortunately the main fraction obtained was the starting material (entry 1, Table 5.1).

One possible issue could have been that the HCl was added too fast and therefore, in the next attempt more emphasis was laid on adding the conc. HCl dropwise (entry 2, Table 5.1). The reaction was repeated on a scale of 100 mg of the substituted anthraquinone **5.35**. This time 0.4 mL conc. HCl was added instead of 0.3 mL. The HCl was added in very small portions over 1.45 h and the reaction was performed under an argon atmosphere. After the addition of HCl, the reaction was heated to 140 °C and stirred at this temperature for another 1.45 h. The reaction was stopped once all of the starting material was consumed. However, purification turned out to be more difficult than expected. Since the bisanthracene **5.36** is not very stable on silica, column chromatography had to be completed as fast as possible. In the end, only traces of the desired compound could be isolated, which might also be due to degradation.

In an attempt to optimise the reaction, another reduction reaction was set up and the reaction conditions were varied (entry 3, Table 5.1). This time the anthraquinone **5.35** (1 eq.), was dried for 30 min under vacuum. The anthraquinone **5.35** was suspended in glacial acetic acid (5 mL) and heated to 60 °C under argon. Then tin (10 eq.) was added and the reaction was heated to 140 °C. Once the reaction temperature had been reached, conc. HCl (0.4 mL) was added dropwise over ~2 h. The reaction was heated for a further 2.5 h. Once cooled, the reaction mixture was poured into H_2O and extracted with DCM. The organic layer was washed with sat. NH_4Cl solution and the solvents were removed. Since the compound degrades on silica, an attempt was made to purify the crude reaction mixture without the use of silica gel and, thereby avoiding column chromatography for the work up. However, TLC analysis showed several different compounds which could not be removed by crystallisation or aqueous workup and therefore column chromatography was indispensable. Again, only traces of the desired target compound were obtained. As so far only traces of the bisanthracene **5.36** had been found, it was suspected that maybe more tin was necessary in order to reduce the anthraquinone **5.35** (entry 4, Table 5.1). The

anthraquinone was again suspended in glacial acetic acid with 7 eq. of tin and heated to 140 °C under argon. Once the reaction temperature had been reached, conc. HCl was added dropwise. The reaction was further heated for 3 h. After this another 7 eq. of tin and 0.54 mL conc. HCl were added and the reaction was stirred at the reaction temperature for 3 h. After work up, the target compound was isolated in 3% yield.

Table 5.1. Synthesis of bisanthracene **5.36** utilising tin:

Entry	Metal [eq.]	Temp. [°C]	Time [h]	Reaction Condition	Specifics	Outcome
1	Tin [7]	120	1.5	Atmosph.	HCl was added dropwise	Mostly SM
2	Tin [7]	140	1.45	Ar		Traces
3	Tin [7]	1) 60 2) 140		Ar	Tin was heated first to 60 °C HCl (0.4mL) was added over 2 h,	Traces
4	Tin [14]	140	3	Ar	-	3%
5	Tin [7]	140	24	Ar	-	No product
6	Tin [7]	rt	3	Ar	-	No product

Even though the product was obtained on this occasion, the yield was still too low to continue with the next reaction step. Therefore, the reaction concentration was altered and the amount of glacial acetic acid was reduced. The anthraquinone 5.35 and 7 eq. of tin were dried and then suspended in glacial acetic acid (1.1 mL) and heated to 140 °C under argon in a MW vial (entry 5, Table 5.1). Once the reaction temperature had been reached, conc. HCl was added dropwise (0.1 mL every 30 min). The reaction was further heated for 3 h. After cooling, the reaction mixture was poured into H_2O and extracted with DCM. The organic layer was washed with sat. NH_4Cl solution and $NaHCO_3$ and the solvents were removed. A column was carried out starting with DCM:hexane = 1:1 and the polarity was increased to DCM + 3% MeOH. Only a small amount of product was obtained. The largest fraction separated was the anthraquinone fraction. An attempt to only stir the reaction at rt resulted in no product formation (entry 6, Table 5.1). To see if the bisanthracene **5.36** would be formed following a longer reaction time, the above

reaction was repeated and heated to 140 °C for 24 h. Unfortunately, no product was obtained.

Since the synthesis of the substituted bisanthracene **5.36** proved to be rather difficult, the decision was made to use the unsubstituted anthraflavic acid **5.34** in order to see if the long alkoxy chains might cause problems in the formation of the bisanthracene. Therefore, the same reduction reaction was attempted with the unsubstituted anthraflavic acid **5.34** (Scheme 5.6). Anthraflavic acid **5.34** (1 eq.) and tin (7 eq.) were suspended in glacial acetic acid (1.1 mL) and heated under argon to 140 °C. Once the reaction temperature was reached, 0.54 mL conc. HCl was added dropwise and the reaction was stirred at this temperature. On this attempt, no additional tin or HCl was added. Unfortunately, no product 5.37 was formed. The reaction was again repeated using 3 mL conc. HCl and the entire reaction was stirred at room temperature; however, the desired bisanthracene was not obtained.

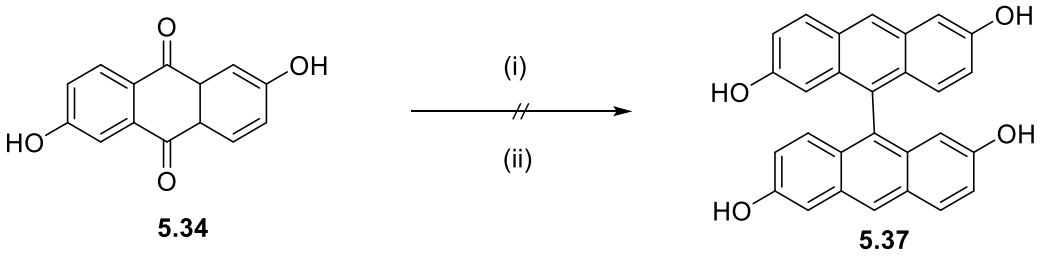

5.34 **5.37**

Scheme 5.6. Attempted synthesis of unsubstituted bisanthracene precursor **5.37**: (i) tin powder (7 eq.), glacial acetic acid, conc. HCl, 140 °C, 1.5 h. (ii) tin powder (7 eq.), glacial acetic acid, conc. HCl, rt, 1.5 h.

Since several reaction conditions were varied (concentration, eq. of tin, reaction time, reaction temperature, argon/no argon) without success, different synthetic procedures were explored.

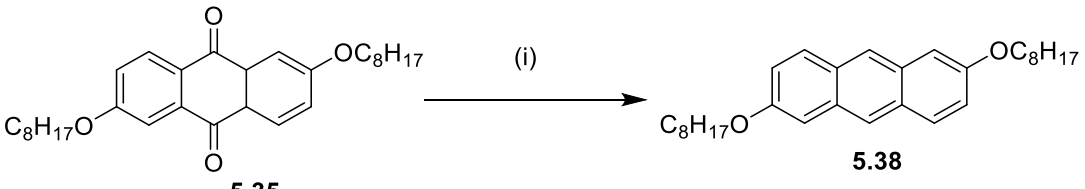

5.35 **5.38**

18%

Scheme 5.7. Reduction of anthraquinone: (i) zinc powder (63 eq.), NaOH (30 eq.)/H_2O, conc. HCl, 100 °C, 48 h.

In order to find an alternative way of synthesising the bisanthracene, the reduction of anthraquinone **5.35** to the anthracene **5.38** was attempted (Scheme 5.7). The anthracene could then be brominated in the next step and converted into the boronic ester which in turn could be coupled *via* a Suzuki cross-coupling reaction to form the bisanthracene. Even though this would add several synthetic steps to the formation of the bisanthracene, it was considered an alternative worth trying, as long as the single steps could be performed in high yields. This time the anthraquinone **5.35** and activated zinc powder were put in a 50 mL RB flask and dried under vacuum (Scheme 5.7). The flask was charged with argon and NaOH in H_2O was added. The reaction was heated to 100 °C for 48 h. After cooling to room temperature 3 mL conc. HCl was added and the reaction was stirred for 1 h. However, anthracene **5.38** was only obtained in 18% yield which was not sufficient considering the fact that two more steps had to be performed prior to the coupling reaction to form the bisanthracene **5.36**.

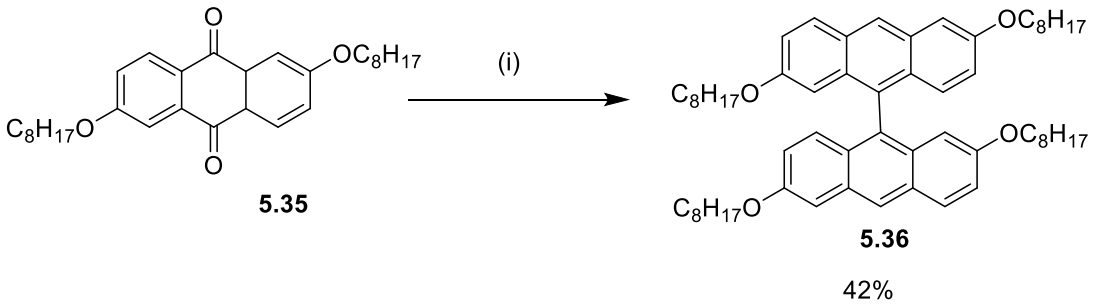

5.35 **5.36**

42%

Scheme 5.8. Synthesis of bisanthracene using zinc powder: (i) zinc (29 eq.), glacial acetic acid, conc. HCl, 140 °C, 4 h.

Upon renewed review of the literature, a patent was found in which zinc powder was used instead of tin to form various bisanthracenes (Scheme 5.8).[269] 0.18 mmol of the substituted anthraquinone **5.35** was put into a 20 mL MW vial. Activated zinc powder (29 eq.) was added along with 1.5 mL of glacial acetic acid. The reaction was stirred at room temperature and 1 mL conc. HCl was added. After stirring for 5 min at room temperature, the reaction was heated to 140 °C for 4 h. The reaction was then cooled down and another 300 mg of zinc powder as well as 1 mL conc. HCl were added. The reaction was stirred for 5 min at room temperature and then heated once again to 140 °C for 4 h. The crude reaction mixture was cooled to room temperature, poured into water and extracted with

DCM. After purification, the target compound **3.36** was obtained in 42% yield, in addition to some anthracene as a side product.

Since the bisanthracene could now be synthesised in reasonable yields, the reaction was upscaled in order to stockpile this valuable starting material. Therefore, 402 mg of the substituted anthraquinone **3.35** and 1.44 g zinc (22 mmol, 13 eq.) were dissolved in 7 mL of glacial acetic acid. The reaction was stirred at rt and 4.8 mL conc. HCl was added dropwise. The reaction was allowed to stir at rt for 5 min before being heated to 140 °C. After 4 h an additional 1.44 g zinc and 4.8 mL conc. HCl were added as before. After 5 min of stirring at rt, the reaction was once again heated to 140 °C for 4 h. After purification, the bisanthracene **5.36** was obtained in 32% yield. This proved that the reaction can be possibly even further upscaled. Indeed, when 1.5 g of anthraquinone was used the desired target **5.36** was obtained in 53% yield.

5.4 Bromination of Bisanthracene

After the successful synthesis of the bisanthracene precursor, the following step was to monobrominate the anthracene building block **3.36** in order to facilitate subsequent coupling with a porphyrin molecule.

Therefore anthracene **3.36** was dissolved in DCM with 1.1 eq. of NBS and 2,4,6-trimethylaniline was added in catalytic amounts (Scheme 5.9).[270] The reaction mixture was then cooled down to –30 °C in order to slow down the reaction rate and therefore be able to direct the formation of monobrominated bisanthracene (Table 5.2, entry 1).

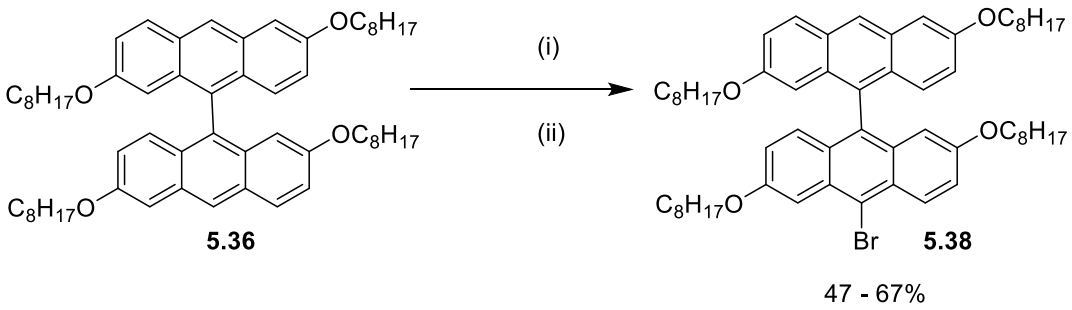

5.36 **5.38**

47 - 67%

Scheme 5.9. Monobromination of bisanthracene 5.36: (i) NBS (1.1 eq.), 2,4,6-trimethylaniline, DCM, –30 °C, 4 h. (ii) NBS (1.1 eq.), pyridine, DCM, –30 °C, 4 h.

The reaction was stirred for 4 h before being quenched and worked up. After column chromatography, the monobrominated species could be isolated along with a minor fraction of dibrominated side product. Recrystallisation from DCM and MeOH gave the target compound **5.38** in 67% yield. Since purification had some minor issues, it was decided to use pyridine as a base to see if this would cause fewer impurities (Table 5.2, entry 2). The reaction was repeated exactly as before except with the addition of pyridine. The reaction was quenched with acetone and a column was carried out using DCM:hexane = 1:6. The first fraction contained the dibrominated species and the second fraction the monobrominated anthracene. After recrystallisation from DCM/MeOH 19 mg of the desired compound **5.38** was obtained (56%). Since the yield of this reaction was slightly lower than for 2,4,6-trimethylaniline the decision was made to change back to the original conditions for upscaling. One eq. of bisanthracene and NBS (1.1 eq.) was dissolved in $CHCl_3$ and 2,4,6-trimethylaniline was added (Table 5.2, entry 3). The reaction was stirred for 3 h at –30 °C. Then the reaction was slowly warmed to –20 °C and another 0.2 eq. NBS was added. After an additional 1.5 h, the reaction was quenched with acetone and the workup was done as previously described. The target compound **5.38** was obtained in 47% yield. Even though acceptable yields for the monobrominated species were obtained, the issue was that there was still always some amount of starting material present when the reactions were quenched.

Table 5.2. Synthesis of monobrominated bisanthracene precursor:

Entry	Bisanthracene 5.36 [mmol]	NBS [eq.]	Temp. [°C]	Time [h]	Base	Solvent	Yield [%]
1	0.036	1.1	-30	4	2,4,6-trimethylaniline	DCM	67
2	0.036	1.1	-30	4	pyridine	DCM	56
3	0.09	1.1	-30 –(-20)	4.5	2,4,6-trimethylaniline	$CHCl_3$	47
4	0.368	1.1	0	4	2,4,6-trimethylaniline	DCM	52
5	0.294	1.3	0	4	pyridine	$CHCl_3$	83

Therefore, it was decided to perform the reaction at a higher temperature to speed up the reaction rate, while still maintaining a certain amount of selectivity for the

monobrominated anthracene (Table 5.2, entry 4). Hence, the reaction was performed at 0 °C instead of –30 °C. However, the reaction was still not completed after 4 h and another 0.6 eq. of NBS was added. After the workup, 52% of the monobrominated species **5.38** was obtained. Since the difference in yield upon utilization of 2,4,6-trimethylaniline or pyridine was not too grave, another reaction, this time on a larger scale, was attempted with pyridine. As the yield stayed more or less the same when the reaction with 2,4,6-trimethylaniline was either performed at –30 °C or 0 °C, it was decided to also try the reaction at 0 °C. Compound 5.36 was dissolved in $CHCl_3$ and 1.3 eq. of NBS were added together with pyridine. The reaction was stirred at 0 °C for 4 h (Table 5.2, entry 5). TLC analysis showed full conversion of the starting material and a yield of 83% was obtained after recrystallisation.

5.5 Borylation of Bisanthracene

Having optimised the synthesis of the monobrominated bisanthracene, further functional group interconversions were explored. To examine the full potential and reactivity of the bisanthracene building block the bromo unit on the bisanthracene was transformed into a boronic ester moiety (Scheme 5.10).

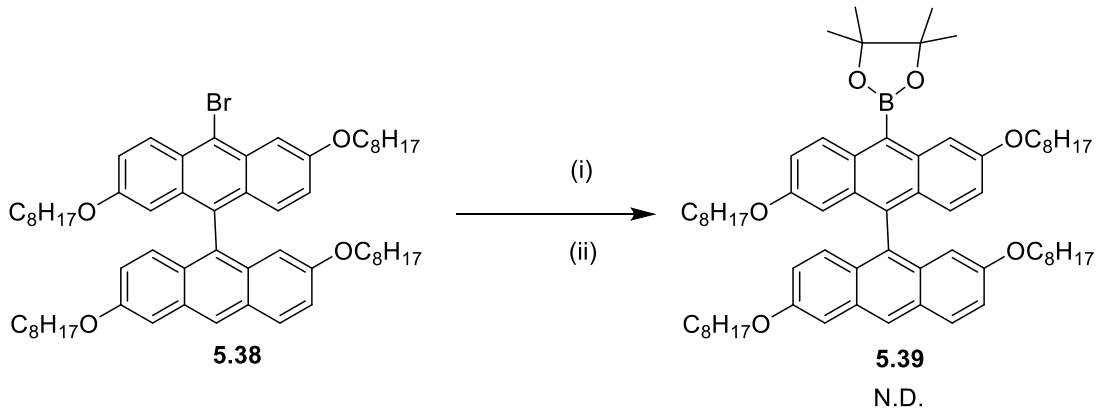

5.38 **5.39**

N.D.

Scheme 5.10. Synthesis of boronic ester bisanthracene **5.39**: (i) B_2pin_2 (1.5 eq.), $Pd(OAc)_2$ (0.05 eq.), S-Phos (0.1 eq.), K_3PO_4 (3 eq.), dry dioxane, 90 °C, 48 h. (ii) $PdCl_2(PPh_3)_2$ (10 mol%), pinacolborane (10 eq.), TEA, dry dichloroethane, 85 °C, 1.5 h.

This would give potential access to even larger building blocks through Suzuki cross-coupling reactions between several anthracene units. Therefore, bromoanthracene **5.38** (1 eq.), B_2pin_2 (1.5 eq.), S-Phos (0.1 eq.) and K_3PO_4 (3

eq.) were dried under vacuum for 4 h. Dry dioxane was added and the reaction was heated to 90 °C for 48 h (Scheme 5.10, (i)). However, only starting material and the debrominated species were recovered. Thus, a different borylating agent was used. A test reaction was set up on a small scale and 10 mg bromoanthracene 5.38 (0.01 mmol, 1 eq.), $PdCl_2(PPh_3)_2$ (10 mol%) were dried under vacuum for 3 h. TEA (0.01 mL) and dry dichloroethane (2 mL), as well as pinacolborane (10 eq.), were added and the reaction was heated to 85 °C for 1.5 h (Scheme 5.10, (ii)). The reaction was quenched and after purification the formation of the desired target compound **5.39** was confirmed through mass spec. and NMR, however, a yield was not determined due to the small scale.

5.6 Synthesis of anthracene substituted porphyrins

Once the bromination step had been optimised, an initial coupling reaction between a porphyrin and the bisanthracene was attempted (Scheme 5.11). The porphyrin starting material **5.40** was synthesised according to a literature procedure.[262b] Porphyrin **5.40** (1 eq.), bromoanthracene **5.38** (1.3 eq.), $Pd(dba)_3$ (0.1 eq.), S-Phos (0.41 eq.) and KOH (289 eq.) were put into a 20 mL MW vial and dried under vacuum for 5 h.

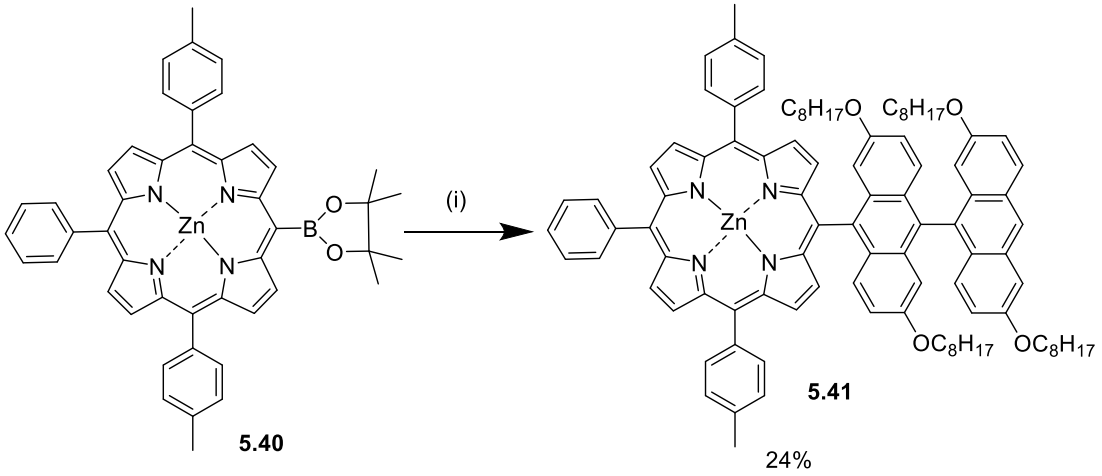

Scheme 5.11. Synthesis of anthracene substituted porphyrin **5.41**: (i) $Pd(dba)_3$ (0.1 eq), S-Phos (0.41 eq.), KOH (298 eq.), bromoanthracene **5.38** (1.3 eq.), dry toluene, 90 °C, 17 h.

The reaction was then heated to 90 °C for 17 h. After work up the target compound **5.41** was obtained in 24% yield. This showed that the bisanthracene unit can be attached to the porphyrin.

The next step involved a test reaction of the fusing step. The previously obtained porphyrin **5.41** was dried along with scandium triflate and DDQ. The reaction was then stirred for 1.5 h in dry toluene at rt (Scheme 5.12).

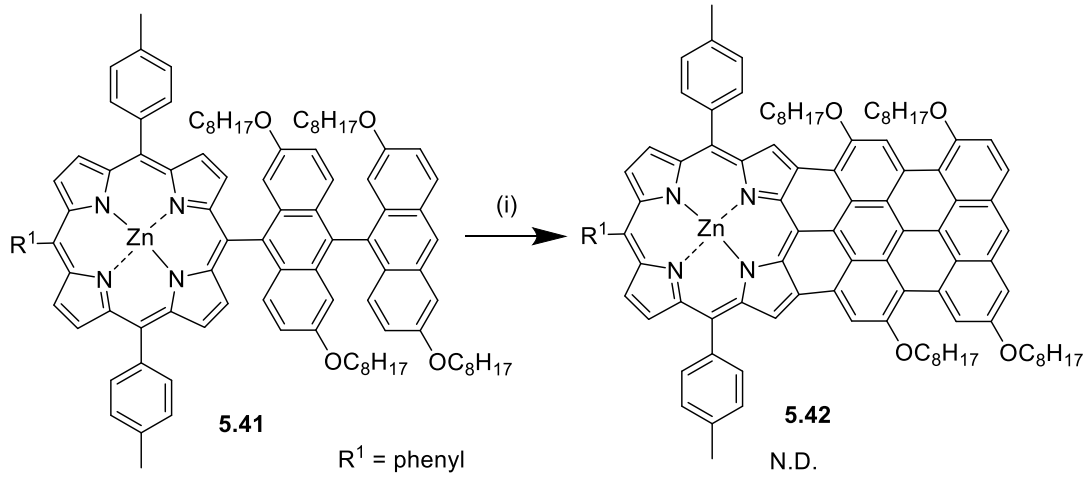

Scheme 5.12. Attempted synthesis of fused anthracene-porphyrin 5.42: DDQ (4.9 eq.), $Sc(Otf)_3$ (4.9 eq.), dry THF, rt, 1.5 h

Various different attempts were undertaken to purify this compound, however the low solubility made it very difficult to purify the porphyrin and unfortunately, the formation of target compound **5.42** could not be verified at this stage.

5.7 Exploration of oxidative fusing reactions

In order to try different fusing reaction conditions without losing precious porphyrin material, some initial studies were carried out utilising the bisanthracene building block. This should give an indication if the two anthracene units can be fused together. Since this compound can be easily synthesised in a large amount, it was deemed the perfect entry point for optimisation reactions.

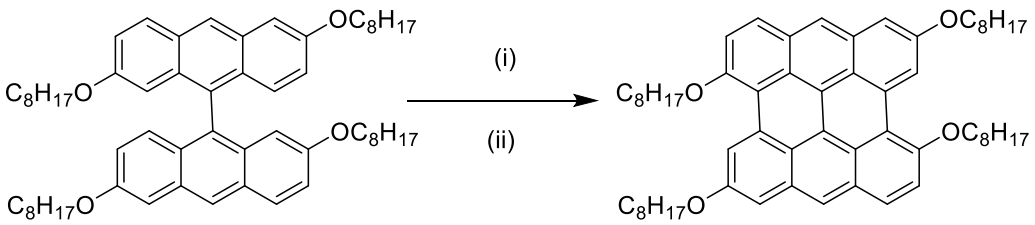

5.36 **5.43**

N.D.

Scheme 5.13. Oxidative fusing reactions on simple precursor **5.36**: (i) Scandium triflate (4.88 eq.), DDQ (4.88 eq.), dry toluene, rt, 2 h. (ii) $FeCl_3$ (10.5 eq.), AgOTf (31.5 eq.), dry toluene, dry nitromethane, rt, 15 min.

The initial reaction conditions explored were also used to synthesise the first anthracene-fused porphyrin which was reported in 2008 by Davis *et al*.[262b] Bisanthracene **5.36** was dried along with scandium triflate and DDQ. The reaction was performed in dry toluene and was stirred for 2 h at rt (Scheme 5.13). Since the reaction had not gone to completion, it was decided to heat the mixture to 120 °C for 1.5 h. This time all of the starting material was consumed. However, purification proved to be difficult and it was therefore not possible to confirm the formation of the product. A multitude of different compounds were formed during the reaction yet the fused anthracene could not be isolated, it was decided to perform the reaction at a lower temperature to prevent degradation. The reaction was repeated however, again a mass spectrum from the crude reaction mixture did not confirm the formation of the fused bisanthracene **5.43**. At this stage, a different type of fusing reaction was explored to see if it would generate more promising results. Iron chloride is a widely used reagent when it comes to the formation of oxidative ring closure.[271] Besides having been used for reactions with graphene, this chemical has also been used for the synthesis of fused porphyrins.[272] One unwanted side reaction, however, could be halogenation of the porphyrin or anthracene unit due to the chlorine atoms in the solution. Therefore, silver triflate was used as a chloride ion scavenger in this reaction (Scheme 5.13).

The bisanthracene **5.36**, $FeCl_3$ (10.5 eq.) and AgOTf (31.5 eq.) were dried under vacuum in separate vials for 2.5 days (Scheme 5.13). Dry nitromethane (1 mL) was added to the $FeCl_3$. The yellow solution was then transferred into the vial with AgOTf which resulted in a white precipitate of silver chloride salts in the yellow

solution. The solution was again removed with a syringe and added to bisanthracene **5.36** which had been dissolved prior to this in dry toluene (2 mL). The reaction was stirred for 15 min at rt, however once again the fused bisanthracene **5.43** could not be identified.

5.8 Optimised synthesis of anthracene-substituted porphyrins

As previous attempts in chapter 5.6 to couple a bisanthracene unit with a porphyrin had shown to be successful, a porphyrin with higher solubility was synthesised in order to circumvent difficulties in purification of the final fused target compound. Therefore, compound **5.44** was synthesised using standard literature procedures.[262b]

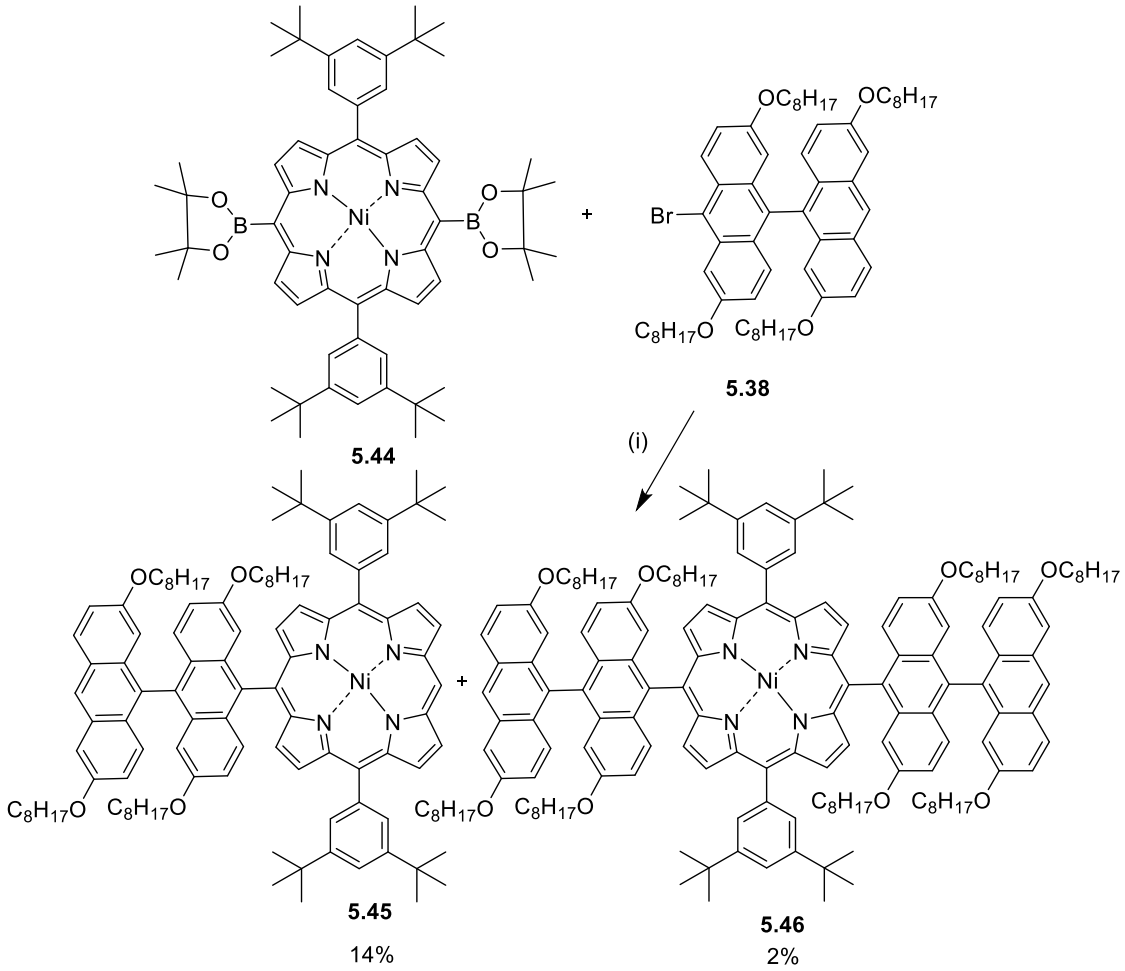

Scheme 5.14. Synthesis of porphyrin bisanthracene trimer **5.55**: (i) bisanthracene **5.38** (2.1 eq.), KOH (89 eq.), S-Phos (1.7 eq.), $Pd_2(dba)_3$ (0.2 eq.), dry toluene, 90 °C, 4 h.

This porphyrin was then subjected to Suzuki coupling reaction conditions utilising the monobrominated bisanthracene **5.38** as a coupling partner (Scheme 5.14). Porphyrin **5.44** was dried along with the bromobisanthracene **5.38**, KOH, S-Phos and $Pd_2(dba)_3$ for 6 h under high vacuum. Dry toluene was added and three freeze-thaw cycles were carried out. The reaction was stirred at 90 °C for 18 h. However, after workup, neither of the desired compounds **5.45** or **5.46** could be isolated. It was assumed that stirring the reaction for 18 h might have resulted in degradation and deborylation of the porphyrin species. Therefore, the reaction was repeated. All of the reagents were dried for 5 h under high vacuum. Dry toluene was added and after four freeze-thaw cycles, the reaction was heated to 90 °C. This time the reaction was set up during the day and was monitored *via* TLC analysis. After 4 h, all of the porphyrin starting material was consumed and the reaction was quenched. After an aqueous wash and filtration through silica, using DCM as eluent, a prep TLC was carried out using DCM:petroleum ether = 1:5. As can be seen in Figure 5.6, the reaction resulted in several products/side-products and hence purification proved to be difficult.

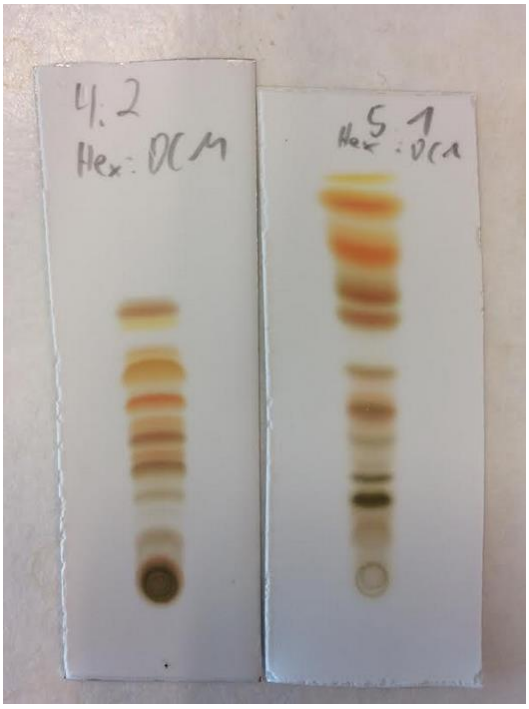

Figure 5.6. Fractions after Suzuki cross-coupling reaction.

Unfortunately, the three prominent orange fractions at the top turned out to be the debrominated anthracene, brominated anthracene and debrominated porphyrin. Mass spectrometry further confirmed the presence of the two target compounds

5.45 and **5.46** in two other fractions (F6 and F8). However, these fractions split into another 5-9 fractions, which made purification difficult. In addition to this, a small amount of the debrominated bisanthracene seemed to always co-elute with the porphyrin and was present in every single porphyrin fraction. Each fraction was again subjected to separation with a prep TLC plate using 1:2 = DCM:hexane for the dimer and 1:3 = DCM: hexane for the monomer. As these compounds also tended to degrade when exposed to silica gel or ALOX for too long, it was decided to use size exclusion chromatography for further purification. In the end, 1.5 mg of the disubstituted porphyrin **5.46** (2%) and 9 mg of the monosubstituted porphyrin **5.45** (14%) were isolated. The low yields might result from the cumbersome and repeated attempts to purify the porphyrins and consequential degradation due to the exposure to silica gel. Therefore, it was decided to use size exclusion chromatography straight away going forward..

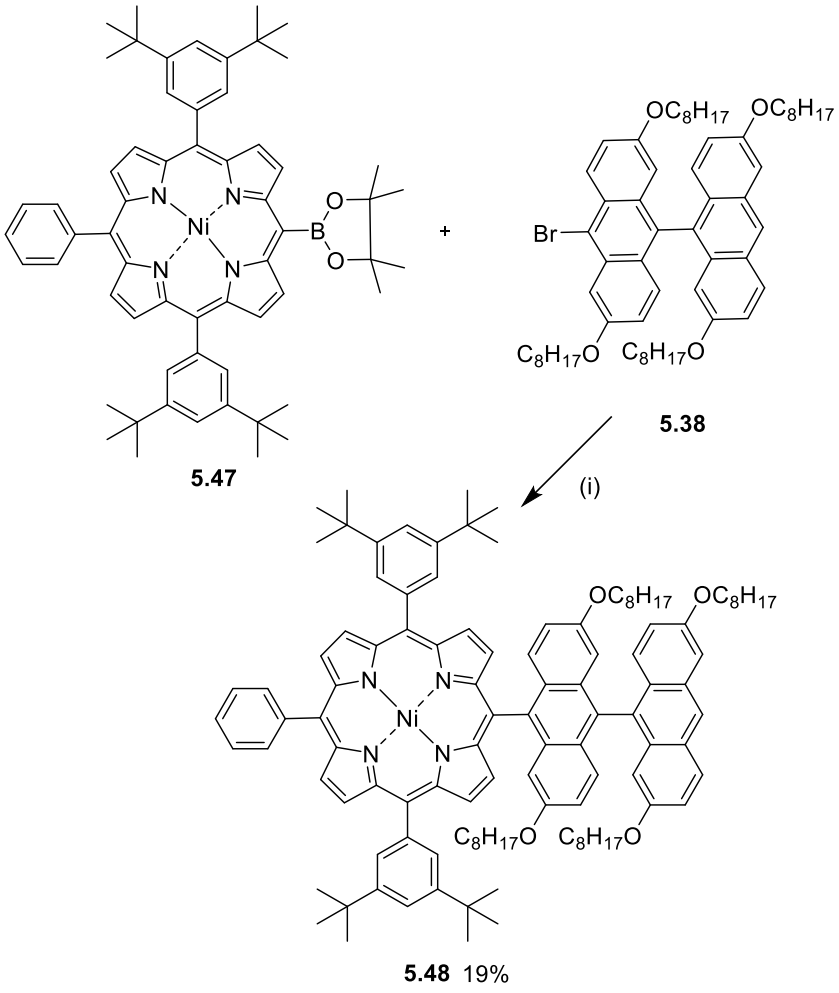

Scheme 5.15. Synthesis of monosubstituted anthracene porphyrin **5.48**: (i) compound **5.38** (1.3 eq.), $Pd_2(dba)_3$ (0.1 eq.), SPhos (0.41 eq.), KOH (289 eq.) dry toluene, 90 °C, 2 h.

As the separation of the dimer from the monomer was still challenging even with size exclusion chromatography, it was decided to use a mono-borylated porphyrin. This should not only result in higher reaction yields but also in an easier and faster purification which would hopefully minimise the degradation of the target compoundTherefore, porphyrin **5.47** was dried for 4 h under vacuum along with the bisanthracene **5.38**, $Pd_2(dba)_3$, SPhos and KOH (Scheme 5.15). Dry toluene was added and four freeze-thaw cycles were carried out. The reaction was heated to 90 °C for 2 h. The solvent was removed and filtration through silica was carried out using DCM, followed by size exclusion chromatography using THF as eluent. Compound **5.48** was obtained in 19% yield. As a higher yield for this coupling reaction was expected, the purity of starting materials was inspected. Unfortunately, it transpired that the monobrominated bisanthracene compound had partially degraded, which would have contributed to the low yields obtained. This comes as a surprise as the dibrominated bisanthracene species, which had been stored in exactly the same way, was still stable and pure. On these grounds, all of the bisanthracene products were stored in the dark in the freezer from that point. To determine if the degradation of the brominated bisanthracene species is the sole reason for the low reaction yield or if the reaction conditions also need to be optimised, it was decided to synthesise more of the monobrominated anthracene and use it immediately in the next coupling reaction to avoid any degradation.

5.9 Fusing of an anthracene-substituted porphyrin

A test reaction was set up in an attempt to fuse the bisanthracene unit to the porphyrin macrocycle. Therefore porphyrin **5.45** (6 mg, 1 eq.), $FeCl_3$ (10.5 eq.) and AgOTf (31.5 eq.) were dried in separate vials for 3 days to remove any water from the compounds (Scheme 5.16). The porphyrin was then dissolved in dry toluene. At the same time, $FeCl_3$ was dissolved in dry nitromethane and the resulting yellow solution was then added to the AgOTf. This was done in order to remove the chlorine atoms from the solution and avoid unwanted chlorination of the porphyrin species.

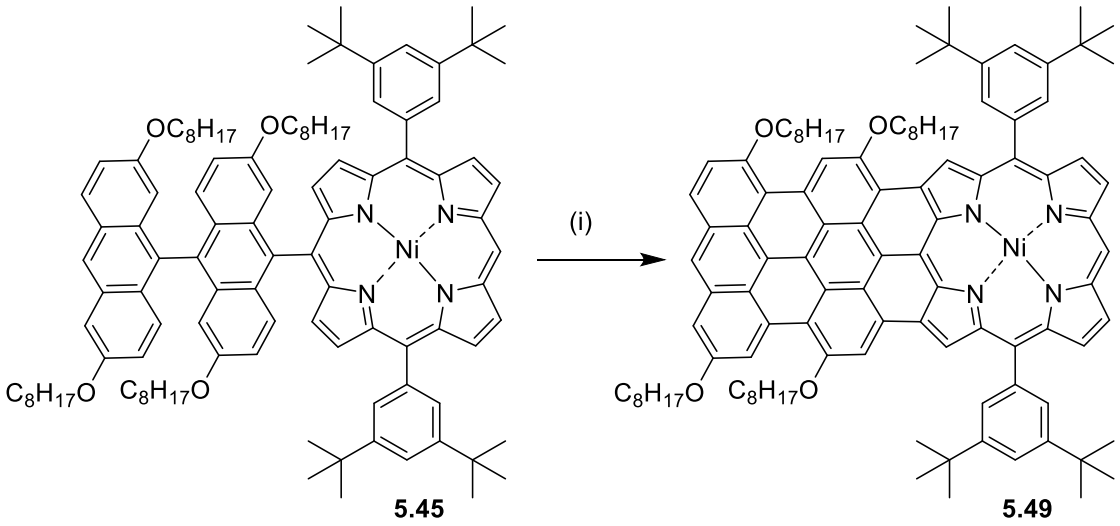

Scheme 5.16. Fusing of bisanthracene porphyrin **5.45**: (i) $FeCl_3$ (10.5 eq.), AgOTf (31.5 eq.), dry toluene, dry nitromethane, rt, 1 h.

The solution was then added to porphyrin **5.45** and the reaction was stirred at rt. The progress of the fusing process was monitored by TLC. After 1 h no further changes could be observed and the reaction was quenched. The crude mixture was washed with water and the different fractions were separated using filtration through silica gel, starting with DCM as eluent, DCM + 1% pyridine, and finally MeOH to elute all of the compounds. Mass spectrometry confirmed the formation of the fused porphyrin. However, instead of compound **5.49** the β-fused porphyrin **5.50** was obtained (Fig. 5.7).

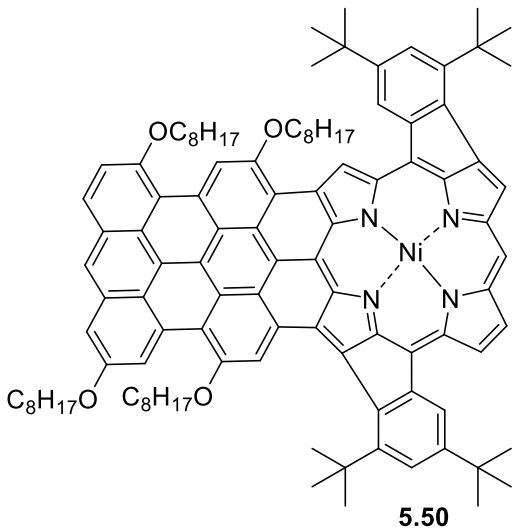

Figure 5.7. Fused porphyrin **5.50**

5.10 UV/Vis studies

In Figure 5.7 the UV/Vis spectra of bisanthracene substituted porphyrin **5.45**, as well as the fused porphyrin **5.50**, were investigated. Porphyrin **5.45** (orange, Figure 5.4) shows a characteristic absorption pattern of a monomeric metalloporphyrin.[273] When the absorption spectrum of porphyrin **5.50** is analysed, however, an extensive red-shift can be observed up to 890 nm with the longest wavelength absorption maxima at 825 nm.

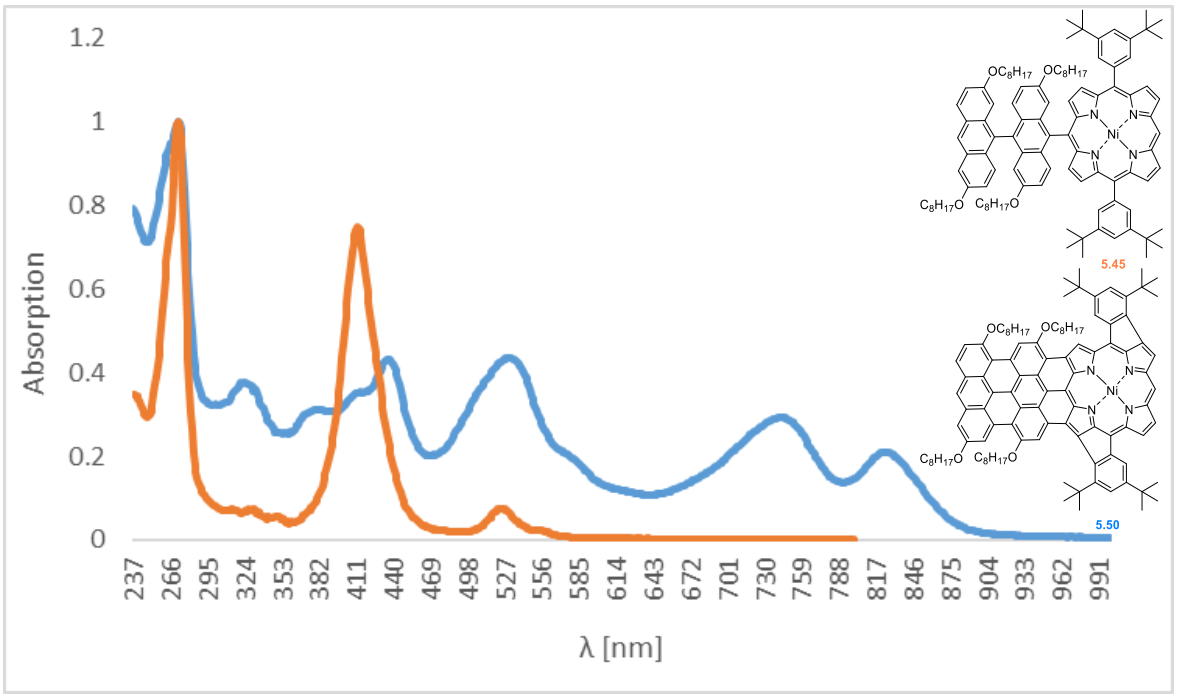

Figure 5.7. UV/vis spectra of fused porphyrin **5.50** (blue) and porphyrin **5.45** (orange) in DCM (normalized).

These results are due to an expansion of the π-system. Furthermore, when compared to the absorption spectrum of the monoanthracene-fused porphyrin synthesised by Davis *et al.* in 2008,[262b] striking similarities can be observed, further fortifying the assumption that the bisanthracene unit is fused to the porphyrin.

5.11 Conclusion

In this chapter, the synthesis of bisanthracene-substituted porphyrins was attempted. The investigation towards these target materials started with the synthesis of symmetric tetra-substituted bisanthracene precursors. While the substitution of catechol with long alkyloxy chains was successful, the subsequent formation of the tetra-substituted anthracene could only be achieved in low yields of 8%. Transformation of the anthracene to the anthraquinone resulted, however, in ring-opened products and was therefore abandoned at this stage. Due to this setback, the synthetic route was revised and the decision was made to synthesise bisanthracene precursors based on anthraflavic acid. The substitution of anthraflavic acid with long alkyloxy chains was optimised and resulted in a 98% yield of the desired compound. This compound was then subjected to dissolving metal oxidation to form the bisanthracene unit. While the reaction, when using tin, was largely unsuccessful (only 3% yield), the bisanthracene unit could be obtained in up to 53% yield when zinc was utilised. In order to be able to attach this precursor to a porphyrin, further functionalisation was necessary. Therefore, the bisanthracene unit was monobrominated. Varying the reaction temperature, as well as the base, resulted in yields from 47–83%, with the best results obtained when pyridine was used as a base at 0 °C. To investigate the reactivity of this compound, a test reaction was performed with the monobrominated bisanthracene to form the boronic ester. This compound could be very useful in further functionalisation reactions and could allow the formation of multiple anthracene units being coupled together. Additionally, a coupling reaction was attempted with boronic ester-substituted porphyrins and the monobrominated bisanthracene. This resulted in the successful formation of porphyrins with one or two bisanthracene units appended in low to moderate yields. Unfortunately, it was discovered that the monobrominated bisanthracene precursor is not stable and degrades over time, while the bisbrominated side product remains intact even over long periods. This could be responsible for the low yields during the coupling reaction with the porphyrin and the monobrominated species should, therefore, be directly used after its synthesis. Finally, fusing reactions were attempted for the bisanthracene precursor as well as the bisanthracene-substituted porphyrin. While the fused bisanthracene precursor could be not isolated, the fused porphyrin **5.50** was obtained and characterised through Mass spectrometry. The UV/vis spectra of this

fused system bears striking similarities to the anthracene-fused porphyrin reported by Davis *et al.*[262b] Due to the small reaction scale no further characterisation of the target compound was possible. Future work includes the optimisation of the Suzuki coupling reaction between the porphyrin and the bisanthracene precursor as well as further investigation into the fusing to confirm the formation of the fused anthracene-substituted porphyrin. Furthermore the synthesis of a symmetrically substituted bisanthracene precursor has to be developed to avoid the formation of isomeric porphyrin species. This can be achieved through the reaction of di-substituted phtalic anhydride with the di-substituted catechol in a Friedel-Crafts reaction. The resulting 2-benzoylbenzoic acid will then be dehydrated to form the tetra-substituted anthraquinone. The final anthraquinone will then be subjected to the same reaction condition as earlier to form the bis-anthracene building block.

6 Experimental

6.1 General Methods*:*

General chemicals were purchased from industrial suppliers and were used without further purification. Anhydrous DCM was obtained *via* distillation over phosphorus pentoxide. Fluka Silica Gel 60 (230-400 mesh; Merck) was used for column chromatography and analytical thin-layer chromatography (TLC) was performed using silica gel 60 (fluorescence indicator F254, precoated sheets, 0.2 mm thick, 20 cm × 20 cm; Merck) or aluminium oxide 60 (neutral, F254; Merck) plates. MW reactions were performed in a CEM Discover 600 W MW reactor. NMR spectra were measured on a Bruker Advance III 400 MHz, Bruker DPX 400 and an Agilent 400 spectrometer were employed for ^{1}H (400.13 MHz) and ^{13}C (100.61 MHz) or a Bruker AV 600 instrument (600.13 MHz for ^{1}H NMR; 150.90 MHz for ^{13}C NMR) was used. All NMR studies were carried out at room temperature. Resonances δ are given in ppm units and referenced to the deuterium peak in the NMR solvent. HRMS investigations were carried out on a Waters Maldi-quadrupole time-of-flight (Q-Tof) premier equipped with Z-spray electrospray ionisation (ESI) and matrix-assisted laser desorption ionisation (MALDI). Photophysical measurements were measured on a Specord 250. Melting points were determined with a Digital Stuart SMP10 melting point apparatus and are uncorrected. IR measurements were done on a PerkinElmer Spectrum 100 FT-IR.

General procedure A: Condensation reaction for 5,10-A_2 porphyrins: A flask was charged with anhydrous DCM (1.5 L) and purged with argon. Tripyrrane (1 eq.), Pyrrole (1 eq.), the according to aldehyde (2 eq.) and TFA (0.61 eq.) were added. The flask was shielded from light and the reaction was stirred at rt for 16 h. The reaction was oxidised with DDQ (3.8-5 eq.) followed by stirring for 30 min. The reaction was quenched with triethylamine and the solvent was removed *in vacuo.* The reaction mixture was filtered through silica using DCM as eluent followed by purification by column chromatography using DCM/hexane (1:2, v/v).

General Procedure B: Monobromination of 5,10-A_2 porphyrins: A 3-neck flask was purged with argon. The porphyrin (1 eq.) was dissolved in $CHCl_3$. The flask was shielded from light and cooled to 0 °C. NBS (0.90 eq.) and pyridine were

added and the reaction was stirred TLC analyses indicated the disappearance of the starting material at which point the reaction was quenched with acetone. The solvents were removed under vacuum and the product was purified by column chromatography using toluene/hexane (1:3, v/v).

General Procedure C: Insertion of zinc(II): Bromoporphyrin (1 eq.) was dissolved in $CHCl_3$ at rt zinc(II)acetate (3 eq.) was dissolved in MeOH and added to the reaction. The reaction was stirred at rt and monitored by TLC. The products were filtered through a plug of silica using DCM as eluent and the solvent was removed.

General Procedure D: Buchwald-Hartwig amination (bench reaction): Cs_2CO_3 (4 eq.) and *N,N*-bis(4-*tert*-butylphenyl)amine (4 eq.) and dry THF were placed in an oven-dried Schlenk flask, three freeze-thaw cycles and were reacted together for 30 min at the reaction temperature. Bromoporphyrin (1 eq.), palladium(II)acetate (10 mol-%), (*S*)-(−)-2,2′-bis(diphenylphosphino)-1,1′-binaphthalene (BINAP) (20 mol-%.) were added and the solution was subjected to three freeze-pump-thaw cycles before it was released to argon. The reaction mixture was heated to 65 °C. The reaction was monitored by TLC and quenched by pouring into the water after full consumption of the starting material. The product was extracted with DCM (3 × 100 mL), washed with $NaHCO_3$ (3 × 100 mL) and NaCl (3 × 100 mL) and dried over $MgSO_4$. The solvents were removed *in vacuo*. The reaction mixture was filtered through a plug of silica using DCM as eluent. Purification by column chromatography using DCM/hexane (1:2, v/v) gave the desired product.

General procedure E: Buchwald-Hartwig amination (MW reaction): Bromoporphyrin (1 eq.), *N,N*-bis(4-*tert*-butylphenyl)amine (4 eq.), palladium(II) acetate (0.05 eq.), (BINAP) (0.05 eq.) and Cs_2CO_3 (4 eq.) were placed in a MW vial, dissolved in anhydrous DMF, and degassed with argon for 10 minutes. The vial was sealed and subjected to MW radiation for 6 minutes at 160 °C. Work up followed General procedure D.

General procedure F: Bromination of tri-substituted porphyrins: To a solution of porphyrin (1 eq.) in $CHCl_3$, NBS (1.50 eq.) and pyridine were added. The reaction was stirred at rt, monitored by TLC and quenched with acetone. The

solvents were removed and the compound was purified by filtration through a plug of silica using DCM as eluent.

General procedure G: Sonogashira cross-coupling reaction: Bromoporphyrin (1 eq.), methyl 4-ethynylbenzoate (5 eq.), $PdCl_2(PPh_3)_2$ (0.10 eq.) and CuI (0.31 eq.) were placed in an oven-dried Schlenk flask and heated under vacuum for 10 minutes. Anhydrous DMF and diethylamine (3:1, v/v) were added. The reaction mixture was heated to 120 °C for 16 h until TLC analysis indicated complete consumption of the starting material after three freeze-thaw cycles. The product was extracted with DCM (3 × 50 mL). The combined organic phases were washed with sat. NH_4Cl solution (3 × 100 mL) and $NaHCO_3$ (3 × 100 mL) before drying over $MgSO_4$. The solvents were removed and the reaction mixture was filtered through a plug of silica using DCM as eluent prior to column chromatography (silica gel) using DCM/hexane (2:3, v/v).

General Procedure H: Ester deprotection: To a solution of the porphyrin ester (1 eq.) in THF, NaOH in MeOH (2 M, 353 eq.) was added, the solution was purged with argon and heated to 70 °C for 16 h. The solvents were removed *in vacuo.* The addition of water gave a green solution. HCl (1 M) was added dropwise until pH 5 was reached. The product was extracted with DCM (3 × 100 mL) and washed with sat. NH_4Cl solution (1 × 100 mL) and $NaHCO_3$ (1 × 100 mL) before drying over $MgSO_4$. The solvents were removed *in vacuo* and the product was recrystallised from MeOH/DCM.

General Procedure I: Reaction with organolithium compounds: The porphyrin (1 eq.) and 4-bromodimethylaniline (12 eq.) were heated in two flasks for 10 minutes under vacuum and then refilled with argon. Dry diethyl ether was added to the 4-bromodimethylaniline (12 eq.) and the solution was cooled to 0 °C or -70 °C. *n*-BuLi (12 eq.) was added dropwise over 1 h. After the addition was completed the reaction was allowed to stir at rt for 2 h. Meanwhile, the porphyrin (1 eq.) was dissolved in dry THF. The solution was added to the organolithium reagent and was stirred at rt for 2 h. The reaction was hydrolysed with sat. NH_4Cl solution followed by stirring for 20 minutes. DDQ (4.50 eq.) was added and the reaction was stirred for another hour. The solvents were removed *in vacuo*. The product was purified by filtration through silica gel using DCM as eluent, followed by filtration through silica gel using hexane/DCM (5:1, v/v) to remove traces of

starting material and a third filtration through silica gel using DCM/hexane (1:1) to obtain the pure product.

6.2 Chapter 2: Synthesis of unsymmetrical push-pull porphyrins

All starting materials such as 2,5-bis(hydroxymethyl)pyrrole (**1**),[274] tripyrrane (**2**),[142] 2,6-dioctyloxybenzaldehyde,[116c] 3,5-di-*tert*-butylbenzaldehyde,[275] or 5,15-disubstituted porphyrins[139a] were synthesized according to standard procedures.

5,10-Bis(3,5-di-*tert*-butylphenyl)porphyrin 2.13a:[150a]

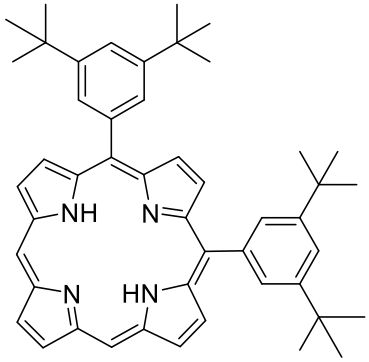

Porphyrin **2.13a** was synthesised according to general procedure A. Tripyrrane (0.92 g, 4.12 mmol), 3,5-di-*tert*-butylbenzaldehyde (1.80 g, 8.24 mmol), pyrrole (0.28 mL, 4.12 mmol) and TFA (0.20 mL, 0.63 eq.) were dissolved in 1.50 L dry DCM. Recrystallization gave purple crystals (150 mg, 0.22 mmol, 5%). M.p.: >300 °C (lit. M.p.[139b] >300 °C). R_f = 0.47 (hexane/DCM, 1:1, v/v). ^{1}H NMR (400 MHz, $CDCl_3$, 25 °C): δ =10.12 (s, 2H, H_{meso}), 9.74 (d, J = 4.6 Hz, 1H, H_β), 9.65 (d, J = 4.6 Hz, 1H, H_β), 9.36 (d, J = 4.6 Hz, 1H, H_β), 9.27 (d, J = 4.6 Hz, 1H, H_β), 9.00 (d, J = 4.6 Hz, 1H, H_β), 8.93 (d, J = 4.6 Hz, 1H, H_β), 8.85-8.90 (m, 2H, H_β), 8.03 (s, 4H, Ar-*o*-C*H*), 7.79 (s, 2H, Ar-*p*-C*H*), 1.51 (s, 36H, *t*-butyl-CH_3) and -2.93 ppm (s, 2H, N*H*). UV/Vis (DCM): λ_{max} (log ε) = 408 (6.11), 503 (4.76), 580 nm (4.35). HRMS (MALDI) *m/z*calcd. for $C_{48}H_{54}N_4(M^+)$: 686.4348; found 686.4354.

5,10-Bis(2,6-dioctyloxyphenyl)porphyrin 2.13b:

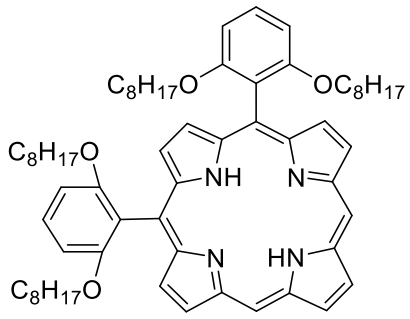

Porphyrin **2.13b** was synthesised according to general procedure A. Tripyrrane (0.962 g, 4.26 mmol), 2,6-dioctoxybenzaldehyde (2.96 g, 8.24 mmol), TFA (0.2 mL, 2.6 mmol) and pyrrole (0.28 mL, 4.12 mmol) were dissolved in anhydrous DCM (2 L). Purification by column chromatography (silica gel; hexane/DCM, 2:1, v/v) and removal of solvents followed by recrystallisation ($CHCl_3$/MEOH) gave the title compound as purple crystals (270 mg, 0.277 mmol, 6.4%). M.p 75-77 °C. R_f = 0.31 (hexane/DCM, 1:1, v/v). ^{1}H NMR (400 MHz, $CDCl_3$, 25 °C): δ = 10.10 (s, 2H, H_{meso}), 9.38 (s, 2H, H_β), 9.22 (d, J= 4.2 Hz, 2H, H_β), 8.92 (d, J = 4.2 Hz, 2H, H_β), 8.78 (s, 2H, H_β), 7.66 (t, J = 8.3 Hz, 2H, Ar-*p*-C*H*), 6.97 (d, J = 8.3 Hz, 4H, Ar-*m*-C*H*), 3.75-3.78 (m, 8H, OCH_2), 0.74-0.87 (m, 16H, CH_2), 0.38-0.59 (m, 44H, CH_2/CH_3) and -3.22 ppm (s, 2H, N*H*). ^{13}C NMR (100 MHz, $CDCl_3$, 25 °C): δ = 160.1, 130.6, 130.5, 130.4, 130.3, 130.2, 130.1, 129.9, 129.8, 120.9, 111.9, 105.3, 103.3, 68.7, 31.3, 28.6, 28.5, 28.4, 25.1, 22.2 and 13.8 ppm. UV/Vis (DCM): λ_{max} (log ε) = 407 (5.60), 502 (4.24), 576 nm (3.49). HRMS (MALDI) *m/z* calcd. for $C_{64}H_{86}N_4O_4$ (M^+): 974.6649; found 974.6656.

5-Bromo-10,15-bis(3,5-di-*tert*-butylphenyl)porphyrin 2.14a:[144]

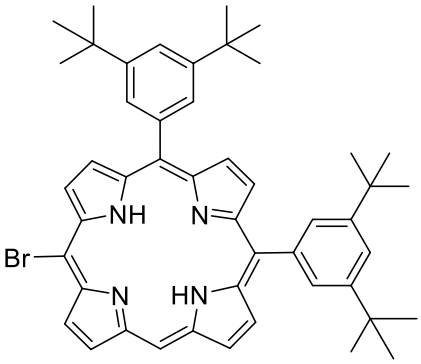

Porphyrin **2.14a** was synthesised according to procedure B. Porphyrin **2.13a** (425 mg, 0.69 mmol), NBS (100 mg, 0.58 mmol) and pyridine (0.15 mL) were dissolved in $CHCl_3$ (150 mL). The product was recrystallised from MeOH/DCM and gave purple crystals (386 mg, 0.50 mmol, 78%) with analytical data identical to the literature.[144] M.p.: >300 °C. R_f = 0.56 (hexane/DCM, 2:1, v/v). HRMS (MALDI) *m/z* calcd. for $C_{48}H_{53}BrN_4(M^+)$: 764.3454; found 764.3480.

5-Bromo-10,15-bis(2,6-dioctyloxyphenyl)porphyrin 2.14b:

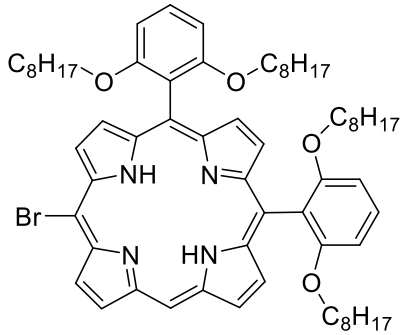

Porphyrin **2.14b** was synthesised according to general procedure B. Porphyrin **2.13b** (400 mg, 0.38 mmol) was dissolved in $CHCl_3$ (150 mL), purged with argon and cooled to 0 °C. Pyridine (0.50 mL) and NBS (58 mg, 0.33 mmol) were added and the solution stirred at 0 °C. The product was purified by column chromatography (silica gel) using toluene/hexane (1:3, v/v) as eluent. The target was obtained in the second porphyrin-containing fraction as a purple solid (292 mg, 0.28 mmol, 73%). M.p.: 72-74 °C. R_f = 0.44 (hexane/DCM, 1:1, v/v). ^{1}H NMR (400 MHz, $CDCl_3$, 25 °C): δ = 10.00 (s, 1H, H_{meso}), 9.68 (d, J = 4.5 Hz, 1H, H_β), 9.54 (d, J = 4.5 Hz, 1H, H_β), 9.30 (d, J = 4.5 Hz, 1H, H_β), 9.14 (d, J = 4.5 Hz, 1H, H_β), 8.83-8.85 (m, 2H, H_β), 8.70 (s, 2H, H_β), 7.63-7.68 (m, 2H, Ar-*p*-C*H*), 6.94-6.97 (m, 4H, Ar-*m*-C*H*), 3.76-3.79 (m, 8H, OCH_2), 0.85-0.93 (m, 8H, CH_2), 0.71-0.77 (m, 8H, CH_2), 0.37-0.57 (m, 44H, CH_2/CH_3) and -2.86 ppm (s, 2H, N*H*). ^{13}C NMR (100 MHz, $CDCl_3$, 25 °C): δ = 160.0, 159.9, 131.3, 131.1, 131.0, 130.0, 129.9, 120.8, 120.1, 113.2, 112.4, 105.3, 105.2, 104.5, 101.1, 68.6, 31.3, 28.6, 28.5, 28.4, 25.1, 22.2 and 13.8 ppm. UV/Vis (DCM): λ_{max} (log ε) = 415 (5.61), 511 (4.27), 546 (3.65), 587 (3.69), 641 nm (3.35). HRMS (MALDI) *m/z* calcd. for $C_{64}H_{85}BrN_4O_4$ (M^+): 1052.5754; found 1052.5739.

[**5-Bromo-10,15-bis(3,5-di-*tert*-butylphenyl)porphyrinato]zinc(II) 2.15a:**

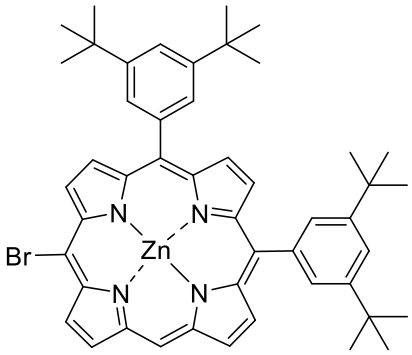

The title compound was synthesised according to general procedure C. Bromoporphyrin **2.14a** (768 mg, 1 mmol), zinc(II) acetate (652 mg, 3 mmol) were dissolved in $CHCl_3$ (150 mL). Recrystallisation from $CHCl_3$/MEOH gave purple crystals (839 mg, 1 mmol, >99%). M.p.: >300 °C. R_f = 0.33 (hexane/DCM, 2:1, v/v). ^{1}H NMR (600 MHz, $CDCl_3$, 25 °C): δ = 9.75 (s, 1H, H_{meso}), 9.71 (d, J = 4.4 Hz, 1H, H_β), 9.52 (d, J = 4.6 Hz, 1H, H_β), 9.22 (d, J = 4.6 Hz, 1H, H_β), 9.02-9.07 (m, 5H, H_β), 8.13 (s, 4H, Ar-*o*-C*H*), 7.84 (s, 2H, Ar-*p*-C*H*) and 1.58 ppm (s, 36H, *t*-butyl-CH_3). ^{13}C NMR (100 MHz, $CDCl_3$, 25 °C): δ = 151.0, 150.9, 150.5, 150.4, 149.9, 149.7, 149.4, 149.2, 148.9, 148.8, 141.8, 141.6, 133.6, 133.3, 132.8, 132.8, 132.7, 132.5, 132.3, 131.9, 129.9, 129.9, 123.7, 122.9, 121.2, 121.1, 105.8, 103.4, 35.3 and 32.0 ppm. UV/Vis (DCM): λ_{max} (log ε) = 417 (5.43), 547 (3.96), 585 nm (3.16). MS (MALDI) *m/z* (%): 830.29 (66) [M^+], 828.28 (100) [M^+], 826.29 (66) [M^+], 732.36 (24) [M-C_2H_6Zn], 675.28 (12) [M-$C_{10}H_{33}$]. HRMS (MALDI) *m/z* calcd. for $C_{48}H_{51}BrN_4Zn$ (M^+): 826.2589; found 826.2620. Anal. Calcd. for $C_{48}H_{51}BrN_4Zn$: C 69.52, H 6.2, N 6.76%; found: C 69.19, H 6.25, N 6.51%.

[5-Bromo-10,15-bis(2,6-dioctyloxyphenyl)porphyrinato]zinc(II) 2.15b:

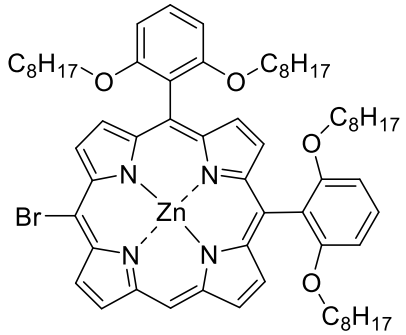

Porphyrin **2.15b** was synthesised following general procedure C. Bromoporphyrin **2.14b** (246 mg,, 0.233 mmol) was dissolved in $CHCl_3$ (70 mL) at rt. Zinc(II) acetate (153 mg, 0.7 mmol) was dissolved in MeOH (5 mL) and added to the reaction. The reaction products were filtered through a plug of silica using DCM as eluent. The removal of solvents gave a quantitative yield of purple crystals (240 mg, 0.231 mmol, 99%). M.p.: 88-91 °C. R_f = 0.39 (hexane/DCM, 1:1, v/v). ^{1}H NMR (400 MHz, $CDCl_3$, 25 °C): δ = 9.68 (d, J = 4.6 Hz, 1H, H_β), 9.57 (s, 1H, H_{meso}), 9.23 (d, J = 4.5 Hz, 1H, H_β), 9.14 (d, J = 4.6 Hz, 1H, H_β), 8.98-8.99 (m, 2H, H_β), 8.69 (s, 2H, H_β), 8.68 (d, J = 4.6 Hz, 1H, H_β), 7.68-7.73 (m, 2H, Ar-*p*-C*H*), 7.02-7.04 (m, 4H, Ar-*m*-C*H*), 3.85-3.88 (m, 8H, OCH_2), 0.89-1.05 (m, 8H, CH_2), 0.71-0.78 (m, 8H, CH_2) and 0.40-0.56 ppm (m, 44H, CH_2/CH_3). ^{13}C NMR (100 MHz, $CDCl_3$, 25 °C): δ = 160.0, 151.4, 151.2, 150.9, 150.8, 149.3, 148.7, 148.1, 132.3, 132.1, 131.9, 131.8, 131.7, 131.2, 129.7, 121.5, 121.4, 113.8, 112.9, 105.5, 105.4, 105.3, 105.2, 102.9, 68.7, 31.3, 31.2, 28.6, 28.5, 25.2, 25.1, 22.2 and 13.8 ppm. UV/Vis (DCM): λ_{max} (log ε) = 417 (5.58), 546 (4.14), 583 nm (2.91). MS (MALDI) *m/z* (%): 1118.52 (82) [M^+], 1116.5 (100) [M^+], 1114.52 (68) [M^+]. HRMS (MALDI) *m/z* calcd. for $C_{64}H_{85}BrN_4O_4Zn$ (M^+): 1114.4889; found 1114.4885.

[5,10-Bis(3,5-di-*tert*-butylphenyl)-15-*N,N*-bis(4-*tert*-butylphenyl)amino)porphyrinato]zinc(II) 2.16a:.

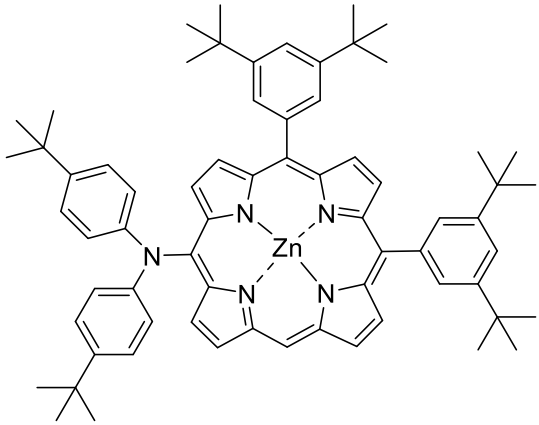

Bromoporphyrin **2.15a** (200 mg, 0.24 mmol), *N,N*-bis(4-*tert*-butylphenyl)amine (272 mg, 0.97 mmol), palladium(II)acetate (13 mg, 0.06 mmol), BINAP (54 mg, 0.09 mmol) and NaH (23 mg, 0.97 mmol) were put into a Schlenk tube. The compounds were heated under vacuum for 10 min. Anhydrous toluene (24 mL) was added and the solution was subjected to three freeze-pump-thaw cycles before it was released to argon. The reaction mixture was heated to 110 °C. The reaction was monitored by TLC and quenched by pouring into water after full consumption of the starting material. The product was extracted with DCM (3 × 100 mL), washed with $NaHCO_3$ (3 × 100 mL) and NaCl (3 × 100 mL) and dried over $MgSO_4$. The solvents were removed *in vacuo*. The reaction mixture was filtered through a plug of silica using DCM as eluent. Purification by column chromatography using DCM/hexane (1:2, v/v) gave the desired porphyrin (100 mg, 0.10 mmol, 40%). Porphyrin **2.16a** was also synthesised using general procedure E. Bromoporphyrin **2.15a** (50 mg, 0.06 mmol), *N,N*-bis(4-*tert*-butylphenyl)amine (67 mg, 0.24 mmol), palladium(II)acetate (0.7 mg, 3 µmol), BINAP (2 mg, 3 µmol) and Cs_2CO_3 (78 mg, 0.24 mmol) were used yielding porphyrin **2.16a** as a purple solid (15 mg, 0.02 mmol, 24%). M.p.: 254-255 °C. R_f = 0.45 (hexane/DCM 2:1, v/v). ^{1}H NMR (600 MHz, $CDCl_3$): δ = 10.12 (s, 1H, H_{meso}), 9.49 (d, J = 4.6 Hz, 1H, H_β), 9.40 (d, J = 4.6 Hz, 1H, H_β), 9.33 (d, J = 4.6 Hz, 1H, H_β), 9.30 (d, J = 4.6 Hz, 1H, H_β), 9.08 (d, J = 4.6 Hz, 1H, H_β), 8.99 (d, J = 4.6 Hz, 1H, H_β), 8.95 (d, J = 4.6 Hz, 1H, H_β), 8.93 (d, J = 4.6 Hz, 1H, H_β), 8.09 (s, 2H, Ar-o-C*H*), 8.04 (s, 2H, Ar-o-C*H*), 7.80 (s, 1H, Ar-*p*-C*H*), 7.76 (s, 1H, Ar-*p*-C*H*), 7.27 (d, J = 8.1 Hz, 4H, N-Ar-C*H*), 7.18 (d, J = 8.1 Hz, 4H, N-Ar-C*H*), 1.55 (s, 16H, *t*-butyl-CH_3), 1.50 (s, 20H, *t*-butyl-CH_3) and1.24 ppm (s, 18H, *t*-butyl-CH_3). ^{13}C NMR (100 MHz, $CDCl_3$, 25 °C):

δ = 153.0, 152.9, 150.6, 150.5, 150.3, 149.5, 149.3, 148.8, 148.7, 143.0, 141.8, 133.6, 133.1, 132.8, 132.4, 132.3, 131.6, 131.4, 130.6, 129.8, 129.7, 125.9, 123.0, 122.9, 122.0, 121.7, 121.0, 121.0, 105.8, 35.2, 35.2, 34.2, 31.9, 31.9 and 31.6 ppm. UV/Vis (DCM): λ_{max} (log ε) = 410 (5.49), 556 (4.24), 606 nm (4.01). HRMS (MALDI) *m/z* calcd. for $C_{68}H_{77}N_5Zn$ (M^+):1027.5470; found 1027.5493. MS (MALDI) *m/z* (%): 1027.55 (100) [M^+], 1012.53 (49) [M-CH_3].

[5-(*N,N*-Bis(4-*tert*-butylphenyl)amino)-10,15-bis(2,6-dioctyloxyphenyl)porphyrinato]zinc(II) 2.16b:

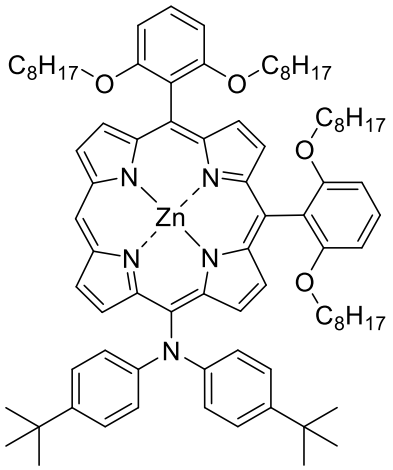

Porphyrin **2.16b** was synthesised following general procedure D. Bromoporphyrin **2.15b** (62 mg, 0.06 mmol), *N,N*-bis(4-*tert*-butylphenyl)amine (68 mg, 0.24 mmol), palladium(II) acetate (0.7 mg, 3 µmol), BINAP (2 mg, 3 µmol) and Cs_2CO_3 (78 mg, 0.24 mmol) were placed in an oven-dried Schlenk flask. Anhydrous DMF (2.7 mL) was used to dissolve the compounds. Recrystallisation ($CHCl_3$/MeOH) gave purple crystals (170 mg, 0.13 mmol, 68%). M.p.: 85-87 °C. R_f = 0.27 (hexane/DCM, 2:1, v/v). ^{1}H NMR (400 MHz, $CDCl_3$, 25 °C): δ = 9.99 (s, 1H, H_{meso}), 9.41 (d, J = 4.5 Hz, 1H, H_β), 9.28 (d, J = 4.5 Hz, 1H, H_β), 9.23 (d, J = 4.5 Hz, 1H, H_β), 9.21 (d, J = 4.5 Hz, 1H, H_β), 8.92 (d, J = 4.5 Hz, 1H, H_β), 8.78-8.80 (m, 3H, H_β), 7.60-7.68 (m, 2H, Ar-*p*-C*H*), 7.24 (d, J = 8.9 Hz, 4H, N-Ar-*o*-C*H*), 7.13 (d, J = 8.9 Hz, 4H, N-Ar-*m*-C*H*), 6.93-6.99 (m, 4H, Ar-*m*-C*H*), 3.76-3.80 (m, 8H, OCH_2), 1.23 (s, 18H, C(CH_3)$_3$), 0.86-0.96 (m, 8H, CH_2), 0.67-0.75 (m, 8H, CH_2) and 0.37-0.55 ppm (m, 44H, CH_2/CH_3). ^{13}C NMR (100 MHz, $CDCl_3$, 25 °C): δ = 160.0, 151.9, 151.8, 151.6, 150.9, 150.8, 150.1, 149.8, 149.4, 148.3, 142.5, 131.9, 131.7, 131.6, 131.4, 131.1, 130.3, 130.2, 129.5, 125.5, 121.6, 121.3, 121.1, 112.9, 112.8, 105.0, 68.7, 68.6, 34.0, 31.4, 31.3, 28.7, 28.6, 28.5, 28.3, 25.1, 24.9, 22.2, 22.1, 13.8 and 13.7 ppm. UV/Vis (DCM): λ_{max} (log ε) = 410 (5.08), 555 (3.98), 600 nm (3.52). MS (MALDI) *m/z* (%): 1315.84 (96) [M$^+$].HRMS (MALDI) *m/z* calcd. for $C_{84}H_{109}N_5O_4Zn$ (M^+): 1315.7771; found 1315.7756.

[5-Bromo-10,15-bis(3,5-di-*tert*-butylphenyl)-20-(*N,N*-bis(4-*tert*-butylphenyl)amino)porphyrinato]zinc(II) 2.18a:

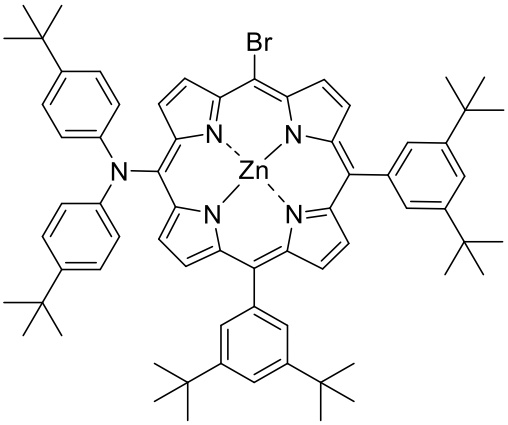

Porphyrin **2.18a** was synthesised in accordance to general procedure F. Porphyrin **2.16a** (120 mg, 0.12 mmol), NBS (31 mg, 0.18 mmol) and pyridine (0.3 mL) were dissolved in $CHCl_3$ (25 mL) for this reaction. Recrystallisation from MeOH/DCM yielded green crystals (100 mg, 0.09 mmol, 77%). M.p.: >300 °C. R_f = 0.43 (hexane/DCM, 2:1, v/v). ^{1}H NMR (600 MHz, $CDCl_3$): δ = 9.69 (d, J = 5.0 Hz, 1H, H_β), 9.66 (d, J = 5.0 Hz, 1H, H_β), 9.40 (d, J = 5.0 Hz, 1H, H_β), 9.30 (d, J = 5.0 Hz, 1H, H_β), 8.96 (d, J = 5.0 Hz, 1H, H_β), 8.86-8.88 (m, 2H, H_β), 8.84 (d, J = 5.0 Hz, 1H, H_β), 8.03 (s, 2H, Ar-o-C*H*), 7.98 (s, 2H, Ar-o-C*H*), 7.79 (s, 1H, Ar-*p*-C*H*), 7.75 (s, 1H, Ar-*p*-C*H*), 7.23 (d, J = 8.09 Hz, 4H, N-Ar-C*H*), 7.17 (d, J = 8.09 Hz, 4H, N-Ar-C*H*), 1.53 (s, 20H, *t*-butyl-CH_3), 1.49 (s, 16H, *t*-butyl-CH_3) and 1.25 ppm (s, 18H, *t*-butyl-CH_3). ^{13}C NMR (100 MHz, $CDCl_3$, 25 °C): δ = 153.3, 151.1, 150.9, 150.3, 150.2, 149.9, 148.9, 148.8, 148.8, 143.1, 141.5, 141.4, 134.0, 133.9, 133.7, 132.7, 132.7, 132.0, 131.0, 129.7, 129.6, 126.0, 124.0, 122.9, 121.7, 121.2, 121.1, 115.9, 104.4, 35.2, 35.2, 34.2, 31.9, 31.9, 31.7 and 31.5 ppm. UV/Vis (DCM): λ_{max} (log ε) = 418 (4.61), 450 (3.70), 564 (3.28), 616 nm (3.15). MS (MALDI) *m/z* (%): 1109.45 (82) [M^+], 1107.45 (100) [M^+], 1105.45 (46) [M^+], 1092.41 (31) [M-CH_3]. HRMS (MALDI) *m/z* calcd. for $C_{68}H_{76}BrN_5Zn$ (M^+): 1105.4576; found 1105.4548.

[5,10-Bis(3,5-di-*tert*-butylphenyl)-15-(*N,N*-bis(4-*tert*-butylphenyl)amino)-20-(4-Carbomethoxyphenylethynyl)porphyrinato]zinc(II) 2.19a:

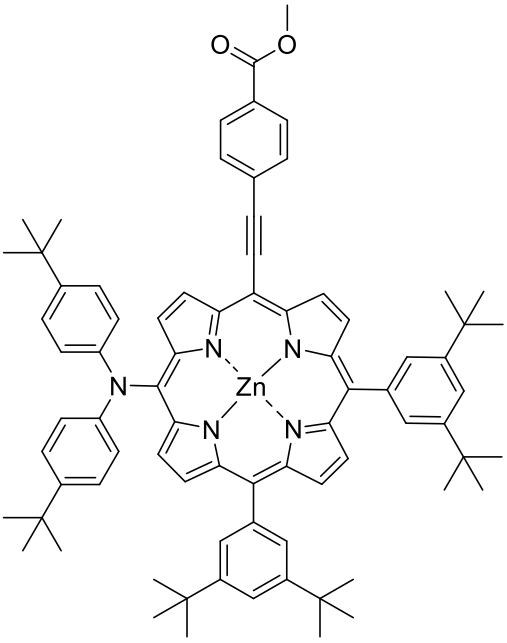

Porphyrin **2.19a** was synthesised according to general procedure G. Bromoporphyrin **2.18a** (100 mg, 0.09 mmol), methyl 4-ethynylbenzoate (79 mg, 0.48 mmol), $PdCl_2(PPh_3)_2$ (7 mg, 0.01 mmol), CuI (6 mg, 0.03 mmol), DMF (9 mL) and DEA (2.6 mL) were used for this reaction. The resultant porphyrin was recrystallised from MeOH/DCM yielding a green solid (57 mg, 0.05 mmol, 53%). M.p.: >300 °C. R_f = 0.41 (hexane/DCM, 2:1, v/v). ^{1}H NMR (400 MHz, $CDCl_3$): δ = 9.72-9.77 (m, 2H, H_β), 9.43 (d, J = 4.9 Hz, 1H, H_β), 9.29 (d, J = 4.9 Hz, 1H, H_β), 9.01 (d, J = 4.9 Hz, 1H, H_β), 8.83-8.88 (m, 3H, H_β), 8.16 (d, J = 8.1 Hz, 2H, alkynyl-Ar-C*H*), 8.05 (s, 2H, Ar-o-C*H*), 8.03 (d, J = 8.1 Hz, 2H, alkynyl-Ar-C*H*), 7.99 (s, 2H, Ar-o-C*H*), 7.81 (s, 1H, Ar-*p*-C*H*), 7.78 (s, 1H, Ar-*p*-C*H*), 7.26 (d, J = 8.4 Hz, 4H, N-Ar-C*H*), 7.20 (d, J = 8.4 Hz, 4H, N-Ar-C*H*), 3.96 (s, 3H, OCH_3), 1.55 (s, 18H, *t*-butyl-CH_3), 1.50 (s, 18 H, *t*-butyl-CH_3) and 1.25 ppm (s, 18H, *t*-butyl-CH_3).^{13}C NMR (100 MHz, $CDCl_3$, 25 °C): δ = 166.8, 153.4, 152.6, 152.6, 151.6, 151.1, 150.7, 150.3, 150.2, 149.7, 148.9, 148.8, 143.2, 141.4, 141.3, 133.9, 133.6, 132.7, 132.3, 131.9, 131.8, 131.4, 130.7, 130.6, 129.9, 129.7, 129.6, 129.3, 129.2, 129.1, 126.0, 124.7, 124.5, 123.7, 121.8, 121.2, 99.0, 95.9, 95.5, 52.4, 35.2, 35.2, 34.2, 31.9, 31.9 and 31.6 ppm. UV/Vis (DCM): λ_{max} (log ε) = 438 (4.75), 579 (3.49), 631 nm (3.64). HRMS (MALDI) *m/z* calcd. for$C_{78}H_{83}N_5O_2Zn$ (M^+): 1185.5838; found 1185.5842. MS (MALDI) *m/z* (%): 1185.55 (100) [M^+], 1170.54 (14) [M-CH_3].

[5,10-Bis(3,5-di-*tert*-butylphenyl)-15-(*N,N*-bis(4-*tert*-butylphenyl)amino)-20-(4-Carboxyphenylethynyl)porphyrinato]zinc(II) 2.10a:

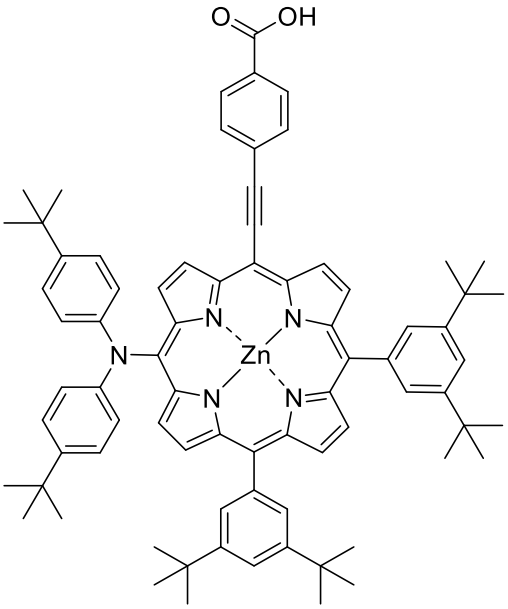

2.10a was synthesised in accordance to general procedure H. Porphyrin **2.19a** (64 mg, 0.0539 mmol), NaOH (760 mg, 19 mmol), THF (9.5 mL) and MeOH (9.5 mL) were used. Recrystallisation from MeOH/DCM yielded a dark green solid (60 mg, 0.05 mmol, 95%). M.p.: >300 °C. R_f = 0.21 (DCM + drop of MeOH). ^{1}H NMR (400 MHz, $CDCl_3$): δ = 9.76 (d, *J* = 4.4 Hz, 1H, H_β), 9.73 (d, *J* = 4.4 Hz, 1H, H_β), 9.44 (d, *J* = 4.4 Hz, 1H, H_β), 9.29 (d, *J* = 4.4 Hz, 1H, H_β), 9.01 (d, *J* = 4.4 Hz, 1H, H_β), 8.82-8.88 (m, 3H, H_β), 8.22 (d, *J* = 8.4 Hz, 2H, alkynyl-Ar-C*H*), 8.06 (s, 2H, Ar-o-C*H*), 8.05 (d, *J* = 8.1 Hz, 2H, alkynyl-Ar-C*H*), 8.00 (s, 2H, Ar-o-C*H*), 7.82 (s, 1H, Ar-*p*-C*H*), 7.76 (s, 1H, Ar-*p*-C*H*), 7.28 (d, J = 8.5 Hz, 4H, N-Ar-C*H*), 7.20 (d, *J* = 8.5 Hz, 4H, N-Ar-C*H*), 1.55 (s, 18H, *t*-butyl-CH_3), 1.50 (s, 18 H, *t*-butyl-CH_3) and 1.26 ppm (s, 18H, *t*-butyl-CH_3).^{13}C NMR (100 MHz, $CDCl_3$, 25 °C): δ = 169.3, 153.5, 152.7, 152.6, 151.6, 151.2, 150.7, 150.4, 150.2, 149.7, 148.9, 148.8, 143.3, 141.4, 141.4, 134.0, 133.6, 132.8, 132.3, 132.0, 131.8, 131.5, 130.7, 130.6, 130.6, 130.0, 129.8, 129.6, 128.2, 126, 124.8, 124.5, 123.8, 121.8, 121.2, 98.8, 97.1, 96.5, 95.5, 35.2, 35.2, 34.3, 31.9, 31.9 and 31.6 ppm. UV/Vis (DCM): λ_{max} (log ε) = 438 (4.78), 580 (3.52), 631 nm (3.68). HRMS (MALDI) *m/z* calcd. for $C_{77}H_{81}N_5O_2Zn$ (M^+): 1171.5682; found 1171.5698. MS (MALDI) *m/z* (%): 1171.55 (100) [M^+], 1156.54 (19) [M-CH_3].

5,10-Bis(3,5-di-*tert*-butylphenyl)-15-(*N,N*-dimethylaniline)porphyrin 2.17a:

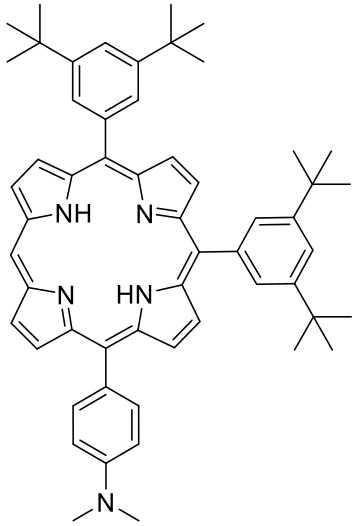

Porphyrin **2.17a** was synthesised in accordance with general procedure I. Porphyrin **2.13a** (223 mg, 0.29 mmol), 4-bromo-dimethylaniline (699 mg, 3.49 mmol), *n*-BuLi (2.2 mL, 3.49 mmol, 1.6 M in hexane),diethylether (8mL) and THF (40 mL) were used. Recrystallisation from $CHCl_3$/MeOH gave purple crystals (89 mg, 0.11 mmol, 38%). M.p.: 269-270 °C. R_f = 0.30 (hexane/DCM, 1:1, v/v). ^{1}H NMR (400 MHz, $CDCl_3$, 25 °C): δ = 10.19 (s, 1H, H_{meso}), 9.34 (d, J = 4.6 Hz, 1H, H_β), 9.32 (d, J = 4.6 Hz, 1H, H_β), 9.13 (d, J = 4.6 Hz, 1H, H_β), 9.05 (d, J = 4.6 Hz, 1H, H_β), 9.01 (d, J = 4.6 Hz, 1H, H_β), 8.95 (d, J = 4.6 Hz, 1H, H_β), 8.92 (d, J = 4.6 Hz, 1H, H_β), 8.89 (d, J = 4.6 Hz, 1H, H_β), 8.14 (d, J = 8.3 Hz, 2H, N-Ar-C*H*), 8.11 (d, J = 2.0 Hz, 2H, Ar-*o*-C*H*), 8.07 (d, J = 2.0 Hz, 2H, Ar-*o*-C*H*), 7.79-8.11 (m, 2H, Ar-*p*-C*H*), 7.15 (d, J = 8.3 Hz, 2H, N-Ar-C*H*), 3.26 (s, 6H, NCH_3), 1.55 (s, 18H, *t*-butyl-CH_3), 1.52 (s, 18H, *t*-butyl-CH_3) and -2.88 ppm (s, 2H, N*H*).^{13}C NMR (100 MHz, $CDCl_3$, 25 °C): δ = 150.2, 149.1, 148.7, 142.0, 141.1, 136.1, 131.8, 130.9, 130.0, 122.0, 121.2, 121.1, 120.7, 120.6, 111.2, 104.5, 41.0, 35.3, 35.2, 32.9, 32.0 and 31.2 ppm. UV/Vis (DCM): λ_{max} (log ε) = 415 (5.09), 515 (3.92), 556 (3.76), 590 (3.55), 646 nm (3.41). HRMS (MALDI) *m/z*calcd. for $C_{56}H_{63}N_5$(M^+): 805.5083; found 805.5056. MS (MALDI) *m/z* (%): 805.46 (100) [M^+], 790.45 (39) [M^+–CH_3].

5-*(N,N*-Dimethylaniline)-10,20-bis(2,6-dioctyloxyphenyl)porphyrin 2.17b:

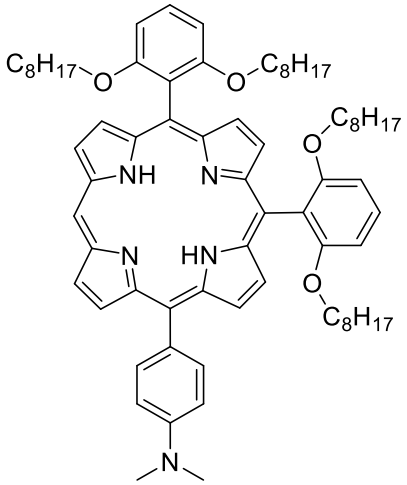

4-Bromo-dimethylaniline (1024 mg, 5.12 mmol) was dissolved in diethylether (26 mL) and cooled to -70 °C and *n*-BuLi (2.1 mL, 5.12 mmol, 1.6 M in hexane) was added dropwise over 45 min. The mixture of porphyrin **2.13b** (50 mg, 0.05 mmol) in THF (10 mL) was cooled to –70 °C and the organolithium reagent was added dropwise over 20 min. The cold bath was removed and the reaction mixture was stirred for 1.5 h at rt Once all the starting material was consumed NH_4CL (5 mL) was added and the reaction was stirred for 20 min. In the end DDQ (575 mg, 0.77 mmol) was added and the reaction was stirred for 1 h at rt. The crude product was purified by a filtration through silica using DCM followed by column chromatography with first 2 L of hexane and then hexane/DCM (5:1, v/v). Recrystallisation from $CHCl_3$/MeOH gave the pure compound as purple crystals (32 mg, 0.029 mmol, 57%). M.p.: 65-67 °C. R_f = 0.36 (hexane/DCM, 1:1, v/v). ^{1}H NMR (400 MHz, $CDCl_3$, 25 °C): δ = 10.08 (s, 1H, H_{meso}), 9.28 (d, J = 4.6 Hz, 1H, H_β), 9.21 (d, J = 4.6 Hz, 1H, H_β), 9.06 (d, J = 4.6 Hz, 1H, H_β), 8.90 (m, 2H, H_β), 8.80 (d, J = 4.6 Hz, 1H, H_β), 8.75 (s, 2 H, H_β), 8.11 (d, J = 8.3 Hz, 2H, N-Ar-C*H*), 7.65-7.71 (m, 2H, Ar-*p*-C*H*), 7.13 (d, J = 8.3 Hz, 2H, N-Ar-C*H*), 6.96-7.00 (m, 4H, Ar-*m*-C*H*), 3.79 (m, 8H, OCH_2), 3.25 (s, 6H, N-CH_3), 0.96-0.37 (m, 60H, $CH_3(CH_2)_6$) and -2.79 ppm (s, 2H, N*H*). ^{13}C NMR (100 MHz, $CDCl_3$, 25 °C): δ = 160.3, 150.0, 135.8, 130.7, 129.9, 129.8, 121.7, 120.9, 119.7, 112.3, 111.0, 111.0, 105.7, 105.5, 103.9, 68.9, 68.8, 40.9, 31.5, 31.5, 28.8, 28.8, 28.7, 28.7, 28.6, 25.3, 22.4 and 14.0 ppm. UV/Vis (DCM): λ_{max} (log ε) = 417 (5.58), 513 (4.43), 551 (4.12), 588 (3.99), 646 nm (3.62). HRMS (MALDI) *m/z* calcd. for $C_{72}H_{95}N_5O_4(M^+)$: 1093.7384; found 1093.7384.

5-Bromo-10,15-bis(3,5-di-*tert*-butylphenyl)-20-(*N,N*-dimethylaniline)porphyrin 2.20a:

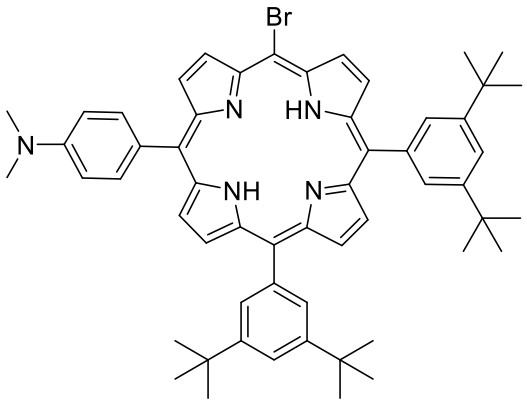

The title compound was synthesised in accordance with general procedure F. Porphyrin **2.17a** (89 mg, 0.11 mmol), NBS (18 mg, 0.10 mmol) were dissolved in $CHCl_3$ (30 mL). Recrystallisation from $CHCl_3$/MeOH gave purple crystals in good yield (89 mg, 0.10 mmol, 91%). M.p.: 259-260 °C. R_f = 0.50 (hexane/DCM, 1:1, v/v). ^{1}H NMR (400 MHz, $CDCl_3$, 25 °C): δ = 9.66 (d, J = 4.9 Hz, 2H, H_β), 9.01 (d, J = 4.8 Hz, 1H, H_β), 8.89-8.95 (m, 2H, H_β), 8.80-8.85 (m, 3H, H_β), 8.07 (d, J = 8.1 Hz, 2H, N-Ar-C*H*), 8.03 (m, 4H, Ar-*o*-C*H*), 7.79 (d, 2H, J = 8.2 Hz, Ar-*p*-C*H*), 7.12 (d, J = 8.1 Hz, 2H, N-Ar-C*H*), 3.25 (s, 5H, N-CH_3), 3.13 (s, 1H, N-CH_3), 1.53 (s, 18H, *t*-butyl-CH_3), 1.51 (s, 18H, *t*-butyl-CH_3), -2.64 (s, 1.6H, N*H*) and -2.71 ppm (s, 0.4H, N*H*). ^{13}C NMR (100 MHz, $CDCl_3$, 25 °C): δ = 150.2, 149.0, 148.9, 141.2, 141.1, 135.9, 130.1, 129.9, 129.9, 121.8, 121.4, 121.3, 121.2, 110.9, 102.5, 44.7, 40.9, 35.2, 35.2, 31.9 and 31.8 ppm. UV/Vis (DCM): λ_{max} (log ε) = 303 (3.76), 423 (4.93), 522 (3.67), 562 (3.57), 600 (3.14), 658 nm (3.14). HRMS (MALDI) *m/z* calcd. for $C_{56}H_{62}N_5Br$ (M^+): 883.4189; found 883.4227. MS (MALDI) *m/z* (%): 885.38 (100) [M^+], 870.37 (16) [M^+–CH_3].

[5-Bromo-10,15-bis(3,5-di-*tert*-butylphenyl)-20-(*N,N*-dimethylaniline)porphyrinato]zinc(II) 2.21a:

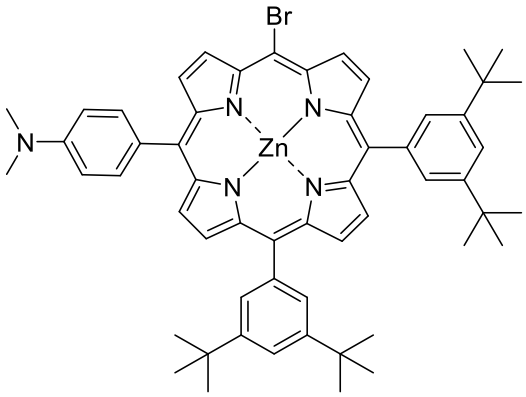

Porphyrin **2.21a** was obtained using general procedure C. Porphyrin **2.20a** (127 mg, 0.14 mmol) and $Zn(OAc)_2$ (95 mg, 0.43 mmol) were dissolved in $CHCl_3$ (50 mL). Recrystallisation from $CHCl_3$/MeOH gave purple crystals (117 mg, 0.12 mmol, 86%). M.p.: 128-129 °C. R_f = 0.14 (hexane/DCM, 2:1, v/v). ^{1}H NMR (400 MHz, $CDCl_3$, 25 °C): δ = 9.74-9.80 (m, 2H, H_β), 9.03-9.08 (m, 2H, H_β), 8.92-8.98 (m, 4H, H_β), 8.06 (s, 2H, Ar-*o*-C*H*), 8.04 (s, 2H, Ar-*o*-C*H*), 8.00 (bs, 2H, N-Ar-C*H*), 7.79 (d, 2H, *J* = 10.4 Hz, Ar-*p*-C*H*), 6.83 (bs, 2H, N-Ar-C*H*), 3.13 (s, 1H, N-CH_3), 2.82 (s, 5H, N-CH_3), 1.53 (s, 18H, *t*-butyl-CH_3) and 1.50 ppm (s, 18H, *t*-butyl-CH_3). ^{13}C NMR (100 MHz, $CDCl_3$, 25 °C): δ = 151.0, 150.9, 150.9, 149.7, 148.8, 148.7, 141.9, 141.8, 141.7, 141.7, 139.6, 138.3, 135.3, 133.6, 133.0, 132.8, 132.7, 132.6, 129.8, 129.8, 121.1, 121.0, 111.0, 104.2, 44.8, 41.0, 35.2 and 31.9 ppm. UV/Vis (DCM): λ_{max} (log ε) = 425 (4.99), 556 (3.78), 598 nm (3.44). HRMS (MALDI) *m/z* calcd. for $C_{56}H_{60}BrN_5Zn$ (M^+): 945.3324; found 945.3344. MS (MALDI) *m/z* (%): 947.36 (100) [M^+], 851.44 (12) [M^+–CH_4Br].

[5,10-Bis(3,5-di-*tert*-butylphenyl)-15-(4-carbomethoxyphenylethynyl)-20-(*N*,*N*-dimethylaniline)porphyrinato]zinc(II) 2.22a:

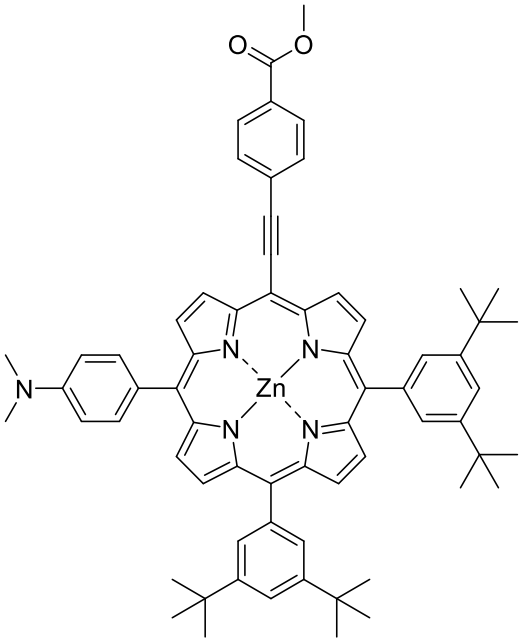

The target compound was obtained using general procedure G. Porphyrin **2.21a** (94 mg, 0.10 mmol), methyl 4-ethynylbenzoate (81 mg, 0.50 mmol), $PdCl_2(PPh_3)_2$ (7 mg, 0.01 mmol), CuI (6 mg, 0.03 mmol), DMF (9.3 mL) and DEA (2.75 mL) were used for this reaction. Recrystallisation from $CHCl_3$/MeOH gave dark purple crystals (64 mg, 0.06 mmol, 63%). M.p.: >300 °C. R_f = 0.47 (DCM).^{1}H NMR (400 MHz, $CDCl_3$, 25 °C): δ = 9.83 (d, J = 4.6 Hz, 1H, H_β), 9.80 (d, J = 4.6 Hz, 1H, H_β), 9.10 (bs, 1H, H_β), 9.06 (d, J = 4.6 Hz, 1H, H_β), 8.90-8.97 (m, 4H, H_β), 8.15 (d, J = 8.2 Hz, 2H, alkynyl-Ar-C*H*), 8.08 (d, 2H, J = 1.9 Hz, Ar-*o*-C*H*), 8.07 (bs, 2H, N-Ar-C*H*), 8.04 (d, 2H, J = 1.9 Hz, Ar-*o*-C*H*), 8.01 (d, J = 8.3 Hz, 2H, alkynyl-Ar-C*H*), 7.80 (s, 1H, Ar-*p*-C*H*), 7.77 (s, 1H, Ar-*p*-C*H*), 6.85 (bs, 2H, N-Ar-C*H*), 3.95 (s, 3H, OCH_3), 2.87 (s, 4H, N-CH_3), 2.75 (s, 2H, N-CH_3), 1.53 (s, 18H, *t*-butyl-CH_3) and 1.49 ppm (s, 18H, *t*-butyl-CH_3). ^{13}C NMR (100 MHz, $CDCl_3$, 25 °C): δ = 166.8, 162.5, 152.4, 152.3, 151.4, 151.0, 150.5, 150.3, 150.2, 149.6, 148.8, 148.6, 141.8, 141.7, 135.2, 133.5, 133.4, 132.6, 132.6, 132.3, 132.1, 131.4, 130.5, 130.3, 129.9, 129.7, 129.3, 129.2, 124.8, 123.5, 122.9, 121.0, 111.3, 98.5, 96.6, 95.3, 52.4, 40.9, 35.2, 35.1, 31.9 and 31.8 ppm. UV/Vis (DCM): λ_{max} (log ε) = 443 (4.88), 570 (3.56), 619 nm (3.80). HRMS (MALDI) *m/z* calcd. for $C_{66}H_{67}N_5O_2Zn$ (M^+): 1025.4586; found 1025.4580. MS (MALDI) *m/z* (%): 1025.44 (100) [M^+], 1010.45 (12) [M^+–CH_3].

[5,10-Bis(3,5-di-*tert*-butylphenyl)-15-(4-carboxyphenylethynyl)-20-(*N,N*-dimethylaniline)porphyrinato]zinc(II) 2.11a:

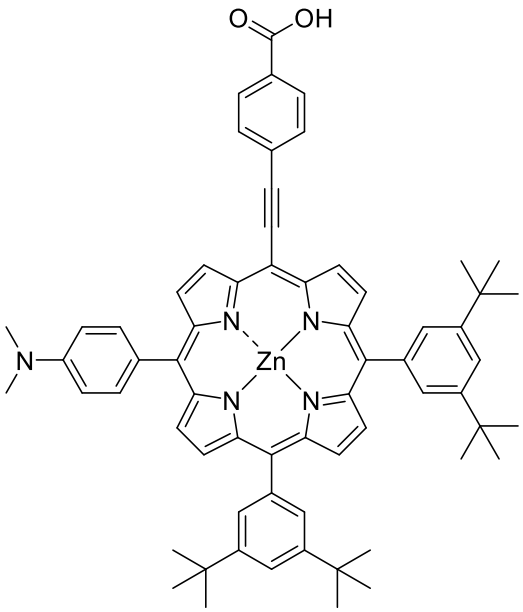

The title compound was synthesised in accordance to general procedure H. Porphyrin **2.22a** (40 mg, 0.04 mmol), NaOH (550 mg, 13.74 mmol), THF (6.9 mL) and MeOH (6.9 mL) were used. Recrystallisation yielded a dark green solid (33 mg, 0.03 mmol, 84%). M.p.: 108-110 °C. R_f = 0.14 (DCM + drop MeOH). ^{1}H NMR (400 MHz, $CDCl_3$, 25 °C): δ = 9.79-9.84 (m, 2H, H_β), 9.13 (d, J = 4.7 Hz, 1H, H_β), 9.06 (d, J = 4.7 Hz, 1H, H_β), 8.89-8.97 (m, 4H, H_β), 8.23 (d, J = 8.0 Hz, 2H, alkynyl-Ar-C*H*), 8.11 (d, J = 8.0 Hz, 2H, alkynyl-Ar-C*H*), 8.07 (d, 2H, J = 1.9 Hz, Ar-*o*-C*H*), 8.03 (d, 2H, J = 1.9 Hz, Ar-*o*-C*H*), 7.80 (s, 1H, Ar-*p*-C*H*), 7.77 (s, 1H, Ar-*p*-C*H*), 7.37 (bs, 2H, N-Ar-C*H*),7.02 (bs, 2H, N-Ar-C*H*),3.09 (s, 6H, N-CH_3),1.55 (s, 18H, *t*-butyl-CH_3) and 1.51 ppm (s, 18H, *t*-butyl-CH_3). ^{13}C NMR (100 MHz, $CDCl_3$, 25 °C): δ = 152.5, 152.4, 151.5, 151.1, 150.6, 150.3, 150.2, 149.8, 148.8, 148.7, 141.8, 141.6, 135.3, 133.6, 133.5, 132.7, 132.6, 132.3, 132.1, 131.5, 130.6, 130.4, 130.2, 129.8, 129.7, 124.9, 123.6, 121.1, 111.2, 98.5, 95.4, 40.9, 35.2, 35.1, 31.9 and 31.9 ppm. UV/Vis (DCM): λ_{max} (log ε) = 443 (3.81), 568 (2.58), 619 nm (2.73). HRMS (MALDI) *m/z* calcd. for $C_{65}H_{65}N_5O_2Zn$ (M^+): 1011.4430; found 1011.4462. MS (MALDI) *m/z* (%): 1011.43 (100) [M^+], 996.41 (11) [M^+–CH_3].

5-Bromo-10,20-bis(3,5-di-*tert*-butylphenyl)porphyrin 2.24a:[276]

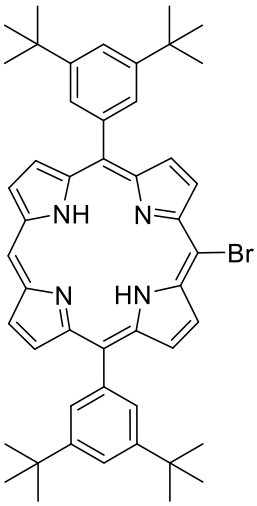

Porphyrin **2.24a** was synthesised in accordance with general procedure B. 5,15-Bis(3,5-di-*tert*-butylphenyl)porphyrin **2.23a** (1.0 g, 1.46 mmol), NBS (0.23 g, 1.29 mmol) and pyridine (0.5 mL) were used. The reaction was monitored by TLC. The product was recrystallised from DCM/MeOH to yield purple crystals (680 g, 0.89 mmol, 60%). M.p.: >300 °C. R_f = 0.76 (hexane/DCM 1:5, v/v). ^{1}H NMR (400 MHz, $CHCl_3$): δ = 10.16 (s, 1H, H_{meso}), 9.71 (d, J = 4.9 Hz, 2H, H_β), 9.28 (d, J = 4.4 Hz, 2H, H_β), 9.00 (t, J = 4.8 Hz, 4H, H_β), 8.07 (d, J = 1.8 Hz, 4H, Ar-*o*-C*H*), 7.83 (t, J = 1.8 Hz, 2H, Ar-*p*-C*H*), 1.55 (s, 36H, *t*-butyl-CH_3) and -2.93 ppm (s, 2H, N*H*). HRMS (ESI) *m/z* calcd. for $C_{48}H_{53}BrN_4(M^+)$: 764.3454; found 764.3469.

[5-Bromo-10,20-bis(3,5-di-*tert*-butylphenyl)porphyrinato]zinc(II) 2.25a:[276-277]

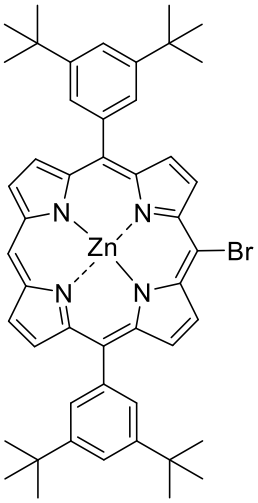

Porphyrin **2.25a** was synthesised in accordance with general procedure C. 5-Bromo-10,20-bis(3,5-di-*tert*-butylphenyl)porphyrin **2.24a** (720 mg, 0.94 mmol), $Zn(OAc)_2$ (0.52 g, 2.82 mmol), MeOH (10 mL) and $CHCl_3$ (200 mL) were used. The product was obtained as a purple solid (615 mg, 0.74 mmol, 79%). M.p.: >300 °C. R_f = 0.58 (hexane/DCM, 2:1, v/v). HRMS (ESI) *m/z* calcd. for $C_{48}H_{51}BrN_4Zn$ (M^+): 826.2589; found 826.2624. Other data were as reported before.[276-277]

[5,15-Bis(3,5-di-*tert*-butylphenyl)-10-(*N*,*N*-bis(4-(*tert*-butylphenyl)amino)porphyrinato]zinc(II) 2.26a:

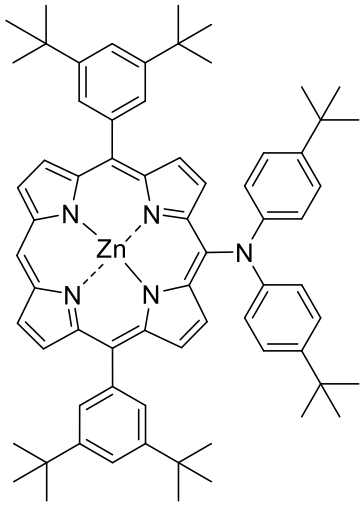

[5-Bromo-10,20-bis(3,5-di-*tert*-butyl)phenylporphyrinato]zinc(II) **2.25a** (400 mg, 0.48 mmol) was dissolved in DMF (10 mL) in a 20 mL MW vial. Bis(4-(*tert*-butyl)phenyl)amine (543 mg, 1.93 mmol), $Pd(OAc)_2$ (6 mg, 24 µmol), BINAP (15 mg, 24 µmol) and Cs_2CO_3 (629 mg, 1.93 mmol) were added according to general procedure E. The crude residue was redissolved in DCM/hexane, (25 mL, 1:3, v/v) and filtered through a short plug of silica using DCM/hexanes, (25 mL, 1:3, v/v) as eluent. The brown/red fraction was isolated (other faint fractions were discarded) and the solvents were removed *in vacuo*. The residue was subjected to column chromatography (DCM/hexane, 1:3, v/v), with the main fraction (red in color) containing the desired product. The solvents were removed i*n vacuo* and the purple residue was recrystallised from DCM/hexane to yield a purple solid (180 mg, 0.18 mmol, 36%). M.p.: >300 °C. R_f = 0.32 (DCM/hexane, 1:3, v/v). ^{1}H NMR (400 MHz, $CDCl_3$ +pyridine-d_5, 50:1, v/v): δ = 10.21 (s, 1H, H_{meso}), 9.40 (d, J = 4.5 Hz, 2H, H_β), 9.36 (d, J = 4.5 Hz, 2H, H_β), 9.07 (d, J = 4.5 Hz, 2H, H_β), 8.96 (d, J = 4.5 Hz, 2H, H_β), 8.07-8.09 (m, 4H, Ar-*o*-C*H*), 7.78-7.80 (m, 2H, Ar-*p*-C*H*), 7.24 (d, J = 8.8 Hz, 4H, N-Ar-C*H*), 7.15 (d, J = 8.8 Hz, 4H, N-Ar-C*H*), 1.53 (s, 36H, *t*-butyl-CH_3) and 1.21 ppm (s, 18H, *t*-butyl-CH_3). ^{13}C NMR (100 MHz, $CDCl_3$,25 °C): δ = 152.6, 150.9, 150.2, 149.9, 149.9, 148.8, 142.9, 141.5, 133.5, 133.0, 131.7, 130.9, 129.9, 125.9, 122.6, 122.0, 121.6, 121.0, 106.6, 35.2, 34.2, 31.9 and 31.5 ppm. UV/Vis (DCM): λ_{max} (log ε) = 411 (5.64), 453 (4.81), 556 (4.39), 604 nm (3.97). HRMS (MALDI): *m/z*calcd. for $C_{68}H_{77}N_5Zn$ (M^+): 1027.5470; found 1027.5461.

[5-Bromo-10,20-bis(3,5-di-*tert*-butylphenyl)-15-(*N*,*N*-bis(4-*tert*-butylphenyl)amino)porphyrinato]zinc(II) 2.27a:

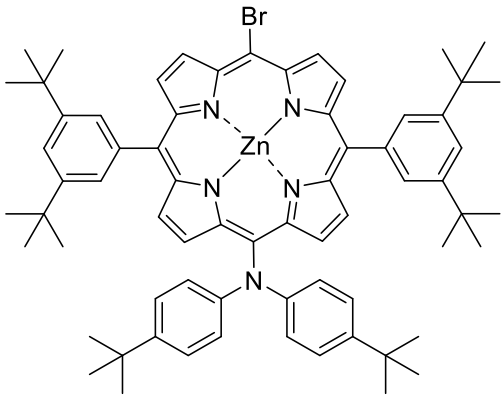

Porphyrin **2.27a** was synthesised following general procedure F. [5,15-bis(3,5-di-*tert*-butyl)phenyl-10-*N*,*N*-Bis(4-(*tert*-butylphenyl)amino)porphyrinato]zinc(II) **2.26a** (10 mg. 0.01 mmol) was dissolved in $CHCl_3$ (10 mL). NBS (1.70 mg, 0.01 mmol) and pyridine (0.01 mL) were added. The reaction was stirred at rt and monitored by TLC. The reaction was quenched with acetone and filtered through a plug of silica using DCM. The solvent was removed and the product was obtained in 93% yield as a purple solid (10 mg, 0.9 µmol, 93%). M.p.: >300 °C. R_f = 0.39 (DCM/hexane, 1:3, v/v). ^{1}H NMR (400 MHz, $CDCl_3$): δ = 9.72 (d, J = 4.5 Hz, 2H, H_β), 9.33 (d, J = 4.5 Hz, 2H, H_β), 8.97 (d, J = 4.5 Hz, 2H, H_β), 8.87 (d, J = 4.5 Hz, 2H, H_β), 8.01-8.03 (m, 4H, Ar-*o*-C*H*), 7.79 (s, 2H, Ar-*p*-C*H*), 7.23 (d, J = 8.6 Hz, 4H, N-Ar-C*H*), 7.16 (d, J = 8.6 Hz, 4H, N-Ar-C*H*), 1.52 (s, 36H, *t*-butyl-CH_3) and 1.22 ppm (s, 18H, *t*-butyl-CH_3). ^{13}C NMR (100 MHz, $CDCl_3$, 25 °C): δ = 153.5, 151.4, 150.2, 150.1, 149.8, 148.9, 143.1, 141.3, 133.9, 133.6, 132.8, 131.2, 129.8, 125.9, 123.1, 121.7, 121.2, 105.2, 35.2, 34.2, 31.9 and 31.5 ppm. UV/Vis (DCM): λ_{max} (log ε) = 419 (5.38), 566 (4.05), 620 nm (3.98). HRMS (MALDI): *m/z* calcd. for $C_{68}H_{76}N_5ZnBr$ (M^+): 1105.4576; found 1105.4561.

[5,15-Bis(3,5-di-*tert*-butylphenyl)-10-(*N*,*N*-bis(4-*tert*-butyl)phenylamino)-20-(4-carbomethoxyphenylethynyl)porphyrinato]zinc(II) 2.28a:

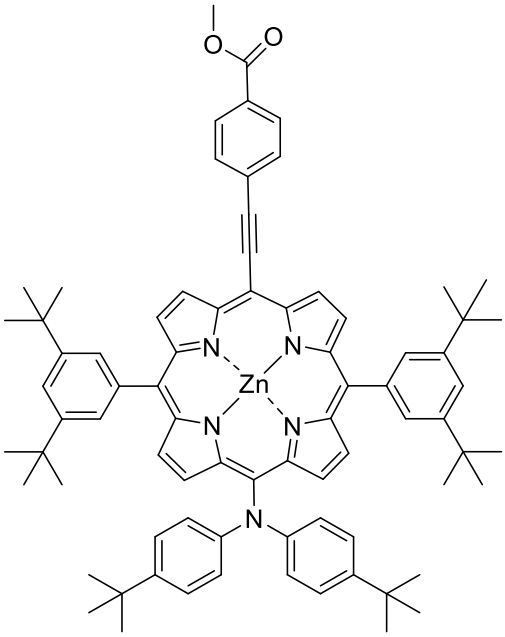

The target porphyrin was synthesised using [5-bromo-10,20-bis(3,5-di-*tert*-butyl)phenyl-15-*N*,*N*-bis(4-(*tert*-butyl)phenylamino)porphyrinato]zinc(II) **2.27a** (150 mg, 0.14 mmol), methyl-4-ethynylbenzoate (108 mg, 0.68 mmol), $PdCl_2(PPh_3)_2$ (10 mg, 14 µmol) and copper(I)iodide (8 mg, 41 µmol) in dry DMF (10 mL) and diethylamine (6 mL) according to procedure G. The crude product was filtered through a plug of silica using DCM before column chromatography (silica gel) using hexane/DCM (3:2, v/v) as eluent gave a glossy purple solid (111 mg, 0.09 mmol, 69%). (Recrystallisation from DCM/MeOH, yield 50 mg, loss due to solubility of the product in MeOH). M.p.: >300 °C. R_f = 0.72 (DCM/hexane 1:1 v/v + 1% MeOH). ^{1}H NMR (400 MHz, $CDCl_3$ + pyridine-d_5, 30:1, v/v): δ = 9.68 (d, *J* = 4.6 Hz, 2H, H_β), 9.18 (d, *J* = 4.6 Hz, 2H, H_β), 8.88 (d, *J* = 4.6 Hz, 2H, H_β), 8.72 (d, *J* = 4.6 Hz, 2H, H_β), 8.18 (d, *J* = 8.2 Hz, 2H, alkynyl-Ar-C*H*), 8.03 (d, *J* = 8.2 Hz, alkynyl-Ar-C*H*), 7.93-7.96 (m, 4H, Ar-*o*-C*H*), 7.72-7.73 (m, 2H, Ar-*p*-C*H*), 7.11 (d, *J* = 7.8 Hz, 4H, N-Ar-C*H*), 7.08 (d, *J* = 7.8 Hz, 4H, N-Ar-C*H*), 3.96 (s, 3H, N-CH_3) and 1.48 ppm (s, 54H, *t*-butyl-CH_3). ^{13}C NMR (150 MHz, $CDCl_3$ + pyridine-d_5, 30:1, v/v): δ = 167.1, 152.3, 152.2, 150.2, 150.1, 150.0, 149.7, 148.4, 142.6, 141.7, 133.1, 132.9, 131.1, 130.7, 130.0, 129.8, 129.7, 129.0, 125.6, 121.4, 120.7, 98.2, 95.0, 52.2, 35.0, 34.0, 31.7 and 31.4 ppm. UV/Vis (MeOH): λ_{max} (log ε) = 442 (5.00), 588 (3.94), 652 nm (4.36). HRMS (MALDI): *m/z* calcd. for $C_{78}H_{83}N_5O_2Zn$ (M^+): 1185.5838; found 1185.5844.

5,15-Bis(3,5-di-*tert*-butylphenyl)-10-(*N,N*-dimethylaniline)porphyrin 2.29a:

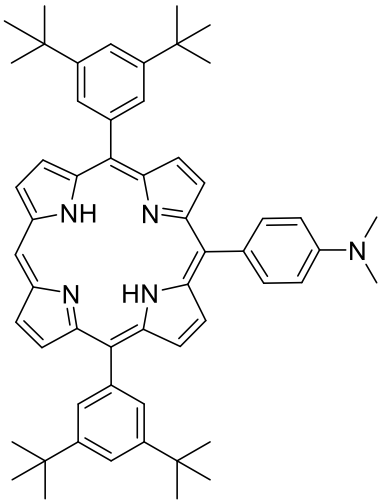

The title compound was synthesised in accordance with general procedure I. 4-Bromo-4-*N,N*-dimethylalanine (699 mg, 3.49 mmol), 5,15-Bis(3,5-di-*tert*-butylphenyl)porphyrin **2.23a** (200 mg, 0.29 mmol), (8 mL), *n*-BuLi (2.2 mL, 3.49 mmol), THF (40 mL), sat. aq. NH_4Cl (2 mL) and DDQ (396 mg, 1.30 mmol) were used. The product was obtained as purple/red crystals after recrystallisation from MeOH/$CHCl_3$ (170 mg, 0.21 mmol, 72%). M.p.: >300 °C. R_f = 0.68 (hexane/DCM, 1:1, v/v). ^{1}H NMR (400 MHz, $CDCl_3$): δ = 10.18 (s, 1H, meso-*H*), 9.33 (d, *J* = 4.6 Hz, 2H, H_β), 9.06 (d, *J* = 4.6 Hz, 2H, H_β), 8.99 (d, *J* = 4.8 Hz, 2H, H_β), 8.94 (d, *J* = 4.8 Hz, 2H, H_β), 8.13 (d, *J* = 1.8 Hz, 4H, Ar-*o*-C*H*), 8.10 (d, *J* = 8.6 Hz, 2H, N-Ar-C*H*), 7.81 (t, *J* = 1.8 Hz, 2H, Ar-*p*-C*H*), 7.11 (d, *J* = 8.6 Hz, 4H, N-Ar-C*H*), 3.24 (s, 6H, N-CH_3), 1.56 (s, 36H, *t*-butyl-CH_3) and -2.87 ppm (s, 2H, N*H*). ^{13}C NMR (100 MHz, $CDCl_3$): δ = 150.1, 149.0, 141.1, 135.7, 131.8, 131.7, 131.0, 130.8, 130.2, 121.6, 121.1, 120.9, 110.7, 104.2, 40.9, 35.2 and 31.9 ppm. UV/Vis (DCM): λ_{max} (log ε) = 416 (5.24), 514 (4.04), 554 (3.79), 588 (3.59), 646 nm (3.49). HRMS (MALDI): *m/z* calcd. for $C_{56}H_{63}N_5(M^+)$: 805.5083; found 805.5074.

5-(*N,N*-Dimethylaniline)-10,15-bis(2,6-dioctyloxyphenyl)porphyrin 2.29b:

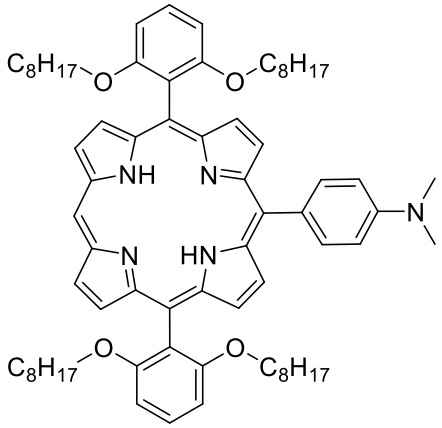

The porphyrin was prepared in accordance with general procedure I. 4-Bromo-4-*N,N*-dimethylalanine (699 mg, 3.49 mmol), 5,15-bis(2,6-dioctyloxyphenyl)porphyrin **2.23b** (284 mg, 0.29 mmol), Et_2O (8 mL), *n*-BuLi (2.2 mL, 3.49 mmol) , THF (40 mL), sat. aq. NH_4Cl and DDQ (396 mg, 1.30 mmol) were used. The product was obtained as purple/red crystals after recrystallisation from MeOH/$CHCl_3$ (171 mg, 0.15 mmol 54%). M.p.: 95-96 °C. R_f = 0.31 (hexane/DCM, 1:1, v/v). ^{1}H NMR (400 MHz, $CDCl_3$): δ= 10.02 (s, 1H, H_{meso}), 9.20 (d, J = 4.9 Hz, 2H, H_β), 8.92 (d, J = 4.9 Hz, 2H, H_β), 8.88 (d, J = 4.9 Hz, 2H, H_β), 8.82 (d, J = 4.9 Hz, 2H, H_β), 8.08 (d, J = 8.6 Hz, 2H, N-Ar-C*H*), 7.70 (t, J = 8.4 Hz, 2H, Ar-*p*-C*H*), 7.09 (d, J = 8.6 Hz, 2H, N-Ar-C*H*), 7.02 (d, J = 8.6 Hz, 4H, Ar-*m*-C*H*), 3.83 (t, J = 6.3 Hz, 8H, OCH_2), 1.00-0.93 (m, 8H, CH_2), 3.23 (s, 6H, N-CH_3), 0.44-0.92 (m, 60H, CH_3(CH_2)$_6$) and -2.82 ppm (s, 2H, N*H*). ^{13}C NMR (100 MHz, $CDCl_3$): δ_c = 159.3, 148.9, 134.7, 130.4, 128.9, 119.8, 119.1, 110.9, 109.7, 104.4, 102.2, 67.8, 39.4, 30.5, 27.8, 27.8, 24.4, 21.4 and 12.9 ppm. UV/Vis (DCM): λ_{max} (log ε) = 413 (5.90), 508 (4.58), 586 (4.11), 644 nm (3.89). HRMS (MALDI): *m/z* calcd. for $C_{56}C_{72}H_{95}N_5O_4(M^+)$: 1093.7384; found 1093.7384.

5-Bromo-10,20-bis(3,5-di-*tert*-butylphenyl)-15-(*N,N*-dimethylaniline)porphyrin 2.30a:

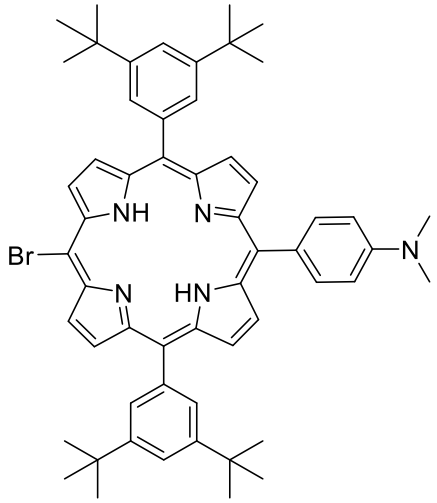

Porphyrin **2.30a** was synthesised in accordance with general procedure F. 5,15-bis(3,5-di-*tert*-butylphenyl)-10-(4-*N,N*-Dimethylanilinyl)porphyrin **2.29a** (250 mg, 0.31 mmol), $CHCl_3$ (50 mL), pyridine (0.2 mL), NBS (66 mg, 0.37 mmol) and acetone (5 mL) were used. The product was obtained as purple crystals (200 mg, 0.23 mmol, 74%). M.p.: >300 °C. R_f = 0.60 (hexane/DCM, 1:1, v/v). ^{1}H NMR (400 MHz, $CDCl_3$): δ = 9.63 (d, J = 4.6 Hz, 2H, H_β), 8.90 (d, J = 8.8 Hz, 2H, H_β), 8.89 (d, J = 5.2 Hz, 2H, H_β), 8.80 (d, J = 4.9 Hz, 2H, H_β), 8.04 (d, J = 2.3 Hz, 4H, Ar-*o*-C*H*), 8.03 (d, J = 4.3 Hz, 2H, N-Ar-C*H*), 7.80-7.79 (m, 2H, Ar-*p*-C*H*), 7.08 (d, J = 8.9 Hz, 2H, N-Ar-C*H*), 3.21 (s, 6H, N-CH_3), 1.52 (s, 36H, *t*-butyl-CH_3) and -2.66 ppm (s, 2H, N*H*). ^{13}C NMR (100 MHz, $CDCl_3$): δ_c = 150.2, 148.9, 141.1, 135.7, 131.9, 130.2, 130.1, 122.1, 121.3, 110.9, 102.2, 40.9, 35.2 and 31.9 ppm. UV/Vis (DCM); λ_{max} (log ε) =423 (5.75), 524 (4.47), 565 (4.42), 603 (3.99), 659 nm (4.17 HRMS (ESI): *m/z* calcd. for $C_{56}H_{62}BrN_5$ (M^+): 884.4267; found 884.4265.

5-Bromo-10,20-bis(2,6-dioctyloxyphenyl)-15-(*N,N*-dimethylaniline)porphyrin 2.30b:

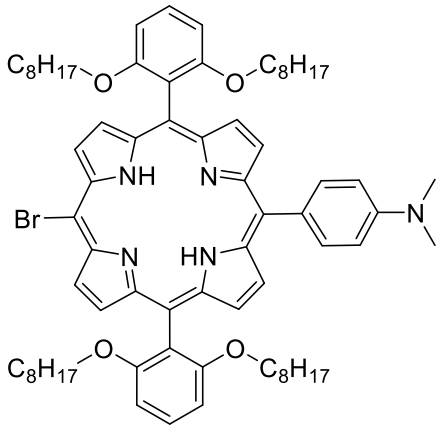

The porphyrin was synthesised in accordance with general procedure F. 5-(4-*N,N*-Dimethylanilinyl)-10,20-bis(2,6-dioctyloxyphenyl)porphyrin **2.29b** (56 mg, 0.05 mmol), $CHCl_3$ (20 mL), NBS (82 mg, 0.05 mmol), pyridine (5 µL) and acetone (5 mL) were used to obtained the product as purple crystals (50 mg, 0.43 mmol, 84%). M.p.: 52 °C. R_f = 0.51 (hexane/DCM, 1:1, v/v). ^{1}H NMR (600 MHz, $CDCl_3$): δ= 9.56 (d, J = 4.6 Hz, 2H, H_β), 8.85 (dd, J = 4.7, 8.5 Hz, 4H, H_β), 8.76 (d, J = 4.7 Hz, 2H, H_β), 9.56 (d, J = 4.7 Hz, 2H, N-Ar-C*H*), 7.72 (t, J = 8.9 Hz, 2H, Ar-*p*-C*H*), 7.10 (d, J = 8.4 Hz, 2H, N-Ar-C*H*), 7.02 (d, J = 8.6 Hz, 4H, Ar-*m*-C*H*), 3.85 (t, J = 6.4 Hz, 8H, OCH_2), 1.01-0.45 (m, 60H, $CH_3(CH_2)_6$) and -2.53 ppm (s, 2H, N*H*). ^{13}C NMR (100 MHz, $CDCl_3$): δ_c = 160.1, 149.8, 135.7, 131.2, 130.1, 120.7, 113.3, 110.8, 105.3, 68.7, 40.9, 31.5, 28.8, 28.7, 25.4, 22.4 and 13.9 ppm. UV/Vis (DCM): λ_{max} (log ε) = 423 (5.73), 523 (4.50), 561 (4.29), 600 (4.05), 657 nm (3.96). HRMS (MALDI): *m/z* calcd. for $C_{72}H_{94}BrN_5O_4$ (M^+): 1171.6489; found1171.6497.

[5-Bromo-10,20-bis(3,5-di-*tert*-butylphenyl)-15-(*N,N*-dimethylaniline)porphyrinato]zinc(II) 2.31a:

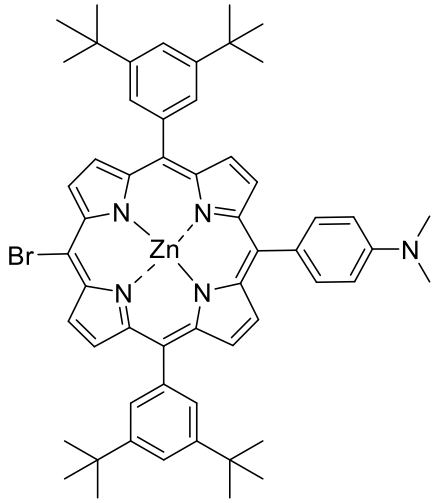

Porphyrin **2.31a** was synthesised in accordance with general procedure C using 5-bromo-10,20-bis(3,5-di-*tert*-butylphenyl)-15-(4-*N,N*-dimethylanilinyl)porphyrin **2.30a** (200 mg, 0.22 mmol) in $CHCl_3$ (30 mL) and $Zn(OAc)_2$ (12 mg, 0.68 mmol) in MeOH (10 mL) was added. The product was obtained as green crystals after recrystallisation from MeOH/$CHCl_3$ (150 mg, 0.16 mmol, 72%). M.p.: >300 °C. R_f = 0.42 (hexane/DCM, 1:1, v/v). ^{1}H NMR (400 MHz, $CDCl_3$): δ= 9.82 (d, J = 5.6 Hz, 2H, H_β), 9.10 (d, J = 4.6 Hz, 2H, H_β), 9.00 (dd, J = 9.4 Hz, 4H, H_β), 8.44 (d, J = 1.9 Hz, 1H, N-Ar-C*H*), 8.11 (s, 4H, Ar-*o*-C*H*), 8.07 (s, 1H, N-Ar-C*H*), 7.85 (s, 2H, Ar-*p*-C*H*), 7.82 (d, J = 13.9 Hz, 1H, N-Ar-C*H*), 7.45 (d, J = 8.4 Hz, 1H, N-Ar-C*H*), 3.12 (s, 6H, N-CH_3) and 1.57 ppm (s, 36H, *t*-butyl-CH_3). ^{13}C NMR (100 MHz, $CDCl_3$): δ_c = 151.3, 151, 150.8, 150.5, 149.7, 148.7, 148.7, 148.5, 141.4, 139.3, 138.3, 134.9, 133.6, 132.8, 132.6, 132.5, 129.9, 123.1, 121.1, 111.3, 104.1, 40.9, 35.2, 31.9 ppm. UV/Vis (DCM): λ_{max} (log ε) = 425 (4.79), 556 (3.52), 596 nm (3.21). HRMS (MALDI): *m/z* calcd. for $C_{56}H_{60}BrN_5Zn$ (M^+): 945.3324; found 945.3356.

[5-Bromo-10,20-bis(2,6-dioctyloxyphenyl)-15-(*N,N*-dimethylaniline)porphyrinato]zinc(II) 2.31b:

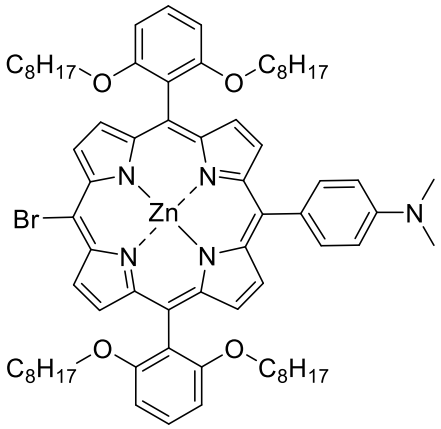

Porphyrin **2.31b** was synthesised in accordance with general procedure C using 5-bromo-10,20-bis(2,6-dioctyloxyphenyl)-15-(4-*N,N*-dimethylanilinyl)porphyrin **2.30b** (150 mg, 0.13 mmol) in $CHCl_3$ (50 mL) and $Zn(OAc)_2$ (84 mg, 0.38 mmol) in MeOH (5 mL) was added. The crude product was filtered through silica gel using DCM as eluent to yield a dark purple/green solid (155 mg, 0.13 mmol, 98%). M.p.: 134 °C. R_f = 0.42 (hexane/DCM, 1:1, v/v). ^{1}H NMR (600 MHz, $CDCl_3$): δ= 9.65 (d, J = 4.7 Hz, 2H, H_β), 8.91 (d, J = 4.7 Hz, 2H, H_β), 8.87 (d, J = 4.5 Hz, 2H, H_β), 8.81 (d, J = 4.8 Hz, 2H, H_β), 7.94 (d, J = 8.3 Hz, 2H, N-Ar-C*H*), 7.68 (t, J = 8.4 Hz, 2H, Ar-*p*-C*H*), 6.99 (d, J = 8.8 Hz, 4H, Ar-*m*-C*H*), 6.73 (d, J = 8.8 Hz, 2H, N-Ar-C*H*), 3.82 (t, J = 6.3 Hz, 8H, CH_2), 2.71 (s, 6H, N-CH_3) and 0.98-0.39 ppm (m, 60H, CH_3(CH_2)$_6$). ^{13}C NMR (100 MHz, $CDCl_3$): δ_c = 160.2, 150.9, 149.2, 135.4, 132.4, 131.3, 129.8, 121.5, 114.1, 105.4, 68.8, 31.4, 28.8, 28.8, 28.7, 25.4, 22.4 and 13.9 ppm. UV/Vis (DCM): λ_{max} (log ε) = 426 (5.70), 555 (4.50), 599 nm (4.02). HRMS (MALDI): *m/z* calcd. for $C_{72}H_{92}BrN_5O_4Zn$ (M^+): 1233.5624; found 1233.4647.

[5,15-Bis(3,5-di-*tert*-butylphenyl)-10-(4-Carbomethoxyphenylethynyl)-20-(*N,N*-dimethylaniline)porphyrinato]zinc(II) 2.32a:

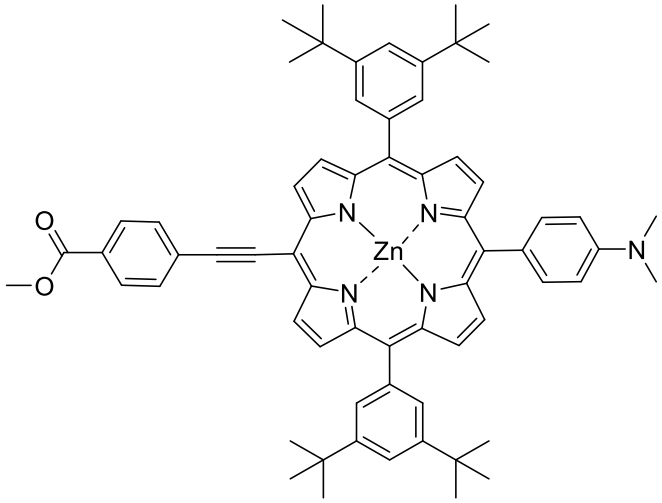

Porphyrin **2.32a** was synthesised in accordance with general procedure G. [5-bromo-10,20-bis(3,5-di-*tert*-butylphenyl)-15-(4-*N,N*-dimethylanilinyl)porphyrinato]zinc(II) **2.31a** (100 mg, 0.12 mmol), methyl-4-ethylbenzonate (83 mg, 0.52 mmol), $PdCl_2(PPh_3)_2$ (7 mg, 0.12 µmol), CuI (6 mg, 0.32 µmol), (10 mL), diethylamine (2.9 mL) and water (100 mL) were used to yield green crystals after recrystallisation from MeOH/$CHCl_3$ (60 mg, 0.06 mmol, 52%). M.p.: 182 °C. R_f = 0.58 (hexane/DCM, 2:1, v/v). ^{1}H NMR (400 MHz, $CDCl_3$): δ = 9.86 (d, J = 4.5 Hz, 2H, H_β). 9.09 (d, J = 4.6 Hz, 2H, H_β), 9.03 (d, J = 4.8 Hz, 2H, H_β), 8.94 (d, J = 4.6 Hz, 2H, H_β), 8.25 (d, J = 8.1 Hz, 2H, alkynyl-Ar-C*H*), 8.12 (d, J = 8.4 Hz, 4H, alkynyl-Ar-C*H*), 8.07 (d, J = 8.1 Hz, 2H, N-Ar-C*H*), 7.85-7.84 (m, 2H, Ar-*p*-C*H*), 7.10 (d, J = 8.1 Hz, 2H, N-Ar-CH), 4.03 (s, 3H, OCH_3), 3.22 (s, 6H, N-CH_3) and 1.58 ppm (s, 36H *t*-butyl-CH_3). ^{13}C NMR (100 MHz, $CDCl_3$): δ_c = 152.4, 150.9, 150.0, 148.5, 142.2, 135.5, 133.2, 132.2, 131.7, 131.2, 130.4, 130.0, 129.8, 129.0, 123.4, 120.7, 113.6, 110.9, 97.8, 97.1, 94.9, 52.4, 41.1, 35.2, 31.9 and 31.1 ppm. UV/Vis (DCM): λ_{max} (log ε) = 444 (6.31), 570 (4.98), 620 nm (5.29). HRMS (MALDI): *m/z* calcd. for $C_{66}H_{67}N_5O_2Zn$ (M^+): 1025.4586; found 1025.4613.

[5-(4-Carbomethoxyphenylethynyl)-10,20-bis(2,6-dioctyloxyphenyl)-15-(*N,N*-dimethylaniline)porphyrinato]zinc(II) 2.32b:

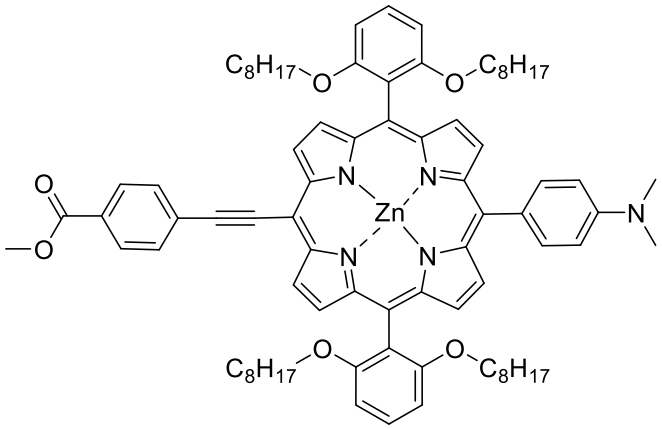

Following procedure G [5-bromo-10,20-bis(2,6-dioctyloxyphenyl)-15-(4-*N,N*-dimethylanilinyl)porphyrinato]zinc(II) **2.31b** (140 mg, 0.12 µmol), methyl-4-ethylbenzonate (96 mg, 0.60 mmol), $PdCl_2(PPh_3)_2$ (9 mg, 12.20 µmol), CuI (7 mg, 36.50 µmol), DMF (11 mL), diethylamine (2.8 mL) gave green crystals after recrystallisation from MeOH/$CHCl_3$ (80 mg, 0.06 mmol, 50%). M.p.: 87 °C. R_f = 0.42 (hexane/DCM, 1:2, v/v). ^{1}H NMR (400 MHz, $CDCl_3$): δ= 9.74 (d, *J* = 4.4 Hz, 2H, H_β), 8.97 (d, *J* = 4.7 Hz, 2H, H_β), 8.91 (s, 2H, H_β), 8.82 (d, *J* = 4.7 Hz, 2H, H_β), 8.25 (d, *J* = 8.2 Hz, 2H, alkynyl-Ar-C*H*), 8.04 (d, *J* = 8.4 Hz, 2H, alkynyl-Ar-C*H*), 8.06 (s, 2H, N-Ar-C*H*), 7.72 (t, *J* = 9.4 Hz, 2H, Ar-*p*-C*H*), 7.08 (s, 2H, N-Ar-C*H*), 7.03 (d, *J* = 9.01 Hz, 4H, Ar-*m*-C*H*), 4.04 (s, 3H, OCH_3), 3.86 (t, *J* = 6.6 Hz, 8H, OCH_2), 3.20 (s, 6H, N-CH_3), and 0.99-0.42 ppm (m, 60H, $CH_3(CH_2)_6$). ^{13}C NMR (100MHz, $CDCl_3$): δ_c = 160.2, 135.6, 132.0, 131.9, 131.1, 130.4, 129.9, 129.8, 129.5, 128.2, 105.4, 68.7, 52.3, 31.6, 28.9, 28.9, 25.4 and 22.5 ppm. UV/Vis (DCM): λ_{max} (log ε) = 446 (5.69), 569 (4.42), 619 nm (4.63). HRMS (MALDI): *m/z* calcd. for $C_{82}H_{99}N_5O_6Zn$ (M^+): 1313.6887; found 1313.6887.

[5,15-Bis(3,5-di-*tert*-butylphenyl)-10-(4-carboxyphenylethynyl)-20-(*N,N*-dimethylaniline)porphyrinato]zinc(II) 2.33a:

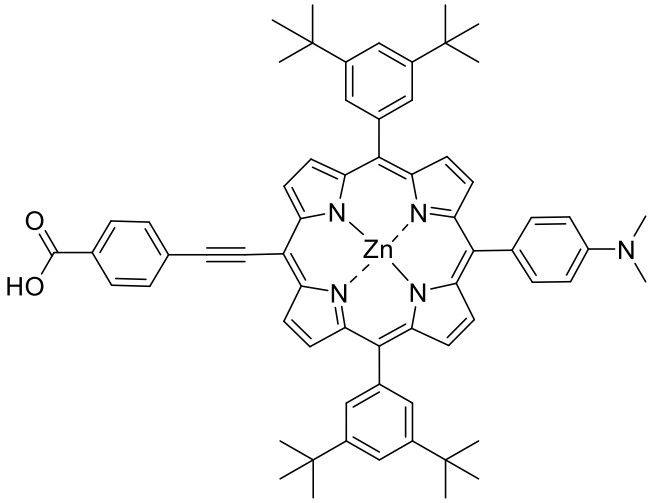

Porphyrin **2.33a** was synthesised using procedure H. Porphyrin **2.32a** (150 mg, 0.15 mmol), NaOH (2.06 g, 51 mmol), MeOH (25.7 mL) and THF (25.7 mL) were used. Recrystallisation from MeOH/ DCM yielded the desired compound as green solid in 85% (128 mg, 0.13 mmol, 85%). M.p.: >300 °C. R_f = 0.14 (DCM + 2% MeOH). ^{1}H NMR (400 MHz, $CDCl_3$): δ = 9.76 (d, J = 4.6 Hz, 2H, H_β), 8.97 (d, J = 4.6 Hz, 2H, H_β), 9.89 (d, J = 4.6 Hz, 2H, H_β), 8.81 (d, J = 4.6 Hz, 2H, H_β), 8.30 (d, J = 6.03 Hz, 2H, alkynyl-Ar-*H*), 8.09 (d, J = 6.03 Hz, 2H, alkynyl-Ar-*H*), 8.02-8.05 (m, 4H, Ar-o-C*H*), 8.02-8.05 (m, 2H, N-Ar-C*H*), 7.78 (s, 2H,Ar-p-C*H*), 7.10 (d, J = 8.5 Hz, 2H, N-Ar-CH), 3.21 (s, 6H, N-CH_3), 1.50 (s, 36H, *t*-butyl-CH_3) and 1.26 ppm (s, 16 H, *t-butyl*-CH_3). ^{13}C NMR (100 MHz, $CDCl_3$): δ_c = 152.4, 150.9, 150.5, 150.0, 149.9, 149.2, 148.9, 148.7, 148.5, 142.2, 135.9, 135.7, 135.5, 135.4, 133.1, 132.2, 131.7, 131.6, 131.2, 130.3, 130.1, 124.0, 123.5, 123.2, 123.0, 120.7, 110.7, 97.4, 97.2, 95.2, 41.0, 35.2, 31.9, 29.8 and 29.5 ppm. UV/Vis: (THF): λ_{max} (log ε) = 447 (5.14), 578 (3.71), 630 nm (4.12). HRMS (MALDI): *m/z* calcd. for $C_{65}H_{65}N_5O_6Zn$ (M^+): 1011.4430; found 1011.4436. MS (MALDI) *m/z* (%): 1011.45 (100) [M^+], 996.46 (9) [M^+–CH_3].

[5-(4-Carboxyphenylethynyl)-10,20-bis(2,6-dioctyloxyphenyl)-15-(*N,N*-dimethylaniline)porphyrinato]zinc(II) 2.32b:

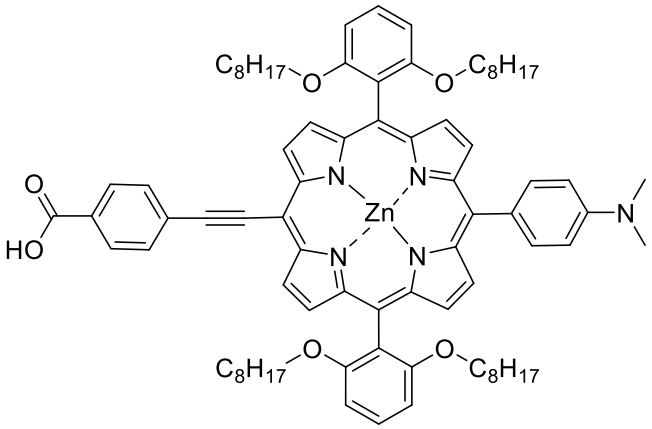

The title compound was synthesised following procedure H. Porphyrin **2.33b** (60 mg, 0.05 mmol), NaOH (644 mg, 16 mmol), MeOH (8 mL) and THF (8 mL) were used. Recrystallisation from DCM/MeOH gave a green solid (42 mg, 33 µmol, 72%). M.p.: 228-232 °C. R_f = 0.36 (DCM + 2% MeOH). ^{1}H NMR (400 MHz, DMSO): δ = 9.56 (d, J = 4.2 Hz, 2H, H_β), 8.72 (d, J = 4.2 Hz, 2H, H_β), 8.66 (d, J = 4.2 Hz, 2H, H_β), 8.57 (d, J = 4.2 Hz, 2H, H_β), 8.07-8.15 (m, 4H, alkynyl-Ar-*H*), 7.86 (d, J = 8.4, 2H, N-Ar-C*H*), 7.71 (m, 2H, Ar-*p*-C*H*), 7.09 (d, J = 8.4, 4H, Ar-m-C*H*), 7.05 (d, J = 8.5 Hz, 2H, N-Ar-C*H*), 3.85 (m, 8H, OCH_2), 3.13 (s, 6H, N-CH_3) and 0.92-0.39ppm (m, 60H, CH_3(CH_2)$_6$). ^{13}C NMR (100 MHz, $CDCl_3$): δ_c = 159.2, 151.2, 150.3, 149.3, 149.2, 149.1, 148.8, 135.9, 135.7, 135.4, 134.9, 130.9, 129.8, 123.6, 123.3, 123.1, 120.4, 114.2, 110.3, 105.2, 67.7, 30.9, 28.2, 28.1, 28.1, 24.8, 21.7 and 13.7 ppm. UV/Vis: (THF): λ_{max} (log ε) = 449 (5.27), 577 (3.86), 630 nm (4.21). HRMS (MALDI): *m/z* calcd. for $C_{81}H_{97}N_5O_6Zn$ (M^+): 1299.6730; found 1299.6735.

6.3 Chapter 3: Connecting two systems – Cubanes and porphyrins

Dipyrromethane was synthesized according to the Lindsey method.[278] 5,15-Disubstituted porphyrins were synthesized *via* standard condensation reactions followed by phenyl lithium insertion reactions using Senge methodologies to afford 10,20-dihexyl-5-phenylporphyrin, 5,10,15-triphenylporphyrin and 5,15-bis-(4-methylphenyl)-10-phenylporphyrin.[20a, 61]

Iodination reactions resulted in 5-iodo-10,20-bis(4-methylphenyl)-15-phenylporphyrin and 5-iodo-10,15,20-triphenylporphyrin. Nickel(II) insertion reactions were performed following literature procedures to afford [5-iodo-10,20-bis(4-methylphenyl)-15-phenylporphyrinato]-nickel(II) **3.36d**, [5-iodo-10,15,20-tris(4-methylphenyl)porphyrinato]nickel(II) **3.36c**.[279] All known porphyrins had analytical data consistent with those reported in the literature.

5,15-dihexyl-10-iodo-20-phenylporphyrin 3.35

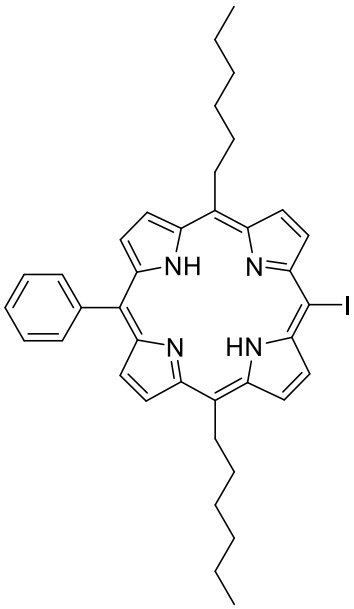

5,15-dihexyl-10-phenylporphyrin (51.6 mg, 93 µmol, 1 eq.) **3.34** was dissolved in $CHCl_3$(25 mL) and purged with argon. Iodine (21 mg, 95 µmol, 1.5 eq.) and bis(trifluoroacetoxy)iodobenzene (40 mg, 93 µmol, 1.1 eq.) were added and the flask shielded from light. The reaction mixture was left to stir at room temperature until consumption of the starting material. The solution was then filtered through silica gel using DCM as eluent, solvents were removed and the product was

recrystallised from $CHCl_3$/MeOH. The product was obtained as purple crystals (76 mg, 73%). M.p.: 114.2 °C (dec.). R_f = 0.26 (SiO_2, hexane/DCM= 2:1, v/v). ^{1}H NMR (400 MHz, $CDCl_3$): δ = 9.71 (d, *J* = 4.9 Hz, 2H, H_β), 9.39 (d, *J* = 4.9 Hz, 2H, H_β), 9.33 (d, *J* = 4.8 Hz, 2H, H_β), 8.81 (d, *J* = 4.8 Hz, 2H, H_β), 8.18–8.13 (m, 2H, phenyl-*H*), 7.83–7.71 (m, 3H, phenyl-*H*), 4.88–4.81 (m, 4H, hexyl-CH_2), 2.47 (m, 4H, hexyl-CH_2), 1.77 (m, 4H, hexyl-CH_2), 1.54–1.45 (m, 4H, hexyl-CH_2), 1.38 (m, 7.0 Hz, 4H, hexyl-CH_2), 0.93 (t, *J* = 7.2 Hz, 6H, hexyl-CH_3) and -2.71 ppm (s, 2H, N*H*). ^{13}C NMR (101 MHz, $CDCl_3$): δ = 142.4, 134.5, 127.9, 126.8, 120.8, 120.2, 78.1, 38.9, 35.5, 32.0, 30.3, 22.9 and 14.3 ppm. UV-Vis (DCM): λ_{max} (log ε) 422 (5.64), 523 (4.02), 559 (3.19), 605.5 (3.58), 659.0 nm (3.82). HRMS (MALDI) *m/z* calcd. for $C_{38}H_{41}N_4I$ $[M]^+$: 680.2376, found 680.2370.

(5,15-dihexyl-10-iodo-20-phenylporphyrinato)nickel(II) 3.36a

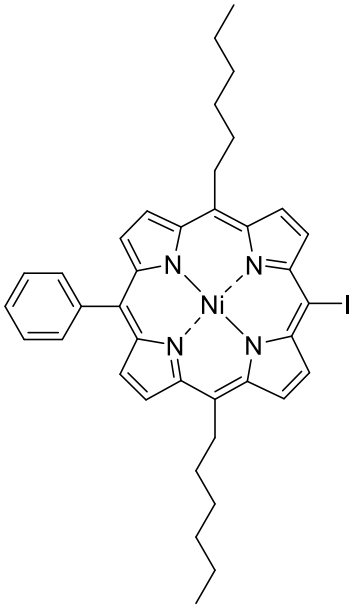

Free-base porphyrin **3.35** (287 mg, 0,42 mmol, 1 eq.) and $Ni(acac)_2$ (120 mg, 0,63 mmol, 1.5 eq.) were dissolved in toluene and heated to reflux. The reaction process was monitored by TLC and once all the starting material was consumed the reaction flask was allowed to cool and filtered through silica gel using DCM as eluent. Removal of the solvents was followed by recrystallisation from $CHCl_3$/MeOH.to yield purple crystals (278 mg, 84%). M.p.: 87 °C (dec.). R_f = 0.26 (SiO_2, hexane/DCM= 6:1, v/v). ^{1}H NMR (400 MHz, $CDCl_3$): δ = 9.43 (d, *J* = 4.9 Hz, 2H, H_β), 9.18 (d, *J* = 4.9 Hz, 2H, H_β), 9.13 (d, *J* = 4.9 Hz, 2H, H_β), 8.66 (d, *J* = 4.9 Hz, 2H, H_β), 7.92 (m, 2H, phenyl-*H*), 7.73–7.61 (m, 3H, phenyl-*H*), 4.41 (t, *J* = 7.4 Hz, 4H, hexyl-CH_2), 2.22 (m, 4H, hexyl-CH_2), 1.60–1.49 (m, 4H, hexyl-CH_2), 1.39 (m, 4H, hexyl-CH_2), 1.30 (m, 4H, hexyl-CH_2) and 0.89 ppm (t, *J* = 7.1 Hz, 6H, hexyl-CH_3). ^{13}C NMR (101 MHz, $CDCl_3$): δ = 143.4, 143.0, 142.5, 141.7, 140.6, 138.1, 133.6, 132.9, 130.9, 129.9, 127.9, 127.0, 118.8, 118.6, 75.8, 37.6, 34.1, 31.9, 30.1, 22.8 and 14.3 ppm. UV-Vis (DCM): λ_{max} (log ε) 421 (5.36), 538 nm (4.22). HRMS (MALDI) *m/z* calcd. for $C_{38}H_{39}N_4INi$ $[M]^+$: 736.1573, found 736.1594.

[5-Iodo-10,15-bis(4-methylphenyl)-20-phenylporphyrinato]nickel(II) 3.36c

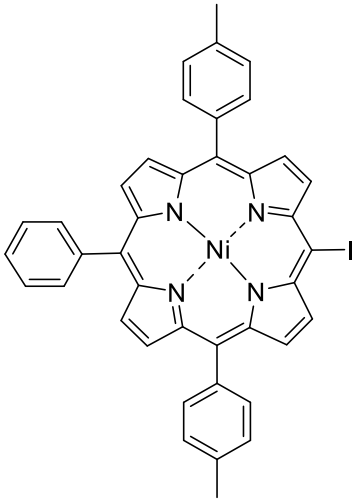

5-Iodo-10,15-bis(4-methylphenyl)-20-phenylporphyrin (517 mg, 0.75 mmol, 1 eq.), $Ni(acac)_2$ (291 mg, 1.12 mmol, 1,5 eq.) were dissolved in toluene (300 ml) and heated to 110 °C. The reaction process was monitored by TLC and once all the starting material was consumed the reaction flask was allowed to cool and filtered through silica gel using DCM as eluent. Removal of the solvents was followed by recrystallisation from $CHCl_3$/MeOH to yield purple crystals (500 mg, 0.67 mmol, 89%). M.p.: 250 °C (dec.). R_f = 0.45 (hexane/DCM, 3:1, v/v). ^{1}H NMR (400 MHz, $CDCl_3$): δ = 9.48 (d, J = 5.0 Hz, 2H, H_β), 8.76 (d, J = 5.0 Hz, 2H, H_β), 8.66–8.70 (m, 4H, H_β), 7.96 (m, 2H, phenyl-*H*), 7.85 (d, J = 7.9 Hz, 4H, tolyl-*H*), 7.67 (m, 3H, phenyl-*H*), 7.48 (d, J = 7.9 Hz, 4H, tolyl-*H*) and 2.65 ppm (s, 6H, CH_3). ^{13}C NMR (100 MHz, $CDCl_3$): δ = 144.5, 143.7, 143.0, 142.9, 140.7, 137.9, 137.7, 137.6, 133.7, 132.8, 132.6, 128.0, 127.8, 127.1, 119.7 and 21.6 ppm. UV/Vis (DCM): λ_{max} (log ε) = 420 (6.61), 534 nm (5.46). HRMS (MALDI) *m/z* calcd. for $C_{40}H_{27}IN_4Ni$ [M]+: 748.0634, found 748.0616.

Bis[5,15-dihexyl-10-phenylporphyrin-20-ylato)nickel(II) S3.1

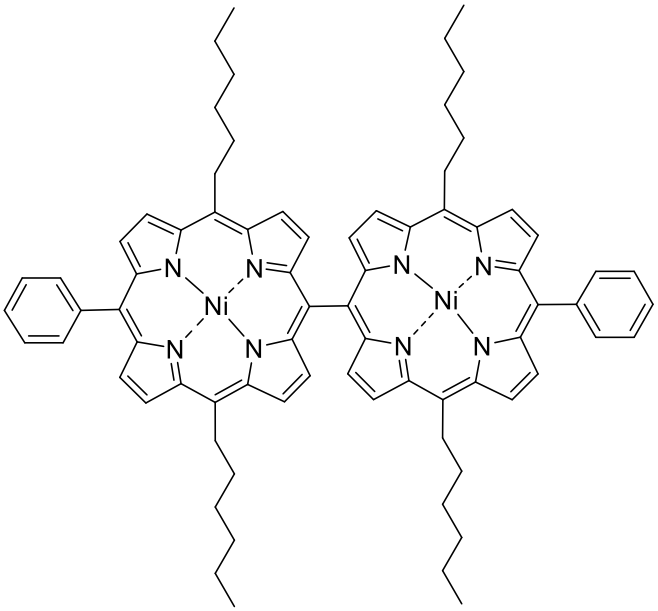

This compound was obtained as a side product in the organolithium reaction with cubanes and porphryins. Iodoporphyrin **3.36a** (74 mg, 0.1mmol, 1eq) was dried and dissolved in 2mL dry THF. The reaction micture was cooled to -98 °C and 0.27 mL of the diluted *n*-BuLi (0.5mL 1.6M *n*-BuLi was dilluted in 1mL dry diethyl ether) (0.15 mmol, 1.5 eq.) was added dropwise over 20 min. The reaction was stirred for 30 min at this temperature. The cubane was dried and a solution of cubane in dry THF was prepared. 79 mg cubane was dissolved in 0.4 mL THF. The cold bath was removed from the porphryin solution and 0.21 mL of the cubane solution (0.15 mmol, 1.5 eq.) were added dropwise over 10 min to the porphyrin solution. The reaction was stirred at rt for 1h. The reaction was quenched with water and the porphryins were seperated using DCM/hexane = 1:6 on a prep. TLC plate. The dimer was isolated in 36% (22 mg, 0.018 mmol) as purple glossy film. M.p.: glossy film, no meassurement of melting point possible. R_f = .0.57 (hexane/DCM, 2:1, v/v). ^{1}H NMR (400 MHz, $CDCl_3$): δ= 9.30 (d, *J* = 5.0 Hz, 4H, H_β), 9.05 (d, *J* = 5.1 Hz, 4H, H_β), 8.82 (d, *J* = 5.0 Hz, 4H, H_β), 8.10 (d, *J* = 5.1 Hz, 4H, H_β), 8.08 – 8.05 (m, 4H, phenyl-*H*), 7.75 – 7.71 (m, 6H, phenyl-*H*), 4.58 – 4.51 (m, 8H, hexyl-CH_2), 2.30 (d, *J* = 7.6 Hz, 8H, hexyl-CH_2), 1.66 – 1.52 (m, 8H, hexyl-CH_2), 1.45 – 1.35 (m, 8H, hexyl-CH_2), 1.30 (m, 8H, hexyl-CH_2) and 0.85 ppm (t, *J* = 7.2 Hz, 12H, hexyl-CH_3). ^{13}C NMR (100 MHz, $CDCl_3$, 25 °C): *δ* =145.8, 143.3, 142.9, 142.1, 141.6, 141.2, 141.2, 138.9, 134.5, 133.8, 132.7, 131.9, 129.7, 129.4,

127.9, 127.0, 124.6, 119.0, 118.6, 114.5, 47.2, 37.6, 34.4, 30.3 and 29.9 ppm. UV/Vis (DCM): λ_{max} (log ε) 412 (5.01), 449 (5.04), 540 (4.39) nm. HRMS (MALDI) *m/z* calcd. for $C_{76}H_{78}N_8Ni_2$ $[M]^+$: 1218.5079, 1218.5056 found;

[5-(4-Cubanyl-1-methylcarboxylate)-10,20-dihexyl-15-phenylporphyrinato]nickel(II) 3.44a

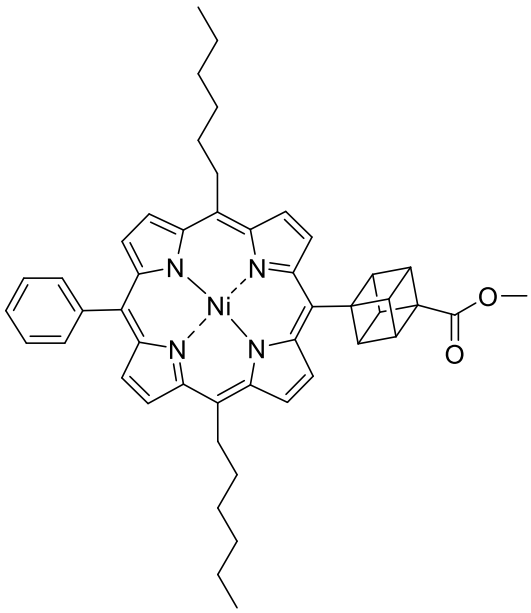

Porphyrin **3.36a** (74 mg, 0.1 mmol, 1 eq.) was dissolved in 2 mL dry THF and cooled to -40 °C. 0.09 mL of the *i*PrMgCl*LiCl solution (0.7 eq., 0.07 mmol, 0.8M.) were added dropwise. The reaction was stirred for 3 h. Another 0.018 mL of the *i*PrMgCl*LiCl solution (0.14 eq.) was added since starting material was still present. After one hour an additional 0.14 eq of the *i*PrMgCl*LiCl solution was added and the reaction was stirred overnight. After 21h the reaction was slowly heated to -25 °C and stirred for 75 min. The cooling bath was removed. After warming to rt 0.1 mL $ZnCl_2$ solution (1.0M in THF, 1 eq.) was added and the reaction was stirred for 30 min at rt. Meanwhile the cubane ester **3.43** (49 mg, 0.1 mmol, 1eq.), $NiCl_2$ (4.4 mg, 0.02 mmol, 0.2 eq.) and dtbppy (11 mg, 0.04 mmol, 0.4 eq.) were dissolved in 1.4 mL fry DMF. The porphyrin solution was added to the cubane solution all at once and the reaction was stirred for 16 h at 40 °C. The reaction mixture was quenched with a sat. solution of ammonium chloride and washed with ammonium chloride, water and sat. NH_4Cl solution. The solvents were removed on the rotavap and the crude was purified on column chromatography using DCM/hexane (1:8, v/v). The cubane-porphryin was obtained in 8% yield as a purple solid (6 mg, 0.008 mmol). M.p.: decomposition at 60 °C. R_f = 0.14 (hexane/DCM, 1:2, v/v). ^{1}H NMR (400 MHz, Acetone): δ= 9.46 (d, *J* = 5.0 Hz, 2H, H_β), 9.42 (d, *J* = 5.1 Hz, 2H, H_β), 9.24 (d, *J* = 5.0 Hz, 2H, H_β), 8.68 (d, *J* = 5.0 Hz, 2H, H_β), 7.99 (d, *J* = 6.3 Hz, 2H, phenyl-*H*), 7.76 (m, 3H, phenyl-*H*), 4.90 – 4.87 (m, 3H, cubane-*H*), 4.63 – 4.57 (m, 4H, hexyl-CH_2), 4.56 – 4.53 (m,

3H, cubane-*H*), 3.77 (s, 3H, OC*H*$_3$), 2.28 (m, 4H, hexyl-C*H*$_2$), 1.63 (m, 4H, hexyl-C*H*$_2$), 1.41 (m, 4H, hexyl-C*H*$_2$), 1.31 (m, 4H, hexyl-C*H*$_2$) and 0.86 ppm (t, J = 7.2 Hz, 6H, hexyl-C*H*$_3$). ^{13}C NMR (100 MHz, acetone, 25 °C): δ = 143.7, 143.7, 013.1, 141.9, 138.4, 134.6, 133.3, 131.3, 131.2, 129.0, 128.1, 120.0, 52.1, 48.8, 48.6, 38.8, 34.8, 32.8, 23.6 and 14.6 ppm; UV/Vis (DCM): λ_{max} (log ε) = 415 (5.47), 531 nm (4.33).

[5-(4-Cubanyl-1-methylcarboxylate)-10,15,20-tri(4-methylphenyl)porphyrinato]nickel(II) 3.44c

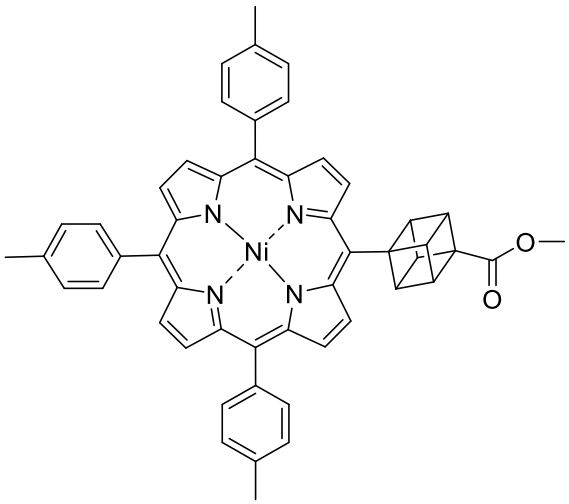

Porphyrin **3.36c** (76 mg, 0.1 mmol, 1eq.) was dissolved in 3ml dry THF and cooled to -40 °C. *i*PrMgCl*LiCl solution 0.11 mL (0.9 eq., 0.13 mmol, 0.8M.) were added dropwise. The reaction was stirred for 3.5 h. Since all the starting material was gone the cooling bath was removed. After warming to rt 0.1 mL $ZnCl_2$ solution (1.0 M in THF, 1 eq.) was added and the reaction was stirred for 30 min at rt. Meanwhile the cubane ester **3.43** (49 mg, 0.1 mmol, 1eq.), $NiCl_2$ (4.4 mg, 0.02 mmol, 0.2 eq.) and dtbppy (11 mg, 0.04 mmol, 0.4 eq.) were dissolved in 1.4 mL fry DMF. The porphryin solution was added to the cubane solution all at once and the reaction was stirred for 16 h at rt. The reaction mixture was quenched with a sat. solution of ammonium chloride and washed with ammonium chloride, water and sat. NH_4Cl solution. The solvents were removed on the rotavap and the crude was purified on column chromatography using DCM/hexane (1:2, v/v) the solvent mixture was slowly increased to DCM/hexane (1:1, v/v) and DCM+5% MeOH. The cubane-porphryin was obtained in 6% yield as a purple solid (5 mg, 0.006 mmol). M.p.: 165-167 °C. R_f = 0.15 (hexane/DCM 1:2, v/v). ^{1}H NMR (400 MHz, $CDCl_3$): δ = 9.06 (d, *J* = 4.9 Hz, 2H, H_β), 8.82 (d, *J* = 4.9 Hz, 2H, H_β), 8.72 (s, 4H, H_β), 7.91 – 7.84 (m, 6H, tolyl-C*H*), 7.48 (m, 6H, tolyl-C*H*), 4.82 – 4.76 (m, 3H, cubane-*H*), 4.55 – 4.50 (m, 3H, cubane-*H*), 3.80 (s, 3H, OCH_3), 2.65 (s, 6H, tolyl-CH_3) and 2.64ppm (s, 3H, tolyl-CH_3). ^{13}C NMR (100 MHz, $CDCl_3$, 25 °C): *δ* = 171.9, 143.4, 143.2, 143.0, 138.1, 138.0, 137.9, 137.6, 137.6, 133.8, 133.7, 132.9, 132.6, 132.4, 127.8, 127.7, 127.3, 126.9, 119.6, 119.4, 56.6, 56.2. 51.9, 47.9, 47.8, 29.9 and 21.6 ppm. UV/Vis (DCM): λ_{max} (log *ε*) = 415 (5.83), 527nm (4.69).

[5-(4-Cubanyl-1-methylcarboxylate)-10,20-bis(4-methylphenyl)-15-phenylporphyrinato]nickel(II) 3.44d

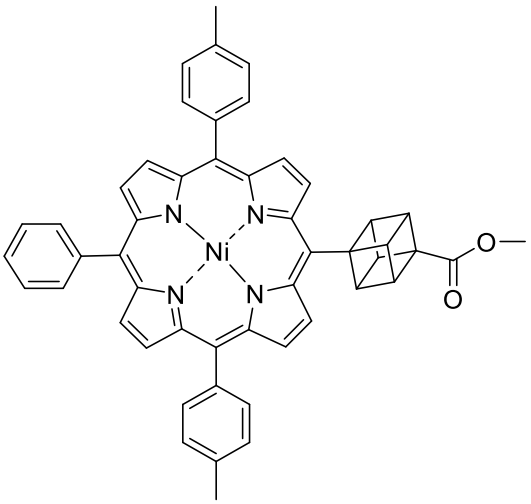

Porphyrin **3.36d** (75 mg, 1 mmol, 1 eq.) was dissolved in 2 mL dry THF and cooled to -40 °C. *i*PrMgCl*LiCl solution 0.19 mL (1.1 eq., 0.11 mmol, 0.6M.) were added dropwise. The reaction was stirred for 3 h. 0.11 mL $ZnCl_2$ solution (1.0 M in THF, 1.1 eq.) was cooled down and added the dropwise to the reaction. The reaction was stirred at for 1h. Meanwhile the cubane ester **3.43** (49 mg, 0.1 mmol, 1 eq.), $NiCl_2$ (4.4 mg, 0.02 mmol, 0.2 eq.) and dtbppy (11 mg, 0.04 mmol, 0.4 eq.) were dissolved in 1.4 mL fry DMF. The porphyrin solution was added to the cubane solution at -40 °C in one step and the reaction was stirred at -40 °C for 23.5 h. The reaction mixture was quenched with a sat. solution of ammonium chloride and washed with ammonium chloride, water and sat. NH_4Cl solution. The solvents were removed on the rotavap and the crude was purified on column chromatography using DCM/hexane (1:2,v/v/) the solvent mixture was slowly increased to DCM/hexane (2:1, v/v). The cubane-porphyrin was obtained in 11.5% yield as a purple solid (9 mg, 0.011 mmol). M.p.: 272-274 °C. R_f = 0.15 (hexane/DCM, 1:2, v/v). ^{1}H NMR (400 MHz, $CDCl_3$): δ = 9.06 (d, *J* = 4.9 Hz, 2H, H_β), 8.82 (d, *J* = 4.9 Hz, 2H, H_β), 8.74 (d, *J* = 5.0 Hz, 2H, H_β), 8.69 (d, *J* = 5.0 Hz, 2H, H_β), 7.99 (d, *J* = 6.5 Hz, 2H, phenyl-*H*), 7.88 (d, *J* = 7.5 Hz, 3H, phenyl-*H*), 7.68 (m, 4H, tolyl-*H*), 7.49 (d, *J* = 7.7 Hz, 4H, tolyl-*H*), 4.81 – 4.78 (m, 3H, cubane-*H*), 4.54 – 4.51 (m, 3H, cubane-*H*), 3.80 (s, 3H, OCH_3) and 2.65 ppm (s, 6H, tolyl-CH_3). ^{13}C NMR (100 MHz, $CDCl_3$, 25 °C): *δ* = 172.0, 171.9, 143.2, 143.2, 143.0, 141.0, 138.1, 137.9, 137.7, 233.8, 132.9, 132.7, 132.3, 127.9, 127.8, 127.4, 127.0, 127.0, 119.8, 119.2, 67.0, 56.6, 56.2, 21.9, 47.9, 47.8, 29.9 and 21.6 ppm. UV/Vis (DCM): λ_{max} (log *ε*) = 414 (5.56), 527 nm (4.42).

[5-(isopropyl)-10,20-bis-(4-methylphenyl)-15-phenylporphyrinato]nickel(II)

S3.2

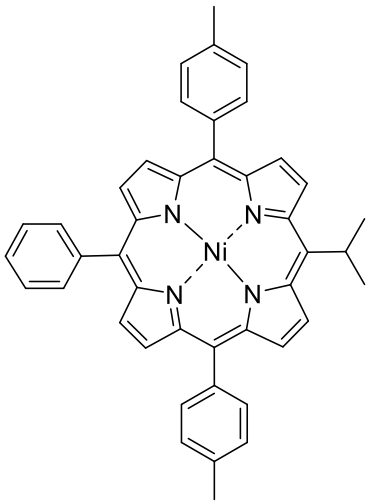

This compound was obtained as a side product in reaction of 4.3.10 and was obtained as a purple solid in a yield of 11% (18 mg, 0.027 mmol). M.p.: >300 °C. R_f = 0.18 (hexane/DCM, 1:1, v/v). ^{1}H NMR (400 MHz, $CDCl_3$): δ= 9.39 (d, *J* = 5.1 Hz, 2H, H_β), 8.79 (d, *J* = 5.1 Hz, 2H, H_β), 8.67 (q, *J* = 4.9 Hz, 4H, H_β), 7.98 – 7.95 (m, 2H, phenyl-*H*), 7.86 (d, *J* = 7.9 Hz, 3H, phenyl-*H*), 7.66 (m, 4H, tolyl-*H*), 7.47 (d, *J* = 7.8 Hz, 4H, tolyl-*H*), 2.64 (s, 3H, tolyl-CH_3) and 2.24 ppm (d, *J* = 7.3 Hz, 6H, isopropyl-*H*). ^{13}C NMR (100 MHz, $CDCl_3$, 25 °C): *δ* =142.2, 142.1, 141.3, 141.2, 140.8, 137.9, 137.5, 133.9, 133.7, 133.7, 132.7, 132.3, 132.2, 130.5, 127.8, 127.0, 123.7, 118.3, 118.2, 34.7, 28.3 and 21.6 ppm. UV/Vis (DCM): λ_{max} (log *ε*) = 418 (5.58), 534 nm (4.41). HRMS (MALDI) *m/z* calcd. for $C_{43}H_{34}N_4Ni$ $[M]^+$: 664.2137, 664.2149 found.

6.4 Chapter 4: Porphyrins as functional building blocks and interactions of porphyrin systems with nanomaterials

Compound **4.1**,[210a, 209] **4.4a**[280], **4.4b**,[280] **4.4c**[281], **4.13**[2] and **4.15**[149] were prepared according to literature procedure

[5,10,15,20-Tetrakis(3'-carboxymethyl)phenylporphyrinato]nickel(II) 4.2.

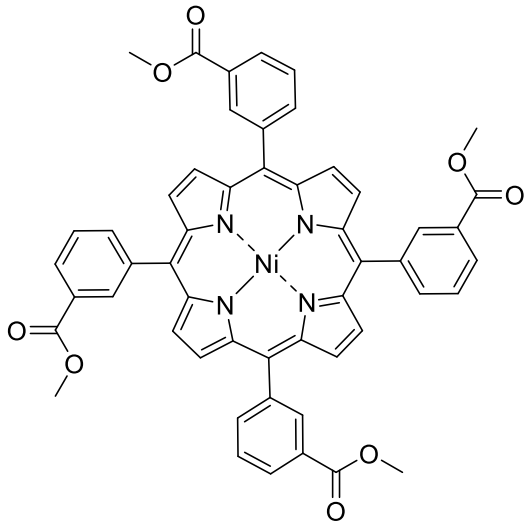

The free base porphyrin **4.1** (260 mg, 0.31 mmol) was reacted with nickel(II) acetate (197 mg, 0.77 mmol) in toluene (30 mL) for 18 h at 120 °C and the crude product purified *via* column chromatography on silica gel (DCM/MeOH, 9:1, v/v) followed by recrystallisation from DCM/MeOH. Yield: 260 mg (0.29 mmol, 94%) of red crystals. Mp.: >300 °C. R_f: 0.61 (DCM/hexane/MeOH, 1:1:0.05, v/v/v, silica gel, 6×3 cm). ^{1}H NMR (400 MHz, $CDCl_3$): δ = 8.67-8.71 (m, 12H, Ar-*H*, H_β), 8.39 (d, *J* = 7.6 Hz, 4H, Ar-*H*), 8.19 (d, *J* = 7.6 Hz, 4H, Ar-*H*), 7.76 (t, *J* = 7.6 Hz, 4H, Ar-*H*) and 3.95 ppm (s, 12H, C*H*$_3$). ^{13}C NMR (100 MHz, $CDCl_3$): δ = 167.1, 142.8, 141.0, 137.6, 134.2, 132.3, 129.2, 129.0, 127.1, 118.1 and 52.3 ppm. UV/vis (DCM) λ_{max} (log ε) = 414 (5.1), 527 nm (4.14). MS (MALDI) *m/z* (%): 902 (30) [M^+], 842 (36) [$M^+ - C_2H_3O_2$], 783 (52) [$M^+ - C_4H_6O_4$], 708 (100) ($M^+ - C_{10}H_{10}O_4$), 648 (80) ($M^+ - C_{12}H_{13}O_6$), 514 (24) [$M^+ - C_{20}H_{20}O_8$). HRMS (EI) *m/z calc. for* $C_{52}H_{36}N_4O_8Ni$ (M^+): 902.1887; found 902.1901.

[5,10,15,20-Tetrakis(3'-carboxy)phenylporphyrinato]nickel(II) 4.3.

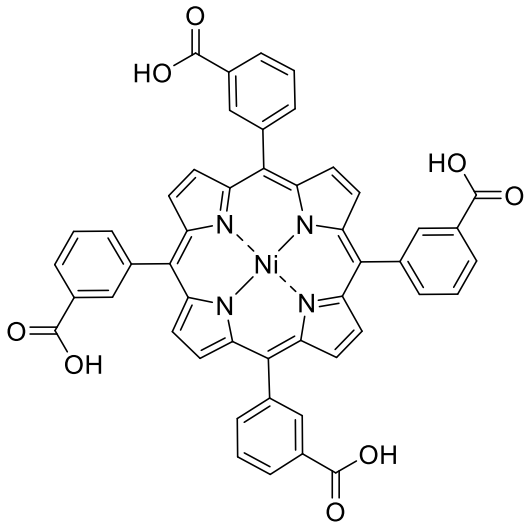

Compound **4.2** (250 mg, 0.28 mmol) in THF/MeOH (100 mL, 1:1, v/v) was heated to 60 °C, followed by reaction with KOH (6.2 g, 111.80 mmol) at 66 °C for 3 days in the absence of light. The reaction was cooled to rt and acidified to pH 4 using 1M HCl. The organic layer was extracted using DCM and dried over Na_2SO_4, filtered and solvent removed under *in vacuo*. The residue was suspended in *n*-hexane and filtered. Yield: 190 mg (0.22 mmol, 81%) of a red solid. Mp.: >300 °C. R_f: 0.25 (DCM/hexane/MeOH, 1:1:0.1, v/v/v, silica gel, 6×3 cm). ^{1}H NMR (400 MHz, $CDCl_3$/pyridine-d^5, 30:1): δ = 8.77-8.75 (m, 12H, Ar-*H*, *H*$_\beta$), 8.45 (d, *J* = 7.6 Hz, 4H, Ar-*H*), 8.13 (d, *J* = 7.6 Hz, 4H, Ar-*H*) and 7.73 ppm (t, *J* = 7.6 Hz, 4H, Ar-*H*). ^{13}C NMR (100 MHz, $CDCl_3$): δ = 169.3, 143.9, 140.7, 137.4, 134.7, 133.6, 130.7, 129.2, 126.9 and 118.6 ppm. UV/vis (DCM/MeOH, 99:1) λ_{max} (log ε) = 411 (5.29), 525 (4.08), 557 nm (3.10). MS (MALDI) *m/z* (%): 846 (16) [M^+], 800 (47) [M^+ –CHO_2], 726 (36) [M^+ – $C_7H_5O_2$], 680 (100) [M^+ – $C_8H_6O_4$], 634 (49) [M^+ – $C_9H_7O_6$], 514 (21) [M^+ – $C_{16}H_{12}O_8$]. HRMS (MALDI) *m/z* calcd. for $C_{48}H_{28}N_4O_8Ni$ (M^+): 846.1461; found 846.1274.

5,15-Bis(3,5-di-*tert*-butyl)-10,20-bis(3'-carboxyethyl)phenyl-phenylporphyrin 4.5b.

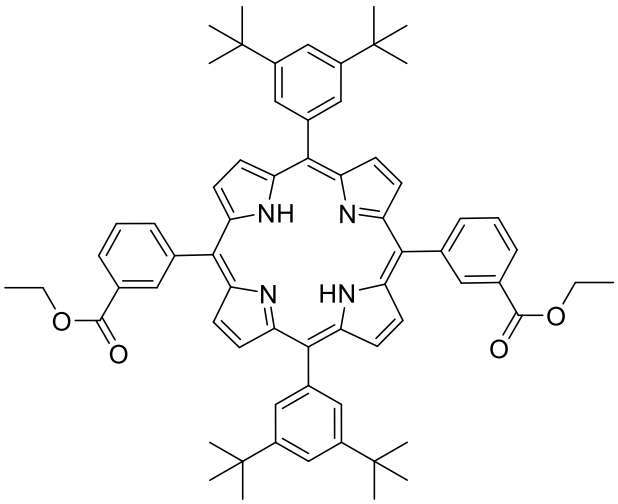

Reaction of 5,15-Dibromo-10,20-bis(3,5-di-*tert*-butyl)phenylporphyrin **4.4b** (200 mg, 0.24 mmol), K_3PO_4 (502 mg, 2.37 mmol), $Pd(PPh_3)_4$ (55 mg, 0.05 mmol) and ethyl 3-(4,4,5,5-tetraethyl-1,3,2-dioxaborolan- 2-yl)benzoate (654 mg, 2.37 mmol) following the procedure given for **5.5a** gave 180 mg (0.18 mmol, 78%) of purple crystals. Mp.: >300 °C. R_f: 0.29 (DCM/hexane, 1:1, v/v, silica gel, 6×3 cm). ^{1}H NMR (400 MHz, $CDCl_3$): δ = 8.66 (d, J = 4.6 Hz, 4H, H_β), 8.69 (m, 2H, Ar-*H*), 8.66 (d, J = 4.6 Hz, 4H, H_β), 8.38 (d, J = 7.3 Hz, 2H, Ar-*H*), 8.20 (d, J = 7.3 Hz, 2H, Ar-*H*), 7.86-7.87 (m, 4H, Ar-*H*), 7.71-7.77 (m, 4H, Ar-*H*), 4.41 (q, J = 7.2 Hz, 4H, CH_2), 1.46 (s, 36H, $H_{t\text{Bu}}$), 1.38 (t, J = 7.2 Hz, 6H, CH_3) and –2.73 ppm (s, 2H, N*H*). ^{13}C NMR(100 MHz, $CDCl_3$): δ = 166.8, 148.8, 142.6, 140.9, 138.2, 134.7, 131.5, 129.9, 129.1, 128.9, 128.2, 126.7, 123.4, 121.8, 121.1, 118.6, 61.2, 35.0, 31.7 and 14.3 ppm. UV/vis (DCM) λ_{max} (log ε) = 420 (5.62), 517 (4.10), 553 (3.66), 593 (3.48), 647 nm (3.55). MS (MALDI) *m/z* (%): 982 (83) [M^+], 954 (100) [$M^+ - C_2H_5$], 895 (40) [$M^+ - C_6H_{14}$], 853 (17) [$M^+ - C_7H_{14}O_2$]. HRMS (MALDI) *m/z* calcd. for $C_{60}H_{70}N_4O_4$ (M^+): 982.5397; found 982.5369.

5,15-Bis(3,5-di-*tert*-butyl)phenyl-10-(3'-Carboxymethyl)phenylporphyrin 4.5c.

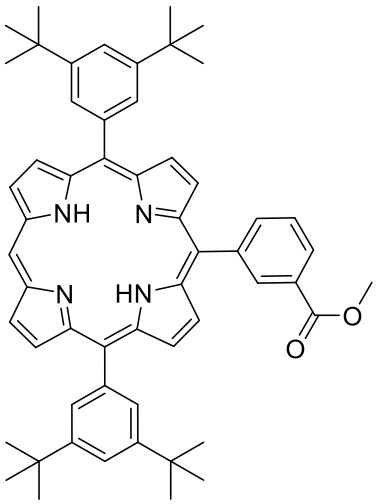

5-Bromo-10,20-bis(3,5-di-*tert*-butyl)phenylporphyrin **4.4b** (300 mg, 0.39 mmol) was dissolved in THF (20 mL). The solution was then degased *via* three freeze-pump-thaw cycle and the flask was purged with argon. 3-Methoxycarbonyl-phenylboronic acid (282 mg, 1.57 mmol), $Pd(PPh_3)_4$ (68 mg, 0.06 mmol) and K_3PO_4 (831 mg, 3.92 mmol) were added. The mixture was stirred at 66 °C for 16 h. The solvent was removed *in vacuo* and the crude product was washed with $NaCO_3$ and H_2O. The solvent was removed and the residue was dissolved in DCM and filtered through silica gel. The porphyrin was purified with column chromatography using DCM/petroleum ether (1:1). The target was obtained in 90% yield (291 mg, 0.35 mmol) after recrystallisation from DCM: MeOH as a purple solid. Mp.: >300 °C. R_f: 0.39 (DCM/hexane = 1:1 + 1 drop MeOH, v/v). ^{1}H NMR (400MHz, $CDCl_3$): δ = 10.24 (s, 1H, H_{meso}), 9.35 (d, J = 4.6 Hz, 2H, H_β), 9.08 (d, J = 4.6 Hz, 2H, H_β), 8.96 (d, J = 4.7 Hz, 2H, H_β), 8.90 (s, 1H, Ar-*H*), 8.78 (d, J = 4.8 Hz, 2H, H_β), 8.48 (d, J = 7.9 Hz, 1H, H_β), 8.40 (d, J = 7.5 Hz, 1H, Ar-*H*), 8.21 (d, J = 1.7 Hz, 4H, Ar-*H*), 7.85 (s, 1H, Ar-*H*), 7.82 (m, 6H, Ar-*H*), 3.97 (s, 3H, OCH_3), 1.55 (s, 30H, $H_{t\text{Bu}}$), 1.53 (s, 6H, $H_{t\text{Bu}}$) and –2.93 ppm (s, 2H, N*H*). ^{13}C NMR (150 MHz, $CDCl_3$): δ = 148.8, 143.0, 142.5, 140.5, 138.1, 134.5, 132.2, 131.5, 131.0, 129.9, 128.8, 128.5, 126.5, 126.0, 121.0, 120.9, 118.4, 105.0, 104.7, 99.8, 52.2, 34.9, 31.9, 31.6 and 29.5 ppm. UV/vis (DCM): λ_{max} (log ε) = 415 (5.69), 511 (4.28), 545 (3.85), 584 (3.77), 639 nm (3.49). HRMS (MALDI) *m/z* calcd. for $C_{56}H_{60}N_4O_2$ (M^+): 820.4716; found 820.4742.

5-(3'-Carboxymethyl)phenyl-10,20-diphenylporphyrin 4.5d.

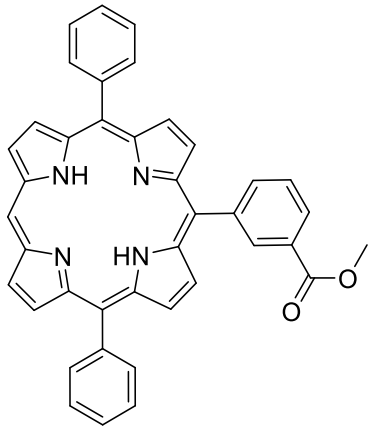

5-Bromo-10,20-di(phenyl)porphyrin **4.4c** (300 mg, 0.55 mmol) was dissolved in THF (20 mL). The solution was degassed *via* freeze-pump-thaw cycles, before the flask was purged with argon. K_3PO_4 (1.175 g, 5.54 mmol), $Pd(PPh_3)_4$ (96 mg, 0.08 mmol) and 3-methoxycarbonylphenyl-boronic acid (399 mg, 2.22 mmol) were added. The reaction was stirred for 16 h at 66 °C. The end of the reaction was monitored by TLC. The solvent was removed *in vacuo*. The residue was washed with a saturated $NaHCO_3$ solution and water. The solvent was removed *in vacuo* and the residue recrystallised using DCM/MeOH yielding purple crystals (260 mg, 78%, 0.43 mmol). Mp.: >300 °C. R_f: 0.12 (DCM/hexane = 1:1 + 2 drops MeOH, v/v). ^{1}H NMR (400 MHz, $CDCl_3$): δ = 10.25 (s, 1H, H_{meso}), 9.36 (d, J = 4.6 Hz, 2H, H_β), 9.03 (d, J = 4.5 Hz, 2H, H_β), 8.90 (d, J = 4.8 Hz, 2H, H_β), 8.88 (s, 1H, Ar-*H*), 8.77 (d, J = 4.7 Hz, 2H, H_β), 8.38 (d, J = 7.5 Hz, 1H, Ar-*H*), 8.23 (d, J = 7.6 Hz, 1H, Ar-*H*), 7.83 (d, J = 7.8 Hz, 1H, Ar-*H*), 7.74-7.81 (m, 6H, Ph-*H*), 3.96 (s, 3H, OCH_3) and –3.02 ppm (s, 2H, N*H*). ^{13}C NMR (150 MHz, $CDCl_3$): δ = 167.5 143.1, 141.8, 138.6, 134.9, 134.8, 131.2, 129.2, 128.9, 127.9, 127.0, 126.9, 120.0, 119.1, 105.2 and 52.5 ppm. UV/vis (DCM): λ_{max} (log ε) = 412 (5.44), 509 (4.09), 543 (3.55), 582 (3.58), 651 nm (3.25). HRMS (MALDI) *m/z* calcd. for $C_{40}H_{28}N_4O_2$ (M^+): 596.2212 found 596.2223.

5-Bromo-15-(3'-carboxymethyl)phenyl-10,20-diphenylporphyrin 4.6c).

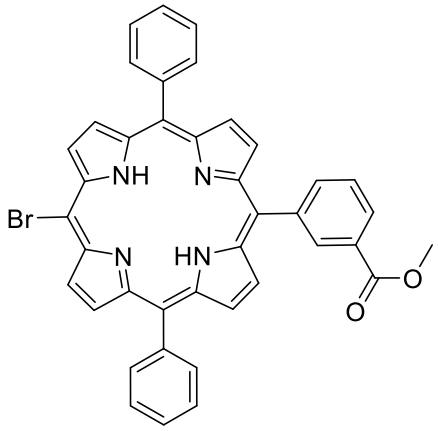

5-(3'-Carboxymethyl)phenyl-10,20-diphenylporphyrin **4.5d** (450 mg, 0,75 mmol) was dissolved in $CHCl_3$ (200 mL). NBS (201 mg, 1.13 mmol) and pyridine (0.15 mL) were added. The mixture was cooled in an ice bath and stirred for 1 h. The solvent was removed *in vacuo* after completion and the residue was filtered through silica gel using DCM. The solvent was evaporated and the desired porphyrin was obtained as a purple solid in 94% yield (478 mg, 0.71 mmol). Mp.: >300 °C. R_f: 0.35 (DCM/hexane, 1:1 + 2 drops MeOH, v/v). ^{1}H NMR (400 MHz, $CDCl_3$): δ = 9.68 (d, J = 4.3 Hz, 2H, H_β), 8.91 (d, J = 4.3 Hz, 2H, H_β), 8.80 (d, J = 4.3 Hz, 2H, H_β), 8.85 (s, 1H, Ar-*H*), 8.72 (d, J = 3.0 Hz, 2H, H_β), 8.46 (d, J = 8.3 Hz, 1H, Ar-*H*), 8.35 (d, J = 6.1 Hz, 1H, Ar-*H*), 8.19 (d, J = 6.6 Hz, 4H, Ph-*H*), 7.83 (s, 1H, Ar-*H*), 7.77 (d, J = 6.6 Hz, 6H, Ph-*H*), 2.82 (s, 3H, OCH_3) and –2.75 ppm (s, 2H, N*H*). ^{13}C NMR (150 MHz, $CDCl_3$): δ = 167.1, 142.0, 141.5, 138.2, 134.6, 134.4, 129.0, 128.8, 127.8, 126.8, 126.6, 120.8, 119.2, 103.1 and 52.2 ppm. UV/vis (DCM): λ_{max} (log ε) = 420 (5.53), 518 (4.16), 553 (3.87), 595 (3.65), 651 nm (3.59). HRMS (MALDI) *m*/*z* calcd. for $C_{40}H_{27}N_4O_2Br$ (M^+): 674.1317; found 674.1351.

5-(3'-Carboxymethyl)phenyl-10,20-diphenyl-15-(trimethylsilyl)ethynyl)porphyrin 4.6d.

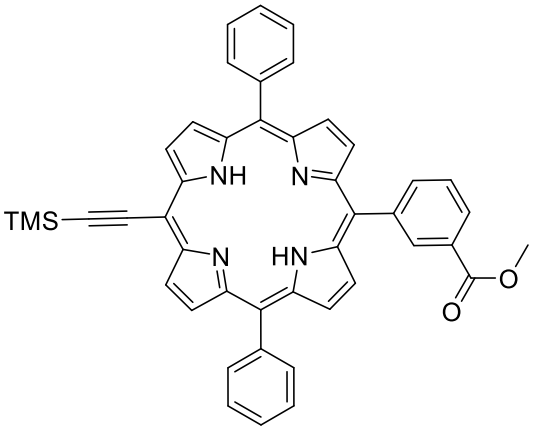

5-Bromo-15-(3'-carboxymethyl)phenyl-10,20-diphenylporphyrin **4.6c** (200 mg, 0.30 mmol) was dissolved in THF (20 mL) The solution was degassed *via* three freeze-pump-thaw cycles, before the flask was purged with argon. $PdCl_2(PPh_3)_2$ (31.2 mg, 0.04 mmol), CuI (11.3 mg, 0.06 mmol) and trimethylsilylacetylene (1.4 mL, 0.02 mmol) were added. The reaction was stirred at 45 °C for 16 h and the solvent removed *in vacuo*. The residue was dissolved in DCM and filtered through silica gel. After evaporation of the solvent the residue was again filtered through silica gel with DCM/petroleum ether (1:1, v/v). Following this the product was eluted from the silica gel with DCM and the solvent was evaporated. The crude product was purified by recrystallisation from DCM/MeOH giving porphyrin **4.6d** as a purple solid in 127 mg (62%, 0.18 mmol). Mp.: >300 °C. R_f: 0.26 (DCM/hexane = 1:1+ 2 drops MeOH, v/v). ^{1}H NMR (400 MHz, $CDCl_3$): δ = 9.67 (d, J = 4.7 Hz, 2H, H_β), 8.90 (d, J = 4.7 Hz, 2H, H_β), 8.85 (s, 1H, Ar-*H*), 8.77 (d, J = 4.7 Hz, 2H, H_β), 8.69 (d, J = 4.7 Hz, 2H, H_β), 8.47 (d, J = 7.9 Hz, 1H, Ar-*H*), 8.35 (d, J = 7.6 Hz, 1H, Ar-*H*), 8.19 (d, J = 7.7 Hz, 4H, Ph-*H*), 7.83 (d, J = 7.8 Hz, 1H, Ar-*H*), 7.73-7.81 (m, 6H, Ph-*H*), 3.98 (s, 3H, OCH_3), 0.61 (s, 9H, TMS-CH_3) and –2.43 ppm (s, 2H, N*H*). ^{13}C NMR (150 MHz, $CDCl_3$): δ = 168.0, 142.3, 139.1, 139.0, 135.4, 135.2, 129.9, 128.6, 127.5 and 53.1 ppm. UV/vis (DCM): λ_{max} (log ε) = 428 (5.66), 527 (4.25), 565 (4.35), 604 (3.83), 661 nm (3.96). HRMS (MALDI) m/z calcd. for $C_{45}H_{36}N_4O_2Si$ (M^+): 692.2608; found 629.2635.

5-(3'-Carboxymethyl)phenyl-10,20-diphenyl-15-(ethynyl)porphyrin 4.6e.

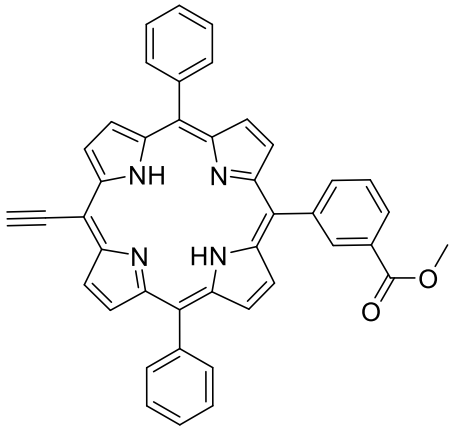

5-(3'-Carboxymethyl)phenyl-10,20-diphenyl-15-(trimethylsilyl)ethynyl)porphyrin **4.6d** (90 mg, 0.13 mmol) was dissolved in DCM and TBAF (1 mL) was added. The mixture was stirred and the reaction was monitored by TLC. Upon completion, the product was filtered through silica gel using DCM and the solvent was removed *in vacuo* yielding the target compound as a purple/red solid in quantitative yield (80 mg, 0.13 mmol). Mp.: >300 °C. R_f: 0.24 (DCM/hexane =1:1 + 2 drops MeOH, v/v). ^{1}H NMR (400 MHz, $CDCl_3$): δ = 9.70 (d, *J* = 4.7 Hz, 2H, H_β), 8.92 (d, *J* = 4.4 Hz, 2H, H_β), 8.85 (s, 1H, Ar-*H*), 8.78 (d, *J* = 4.4 Hz, 2H, H_β), 8.70 (d, *J* = 4.6 Hz, 2H, H_β), 8.47 (d, *J* = 8.2 Hz, 1H, Ar-*H*), 8.36 (d, *J* = 7.3 Hz, 1H, Ar-*H*), 8.20 (d, *J* = 6.9 Hz, 4H, Ph-*H*), 7.84 (d, *J* = 7.6 Hz, 1H, Ar-*H*), 7.79 (m, 6H, Ph-*H*), 4.20 (s, 1H, ethynyl-*H*), 3.98 (s, 3H, OCH_3) and –2.49 ppm (s, 2H, N*H*). ^{13}C NMR (150 MHz, $CDCl_3$): δ = 167.4, 142.4, 141.7, 138.4, 135.1, 134.8, 134.6, 129.3, 128.5, 128.1, 127.0, 122.5, 121.3, 98.1, 89.8, 85.7, 84.8, 84.3 and 52.5 ppm. UV/vis (DCM): λ_{max}(log ε) = 425 (5.82), 524 (4.48), 560 (4.40), 600 (4.06), 657 nm (4.05). HRMS (MALDI) *m*/*z* calcd. for $C_{42}H_{28}N_4O_2$ (M^+): 620.2212; found 620.2181.

5,5-(1,2-Ethyndiyl)-bis[15-(3'-carboxymethyl)phenyl-10,20-diphenylporphyrin] 4.6f.

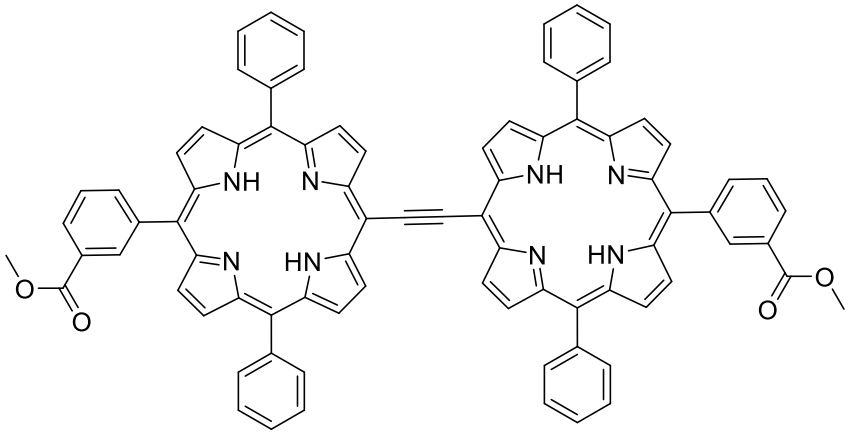

A Schlenk tube was purged with argon and charged with compound 5-(3'-Carboxymethyl)phenyl-15-(ethynyl)-10,20-diphenylporphyrin **4.6d** (62 mg, 0.10 mmol in 12 mL THF) followed by addition of 5-Bromo-15-(3'-carboxymethyl)phenyl-10,20-diphenylporphyrin (67.5 mg, 0.10 mmol), TEA (5 mL), $AsPh_3$ (34 mg, 0.11 mmol) and $Pd_2(dba)_3$ (9 mg, 0.01 mmol). The reaction mixture was stirred at 66 °C for 16 h. The solvent was removed *in vacuo* and the residue was filtered through silica gel. DCM/petroleum ether (1:1, v/v) was used to remove impurities and then the product was eluted with DCM. The crude product was purified by recrystallisation from DCM:MeOH and **6f** was obtained as purple solid in 50% yield (60 mg, 0.05 mmol). Mp.: >300 °C. R_f: 0.23 (DCM). ^{1}H NMR (400 MHz, $CDCl_3$): δ = 10.35 (d, J = 4.6 Hz, 4H, H_β), 9.10 (d, J = 4.5 Hz, 4H, H_β), 8.90 (s, 2H, Ar-*H*), 8.83 (d, J = 4.6 Hz, 4H, H_β), 8.73 (d, J = 4.6 Hz, 4H, H_β), 8.50 (d, J = 7.8 Hz, 2H, Ar-*H*), 8.40 (d, J = 7.2 Hz, 2H, Ar-*H*), 8.29 (d, J = 7.3 Hz, 8H, Ph-*H*), 7.87 (d, J = 7.7 Hz, 2H, Ar-*H*), 7.82 (d, J = 5.5 Hz, 12H, Ph-*H*), 4.00 (s, 6H, OCH_3) and –2.01 ppm (s, 4H, N*H*). ^{13}C NMR (150 MHz, $CDCl_3$): δ = 167.4, 142.4, 141.8, 138.5, 134.9, 134.7, 129.4, 129.1, 128.1, 127.1, 127.0, 121.9, 120.6, 112.0 and 52.5 ppm. UV/vis (DCM): λ_{max} (log ε) = 406 (5.26), 441 (5.18), 473 (5.47), 520 (4.54), 619 (4.69), 713 nm (4.77); HRMS (MALDI) *m/z* calcd. for $C_{82}H_{54}N_8O_4$ (M^+): 1214.4268; found 1214.4248.

[5,15-Dibromo-10,20-diphenylporphyrinato]palladium(II) 4.9

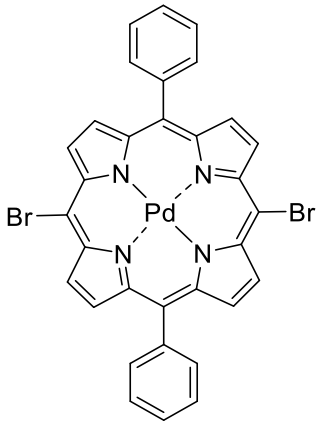

Porphyrin **4.8** (100 mg, 0.16 mmol, 1 eq.) was dissolved in 16 mL $CHCl_3$. 181 mg $Pd(OAc)_2$ (0.8 mmol, 5eq.) was dissolved in 1.6 mL MeOH and added to the reaction which was stirred at rt for 18 h. The solvent was removed and the crude product was immediately filtered through silica using DCM, followed by a column with hexane/toluene (1:1, v/v). The final product was washed with MeOH and resulted in the desired porphyrin in 66% yield as dark purple crystals (77 mg, 0.106 mmol). Mp.: >300 °C. R_f = 0.57 (hexane/DCM, 2:1, v/v). ^{1}H NMR (400 MHz, $CDCl_3$): δ = 9.60 (d, *J* = 5.0 Hz, 4H, H_β), 8.81 (d, *J* = 5.0 Hz, 4H, H_β), 8.11 (d, *J* = 7.1 Hz, 4H, phenyl-*H*) and 7.79 – 7.74 ppm (m, 6H, phenyl-*H*). ^{13}C NMR (100 MHz, $CDCl_3$, 25 °C): δ = 142.5, 142.1, 134.7, 134.2, 132.8, 132.6, 128.3 and 127.0 ppm. UV/Vis (DCM): λ_{max} (log ε) = 420 (5.59), 530 (4.51), 562 nm (3.83). HRMS (MALDI) *m/z* calcd. for $C_{32}H_{18}Br_2N_4Pd$ $[M]^+$: 721.8933; found 721.8957.

(5,15-Diphenyl-10,20-bis-[(4-pyridyl)ethynyl]porphyrinato)palladium(II) 4.11

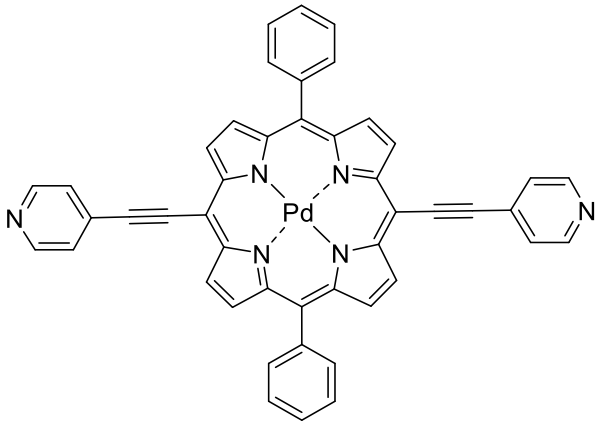

Porphyrin **4.10** (99 mg, 0.137 mmol, 1 eq), 4-ethynylpyridine (42 mg, 0.410 mmol, 3 eq.), $Pd(PPh_3)_4$ (25 mg, 0.022 mmol 0.16 eq.), CuI (4.2 mg, 0.022 mmol, 0.16 eq.) were dried for 3 h under vacuum. 100 mL dry THF and 6.8 mL TEA was added and three freeze-thaw cycles were done. The reaction was then heated to 75 °C for 1 h. The solvent was removed and the resulting solid was washed three times with MeOH. A column was then done with ALOX and DCM= 1% THF. A green fraction was isolated and further washed with sat. NH_4Cl solution, $NaHCO_3$ and $NaSO_4$ before recrystallisation from DCM/MeOH. The target compound was obtained in 52% as dark purple/green crystals (55 mg, 0.072 mmol). Mp.: >300 °C. R_f = 0.18 (DCM+1%, v/v). ^{1}H NMR (600 MHz, $CDCl_3$): δ = 9.51 (d, *J* = 4.6 Hz, 4H,H_β), 8.81 (m, 8H, $H_{\beta,}$ Pyr-*H*), 8.13 (d, *J* = 6.9 Hz, 4H, Phenyl-*H*) and 7.88 – 7.74 ppm (m, 10H, Pheny-*H*, Pyr-*H*). ^{13}C NMR (100 MHz, $CDCl_3$, 25 °C): δ = 150.3, 143.5, 142.0, 140.9, 134.2, 132.3, 130.3, 128.3, 127.1 and 125.6 ppm. UV/Vis (DCM): λ_{max} (log ε) 440 (5.68), 549 (4.32), 599 nm (4.79). HRMS (MALDI) *m/z* calcd. for $C_{46}H_{26}N_6Pd$ $[M]^+$: 768.1254; found 768.1280.

[5-(4-Ethynylphenyl)-10,20-diphenylporphyrinato]nickel(II) 4.16

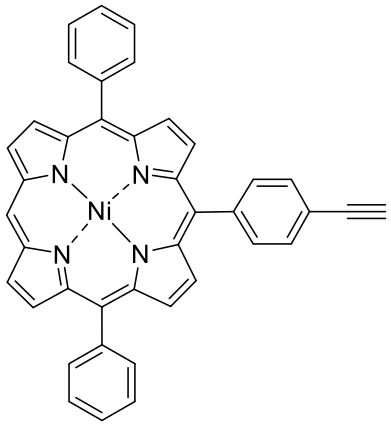

The free base 5-(4-ethynylphenyl)-10,20-diphenylporphyrin **4.15** (50 mg, 0.089 mmol, 1 eq.) and Ni(acac) (28 mg, 0.107 mmol, 1.2 eq.) were dissolved in toluene and heated to 120 °C for 2 h. The solvent was removed and the porphyrin was filtered through silica using DCM. The target compound was obtained as a purple solid in 47% yield (26 mg, 0.042 mmol). Mp.: > 300 °C. R_f = 0.28 (hexane/DCM, 1:2, v/v). ^{1}H NMR (400 MHz, $CDCl_3$): δ = 9.84 (s, 1H, H_{meso}), 9.14 (d, J = 4.8 Hz, 2H, H_β), 8.90 (d, J = 4.8 Hz, 2H, H_β), 8.80 (d, J = 4.9 Hz, 2H, H_β), 8.75 (d, J = 4.9 Hz, 2H, H_β), 8.04 (dd, J = 7.6, 1.6 Hz, 4H, phenyl-*H*), 7.99 (d, J = 8.1 Hz, 2H, phenyl-*H*), 7.82 (d, J = 8.1 Hz, 2H, phenyl-*H*), 7.74 – 7.64 (m, 6H, phenyl-*H*) and 3.28 ppm (s, 1H, C≡C*H*). ^{13}C NMR (100 MHz, $CDCl_3$, 25 °C): δ = 143.0, 142.9, 142.2, 141.9, 141.0, 133.9, 133.8, 132.8, 132.4, 131.9, 130.8, 127.9, 127.0, 121.8, 118.9, 118.5, 104.9, 83.8, 78.3, 32.1, 29.9 and 29.5 ppm. UV/Vis (DCM): λ_{max} (log ε) = 408 (5.42), 522 nm (4.27). HRMS (MALDI) *m/z* calcd. for $C_{40}H_{24}NiN_4$ [M^+]: 618.1354; found 618.1374.

[5,15-Diphenyl-10-(4-(trimethylsilyl)ethynylphenyl)porphyrinato]cobalt(II) 4.20

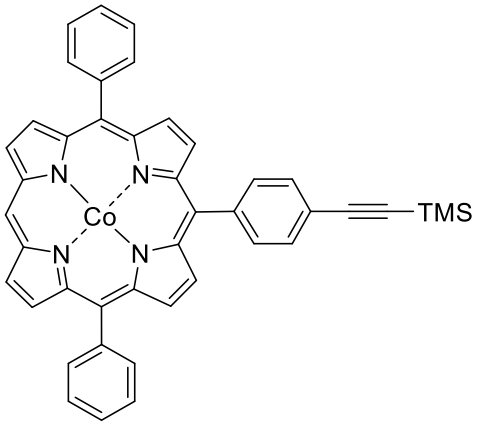

[5-Bromo-10,20-diphenylporphyrinato]cobalt **4.19** (50 mg, 0.077 mmol, 1 eq.) was dried together with $Pd(PPh_3)_4$ (20 mg, 0.017 mmol, 0.22 eq.), K_3PO_4 (164 mg,0.77 mmol, 10 eq.)and the 4-[(Trimethylsilyl)ethynyl]phenylboronic acid pinacol ester (47 mg, 0.157 mmol, 2 eq). The porphyrin was dissolved in 13 mL dry THF. Three freeze-thaw cycles were done and the reaction was stirred at 70 °C for 18 h. After an aqueous work up with $NaHCO_3$ and Na_2SO_4 the crude product was purified using column chromatography with hexane/ethyl acetate (7:1, v/v) as eluent. The target compound was obtained as a purple solid in 68% yield (37 mg, 0.053 mmol). Mp.: 134-135 °C. R_f = 0.22 (hexane/DCM, 1:1, v/v). UV/Vis (DCM): λ_{max} (log ε) 406 (5.22), 525 nm (4.04). HRMS (MALDI) *m/z* calcd. for $C_{43}H_{32}CoN_4Si$ $[M]^+$: 691.1728; found 691.1752.

[5-(4-Ethynylphenyl)-10,20-diphenylporphyrinato]cobalt(II) 4.17

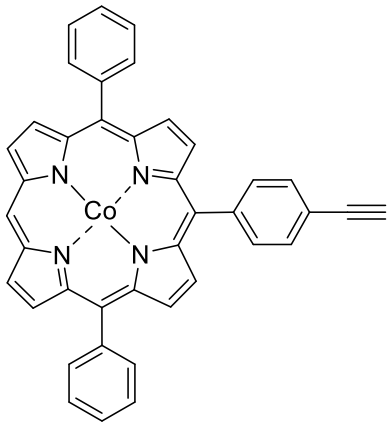

The next step involved a deprotection of the TMS group with TBAF. Therefore, 33 mg porphyrin **4.20** (0.048 mmol, 1 eq.) was dissolved in dry THF and TBAF (0.19 mL, 0.191 mmol, 1M, 4 eq) was added to the reaction. The reaction mixture was stirred until completion at rt. The crude mixture was then poured in H_2O and extracted with DCM. After an aqueous wash, 29 mg of the desired porphyrin (0.047 mmol, 98%) was obtained as a dark purple solid. Mp.: 79-80 °C. R_f = 0.42 (hexane/DCM, 1:1, v/v). UV/Vis (DCM): λ_{max} (log ε) 406 (4.80), 524 nm (3.71). HRMS (MALDI) *m/z* calcd. for $C_{40}H_{24}CoN_4$ $[M]^+$: 619.1333; found 619.1322.

6.5 Chapter 5: Large π-conjugated porphyrin systems

Compound **5.47** was synthesised according to literature.[282]

2,6-Bis(octyloxy)anthraquinone 5.35

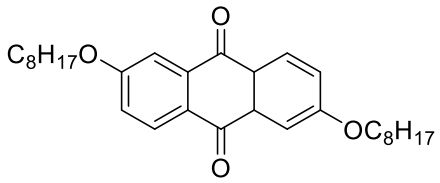

Anthraflavic acid **5.34** (1 g, 4.16 mmol, 1 eq.), 1-bromooctane (1.4 mL, 8.33 mmol, 2 eq.) and potassium carbonate (2.3 g, 16.64 mmol, 4 eq.) were dissolved in 40 mL DMF and heated to 45 °C for 45 h. The reaction was cooled down and the DMF was removed by bubbling N_2 at 90 °C through the solution in a fumehood. The crude product was dissolved in DCM and washed with H_2O purified by column chromatography using DCM/hexane (1:3, v/v). The target compound was obtained in 91% as a yellow solid (1.8 g, 3.8 mmol). Mp.: 104-105 °C. R_f = 0.21 (hexane/DCM, 1:1, v/v). ^{1}H NMR (400 MHz, $CDCl_3$): δ = 8.22 (d, *J* = 8.7 Hz, 2H, Ar-C*H*), 7.70 (d, *J* = 2.6 Hz, 2H, Ar-C*H*), 7.22 (d, *J* = 2.6 Hz, 1H, Ar-C*H*), 7.20 (d, *J* = 2.6 Hz, 1H, Ar-C*H*), 4.14 (t, *J* = 6.6 Hz, 4H, OCH_2), 1.89 – 1.79 (m, 4H, CH_2), 1.51-1.45 (m, 4H, CH_2), 1.40 – 1.27 (m, 16H, CH_2) and 0.89 ppm (t, *J* = 6.8 Hz, 6H, CH_3). ^{13}C NMR (100 MHz, $CDCl_3$, 25 °C): *δ* = 182.5, 164.2, 135.1, 129.8, 127.1, 121.0, 69.0, 32.0, 29.5, 29.4, 29.2, 26.1, 22.8 and 14.3 ppm. UV/Vis (DCM): λ_{max} (log *ε*) = 276 (4.78), 303 (4.55), 351 nm (4.16). HRMS (APCI) *m/z* calcd. for $C_{30}H_{41}O_4$ $[M+H]^+$: 465.3083; found 465.3000. IR (ATR): ṽ = 2920, 1852, 1661, 1629, 1584, 1461, 1313, 1200, 1078 cm^{-1}.

2,2',6,6'-Tetrakis(octyloxy)-9,9'-bisanthracene 5.36

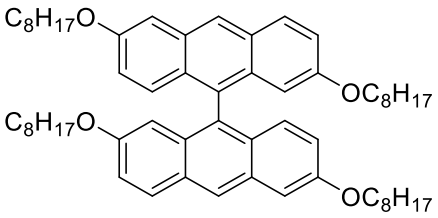

2,6-bis(octyloxy)anthraquinone **5.35** (1.5 g, 3.21 mmol, 2 eq.) was dissolved in 26 mL glacial acetic acid. Zinc (5.4 g, 83 mmol, 13 eq.) was added followed by conc HCl (18 mL) The reaction was stirred at rt for 5 min before being heated to 140 °C for 4 h. After this the reaction was cooled to rt and another 5.4 g of Zinc and 16 mL conc. HCl were added. The reaction was again stirred for 5 min at rt before being heated to 140 °C for another 4 h. The reaction was cooled down and the product was extracted with DCM. The solvent was removed and a column was done using hexane/DCM (3:1, v/v) as eluent. The product was percipitated from DCM/MeOH resulting in 743 mg (0.8567 mmol, 53%) of pure yellow product. Mp.: N.D due to oily consistency. R_f = 0.18 (hexane/DCM, 1:4, v/v). ^{1}H NMR (400 MHz, $CDCl_3$): δ = 8.40 (s, 2H, Ar-C*H*), 7.97 (d, *J* = 9.2 Hz, 2H, Ar-C*H*), 7.30 (s, 2H, Ar-C*H*), 7.17-7.13 (m, 2H, Ar-C*H*), 6.97 (d, *J* = 9.4 Hz, 2H, Ar-C*H*), 6.88-6.83 (m, 2H, Ar-C*H*), 6.31 (s, 2H, Ar-C*H*), 4.12 (t, *J* = 6.4 Hz, 4H, OCH_2), 3.45 (t, *J* = 6.3 Hz, 4H, OCH_2), 1.91 – 1.79 (m, 4H, CH_2), 1.59 – 1.14 (m, 44H, CH_2) and 0.89 ppm (m, 12H, CH_3). ^{13}C NMR (100 MHz, $CDCl_3$, 25 °C): *δ* = 156.1, 156.0, 131.4, 131.2, 129.6, 128.8, 128.5, 128.2, 125.0, 121.0, 120.6, 104.9, 104.0, 68.1, 67.6, 32.0, 31.9, 29.9, 29.6, 29.4, 29.3, 28.9, 26.4, 26.1, 22.8, 22.7, 14.3 and 14.2 ppm. UV/Vis (DCM): λ_{max} (log *ε*) = 271 (6.12), 316 (4.51), 330 (4.66), 348 (4.66), 397 (4.75), 419 nm (4.85). HRMS (MALDI) *m/z* calcd. for $C_{60}H_{82}O_4$ $[M]^+$: 866.6213; found 866.6196. IR (ATR): $\tilde{\nu}$ = 2922, 2854, 1628, 1460, 1198, 885, 804 cm^{-1}.

10-Bromo-2,2‘,6,6‘-tetrakis(octyloxy)-9,9‘-bisanthracene 5.38

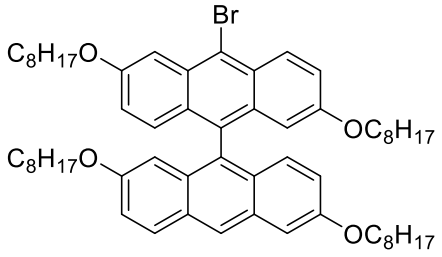

The bisanthracene **5.36** (255 mg, 0.294 mmol, 1 eq.) was dissolved in $CHCl_3$ and 1.3 eq. NBS (67 mg, 0.378 mmol) were added together with 0.5 mL pyridine. The reaction was stirred at 0 °C for 4 h. The reaction was quenched with aceton upon of consumption of all starting material. The solvent was removed and the crude product was purified by column chromatography using DCM/petroleum ether (1:2, v/v). Fraction 1 contained the dibrominated species and fraction 2 the monobrominated species. Recrystallisation from DCM/MeOH resulted in the precipitation of 230 mg of an yellow oil of the mono-brominated anthracene (0.243 mmol, 83%). Mp.: N.D.; oil. R_f = 0.34 (hexane/DCM, 1:4, v/v). ^{1}H NMR (600 MHz, $CDCl_3$) δ = 8.53 (d, *J* = 9.6 Hz, 1H, Ar-C*H*), 8.40 (s, 1H, Ar-C*H*), 7.96 (d, *J* = 9.2 Hz, 1H, Ar-C*H*), 7.79 (d, *J* = 2.3 Hz, 1H, Ar-C*H*), 7.28 (d, *J* = 2.3 Hz, 1H, Ar-C*H*), 7.25-7.23 (m, 1H, Ar-C*H*), 7.14-7.12 (m, 1H, Ar-C*H*), 6.94 (d, *J* = 9.4 Hz, 1H, Ar-C*H*), 6.87 (d, *J* = 9.5 Hz, 1H, Ar-C*H*), 6.83 (d, *J* = 2.3 Hz, 1H, Ar-C*H*), 6.80 (d, *J* = 2.3 Hz, 1H, Ar-C*H*), 6.27 (d, *J* = 2.3 Hz, 1H, Ar-C*H*), 6.23 (d, *J* = 2.1 Hz, 1H, Ar-C*H*), 4.18 (t, *J* = 6.5 Hz, 2H, OCH_2), 4.10 (t, *J* = 6.6 Hz, 2H, OCH_2), 3.49 (d, *J* = 5.5 Hz, 1H, OCH_2), 3.47 – 3.41 (m, 3H, OCH_2), 1.92 – 1.83 (m, 4H, CH_2), 1.55 – 0.98 (m, 44H, CH_2) and 0.93 – 0.80 ppm (m, 12H, CH_3). ^{13}C NMR (100 MHz, $CDCl_3$, 25 °C) δ = 158.0, 156.8, 156.6, 156.4, 132.6, 132.3, 131.7, 131.5, 131.0, 130.8, 130.1, 129.7, 129.5, 129.3, 129.1, 128.8, 128.4, 127.9, 125.8, 122.6, 121.7, 121.6, 121.5, 121.1, 105.3, 104.9, 104.1, 68.6, 68.5, 68.2, 32.4, 32.3, 30.0, 29.9, 29.8, 29.7, 29.3, 26.7, 26.5, 26.4, 23.2, 23.1 and 14.6 ppm. UV/Vis (DCM): λ_{max} (log ε) = 272 (5.20), 316 (3.56), 334 (3.71), 352 (3.69), 406 (3.83), 426 nm (3.93). HRMS (MALDI) *m/z* calcd. for $C_{60}H_{81}BrO_4$ $[M]^+$: 944.5318; found 944.5311. IR (ATR): $\tilde{\nu}$ = 2922, 2853, 1628, 1459, 1200 cm^{-1}.

10,10‘-Dibromo-2,2‘,6,6‘-tetrakis(octyloxy)-9,9‘-bisanthracene S5.1

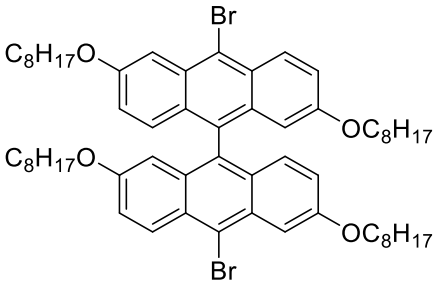

This compound was obtained as a side product during the synthesis of **5.38.**

Mp.: N.D.; oil. R_f = 0.51 (hexane/DCM, 1:4, v/v). ^{1}H NMR (400 MHz, $CDCl_3$) δ = 8.53 (d, *J* = 9.5 Hz, 2H, Ar-C*H*), 7.79 (d, *J* = 2.2 Hz, 2H, Ar-C*H*), 7.24 (d, *J* = 2.4 Hz, 1H, Ar-C*H*), 6.90 (s, 1H, Ar-C*H*), 6.88 (s, 1H, Ar-C*H*), 6.83 (d, *J* = 2.3 Hz, 2H, Ar-C*H*), 6.81 (d, *J* = 2.3 Hz, 1H, Ar-C*H*), 6.25 (d, *J* = 2.3 Hz, 2H, Ar-C*H*), 4.18 (t, *J* = 6.5 Hz, 4H, OCH_2), 3.43 (t, *J* = 6.5 Hz, 4H, OCH_2), 1.92 – 1.83 (m, 4H, CH_2), 1.53 – 1.07 (m, 44H, CH_2) and 0.87-0.80 ppm (m, 12H, CH_3). ^{13}C NMR (100 MHz, $CDCl_3$, 25 °C): *δ* = 157.6, 156.4, 131.8, 131.4, 130.4, 129.4, 129.0, 128.6, 127.5, 104.9, 104.3, 68.3, 67.9, 32.0, 31.9, 29.6, 29.5, 29.4, 29.3, 28.8, 26.3, 26.0, 22.9, 22.8, 22.7, 14.3 and 14.2 ppm. UV/Vis (DCM): λ_{max} (log *ε*) = 277 (5.41), 321 (3.92), 337 (4.04), 353 (4.07), 407 (4.14), 432 nm (4.30). HRMS (MALDI) *m/z* calcd. for $C_{60}H_{80}Br_2O_4$ $[M]^+$: 1022.4423; found 1022.4428. IR (ATR): ṽ = 2923, 2853, 1627, 1459, 1200 cm^{-1}.

[5,15-Bis(3,5-di-*tert*-butyl)phenyl-10,20-bis(2',2'',6',6''-tetrakis(octyloxy)-9',9''-bisanthracene)porphyrinato]nickel(II) 5.46

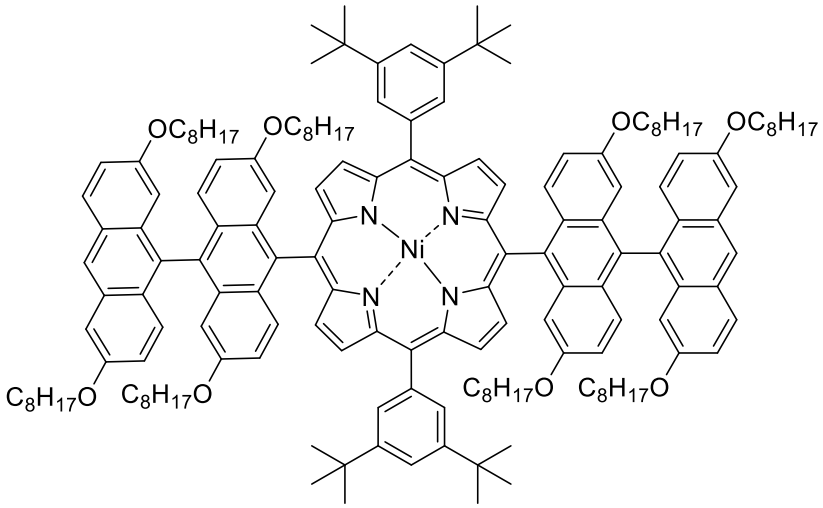

Porphyrin **5.44** (40 mg, 0.04 mmol, 1 eq.) was dried for 4 h under vacuum together with the bisanthracene **5.38** (80 mg, 0.085 mmol, 2.1 eq), $Pd_2(dba)_3$ (8 mg, 0.009 mmol, 0.2 eq.), SPhos (28 mg, 0.068 mmol, 1.7 eq.) and KOH (200 mg, 3.57 mmol, 89 eq.). 3 mL dry toluene were added and four freeze-thaw cycles were done. The reaction was heated to 90 °C for 4h. The solvent was removed and a filtration through silica was done with DCM followed by size exclusion chromatography in THF. The target compound was obtained in 2% yield as a purple glossy film (1.5 mg, 0.0006 mmol). R_f = 0.34 (hexane/DCM, 4:1, v/v). ^{1}H NMR (600 MHz, $CDCl_3$) δ = 8.82 (d, *J* = 4.6 Hz, 1H, Ar-C*H*), 8.80 (d, *J* = 4.6 Hz, 1H, Ar-C*H*), 8.75 (d, *J* = 4.6 Hz, 1H, Ar-C*H*), 8.72 (d, *J* = 4.6 Hz, 1H, Ar-C*H*), 8.62 – 8.58 (m, 2H, Ar-C*H*), 8.51 (bs, 1H, Ar-C*H*), 8.42 – 8.38 (m, 2H, Ar-C*H*), 8.06 (d, *J* = 8.9 Hz, 2H, Ar-C*H*), 7.98 – 7.94 (m, 3H, Ar-C*H*), 7.72 (bs, 2H, Ar-C*H*), 7.47 – 7.43 (m, 2H, Ar-C*H*), 7.40 (bs, 1H, Ar-C*H*), 7.24 – 7.19 (m, 4H, Ar-C*H*), 7.09 – 7.05 (m, 2H, Ar-C*H*), 6.92 (d, *J* = 9.7 Hz, 1H, Ar-C*H*), 6.88-6.81 (m, 4H, Ar-C*H*), 6.75 (bs, 1H, Ar-C*H*), 6.69-6.58 (m, 5H, Ar-C*H*), 6.50 – 6.44 (m, 4H, Ar-C*H*), 4.25-4.20 (m, 4H, OCH_2), 3.78-3.72 (m, 4H, OCH_2), 3.47-3.40 (m, 4H, OCH_2), 3.20-3.16 (m, 2H, OCH_2), 3.13-3.10 (m, 2H, OCH_2), 2.09-2.04 (m, 2H, CH_2), 1.97 – 1.92 (m, 4H, CH_2) and 1.66 – 0.63 ppm (m, 150 H, CH_2, CH_3). UV/Vis (DCM): λ_{max} (log ε) = 272 (5.19), 419 (4.83), 533 nm (4.00). HRMS (MALDI) *m/z* calcd. for $C_{168}H_{212}N_4O_8Ni$ $[M]^+$: 2471.5659; found 2471.5552.

[5,15-Bis(3,5-di-*tert*-butyl)phenyl-10-(2',2'',6',6''-tetrakis(octyloxy)-9',9''-bisanthracene)porphyrinato]nickel(II) 5.45

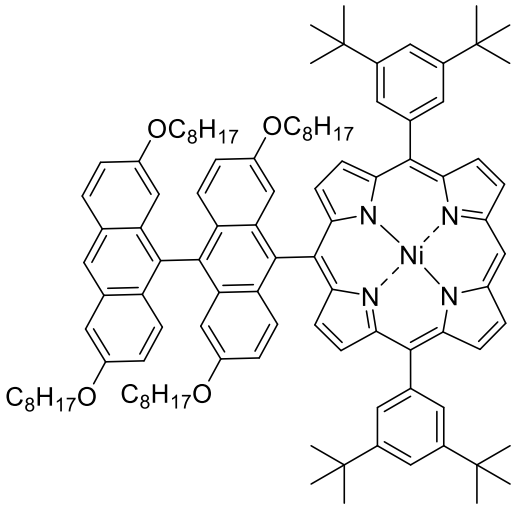

Compound **5.45** was obtained as side product of compound **5.46** as a purple glossy film in 14% yield (8 mg, 0.005 mmol). R_f = 0.48 (hexane/DCM, 4:1, v/v). ^{1}H NMR (600 MHz, $CDCl_3$) δ = 9.94 (s, 1H, H_{meso}), 9.22 – 9.19 (m, 2H, Ar-C*H*), 9.00 (d, *J* = 4.7 Hz, 1H, Ar-C*H*), 8.98 (d, *J* = 4.7 Hz, 1H, Ar-C*H*), 8.82 (d, *J* = 4.8 Hz, 1H, Ar-C*H*), 8.74 (d, *J* = 4.8 Hz, 1H, Ar-C*H*), 8.58 (d, *J* = 4.9 Hz, 1H, Ar-C*H*), 8.50 (s, 1H, Ar-C*H*), 8.39 (d, *J* = 4.9 Hz, 1H, Ar-C*H*), 8.05 (d, *J* = 8.9 Hz, 1H, Ar-C*H*), 7.95 (d, *J* = 8.1 Hz, 3H, Ar-C*H*), 7.75 (s, 2H, Ar-C*H*), 7.42 (d, *J* = 9.3 Hz, 1H, Ar-C*H*), 7.39 (s, 1H, Ar-C*H*), 7.22 (d, *J* = 9.0 Hz, 1H, Ar-C*H*), 7.18 (d, *J* = 9.6 Hz, 1H, Ar-C*H*), 7.05 (d, *J* = 9.3 Hz, 1H, Ar-C*H*), 6.84-6.77- (m, 3H, Ar-C*H*), 6.61 (d, *J* = 9.9 Hz, 2H, Ar-C*H*), 6.48 (s, 1H, Ar-C*H*), 6.35 (s, 1H, Ar-C*H*), 4.19 (s, 2H, OCH_2), 3.71 (t, *J* = 6.5 Hz, 2H, OCH_2), 3.41 (t, *J* = 6.5 Hz, 2H, OCH_2), 2.99 (t, *J* = 6.4 Hz, 2H, OCH_2) and 1.94 – 1.88 ppm (m, 2H, CH_2), 1.79 – 0.54 (m, 94H, CH_2, CH_3). UV/Vis (DCM): λ_{max} (log ε) = 272 (5.75), 412 (5.63), 525 nm (4.63). HRMS (MALDI) *m/z* calcd. for $C_{108}H_{132}N_4O_4Ni$ $[M]^+$: 1606.9602; found 1606.9608.

[5,15-Bis(3,5-di-*tert*-butyl)phenyl-10-phenyl-20-(2',2'',6',6''-tetrakis(octyloxy)-9',9''-bisanthracene)porphyrinato]nickel(II) 5.48

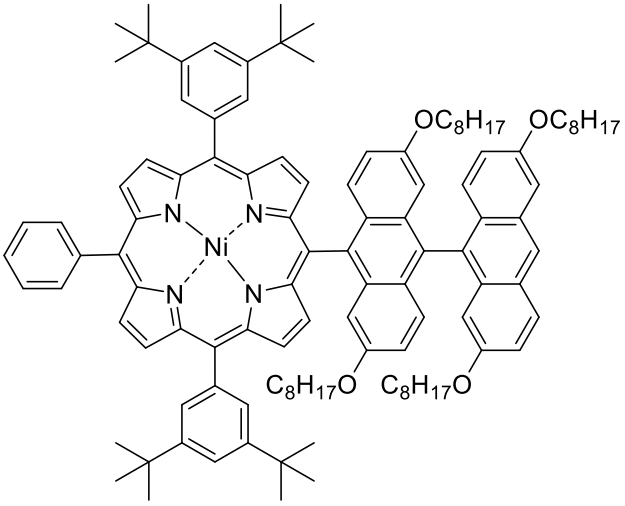

Porphyrin **5.47** (24 mg, 0.025 mmol, 1 eq.) was dried for 4 h under vacuum together with the bisanthracene **5.38** (31 mg, 0.033 mmol, 1.3 eq), $Pd_2(dba)_3$ (2.3 mg, 0.003 mmol, 0.1 eq.), SPhos (4.3 mg, 0.01 mmol, 0.41 eq.) and KOH (411 mg, 7.33 mmol, 289 eq.). 3 mL dry toluene were added and four freeze-thaw cycles were done. The reaction was heated to 90 °C for 2h. The solvent was removed and a filtration through silica was done with DCM followed by size exclusion chromatography in THF. The target compound was obtained in 19% yield as a glossy purple film (8 mg, 0.0047 mmol). Mp.: N.D.: glossy film. R_f = 0.33 (hexane/DCM, 3:1, v/v). ^{1}H NMR (600 MHz, DCM): δ = 8.88 – 8.82 (m, 4H, Ar-C*H*), 8.76 (d, *J* = 4.8 Hz, 1H, Ar-C*H*), 8.58 – 8.56 (m, 2H, Ar-C*H*), 8.42 (d, *J* = 4.8 Hz, 1H, Ar-C*H*), 8.16 – 8.10 (m, 3H, Ar-C*H*), 7.97 (bs, 4H, Ar-C*H*), 7.82 – 7.76 (m, 4H, Ar-C*H*), 7.48 – 7.42 (m, 3H, Ar-C*H*), 7.27– 7.25 (m, 1H, Ar-C*H*), 7.19 (d, *J* = 9.7 Hz, 1H, Ar-C*H*), 7.11 – 7.05 (m, 2H, Ar-C*H*), 6.85 (dd, *J* = 9.8, 2.7 Hz, 2H, Ar-C*H*), 6.69 – 6.64 (m, 2H, Ar-C*H*), 6.52 (d, *J* = 2.4 Hz, 1H, Ar-C*H*), 6.44 (d, *J* = 2.4 Hz, 1H, Ar-C*H*), 4.26 – 4.21 (m, 2H, OCH_2), 3.79 – 3.72 (m, 2H, OCH_2), 3.49 – 3.45 (m, 2H, OCH_2), 3.12 – 3.08 (m, 2H, OCH_2), 1.97 – 1.92 (m, 2H, CH_2), and 1.67 – 0.61 ppm (m, 94H, CH_2, CH_3). ^{13}C NMR (150 MHz, DCM, 25 °C): *δ* = 156.2, 156.1, 156.1, 155.7, 149.2, 149.1, 144.0, 143.9, 143.4, 143.1, 143.0, 142.7, 141.1, 139.9, 134.3, 133.7, 133.3, 133.0, 132.8, 132.7, 132.3, 132.2, 132.1, 131.9, 131.7, 131.5, 131.3, 131.1, 130.4, 129.7, 129.6, 128.9, 128.8, 128.4, 128.0, 127.8, 127.7, 126.9, 126.8, 125.1, 121.4, 121.3, 121.2, 120.6, 120.5, 120.3, 120.1, 119.4, 115.0,

106.0, 105.1, 103.9, 103.8, 69.8, 68.1, 67.6, 67.5, 67.4, 34.9, 31.9, 31.7, 31.4, 39.4, 29.3, 29.2, 29.1, 29.0, 29.0, 28.9, 28.8, 28.6, 28.5, 26.2, 25.9, 25.8, 25.5, 22.7, 22.6, 22.5, 22.3, 13.9, 13.8, 13.7 and 13.6 ppm. UV/Vis (DCM): λ_{max} (log ε) = 277 (5.58), 410 (6.12), 523 nm (4.98). HRMS (MALDI) *m/z* calcd. for $C_{114}H_{136}N_4O_4Ni$ $[M]^+$: 1683.9993; found 1683.9948.

Fused [5,15-Bis(3,5-di-*tert*-butyl)phenyl-10-(2',2'',6',6''-tetrakis(octyloxy)-9',9''-bisanthracene)porphyrinato]nickel(II) 5.50

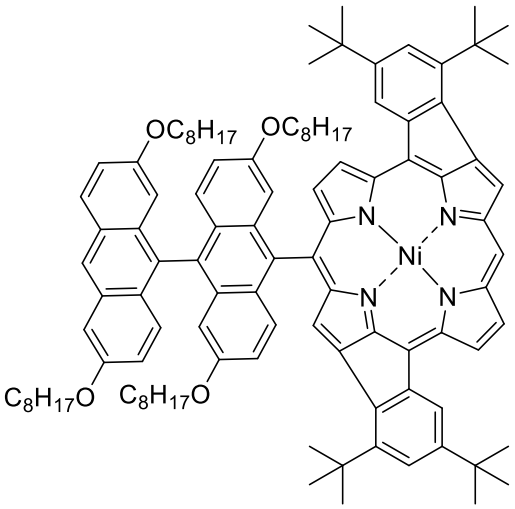

Porphyrin **4.49** (6 mg, 0.004 mmol, 1 eq.), $FeCl_3$ (6.5 mg, 0.039 mmol, 10.5 eq.) and AgOTf (30 mg, 0.117 mmol, 31.5 eq.) were dried under vacuum in three separate vials for 3 days. $FeCl_3$ was dissolved in dry nitromethane (0.4 mL) and the yellow solution was added to the vial with AgOTf. Meanwhle the porphyrin was dissolved in 0.7 mL of dry toluene. The $FeCl_3$ solution was added to the porphyrin and the reaction was stirred at rt. The reaction was monitored by TLC and the reaction was quenched and washed with $NaHCO_3$ after 1 h. The crude compound was filtered through silica using DCM+ 1% pyridine as eluent and the solvent was removed. The target compound was obtained as dark purple solid in 84% yield (5 mg, 0.0031 mmol). UV/Vis (DCM): λ_{max} (log ε) 272 (4.98), 325 (4.55), 379 (4.47), 412 (4.53), 436 (4.61), 531 (4.62), 744 (4.44), 824 nm (4.30). HRMS (MALDI) *m/z* calcd. for $C_{108}H_{120}N_4O_4Ni$ $[M]^+$: 1594.8663; found 1594.8588.

7 References

[1] K. Fujimotot, H. Yorimitsu, A. Osuka, *European Journal of Organic Chemistry* **2014**, *2014*, 4327-4334.
[2] F. Sguerra, V. Bulach, M. W. Hosseini, *Dalton Transactions* **2012**, *41*, 14683-14689.
[3] D. Wohrle, *Advanced Materials* **1997**, *9*, 1191-1192.
[4] W. Küster, *Berichte der deutschen chemischen Gesellschaft* **1912**, *45*, 1935-1946.
[5] a) K. M. Smith, *Porphyrins and Metalloporphyrins*, Elsevier Science Amsterdam, **1975**; b) H. Fischer, J. Klarer, *Justus Liebigs Annalen der Chemie* **1926**, *450*, 181-201.
[6] E. Hückel, *Zeitschrift für Physik* **1931**, *70*, 204-286.
[7] M. O. Senge, *Chemical Communications* **2011**, *47*, 1943-1960.
[8] S. Okada, H. Segawa, *Journal of the American Chemical Society* **2003**, *125*, 2792-2796.
[9] a) M. O. Senge, M. Fazekas, E. G. A. Notaras, W. J. Blau, M. Zawadzka, O. B. Locos, E. M. Ni Mhuircheartaigh, *Advanced Materials* **2007**, *19*, 2737-2774; b) E. S. Nyman, P. H. Hynninen, *Journal of Photochemistry and Photobiology B: Biology* **2004**, *73*, 1-28; c) A. A. Ryan, M. O. Senge, *Photochemical & Photobiological Sciences* **2015**, *14*, 638-660; d) M. R. Wasielewski, *The Journal of Organic Chemistry* **2006**, *71*, 5051-5066.
[10] P. Rothemund, *Journal of the American Chemical Society* **1935**, *57*, 2010-2011.
[11] A. D. Adler, F. R. Longo, W. Shergalis, *Journal of the American Chemical Society* **1964**, *86*, 3145-3149.
[12] A. D. Adler, F. R. Longo, J. D. Finarelli, J. Goldmacher, J. Assour, L. Korsakoff, *The Journal of Organic Chemistry* **1967**, *32*, 476-476.
[13] J. S. Lindsey, in *The Porphyrin Handbook, Vol. 1* (Eds.: K. M. Kadish, K. M. Smith, R. Guilard), Academic Press, New York, **2000**, pp. 45-118;
[14] D. Dolphin, *Journal of Heterocyclic Chemistry* **1970**, *7*, 275-283.
[15] M. G. H. Vicente, K. M. Smith, *Current Organic Synthesis* **2014**, *11*, 3-28.
[16] H. Volz, G. Herb, *Zeitschrift für Naturforschung* **1983**, 1240-1242.
[17] J. S. Lindsey, *Accounts of Chemical Research* **2010**, *43*, 300-311.
[18] J. S. Lindsey, H. C. Hsu, I. C. Schreiman, *Tetrahedron Letters* **1986**, *27*, 4969-4970.
[19] K. M. Smith, in *The Porphyrin Handbook, Vol. 1* (Eds.: K. M. Kadish, K. M. Smith, R. Guilard), Academic Press, New York, **2000**, pp. 1-43.
[20] a) G. P. Arsenault, E. Bullock, S. F. MacDonald, *Journal of the American Chemical Society* **1960**, *82*, 4384-4389; b) T. D. Lash, *Journal of Porphyrins and Phthalocyanines* **2016**, *20*, 855-888.
[21] D. Dolphin, in *The Porphyrins Vol. 1*, Academic Press: New York, **2011**.
[22] S. Plunkett, M. O. Senge, *ECS Transactions* **2011**, *35*, 147-157.
[23] A. Wiehe, Y. M. Shaker, J. C. Brandt, S. Mebs, M. O. Senge, *Tetrahedron* **2005**, *61*, 5535-5564.
[24] A. Treibs, N. Häberle, *Justus Liebigs Annalen der Chemie* **1968**, 183-207.
[25] J. E. Baldwin, M. J. Crossley, T. Klose, E. A. O'Rear, M. K. Peters, *Tetrahedron* **1982**, *38*, 27-39.
[26] C. Brückner, J. J. Posakony, C. K. Johnson, R. W, Boyle, B. R. James, D. Dolphin, *Journal of Porphyrins and Phthalocyanines* **1998**, *2*, 455-465.

[27] L. M. Milgrom, *Journal of Chemical Society, Perkin Transactions 1* **1984**, *0*, 1483-1487.
[28] A. Wiehe, C. Ryppa, M. O. Senge, *Organic Letters* **2002**, *4*, 3807-3809.
[29] R. P. Briñas, C. Brückner, *Tetrahedron* **2002**, *58*, 4375-4381.
[30] S. Hatscher, M. O. Senge, *Tetrahedron Letters* **2003**, *44*, 157-160.
[31] R. K. Pandey, G. K. Zheng in *The Porphyrin Handbook – Applications: Past, Present and Future, Vol. 6*, (Eds.: K. M. Kadish, K. M. Smith, R. Guilard, Academic Press: San Diego, 2000, pp 157-230.
[32] a) J.-H. Furhop, in *The Porphyrins, Vol. 1* (Ed.: D. Dolphin), Academic Press, New York, **1978**, pp. 1311-1159; b) M. G. H. Vincente, in *The Porphyrin Handbook, Vol. 1* (Eds.: K. M. Kadish, M. K. Smith, R. Guilard), Academic Press, New York, **2000**, pp. 149-199.
[33] K. Dahms, M. O. Senge, M. B. Bakar, *European Journal of Organic Chemistry* **2007**, *2007*, 3833-3848.
[34] H. Brockmann, K.-M. Bliesener, H. H. Inhoffen, *Liebigs Annalen der Chemie* **1968**, 148-161.
[35] L.-M. Jin, J.-J. Yin, L. Chen, C.-C. Guo, Q.-Y. Chen, *Synlett* **2005**, *2005*, 2893-2898.
[36] L. R. Nudy, H. G. Hutchinson, C. Schieber, F. R. Longo, *Tetrahedron* **1984**, *40*, 2359-2363.
[37] R. Bonnett, I. A. D. Gale, G. F. Stephenson, *Journal of the Chemical Society C: Organic* **1966**, 1600-1604.
[38] P. Bhyrappa, V. Krishnan, *Inorganic Chemistry* **1991**, *30*, 239-245.
[39] D. Dolphin, T. G. Traylor, L. Y. Xie, *Accounts of Chemical Research* **1997**, *30*, 251-259.
[40] D. E. Chumakov, A. V. Khoroshutin, A. V. Anisimov, K. I. Kobrakov, *Chemistry of Heterocyclic Compounds* **2009**, 259-283.
[41] P. Bhyrappa, *Tetrahedron Letters* **2016**, *57*, 5150-5167.
[42] J. Leroy, A. Bondon, *European Journal of Organic Chemistry* **2008**, *2008*, 417-433.
[43] a) A. Nakano, H. Shimidzu, A. Osuka, *Tetrahedron Letters* **1998**, *39*, 9489-9492; b) S. Shanmugathasan, C. K. Johnson, C. Edwards, E. K. Mathews, D. Dolphin, R. W. Boyle, B. R. W., *Journal of Porphyrins and Phthalocyanines* **2000**, *4*, 228-232.
[44] R. Bonnett, G. F. Stephenson, *The Journal of Organic Chemistry* **1965**, *30*, 2791-2798.
[45] E. Watanabe, S. Nishimura, H. Ogoshi, Z. Yoshida, *Tetrahedron* **1975**, *31*, 1385-1390.
[46] J. E. Baldwin, J. F. DeBernardis, *The Journal of Organic Chemistry* **1977**, *42*, 3986-3987.
[47] M. Palacio, V. Mansuy-Mouries, G. Loire, K. Le Barch-Ozette, P. Leduc, K. M. Barkigia, J. Fajer, P. Battioni, D. Mansuy, *Chemical Communications* **2000**, 1907-1908.
[48] K. M. Smith, G. H. Barnett, B. Evans, Z. Martynenko, *Journal of the American Chemical Society* **1979**, *101*, 5953-5961.
[49] a) G. H. Barnett, K. M. Smith, *Journal of the Chemical Society, Chemical Communications* **1974**, 772-773; b) L. Jaquinod, in *The Porphyrin Handbook, Vol. 1* (Eds.: K. M. Kadish, K. M. Smith, R. Guilard), Academic Press, New York, **2000**, pp. 201-237.
[50] M. O. Senge, *Accounts of Chemical Research* **2005**, *38*, 733-743.
[51] W. W. Kalisch, M. O. Senge, *Angewandte Chemie International Edition* **1998**, *37*, 1107-1109.

[52] M. O. Senge, X. Feng, *Journal of the Chemical Society, Perkin Transactions 1* **2000**, 3615-3621.
[53] M. O. Senge, W. W. Kalisch, I. Bischoff, *Chemistry – A European Journal* **2000**, *6*, 2721-2738.
[54] X. Feng, I. Bischoff, M. O. Senge, *The Journal of Organic Chemistry* **2001**, *66*, 8693-8700.
[55] M. O. Senge, I. Bischoff, *European Journal of Organic Chemistry* **2001**, *2001*, 1735-1751.
[56] M. Ishida, S. W. Park, D. Hwang, Y. B. Koo, J. L. Sessler, D. Y. Kim, D. Kim, *The Journal of Physical Chemistry C* **2011**, *115*, 19343-19354.
[57] a) I. Bischoff, X. Feng, M. O. Senge, *Tetrahedron* **2001**, *57*, 5573-5583; b) N. N. Sergeeva, Y. M. Shaker, E. M. Finnigan, T. McCabe, M. O. Senge, *Tetrahedron* **2007**, *63*, 12454-12464.
[58] M. O. Senge, X. Feng, *Tetrahedron Letters* **1999**, *40*, 4165-4168.
[59] a) B. M. L. Chen, A. Tulinsky, *Journal of the American Chemical Society* **1972**, *94*, 4144-4151; b) M. O. Senge, M. Davis, *Journal of Porphyrins and Phthalocyanines* **2010**, *14*, 557-567.
[60] S. Neya, N. Funasaki, *Tetrahedron Letters* **2002**, *43*, 1057-1058.
[61] M. O. Senge, Y. M. Shaker, M. Pintea, C. Ryppa, S. S. Hatscher, A. A. Ryan, Y. Sergeeva, *European Journal of Organic Chemistry* **2010**, *2010*, 237-258.
[62] B. Krattinger, H. J. Callot, *European Journal of Organic Chemistry* **1999**, *1999*, 1857-1867.
[63] M. J. Crossley, L. G. King, S. M. Pyke, C. W. Tansey, *Journal of Porphyrins and Phthalocyanines* **2002**, *06*, 685-694.
[64] M. J. Crossley, M. M. Harding, C. W. Tansey, *The Journal of Organic Chemistry* **1994**, *59*, 4433-4437.
[65] C. H. Devillers, S. Hebié, D. Lucas, H. Cattey, S. Clément, S. Richeter, *The Journal of Organic Chemistry* **2014**, *79*, 6424-6434.
[66] L.-C. Gong, D. Dolphin, *Canadian Journal of Chemistry* **1985**, *63*, 406-411.
[67] M. Kielmann, K. J. Flanagan, K. Norvaiša, D. Intrieri, M. O. Senge, *The Journal of Organic Chemistry* **2017**, *82*, 5122-5134.
[68] A. A. Ryan, S. Plunkett, A. Casey, T. McCabe, M. O. Senge, *Chemical Communications* **2014**, *50*, 353-355.
[69] S. Hiroto, Y. Miyake, H. Shinokubo, *Chemical Reviews* **2017**, *117*, 2910-3043.
[70] a) D. P. Arnold, R. C. Bott, H. Eldridge, F. M. Elms, G. Smith, M. Zojaji, *Australian Journal of Chemistry* **1997**, *50*, 495-504; b) R. W. Boyle, C. K. Johnson, D. Dolphin, *Journal of the Chemical Society, Chemical Communications* **1995**, *0*, 527-528.
[71] W. M. Sharman, J. E. van Lier, *Journal of Porphyrins and Phthalocyanines* **2000**, *4*, 441-453.
[72] S. G. DiMagno, V. S. Y. Lin, M. J. Therien, *Journal of the American Chemical Society* **1993**, *115*, 2513-2515.
[73] a) K. S. Chan, X. Zhou, B.-S. Luo, T. C. W. Mak, *Journal of the Chemical Society, Chemical Communications* **1994**, *0*, 271-272; b) A. G. Hyslop, M. A. Kellett, P. M. Iovine, M. J. Therien, *Journal of the American Chemical Society* **1998**, *120*, 12676-12677.
[74] a) H. Ali, J. E. van Lier, *Tetrahedron* **1994**, *50*, 11933-11944; b) V. S. Lin, S. G. DiMagno, M. J. Therien, *Science* **1994**, *264*, 1105-1111.
[75] H. L. Anderson, *Chemical Communications* **1999**, 2323-2330.

[76] R. Gauler, N. Risch, *European Journal of Organic Chemistry* **1998**, *1998*, 1193-1200.
[77] O. B. Locos, D. P. Arnold, *Organic & Biomolecular Chemistry* **2006**, *004*, 902-916.
[78] M. Castella, F. Calahorra, D. Sainz, D. Velasco, *Organic Letters* **2001**, *3*, 541-544.
[79] N. N. Sergeeva, A. Scala, M. A. Bakar, G. O'Riordan, J. O'Brien, G. Grassi, M. O. Senge, *The Journal of Organic Chemistry* **2009**, *74*, 7140-7147.
[80] M. J. Frampton, H. Akdas, A. R. Cowley, J. E. Rogers, J. E. Slagle, P. A. Fleitz, M. Drobizhev, A. Rebane, H. L. Anderson, *Organic Letters* **2005**, *7*, 5365-5368.
[81] H. Aihara, L. Jaquinod, D. J. Nurco, K. M. Smith, *Angewandte Chemie International Edition* **2001**, *40*, 3439-3441.
[82] T. Chandra, B. J. Kraft, J. C. Huffman, J. M. Zaleski, *Inorganic Chemistry* **2003**, *42*, 5158-5172.
[83] N. Sugita, S. Hayashi, F. Hino, T. Takanami, *The Journal of Organic Chemistry* **2012**, *77*, 10488-10497.
[84] T. Takanami, M. Yotsukura, W. Inoue, N. Inoue, F. Hino, K. Suda, *Heterocycles* **2008**, 439-453.
[85] S. G. DiMagno, V. S. Y. Lin, M. J. Therien, *The Journal of Organic Chemistry* **1993**, *58*, 5983-5993.
[86] D.-M. Shen, C. Liu, Q.-Y. Chen, *The Journal of Organic Chemistry* **2006**, *71*, 6508-6511.
[87] K. Kato, W. Cha, J. Oh, K. Furukawa, H. Yorimitsu, D. Kim, A. Osuka, *Angewandte Chemie International Edition* **2016**, *55*, 8711-8714.
[88] C. Liu, D.-M. Shen, Q.-Y. Chen, *The Journal of Organic Chemistry* **2007**, *72*, 2732-2736.
[89] T. Dohi, K. Morimoto, A. Maruyama, Y. Kita, *Organic Letters* **2006**, *8*, 2007-2010.
[90] H. Baba, J. Chen, H. Shinokubo, A. Osuka, *Chemistry – A European Journal* **2008**, *14*, 4256-4262.
[91] Y. Chen, X. P. Zhang, *The Journal of Organic Chemistry* **2003**, *68*, 4432-4438.
[92] T. Takanami, M. Hayashi, F. Hino, K. Suda, *Tetrahedron Letters* **2003**, *44*, 7353-7357.
[93] K. B. Fields, J. V. Ruppek, N. L. Snyder, X. P. Zhang, in *Handbook of Porphyrin Science, Vol. 3* (Eds.: K. M. Kadish, K. M. Smith, R. Guilard), World Scientific Publishing, Singapore, **2010**, pp. 367-427.
[94] M. Jurow, A. E. Schuckman, J. D. Batteas, C. M. Drain, *Coordination chemistry reviews* **2010**, *254*, 2297-2310.
[95] A. K. Burrell, M. R. Wasielewski, *Journal of Porphyrins and Phthalocyanines* **2000**, *04*, 401-406.
[96] G. McDermott, S. M. Prince, A. A. Freer, A. M. Hawthornthwaite-Lawless, M. Z. Papiz, R. J. Cogdell, N. W. Isaacs, *Nature* **1995**, *374*, 517-521.
[97] H. E. Zimmerman, T. D. Goldman, T. K. Hirzel, S. P. Schmidt, *The Journal of Organic Chemistry* **1980**, *45*, 3933-3951.
[98] a) J. R. Bolton, T.-F. Ho, S. Liauw, A. Siemiarczuk, C. S. K. Wan, A. C. Weedon, *Journal of the Chemical Society, Chemical Communications* **1985**, 559-560; b) D. N. Beratan, *Journal of the American Chemical Society* **1986**, *108*, 4321-4326; c) A. D. Joran, B. A. Leland, G. G. Geller, J. J. Hopfield, P. B. Dervan, *Journal of the American Chemical Society* **1984**, *106*, 6090-6092.

[99] a) T. A. Reekie, M. Sekita, L. M. Urner, S. Bauroth, L. Ruhlmann, J.-P. Gisselbrecht, C. Boudon, N. Trapp, T. Clark, D. M. Guldi, F. Diederich, *Chemistry – A European Journal* **2017**, *23*, 6357-6369; b) L. M. Urner, M. Sekita, N. Trapp, W. B. Schweizer, M. Wörle, J.-P. Gisselbrecht, C. Boudon, D. M. Guldi, F. Diederich, *European Journal of Organic Chemistry* **2014**, *2015*, 91-108.

[100] a) C. F. Portela, J. Brunckova, J. L. Richards, B. Schöllhorn, Y. Iamamoto, D. Magde, T. G. Traylor, C. L. Perrin, *The Journal of Physical Chemistry A* **1999**, *103*, 10540-10552; b) A. Osuka, R.-P. Zhang, K. Maruyama, N. Mataga, Y. Tanaka, T. Okada, *Chemical Physics Letters* **1993**, *215*, 179-184; c) A. Osuka, S. Marumo, K. Maruyama, N. Mataga, Y. Tanaka, S. Taniguchi, T. Okada, I. Yamazaki, Y. Nishimura, *Bulletin of the Chemical Society of Japan* **1995**, *68*, 262-276.

[101] a) X. Chen, X. Tian, I. Shin, J. Yoon, *Chemical Society Reviews* **2011**, *40*, 4783-4804; b) M. Kamiya, D. Asanuma, E. Kuranaga, A. Takeishi, M. Sakabe, M. Miura, T. Nagano, Y. Urano, *Journal of the American Chemical Society* **2011**, *133*, 12960-12963; c) A. R. Lippert, G. C. Van de Bittner, C. J. Chang, *Accounts of Chemical Research* **2011**, *44*, 793-804; d) X. Li, X. Gao, W. Shi, H. Ma, *Chemical Reviews* **2014**, *114*, 590-659; e) J. Chan, S. C. Dodani, C. J. Chang, *Nature Chemistry* **2012**, *4*, 973-984.

[102] H. Kotani, K. Ohkubo, M. J. Crossley, S. Fukuzumi, *Journal of the American Chemical Society* **2011**, *133*, 11092-11095.

[103] Y. Kubo, M. Yamamoto, M. Ikeda, M. Takeuchi, S. Shinkai, S. Yamaguchi, K. Tamao, *Angewandte Chemie International Edition* **2003**, *42*, 2036-2040.

[104] K. Bera, S. Maiti, M. Maity, C. Mandal, N. C. Maiti, *ACS Omega* **2018**, *3*, 4602-4619.

[105] D. Mondal, S. Bera, *Advances in Natural Sciences: Nanoscience and Nanotechnology* **2014**, *5*, 033002.

[106] J. Malig, N. Jux, D. M. Guldi, *Accounts of Chemical Research* **2013**, *46*, 53-64.

[107] J. F. Lovell, A. Roxin, K. K. Ng, Q. Qi, J. D. McMullen, R. S. DaCosta, G. Zheng, *Biomacromolecules* **2011**, *12*, 3115-3118.

[108] C. F. Pereira, M. M. Simoes, J. P. C. Tomé, F. A. Almeida Paz, Molecules 2016, 21, 1348-1366.

[109] N. U. Day, C. C. Wamser, M. G. Walter, *Polymer International* **2015**, *64*, 833-857.

[110] H. Komiyama, S. Kraines, *Vision 2050: Roadmap for a Sustainable Earth*, Springer, Tokyo Berlin Heidelberg New York, **2008**.

[111] C. C. Stoumpos, M. G. Kanatzidis, *Accounts of Chemical Research* **2015**, *48*, 2791-2802.

[112] B. O'Regan, M. Grätzel, *Nature* **1991**, *353*, 737-740.

[113] a) W. M. Campbell, A. K. Burrell, D. L. Officer, K. W. Jolley, *Coordination Chemistry Reviews* **2004**, *248*, 1363-1379; b) M. J. Griffith, K. Sunahara, P. Wagner, K. Wagner, G. G. Wallace, D. L. Officer, A. Furube, R. Katoh, S. Mori, A. J. Mozer, *Chemical Communications* **2012**, *48*, 4145-4162; c) H. Imahori, T. Umeyama, S. Ito, *Accounts of Chemical Research* **2009**, *42*, 1809-1818; d) K. Ladomenou, T. N. Kitsopoulos, G. D. Sharma, A. G. Coutsolelos, *RSC Advances* **2014**, *4*, 21379-21404; e) L.-L. Li, E. W.-G. Diau, *Chemical Society Reviews* **2013**, *42*, 291-304; f) M. V. Martínez-Díaz, G. de la Torre, T. Torres, *Chemical Communications* **2010**, *46*, 7090-7108.

[114] a) Y. Chiba, A. Islam, Y. Watanabe, R. Komiya, N. Koide, L. Han, *Japanese Journal of Applied Physics* **2006**, *45*, 24-28; b) M. K. Nazeeruddin, F. De

Angelis, S. Fantacci, A. Selloni, G. Viscardi, P. Liska, S. Ito, B. Takeru, M. Grätzel, *Journal of the American Chemical Society* **2005**, *127*, 16835-16847; c) F. Gao, Y. Wang, D. Shi, J. Zhang, M. Wang, X. Jing, R. Humphry-Baker, P. Wang, S. M. Zakeeruddin, M. Grätzel, *Journal of the American Chemical Society* **2008**, *130*, 10720-10728; d) C.-Y. Chen, M. Wang, J.-Y. Li, N. Pootrakulchote, L. Alibabaei, C.-h. Ngoc-le, J.-D. Decoppet, J.-H. Tsai, C. Grätzel, C.-G. Wu, S. M. Zakeeruddin, M. Grätzel, *ACS Nano* **2009**, *3*, 3103-3109; e) L. Han, A. Islam, H. Chen, C. Malapaka, B. Chiranjeevi, S. Zhang, X. Yang, M. Yanagida, *Energy & Environmental Science* **2012**, *5*, 6057-6060; f) M. K. Nazeeruddin, A. Kay, I. Rodicio, R. Humphry-Baker, E. Mueller, P. Liska, N. Vlachopoulos, M. Grätzel, *Journal of the American Chemical Society* **1993**, *115*, 6382-6390; g) M. K. Nazeeruddin, P. Péchy, T. Renouard, S. M. Zakeeruddin, R. Humphry-Baker, P. Comte, P. Liska, L. Cevey, E. Costa, V. Shklover, L. Spiccia, G. B. Deacon, C. A. Bignozzi, M. Grätzel, *Journal of the American Chemical Society* **2001**, *123*, 1613-1624.

[115] a) S. M. LeCours, H.-W. Guan, S. G. DiMagno, C. H. Wang, M. J. Therien, *Journal of the American Chemical Society* **1996**, *118*, 1497-1503; b) K. S. Suslick, C. T. Chen, G. R. Meredith, L. T. Cheng, *Journal of the American Chemical Society* **1992**, *114*, 6928-6930.

[116] a) M. Grätzel, *Journal of Photochemistry and Photobiology C: Photochemistry Reviews* **2003**, *4*, 145-153; b) S. Mathew, A. Yella, P. Gao, R. Humphry-Baker, B. F. E. Curchod, N. Ashari-Astani, I. Tavernelli, U. Rothlisberger, Md. K. Nazeeruddin, M. Grätzel, *Nature Chemistry* **2014**, *6*, 242-247; c) A. Yella, H.-W. Lee, H. N. Tsao, C. Yi, A. K. Chandiran, M. K. Nazeeruddin, E. W.-G. Diau, C.-Y. Yeh, S. M. Zakeeruddin, M. Grätzel, *Science* **2011**, *334*, 629-634.

[117] T. Higashino, H. Imahori, *Dalton Transactions* **2015**, *44*, 448-463.

[118] Q. Wang, W. M. Campbell, E. E. Bonfantani, K. W. Jolley, D. L. Officer, P. J. Walsh, K. Gordon, R. Humphry-Baker, M. K. Nazeeruddin, M. Grätzel, *The Journal of Physical Chemistry B* **2005**, *109*, 15397-15409.

[119] W. M. Campbell, K. W. Jolley, P. Wagner, K. Wagner, P. J. Walsh, K. C. Gordon, L. Schmidt-Mende, M. K. Nazeeruddin, Q. Wang, M. Grätzel, D. L. Officer, *The Journal of Physical Chemistry C* **2007**, *111*, 11760-11762.

[120] a) R. B. Ambre, G.-F. Chang, M. R. Zanwar, C.-F. Yao, E. W.-G. Diau, C.-H. Hung, *Chemistry – An Asian Journal* **2013**, *8*, 2144-2153; b) R. B. Ambre, G.-F. Chang, C.-H. Hung, *Chemical Communications* **2014**, *50*, 725-727; c) M. J. Lee, K. D. Seo, H. M. Song, M. S. Kang, Y. K. Eom, H. S. Kang, H. K. Kim, *Tetrahedron Letters* **2011**, *52*, 3879-3882; d) G. Di Carlo, A. O. Biroli, M. Pizzotti, F. Tessore, V. Trifiletti, R. Ruffo, A. Abbotto, A. Amat, F. De Angelis, P. R. Mussini, *Chemistry – A European Journal* **2013**, *19*, 10723-10740; e) H. Imahori, Y. Matsubara, H. Iijima, T. Umeyama, Y. Matano, S. Ito, M. Niemi, N. V. Tkachenko, H. Lemmetyinen, *The Journal of Physical Chemistry C* **2010**, *114*, 10656-10665; f) K. Kurotobi, Y. Toude, K. Kawamoto, Y. Fujimori, S. Ito, P. Chabera, V. Sundström, H. Imahori, *Chemistry – A European Journal* **2013**, *19*, 17075-17081.

[121] A. Yella, C.-L. Mai, S. M. Zakeeruddin, S.-N. Chang, C.-H. Hsieh, C.-Y. Yeh, M. Grätzel, *Angewandte Chemie International Edition* **2014**, *53*, 2973-2977.

[122] S. Ito, T. N. Murakami, P. Comte, P. Liska, C. Grätzel, M. K. Nazeeruddin, M. Grätzel, *Thin Solid Films* **2008**, *516*, 4613-4619.

[123] W. Shockley, H. J. Queisser, *Journal of Applied Physics* **1961**, *32,* 510-519.

[124] A. Hagfeldt, M. Grätzel, *Accounts of Chemical Research* **2000**, *33*, 269-277.
[125] a) M. Grätzel, *Inorganic Chemistry* **2005**, *44*, 6841-6851; b) A. Listorti, B. O'Regan, J. R. Durrant, *Chemistry of Materials* **2011**, *23*, 3381-3399; c) M. Grätzel, *Journal of Photochemistry and Photobiology A: Chemistry* **2004**, *164*, 3-14; d) H. J. Snaith, L. Schmidt-Mende, *Advanced Materials* **2007**, *19*, 3187-3200; e) L. M. Peter, *Physical Chemistry Chemical Physics* **2007**, *9*, 2630-2642; f) T. W. Hamann, R. A. Jensen, A. B. F. Martinson, H. Van Ryswyk, J. T. Hupp, *Energy & Environmental Science* **2008**, *1*, 66-78; g) S. Ardo, G. J. Meyer, *Chemical Society Reviews* **2009**, *38*, 115-164; h) M. Grätzel, *Nature* **2001**, *414*, 338-344; i) A. Hagfeldt, G. Boschloo, L. Sun, L. Kloo, H. Pettersson, *Chemical Reviews* **2010**, *110*, 6595-6663.
[126] a) E. Palomares, J. N. Clifford, S. A. Haque, T. Lutz, J. R. Durrant, *Journal of the American Chemical Society* **2003**, *125*, 475-482; b) M. Wang, C. Grätzel, S.-J. Moon, R. Humphry-Baker, N. Rossier-Iten, S. M. Zakeeruddin, M. Grätzel, *Advanced Functional Materials* **2009**, *19*, 2163-2172; c) U. Bach, D. Lupo, P. Comte, J. E. Moser, F. Weissortel, J. Salbeck, H. Spreitzer, M. Grätzel, *Nature* **1998**, *395*, 583-585; d) H. Tian, Z. Yu, A. Hagfeldt, L. Kloo, L. Sun, *Journal of the American Chemical Society* **2011**, *133*, 9413-9422; e) T. Daeneke, T.-H. Kwon, A. B. Holmes, N. W. Duffy, U. Bach, L. Spiccia, *Nature Chemistry* **2011**, *3*, 211-215.
[127] a) S. A. Sapp, C. M. Elliott, C. Contado, S. Caramori, C. A. Bignozzi, *Journal of the American Chemical Society* **2002**, *124*, 11215-11222; b) S. M. Feldt, E. A. Gibson, E. Gabrielsson, L. Sun, G. Boschloo, A. Hagfeldt, *Journal of the American Chemical Society* **2010**, *132*, 16714-16724; c) H. Nusbaumer, J.-E. Moser, S. M. Zakeeruddin, M. K. Nazeeruddin, M. Grätzel, *The Journal of Physical Chemistry B* **2001**, *105*, 10461-10464; d) B. A. Gregg, F. Pichot, S. Ferrere, C. L. Fields, *The Journal of Physical Chemistry B* **2001**, *105*, 1422-1429.
[128] a) Z. Zhang, P. Chen, T. N. Murakami, S. M. Zakeeruddin, M. Grätzel, *Advanced Functional Materials* **2008**, *18*, 341-346; b) M. Wang, N. Chamberland, L. Breau, J.-E. Moser, R. Humphry-Baker, B. Marsan, S. M. Zakeeruddin, M. Grätzel, *Nature Chemistry* **2010**, *2*, 385-389.
[129] S. Nishimura, N. Abrams, B. A. Lewis, L. I. Halaoui, T. E. Mallouk, K. D. Benkstein, J. van de Lagemaat, A. J. Frank, *Journal of the American Chemical Society* **2003**, *125*, 6306-6310.
[130] a) L.-L. Tan, J.-F. Huang, Y. Shen, L.-M. Xiao, J.-M. Liu, D.-B. Kuang, C.-Y. Su, *Journal of Materials Chemistry A* **2014**, *2*, 8988-8994; b) W. Zeng, Y. Cao, Y. Bai, Y. Wang, Y. Shi, M. Zhang, F. Wang, C. Pan, P. Wang, *Chemistry of Materials* **2010**, *22*, 1915-1925; cY. Ooyama, Y. Harima, *European Journal of Organic Chemistry* **2009**, *2009*, 2903-2934; d) A. Mishra, M. K. R. Fischer, P. Bäuerle, *Angewandte Chemie International Edition* **2009**, *48*, 2474-2499.
[131] T. Bessho, S. M. Zakeeruddin, C.-Y. Yeh, E. W.-G. Diau, M. Grätzel, *Angewandte Chemie International Edition* **2010**, *49*, 6646-6649.
[132] M. Ishida, D. Hwang, Y. B. Koo, J. Sung, D. Y. Kim, J. L. Sessler, D. Kim, *Chemical Communications* **2013**, *49*, 9164-9166.
[133] T. Higashino, K. Kawamoto, K. Sugiura, Y. Fujimori, Y. Tsuji, K. Kurotobi, S. Ito, H. Imahori, *ACS Applied Materials & Interfaces* **2016**, *8*, 15379-15390.
[134] E. G. A. Notaras, M. Fazekas, J. J. Doyle, W. J. Blau, M. O. Senge, *Chemical Communications* **2007**, 2166-2168.
[135] M. Zawadzka, J. Wang, W. J. Blau, M. O. Senge, *The Journal of Physical Chemistry A* **2013**, *117*, 15-26.

[136] C. Ryppa, M. O. Senge, S. S. Hatscher, E. Kleinpeter, P. Wacker, U. Schilde, A. Wiehe, *Chemistry – A European Journal* **2005**, *11*, 3427-3442.
[137] a) M. S. Driver, J. F. Hartwig, *Journal of the American Chemical Society* **1996**, *118*, 7217-7218; b) J. F. Hartwig, S. Richards, D. Barañano, F. Paul, *Journal of the American Chemical Society* **1996**, *118*, 3626-3633.
[138] K. Sonogashira, Y. Tohda, N. Hagihara, *Tetrahedron Letters* **1975**, *16*, 4467-4470.
[139] a) M. O. Senge, M. Fazekas, M. Pintea, M. Zawadzka, W. J. Blau, *European Journal of Organic Chemistry* **2011**, *2011*, 5797-5816. b) T. A. Pham, F. Song, M. N. Alberti, M.-T. Nguyen, N. Trapp, C. Thilgen, F. Diederich, M. Stöhr, *Chemical Communications* **2015**, *51*, 14473-14476.
[140] A. Meindl, S. Plunkett, A. A. Ryan, K. J. Flanagan, S. Callaghan, M. O. Senge, *European Journal of Organic Chemistry* **2017**, *2017*, 3565-3583.
[141] M. O. Senge, C. Ryppa, M. Fazekas, M. Zawadzka, K. Dahms, *Chemistry – A European Journal* **2011**, *17*, 13562-13573.
[142] S. Taniguchi, H. Hasegawa, M. Nishimura, M. Takahashi, *Synlett* **1999**, 73-74.
[143] Y. Nakamura, I. W. Hwang, N. Aratani, T. K. Ahn, D. M. Ko, A. Takagi, T. Kawai, T. Matsumoto, D. Kim, A. Osuka, *Journal of the American Chemical Society* **2005**, *127*, 236-246.
[144] B. Bašić, J. C. McMurtrie, D. P. Arnold, *European Journal of Organic Chemistry* **2010**, *2010*, 4381-4392.
[145] a) S. Wagaw, R. A. Rennels, S. L. Buchwald, *Journal of the American Chemical Society* **1997**, *119*, 8451-8458; b) J. P. Wolfe, S. Wagaw, S. L. Buchwald, *Journal of the American Chemical Society* **1996**, *118*, 7215-7216; c) A. S. Guram, R. A. Rennels, S. L. Buchwald, *Angewandte Chemie International Edition* **1995**, *34*, 1348-1350; d) F. Paul, J. Patt, J. F. Hartwig, *Journal of the American Chemical Society* **1994**, *116*, 5969-5970; e) J. Louie, J. F. Hartwig, *Tetrahedron Letters* **1995**, *36*, 3609-3612.
[146] a) K. Fujimoto, H. Yorimitsu, A. Osuka, *Organic Letters* **2014**, *16*, 972-975; b) E. A. Mikhalitsyna, V. S. Tyurin, V. N. Khrustalev, I. S. Lonin, I. P. Beletskaya, *Dalton Transactions* **2014**, *43*, 3563-3575; c) K. Ladomenou, T. Lazarides, M. K. Panda, G. Charalambidis, D. Daphnomili, A. G. Coutsolelos, *Inorganic Chemistry* **2012**, *51*, 10548-10556.
[147] a) C. Fischer, B. Koenig, *Beilstein Journal of Organic Chemistry* **2011**, *7*, 59-74; b) J.-N. Heo, Y. S. Song, B. T. Kim, *Tetrahedron Letters* **2005**, *46*, 4621-4625; c) K. Foo, T. Newhouse, I. Mori, H. Takayama, P. S. Baran, *Angewandte Chemie International Ed.* **2011**, *50*, 2716-2719.
[148] M. O. Senge, J. Richter, I. Bischoff, A. A. Ryan, *Tetrahedron* **2010**, *66*, 3508-3524.
[149] X. Feng, M. O. Senge, *Journal of the Chemical Society, Perkin Transactions 1* **2001**, 1030-1038.
[150] a) A. Ryan, A. Gehrold, R. Perusitti, M. Pintea, M. Fazekas, O. B. Locos, F. Blaikie, M. O. Senge, *European Journal of Organic Chemistry* **2011**, *2011*, 5817-5844.
[151] K. Kurotobi, Y. Toude, K. Kawamoto, Y. Fujimori, S. Ito,P. Chabera, V. Sundstrom, H. Imahori, *Chemistry a European Journal* **2013**, *19*, 17075–17081.
[152] P. E. Eaton, T. W. Cole, *Journal of the American Chemical Society* **1964**, *86*, 3157-3158.
[153] B. A. Chalmers, H. Xing, S. Houston, C. Clark, S. Ghassabian, A. Kuo, B. Cao, A. Reitsma, C.-E. P. Murray, J. E. Stok, G. M. Boyle, C. J. Pierce, S.

W. Littler, D. A. Winkler, P. V. Bernhardt, C. Pasay, J. J. De Voss, J. McCarthy, P. G. Parsons, G. H. Walter, M. T. Smith,H. M. Cooper, S. K. Nilsson, J. Tsanaktsidis, G. P. Savage, C. M. Williams, *Angewandte Chemie International Edition* **2016**, *55*, 3580-3585.
[154] W. Weltner, *Journal of the American Chemical Society* **1953**, *75*, 4224-4231.
[155] a) N. Miyaura, A. Suzuki, *Chemical Reviews* **1995**, *95*, 2457-2483; b) R. Chinchilla, C. Nájera, *Chemical Reviews* **2007**, *107*, 874-922.
[156] P. E. Eaton, T. W. Cole, *Journal of the American Chemical Society* **1964**, *86*, 962-964.
[157] a) N. B. Chapman, J. M. Key, K. J. Toyne, *The Journal of Organic Chemistry* **1970**, *35*, 3860-3867; b) M. Bliese, J. Tsanaktsidis, *Australian Journal of Chemistry* **1997**, *50*, 189-192; c) M. J. Falkiner, S. W. Littler, K. J. McRae, G. P. Savage, J. Tsanaktsidis, *Organic Process Research & Development* **2013**, *17*, 1503-1509.
[158] J. R. Griffiths, J. Tsanaktsidis, G. P. Savage, R. Priefer, *Thermochimica Acta* **2010**, *499*, 15-20.
[159] a) G. W. Griffin, A. P. Marchand, *Chemical Reviews* **1989**, *89*, 997-1010; b) P. E. Eaton, *Angewandte Chemie International Edition in English* **1992**, *31*, 1421-1436.
[160] W. v. E. Doering, W. R. Roth, R. Breuckmann, L. Figge, H.-W. Lennartz, W.-D. Fessner, H. Prinzbach, *Chemische Berichte* **1988**, *121*, 1-9.
[161] L. Hedberg, K. Hedberg, P. E. Eaton, N. Nodari, A. G. Robiette, *Journal of the American Chemical Society* **1991**, *113*, 1514-1517.
[162] M. V. Roux, G. Martín-Valcarcel, R. Notario, S. Kini, J. S. Chickos, J. F. Liebman, *Journal of Chemical & Engineering Data* **2011**, *56*, 1220-1228.
[163] a) P. E. Eaton, R. L. Gilardi, M. X. Zhang, *Advanced Materials* **2000**, *12*, 1143-1148; b) P. E. Eaton, M.-X. Zhang, R. Gilardi, N. Gelber, S. Iyer, R. Surapaneni, *Propellants, Explosives, Pyrotechnics* **2002**, *27*, 1-6.
[164] C. M. Marson, *Chemical Society Reviews* **2011**, *40*, 5514-5533.
[165] a) D. Morton, S. Leach, C. Cordier, S. Warriner, A. Nelson, *Angewandte Chemie International Edition* **2008**, *48*, 104-109; b) M. D. Burke, S. L. Schreiber, *Angewandte Chemie International Edition* **2003**, *43*, 46-58.
[166] E. B. Fleischer, *Journal of the American Chemical Society* **1964**, *86*, 3889-3890.
[167] K. F. Biegasiewicz, J. R. Griffiths, G. P. Savage, J. Tsanaktsidis, R. Priefer, *Chemical Reviews* **2015**, *115*, 6719-6745.
[168] L. T. Eremenko, L. B. Romanova, M. E. Ivanova, V. S. Malygina, L. S. Barinova, G. V. Lagodzinskaya, V. P. Lodygina, I. L. Eremenko, G. G. Aleksandrov, *Russian Chemical Bulletin* **2007**, *56*, 1408-1422.
[169] C.-Y. Cheng, L.-W. Hsin, Y.-P. Lin, P.-L. Tao, T.-T. Jong, *Bioorganic & Medicinal Chemistry* **1996**, *4*, 73-80.
[170] R. M. Moriarty, J. S. Khosrowshahi, T. M. Dalecki, *Journal of the Chemical Society, Chemical Communications* **1987**, 675-676.
[171] G. A. Olah, C. S. Lee, G. K. S. Prakash, R. M. Moriarty, M. S. C. Rao, *Journal of the American Chemical Society* **1993**, *115*, 10728-10732.
[172] J. Wlochal, R. D. M. Davies, J. Burton, *Organic Letters* **2014**, *16*, 4094-4097.
[173] R. M. Moriarty, J. S. Khosrowshahi, R. S. Miller, J. Flippen-Andersen, R. Gilardi, *Journal of the American Chemical Society* **1989**, *111*, 8943-8944.
[174] P. E. Eaton, K. Pramod, T. Emrick, R. Gilardi, *Journal of the American Chemical Society* **1999**, *121*, 4111-4123.

[175] S. Plunkett, K. J. Flanagan, B. Twamley, M. O. Senge, *Organometallics* **2015**, *34*, 1408-1414.
[176] a) P. E. Eaton, L. Cassar, J. Halpern, *Journal of the American Chemical Society* **1970**, *92*, 6366-6368; b) L. Cassar, P. E. Eaton, J. Halpern, *Journal of the American Chemical Society* **1970**, *92*, 3515-3518.
[177] F. Toriyama, J. Cornella, L. Wimmer, T.-G. Chen, D. D. Dixon, G. Creech, P. S. Baran, *Journal of the American Chemical Society* **2016**, *138*, 11132-11135.
[178] C. Li, J. Wang, L. M. Barton, S. Yu, M. Tian, D. S. Peters, M. Kumar, A. W. Yu, K. A. Johnson, A. K. Chatterjee, M. Yan, P. S. Baran, *Science* **2017**, *356,* eaam7355.
[179] S. S. R. Bernhard, G. M. Locke, S. Plunkett, A. Meindl, K. J. Flanagan, M. O. Senge, *Chemistry – A European Journal* **2017**, *24*, 1026-1030.
[180] S. Horn, K. Dahms, M. O. Senge, *Journal of Porphyrins and Phthalocyanines* **2008**, *12*, 1053-1077.
[181] L. Rintoul, S. R. Harper, D. P. Arnold, *Physical Chemistry Chemical Physics* **2013**, *15*, 18951-18964.
[182] A. K. Burrell, D. L. Officer, P. G. Plieger, D. C. W. Reid, *Chemical Reviews* **2001**, *101*, 2751-2796.
[183] a) H. Imahori, D. M. Guldi, K. Tamaki, Y. Yoshida, C. Luo, Y. Sakata, S. Fukuzumi, *Journal of the American Chemical Society* **2001**, *123*, 6617-6628; b) D. M. Guldi, *Chemical Society Reviews* **2002**, *31*, 22-36.
[184] a) F. C. Grozema, C. Houarner-Rassin, P. Prins, L. D. A. Siebbeles, H. L. Anderson, *Journal of the American Chemical Society* **2007**, *129*, 13370-13371; b) M. U. Winters, E. Dahlstedt, H. E. Blades, C. J. Wilson, M. J. Frampton, H. L. Anderson, B. Albinsson, *Journal of the American Chemical Society* **2007**, *129*, 4291-4297.
[185] K. Pettersson, A. Kyrychenko, E. Rönnow, T. Ljungdahl, J. Mårtensson, B. Albinsson, *The Journal of Physical Chemistry A* **2006**, *110*, 310-318.
[186] R. D. Hartnell, D. P. Arnold, *European Journal of Inorganic Chemistry* **2004**, *2004*, 1262-1269.
[187] K. Fujimoto, H. Yorimitsu, A. Osuka, *Chemistry – A European Journal* **2015**, *21*, 11311-11314.
[188] J. J. P. Zhou, J. Li, S. Upadhyaya, P. E. Eaton, R. B. Silverman, *Journal of Medicinal Chemistry* **1997**, *40*, 1165-1168.
[189] a) K. M. M. Huihui, J. A. Caputo, Z. Melchor, A. M. Olivares, A. M. Spiewak, K. A. Johnson, T. A. DiBenedetto, S. Kim, L. K. G. Ackerman, D. J. Weix, *Journal of the American Chemical Society* **2016**, *138*, 5016-5019; b) J. Cornella, J. T. Edwards, T. Qin, S. Kawamura, J. Wang, C.-M. Pan, R. Gianatassio, M. Schmidt, M. D. Eastgate, P. S. Baran, *Journal of the American Chemical Society* **2016**, *138*, 2174-2177.
[190] T. Quin, J. Cornella, C. Li, L. R. Malins, J. T. Edwards, S. Kawamura, B. D. Maxwell, M. D. Eastgate, P. S. Baran, *Science* **2016**, *352*, 801-805.
[191] J. Wang, T. Quin, T.-G. Chen, L. Wimmer, J. T. Edwards, J. Cornella, B. Vokits, S. A. Shaw, P. S. Baran, *Angewandte Chemie International Edition* **2016**, *55*, 9676-9679.
[192] J. S. Lindsey, S. Prathapan, T. E. Johnson, R. W. Wagner, *Tetrahedron* **1994**, *50*, 8941-8968.
[193] a) J. P. Collman, R. R. Gagne, C. Reed, T. R. Halbert, G. Lang, W. T. Robinson, *Journal of the American Chemical Society* **1975**, *97*, 1427-1439; b) J. P. Collman, X. Zhang, P. C. Herrmann, E. S. Uffelman, B. Boitrel, A. Straumanis, J. I. Brauman, *Journal of the American Chemical Society* **1994**,

116, 2681-2682; c) L. G. Mackay, R. S. Wylie, J. K. M. Sanders, *Journal of the American Chemical Society* **1994**, *116*, 3141-3142; d) S. Prathapan, T. E. Johnson, J. S. Lindsey, *Journal of the American Chemical Society* **1993**, *115*, 7519-7520.

[194] a) T. Rhauderwiek, S. Waitschat, S. Wuttke, H. Reinsch, T. Bein, N. Stock, *Inorganic Chemistry* **2016**, *55*, 5312-5319; b) A. G. Slater, Y. Hu, L. Yang, S. P. Argent, W. Lewis, M. O. Blunt, N. R. Champness, *Chemical Science* **2015**, *6*, 1562-1569; c) Z. Wang, C. J. Medforth, J. A. Shelnutt, *Journal of the American Chemical Society* **2004**, *126*, 15954-15955; d) O. T. Wilcox, A. Fateeva, A. P. Katsoulidis, M. W. Smith, C. A. Stone, M. J. Rosseinsky, *Chemical Communications* **2015**, *51*, 14989-14991; e) L. Zhang, J. Lei, F. Ma, P. Ling, J. Liu, H. Ju, *Chemical Communications* **2015**, *51*, 10831-10834.

[195] V. Bulach, M. W. Hosseini, in *Handbook of Porphyrin Science, Vol. 13* (Eds.: K. M. Kadish, K. M. Smith, R. Guilard), World Scientific, Singapore, **2011**, pp. 299-390.

[196] M. W. Hosseini, *Accounts of Chemical Research* **2005**, *38*, 313-323.

[197] W. Auwärter, D. Écija, F. Klappenberger, J. V. Barth, *Nature Chemistry* **2015**, *7*, 105-120.

[198] a) F. D'Souza, O. Ito, *Chemical Society Reviews* **2012**, *41*, 86-96; b) V. Sgobba, D. M. Guldi, *Chemical Society Reviews* **2009**, *38*, 165-184.

[199] D. Kiessling, R. D. Costa, G. Katsukis, J. Malig, F. Lodermeyer, S. Feihl, A. Roth, L. Wibmer, M. Kehrer, M. Volland, P. Wagner, G. G. Wallace, D. L. Officer, D. M. Guldi, *Chemical Science* **2013**, *4*, 3085-3098.

[200] H.-J. Son, S. Jin, S. Patwardhan, S. J. Wezenberg, N. C. Jeong, M. So, C. E. Wilmer, A. A. Sarjeant, G. C. Schatz, R. Q. Snurr, O. K. Farha, G. P. Wiederrecht, J. T. Hupp, *Journal of the American Chemical Society* **2013**, *135*, 862-869.

[201] L. G. Arnaut, in *Advances in Inorganic Chemistry, Vol. 63* (Eds.: R. v. Eldik, G. Stochel), Academic Press, **2011**, pp. 187-233.

[202] M. V. Sheridan, K. Lam, W. E. Geiger, *Angewandte Chemie International Edition* **2013**, *52*, 12897-12900.

[203] a) W. Morris, B. Volosskiy, S. Demir, F. Gándara, P. L. McGrier, H. Furukawa, D. Cascio, J. F. Stoddart, O. M. Yaghi, *Inorganic Chemistry* **2012**, *51*, 6443-6445; b) D. Feng, Z.-Y. Gu, J.-R. Li, H.-L. Jiang, Z. Wei, H.-C. Zhou, *Angewandte Chemie International Edition* **2012**, *51*, 10307-10310; c) Y. Chen, T. Hoang, S. Ma, *Inorganic Chemistry* **2012**, *51*, 12600-12602.

[204] a) M. Shmilovits, M. Vinodu, I. Goldberg, *Crystal Growth & Design* **2004**, *4*, 633-638; b) E.-Y. Jeong, A. Burri, S.-Y. Lee, S.-E. Park, *Journal of Materials Chemistry* **2010**, *20*, 10869-10875.

[205] a) G. Wei, M. Yan, L. Ma, C. Wang, *RSC Advances* **2016**, *6*, 3748-3755; b) Z. Hu, Y. Pan, J. Wang, J. Chen, J. Li, L. Ren, *Biomedicine & Pharmacotherapy* **2009**, *63*, 155-164.

[206] F. Gou, X. Jiang, R. Fang, H. Jing, Z. Zhu, *ACS Applied Materials & Interfaces* **2014**, *6*, 6697-6703.

[207] M. B. Bakar, M. Oelgemöller, M. O. Senge, *Tetrahedron* **2009**, *65*, 7064-7078.

[208] N. Hewage, B. Yang, A. G. Agrios, C. Brückner, *Dyes and Pigments* **2015**, *121*, 159-169.

[209] S. V. Bhosale, S. Hackbarth, S. J. Langford, S. V. Bhosale, *Chemistry – An Asian Journal* **2011**, *7*, 176-182.

[210] a) F. Cheng, S. Zhang, A. Adronov, L. Echegoyen, F. Diederich, *Chemistry – A European Journal* **2006**, *12*, 6062-6070; b) F. Cheng, J. Zhu, A. Adronov, *Chemistry of Materials* **2011**, *23*, 3188-3194.
[211] a) N. M. R. Peres, A. H. Castro Neto, F. Guinea, *Physical Review B* **2006**, *73*, 195411-1-194511-8; b) D. V. Khveshchenko, *Physical Review B* **2006**, *74*, 161402-1-161402-4.
[212] V. Strauss, A. Roth, M. Sekita, D. M. Guldi, *Chemistry* **2016**, *1*, 531-556.
[213] a) J. Malig, A. W. I. Stephenson, P. Wagner, G. G. Wallace, D. L. Officer, D. M. Guldi, *Chemical Communications* **2012**, *48*, 8745-8747; b) S. P. Economopoulos, G. Rotas, Y. Miyata, H. Shinohara, N. Tagmatarchis, *ACS Nano* **2010**, *4*, 7499-7507; c) J. M. Englert, C. Dotzer, G. Yang, M. Schmid, C. Papp, J. M. Gottfried, H.-P. Steinrück, E. Spiecker, F. Hauke, A. Hirsch, *Nature Chemistry* **2011**, *3*, 279-286; d) S. Barja, M. Garnica, J. J. Hinarejos, A. L. Vázquez de Parga, N. Martín, R. Miranda, *Chemical Communications* **2010**, *46*, 8198-8200; e) M. Castelaín, H. J. Salavagione, R. Gómez, J. L. Segura, *Chemical Communications* **2011**, *47*, 7677-7679.
[214] a) S. Fukuzumi, T. Kojima, *Journal of Materials Chemistry* **2008**, *18*, 1427-1439; b) G. Bottari, G. de la Torre, D. M. Guldi, T. Torres, *Chemical Reviews* **2010**, *110*, 6768-6816.
[215] a) D. Masih, S. M. Aly, A. Usman, E. Alarousu, O. F. Mohammed, *Physical Chemistry Chemical Physics* **2015**, *17*, 9015-9019; b) C. Bikram K. C. S. K. Das, K. Ohkubo, S. Fukuzumi, F. D'Souza, *Chemical Communications* **2012**, *48*, 11859-11861; c) S. M. Aly, M. R. Parida, E. Alarousu, O. F. Mohammed, *Chemical Communications* **2014**, *50*, 10452-10455.
[216] A. Wang, W. Yu, Z. Xiao, Y. Song, L. Long, M. P. Cifuentes, M. G. Humphrey, C. Zhang, *Nano Research* **2015**, *8*, 870-886.
[217] D. Balbinot, S. Atalick, D. M. Guldi, M. Hatzimarinaki, A. Hirsch, N. Jux, *The Journal of Physical Chemistry B* **2003**, *107*, 13273-13279.
[218] J. R. Lakowicz, *Principles of Fluorescence Spectroscopy*, 3 ed., Springer Science + Business Media, LLC, Singapore, **2006**.
[219] a) H. Furukawa, K. E. Cordova, M. O'Keeffe, O. M. Yaghi, *Science* **2013**, *341,* 1230444-1-1230444-12; b) B. F. Hoskins, R. Robson, *Journal of the American Chemical Society* **1990**, *112*, 1546-1554.
[220] M. C. So, G. P. Wiederrecht, J. E. Mondloch, J. T. Hupp, O. K. Farha, *Chemical Communications* **2015**, *51*, 3501-3510.
[221] A. Bétard, R. A. Fischer, *Chemical Reviews* **2012**, *112*, 1055-1083.
[222] a) K. S. Suslick, P. Bhyrappa, J. H. Chou, M. E. Kosal, S. Nakagaki, D. W. Smithenry, S. R. Wilson, *Accounts of Chemical Research* **2005**, *38*, 283-291; b) T. Ohmura, A. Usuki, K. Fukumori, T. Ohta, M. Ito, K. Tatsumi, *Inorganic Chemistry* **2006**, *45*, 7988-7990.
[223] C. Y. Lee, O. K. Farha, B. J. Hong, A. A. Sarjeant, S. T. Nguyen, J. T. Hupp, *Journal of the American Chemical Society* **2011**, *133*, 15858-15861.
[224] a) J. R. Caram, S. Doria, D. M. Eisele, F. S. Freyria, T. S. Sinclair, P. Rebentrost, S. Lloyd, M. G. Bawendi, *Nano Letters* **2016**, *16*, 6808-6815; b) Y. Wan, A. Stradomska, J. Knoester, L. Huang, *Journal of the American Chemical Society* **2017**, *139*, 7287-7293.
[225] A. T. Haedler, K. Kreger, A. Issac, B. Wittmann, M. Kivala, N. Hammer, J. Köhler, H.-W. Schmidt, R. Hildner, *Nature* **2015**, *523*, 196-199.
[226] F. Dubin, R. Melet, T. Barisien, R. Grousson, L. Legrand, M. Schott, V. Voliotis, *Nature Physics* **2006**, *2*, 32-35.
[227] J. Liu, W. Zhou, J. Liu, I. Howard, G. Kilibarda, S. Schlabach, D. Coupry, M. Addicoat, S. Yoneda, Y. Tsutsui, T. Sakurai, S. Seki, Z. Wang, P.

Lindemann, E. Redel, T. Heine, C. Wöll, *Angewandte Chemie International Edition* **2015**, *54*, 7441-7445.
[228] E. Balasubramaniam, G. Ramachandraiah, P. Natarajan, C. Bied-Charreton, J. Devynck, F. Bedioui, *Journal of Materials Chemistry* **1995**, *5*, 625-629.
[229] S. Drouet, S. Ballut, J. Rault-Berthelot, P. Turban, C. Paul-Roth, *Thin Solid Films* **2009**, *517*, 5474-5481.
[230] M. Kawao, H. Ozawa, H. Tanaka, T. Ogawa, *Thin Solid Films* **2006**, *499*, 23-28.
[231] C. Paul-Roth, J. Rault-Berthelot, G. Simonneaux, C. Poriel, M. Abdalilah, J. Letessier, *Journal of Electroanalytical Chemistry* **2006**, *597*, 19-27.
[232] J. E. Hutchison, T. A. Postlethwaite, C.-h. Chen, K. W. Hathcock, R. S. Ingram, W. Ou, R. W. Linton, R. W. Murray, D. A. Tyvoll, L. L. Chng, J. P. Collman, *Langmuir* **1997**, *13*, 2143-2148.
[233] S. Ssenyange, F. Anariba, D. F. Bocian, R. L. McCreery, *Langmuir* **2005**, *21*, 11105-11112.
[234] a) P. K. B. Palomaki, P. H. Dinolfo, *Langmuir* **2010**, *26*, 9677-9685; b) A. R. McDonald, N. Franssen, G. P. M. van Klink, G. van Koten, *Journal of Organometallic Chemistry* **2009**, *694*, 2153-2162.
[235] a) A. J. Gross, C. Bucher, L. Coche-Guerente, P. Labbé, A. J. Downard, J.-C. Moutet, *Electrochemistry Communications* **2011**, *13*, 1236-1239; b) M. Picot, I. Nicolas, C. Poriel, J. Rault-Berthelot, F. Barrière, *Electrochemistry Communications* **2012**, *20*, 167-170.
[236] a) H. N. Roberts, N. J. Brown, R. Edge, E. C. Fitzgerald, Y. T. Ta, D. Collison, P. J. Low, M. W. Whiteley, *Organometallics* **2012**, *31*, 6322-6335; b) F. Gendron, A. Burgun, B. W. Skelton, A. H. White, T. Roisnel, M. I. Bruce, J.-F. Halet, C. Lapinte, K. Costuas, *Organometallics* **2012**, *31*, 6796-6811; c) F. Lissel, T. Fox, O. Blacque, W. Polit, R. F. Winter, K. Venkatesan, H. Berke, *Journal of the American Chemical Society* **2013**, *135*, 4051-4060.
[237] a) C.-Y. Lin, S.-C. Huang, Y.-C. Chen, *Electrochemistry Communications* **2008**, *10*, 1411-1414; b) S. Jin, H.-J. Son, O. K. Farha, G. P. Wiederrecht, J. T. Hupp, *Journal of the American Chemical Society* **2013**, *135*, 955-958.
[238] T. D. Lash, P. Chandrasekar, A. T. Osuma, S. T. Chaney, J. D. Spence, *The Journal of Organic Chemistry* **1998**, *63*, 8455-8469.
[239] H. Shinokubo, A. Osuka, *Chemical Communications* **2009**, 1011-1021.
[240] a) N. G. Pschirer, C. Kohl, F. Nolde, J. Qu, K. Müllen, *Angewandte Chemie International Edition* **2006**, *45*, 1401-1404; b) P. F. H. Schwab, M. D. Levin, J. Michl, *Chemical Reviews* **1999**, *99*, 1863-1934;
[241] J. P. Lewtak, D. T. Gryko, *Chemical Communications* **2012**, *48*, 10069-10086.
[242] a) G. Sedghi, K. Sawada, L. J. Esdaile, M. Hoffmann, H. L. Anderson, D. Bethell, W. Haiss, S. J. Higgins, R. J. Nichols, *Journal of the American Chemical Society* **2008**, *130*, 8582-8583; b) K. J. McEwan, P. A. Fleitz, J. E. Rogers, J. E. Slagle, D. G. McLean, H. Akdas, M. Katterle, I. M. Blake, H. L. Anderson, *Advanced Materials* **2004**, *16*, 1933-1935; c) P. Kim, T. Ikeda, J. M. Lim, J. Park, M. Lim, N. Aratani, A. Osuka, D. Kim, *Chemical Communications* **2011**, *47*, 4433-4435; d) A. Tsuda, A. Osuka, *Advanced Materials* **2002**, *14*, 75-79; e) H. S. Cho, D. H. Jeong, S. Cho, D. Kim, Y. Matsuzaki, K. Tanaka, A. Tsuda, A. Osuka, *Journal of the American Chemical Society* **2002**, *124*, 14642-14654; f) D. Kim, A. Osuka, *The Journal of Physical Chemistry A* **2003**, *107*, 8791-8816.

[243] M. G. H. Vicente, K. M. Smith, *The Journal of Organic Chemistry* **1991**, *56*, 4407-4418.
[244] H. J. Callot, E. Schaeffer, R. Cromer, F. Metz, *Tetrahedron* **1990**, *46*, 5253-5262.
[245] D. Sengupta, B. C. Robinson, *Tetrahedron* **2002**, *58*, 5497-5502.
[246] M. A. Faustino, M. G. P. M. S. Neves, M. G. H. Vicente, A. M. S. Silva, J. A. S. Cavaleiro, *Tetrahedron Letters* **1995**, *36*, 5977-5978.
[247] T. Tanaka, A. Osuka, *Chemical Society Reviews* **2015**, *44*, 943-969.
[248] a) L. Jaquinod, O. Siri, R. G. Khoury, *Chemical Communications* **1998**, 1261-1262; b) L. Jaquinod, C. Gros, M. M. Olmstead, M. Antolovich, K. M. Smith, *Chemical Communications* **1996**, 1475-1476.
[249] D. H. R. Barton, J. Kervagoret, S. Z. Zard, *Tetrahedron* **1990**, *46*, 7587-7598.
[250] M. G. H. Vicente, M. T. Cancilla, C. B. Lebrilla, K. M. Smith, *Chemical Communications* **1998**, 2355-2356.
[251] M. G. H. Vicente, A. C. Tomé, A. Walter, J. A. S. Cavaleiro, *Tetrahedron Letters* **1997**, *38*, 3639-3642.
[252] A. Osuka, H. Shimidzu, *Angewandte Chemie International Edition in English* **2003**, *36*, 135-137.
[253] A. Tsuda, H. Furuta, A. Osuka, *Angewandte Chemie International Edition* **2000**, *39*, 2549-2552.
[254] N. Yoshida, N. Aratani, A. Osuka, *Chemical Communications* **2000**, 197-198.
[255] A. Tsuda, A. Osuka, *Science* **2001**, *293*, 79-82.
[256] A. Nakano, N. Aratani, H. Furuta, A. Osuka, *Chemical Communications* **2001**, 1920-1921.
[257] K.-i. Sugiura, T. Matsumoto, S. Ohkouchi, Y. Naitoh, T. Kawai, Y. Takai, K. Ushiroda, Y. Sakata, *Chemical Communications* **1999**, 1957-1958.
[258] A. Tsuda, H. Furuta, A. Osuka, *Journal of the American Chemical Society* **2001**, *123*, 10304-10321.
[259] M. Kamo, A. Tsuda, Y. Nakamura, N. Aratani, K. Furukawa, T. Kato, A. Osuka, *Organic Letters* **2003**, *5*, 2079-2082.
[260] Y. Nakamura, N. Aratani, H. Shinokubo, A. Takagi, T. Kawai, T. Matsumoto, Z. S. Yoon, D. Y. Kim, T. K. Ahn, D. Kim, A. Muranaka, N. Kobayashi, A. Osuka, *Journal of the American Chemical Society* **2006**, *128*, 4119-4127.
[261] A. A. Ryan, M. O. Senge, *European Journal of Organic Chemistry* **2013**, *2013*, 3700-3711.
[262] a) N. K. S. Davis, A. L. Thompson, H. L. Anderson, *Journal of the American Chemical Society* **2011**, *133*, 30-31; b) N. K. S. Davis, M. Pawlicki, H. L. Anderson, *Organic Letters* **2008**, *10*, 3945-3947.
[263] O. Yamane, K.-i. Sugiura, H. Miyasaka, K. Nakamura, T. Fujimoto, K. Nakamura, T. Kaneda, Y. Sakata, M. Yamashita, *Chemistry Letters* **2003**, *33*, 40-41.
[264] A. Eftekhari, H. Garcia, *Materials Today Chemistry* **2017**, *4*, 1-16.
[265] Y. He, M. Garnica, F. Bischoff, J. Ducke, M.-L. Bocquet, M. Batzill, W. Auwärter, J. V. Barth, *Nature Chemistry* **2017**, *9*, 33-38.
[266] F. Liu, Y. Xu, L. Zhao, L. Zhang, W. Guo, R. Wang, D. Sun, *Journal of Materials Chemistry A* **2015**, *3*, 21545-21552.
[267] Y. Li, S.-J. Ko, S. Y. Park, H. Choi, T. L. Nguyen, M. A. Uddin, T. Kim, S. Hwang, J. Y. Kim, H. Y. Woo, *Journal of Materials Chemistry A* **2016**, *4*, 9967-9976.

[268] a) C. Liebermann, A. Gimbel, *Berichte der deutschen chemischen Gesellschaft* **1887**, *20*, 1854-1855; b) G. F. Attree, A. G. Perkin, *Journal of the Chemical Society (Resumed)* **1931**, 144-173; c) P. Natarajan, M. Schmittel, *The Journal of Organic Chemistry* **2013**, *78*, 10383-10394; d) P. Xue, B. Yao, X. Liu, J. Sun, P. Gong, Z. Zhang, C. Qian, Y. Zhang, R. Lu, *Journal of Materials Chemistry C* **2015**, *3*, 1018-1025; e) F. Bell, D. H. Waring, *Journal of the Chemical Society (Resumed)* **1949**, 267-269.
[269] Y. Yamada, H. Hayashi, 2015 *Patent No. JP 2017-57182*, Nara Institute of Science and Technology, Japan.
[270] R. C. Samanta, H. Yamamoto, *Chemistry – A European Journal* **2015**, *21*, 11976-11979.
[271] A. A. O. Sarhan, C. Bolm, *Chemical Society Reviews* **2009**, *38*, 2730-2744.
[272] a) K. Kurotobi, K. S. Kim, S. B. Noh, D. Kim, A. Osuka, *Angewandte Chemie International Edition* **2006**, *45*, 3944-3947; b) J. Wu, L. Gherghel, M. D. Watson, J. Li, Z. Wang, C. D. Simpson, U. Kolb, K. Müllen, *Macromolecules* **2003**, *36*, 7082-7089.
[273] A. Meindl, A. A. Ryan, K. J. Flanagan, M. O. Senge, *Heterocycles* **2017**, *94*, 1518-1541.
[274] A. R. Katritzky, K. W. Law, *Magnetic Resonance in Chemistry* **1988**, *26*, 129-133.
[275] M. S. Newman, L. F. Lee, *The Journal of Organic Chemistry* **1972**, *37*, 4468-4469.
[276] R. Shediac, M. H. B. Gray, H. T. Uyeda, R. C. Johnson, J. T. Hupp, P. J. Angiolillo, M. J. Therien, *Journal of the American Chemical Society* **2000**, *122*, 7017-7033.
[277] Y. Liu, H. Lin, J. T. Dy, K. Tamaki, J. Nakazaki, D. Nakayama, S. Uchida, T. Kubo, H. Segawa, *Chemical Communications* **2011**, *47*, 4010-4012.
[278] C.-H. Lee, J. S. Lindsey, *Tetrahedron* **1994**, *50*, 11427-11440.
[279] S. Plunkett, K. Dahms, M. O. Senge, *European Journal of Organic Chemistry* **2013**, *2013*, 1566-1579.
[280] T. S. Balaban, R. Goddard, M. Linke-Schaetzel, J.-M. Lehn, *Journal of the American Chemical Society* **2003**, *125*, 4233-4239.
[281] M. Yeung, A. C. H. Ng, M. G. B. Drew, E. Vorpagel, E. M. Breitung, R. J. McMahon, D. K. P. Ng, *The Journal of Organic Chemistry* **1998**, *63*, 7143-7150.
[282] K. Oda, M. Akita, S. Hiroto, H. Shinokubo, *Organic Letters* **2014**, *16*, 1818-1821.